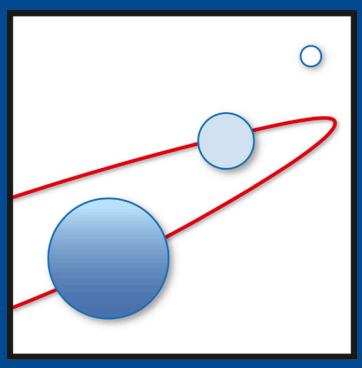

Raumfahrttechnik und Extraterrestrik

Advances in Space Technology and Exploration

Julius-Maximilians-
UNIVERSITÄT WÜRZBURG

Carolin Bösch, Malena Stieler, Salomon Lydon, Martin Hesse, Hassan Ali, Matthias Finzel, Syed Faraz Ali, Yash Salian, Hiba Alnoor, Jeena John, Harsh Lakkad, Devraj Bhosale, Timon Jafarian, Uma Parvathi, Narges Ezzatpoor, Tanuja Datar

Nr. 4

Venus Research Station

Julius-Maximilians-
UNIVERSITÄT
WÜRZBURG

Prof. Dr.-Ing. Hakan Kayal
Chair of Computer Science VIII
Aerospace Information Technology

Venus Research Station

Carolin Bösch, Malena Stieler, Salomon Lydon, Martin Hesse, Hassan Ali, Matthias Finzel, Syed Faraz Ali, Yash Salian, Hiba Alnoor, Jeena John, Harsh Lakkad, Devraj Bhosale, Timon Jafarian, Uma Parvathi, Narges Ezzatpoor, Tanuja Datar

August 2023

Foreword

Because of the extreme conditions in the atmosphere, Venus has been less explored than for example Mars. Only a few probes have been able to survive on the surface for very short periods in the past and have sent data. The atmosphere is also far from being fully explored. It could even be that building blocks of life can be found in more moderate layers of the planet's atmosphere. It can therefore be assumed that the planet Venus will increasingly become a focus of exploration.

One way to collect significantly more data in situ is to build and operate an atmospheric research station over an extended period of time. This could carry out measurements at different positions and at different times and thus significantly expand our knowledge of the planet. But, which scientific questions could be answered with the help of such a research station and how would it have to look like? What challenges would there be to overcome, what bottlenecks are there? Would it even be feasible?

This report was written as part of a student semester project in the course Planetary Bases and Orbital Stations, which addresses these issues in more detail. As a result, a conceptual design has been created, the key features of which have been investigated in more detail. The successful result was developed in a team design project, in which the students also had the opportunity to gain experience in project work in astronautics in a larger team. It can be hoped that this experience will motivate them to participate in such space projects and contribute to their success in the future.

Prof. Dr.-Ing. Hakan Kayal

Acknowledgements

I would like to express our sincere gratitude to Prof. Kayal for granting us the opportunity to participate in such an interesting team project, for the supervision of our project and for the instructions and guidance throughout the project.

My sincere thanks further goes to Christopher Copelan[1] from the NASA Stennis Space Centre and Veronica O. Cavazos[2] of the NASA Technology Transfer Program for granting us the access to the NASA Software Venus-GRAM 2005 [1, 2].

But most importantly I want to thank my entire team: Malena, Salomon, Martin, Hassan, Matthias, Faraz, Yash, Hiba, Jeena, Harsh, Devraj, Timon, Uma, Narges and Tanuja! Thank you guys for your hard work. I know not each step has been easy, but I am grateful we made it through the harder parts as a team. A special thank you to Malena for helping me with special tasks in project management, especially the amazing protocols of the meetings and pretty plots, to Salomon for being an amazing system team leader and guiding them through the hard parts of the discussion, and to Martin (mission leader) for helping with the integration of the final report.

Carolin Bösch

[1]Mail: christopher.r.copelan@nasa.gov
[2]Mail: veronica.o.cavazos@nasa.gov

Contents

List of Figures

List of Tables

CHAPTER 1

Introduction

by Carolin Bösch, Malena Stieler and Syed Faraz Ali

'I haven't heard from Venus for ages, but I understand that she's under a lot of pressure.'
- Anonymous

Venus is one of the most captivating celestial bodies, both for its fascinating planetary science and for its beauty that makes it a delight to watch in the night sky. It is often considered Earth's sister planet for its similarities in mass, size and composition and proximity. It is also famously referred to as the morning or evening star because it is visible near the rising or setting Sun when prominent in the sky. It is the third brightest object in the sky, after the Sun and the Moon, reaching a visible magnitude of -4.3.

Astrobiologists aim to identify environments conducive to life's existence and evolution. The search for life elsewhere in the universe centres around seeking Earth-like conditions and the presence of liquid water. Interestingly, Venus is believed to once possibly be Earth-like and has now evolved into an uninhabitable world, making it an essential case study for understanding the evolution of habitability. Planetary scientists call it a crucial link to understanding habitability on different planets, be it the habitability of humans or the age-old passion of finding out about possible alien life. It might serve as a type of planet that has transitioned from habitable conditions through the inner edge of the Habitable Zone. The significance of Venus in comprehending habitable terrestrial planets cannot be emphasized enough. It is widely acknowledged that the size and orbit of Venus make it a crucial reference point for comparing the evolution of Earth and Earth-sized exoplanets as many of the newly discovered exoplanets are likely direct analogues of Venus.

As detection methods for exoplanets improve, collaborations between the space agencies and communities, especially regarding deep space and exoplanet science become increasingly necessary. Since obtaining in-situ data from exoplanets remains a far-fetched dream, an easier and cheaper way for is to indirectly characterize exoplanet environments through various measurable parameters, such as planetary mass, radius, orbital information, and atmospheric composition. These inferences are derived from detailed models constructed using direct measurable obtained from observations and missions to our own solar system bodies.

Research models of the solar system indicate that Venus likely formed from similar materials as Earth, including both refractory and volatile elements (e.g. [3]). Venus should possess a similar amount of internal heat to Earth, a planet characterized by intense volcanic activity and plate recycling. In fact, the mounting evidence of active volcanism on Venus supports this notion [4, 5].

The atmospheric D/H ratio of Venus indicates the substantial loss of water at some point in its history, e.g. [6–8]. Recent calculations suggest the potential persistence of oceans on

Venus for billions of years[9, 10]. The presence of microbes in Earth's clouds[11] compels us to reconsider the possibility that Venus' clouds may harbour life today[12–14]. Venus represents the most accessible example of an end-state for habitable Earth-sized planets, providing an opportunity to identify the mechanisms that collaborate to create and sustain worlds capable of supporting life, like our own. While every terrestrial planet offers valuable insights into these inquiries, Venus stands out among all the worlds in our solar system due to its size and proximity. This unique position enables us to manipulate and study certain factors that play a role in Earth's geological evolution, such as surface gravity, heat distribution, plate tectonics, and the potential existence of long-lasting oceans. Investigating Venus becomes essential in gaining a better understanding of how water is transported within the inner solar system. Furthermore, the detection of numerous exoplanets similar in size to Earth and Neptune adds a sense of urgency to launch new missions to Venus and the ice giants. The core of our Venus Mission study revolves around fundamental scientific knowledge, which we pursue by analysing measurement data gathered from Venus.

Several space exploration missions have ventured to this neighbour of ours in hope of knowing and understanding it better. However, numerous significant questions about Venus still remain, highlighting substantial gaps in our understanding of terrestrial planet evolution and habitability. Following are some of the questions that the space science community is still pursuing to find the answers to.

1. **Interior Structure and Composition:** A primary question revolves around the interior structure and bulk composition of Venus. Understanding its differences from Earth is vital for modelling exoplanetary interiors accurately.

2. **Venus's Habitability Period:** Did Venus once experience a habitable phase after its synaccretionary runaway greenhouse? (e.g. [9, 15]). The presence of temperate conditions within the cloud layers is also a possible subject of inquiry[13].

3. **Remnants of Ancient Crustal Materials:** Is there evidence of ancient crustal materials on Venus's surface, formed from silica-rich minerals[16]?

4. **Loss of Water:** Venus's water has largely vanished, but the exact mechanisms behind this loss—such as hydrogen escape, abiotic oxygen production, or surface hydration—are not yet fully understood.

5. **Tectonic Activity and Volcanism:** Exploring Venus's history of tectonic activity, deformations, volatile cycling, and volcanic resurfacing is essential for understanding its geology and evolution. The nature of volatiles delivery to the atmosphere also remains a major question.[17]

6. **Venusian Atmosphere:** Detailed information on the Venusian middle and deep atmosphere, including chemical reactions and interactions with the surface, is crucial for atmospheric modelling of terrestrial exoplanets.

It is evident that Venus has undergone a distinct history compared to Earth, making it the only accessible example of an end-state for habitable Earth-sized planets. Given the complex nature of Venus as a highly interactive system, the Venus Mission concept is uniquely equipped to conduct complementary scientific measurements, examining aspects such as the interior, surface, atmosphere, and ionosphere. Following the model of past Venus missions, this mission architecture relies on two collaborative systems to collect surface and atmospheric compositional

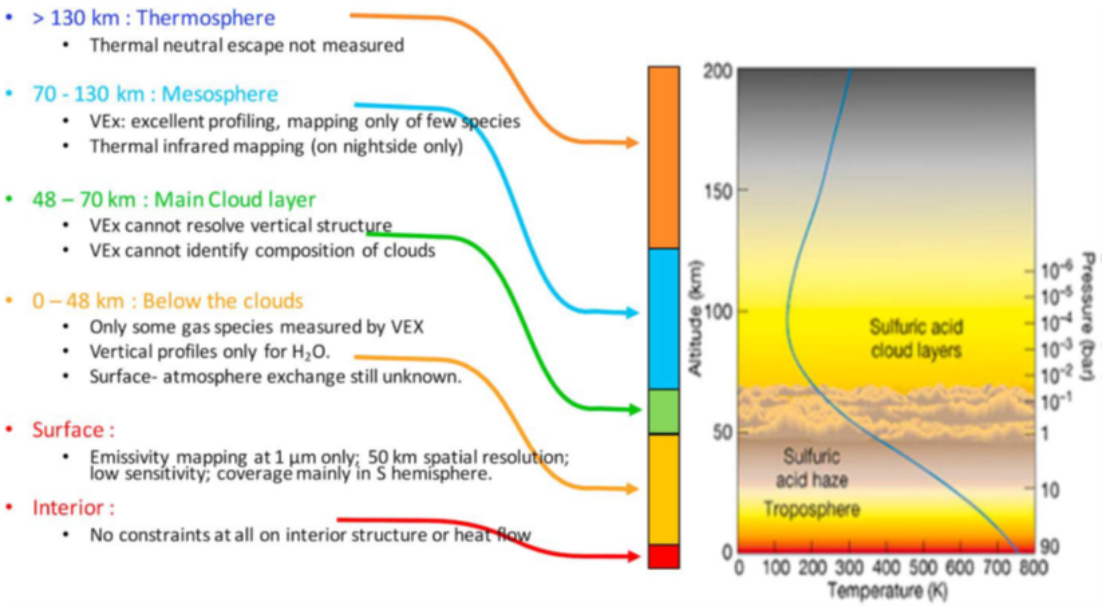

Figure 1.1: Illustration of a few standing questions regarding the Venusian atmosphere and surface.[8]

information, remotely monitor volcanic activity, investigate weather and climate patterns, study cloud formation and analyse other and lesser understood atmospheric phenomenon.

In this work, the design of a Venus Research Station floating within the Venusian atmosphere is presented, which is complemented by the design of deployable atmospheric Scouts. The design of these components is done on a conceptual basis. This means according to the European Cooperation for Space Standardization (ECSS)[18], that this work is mainly limited to Phase 0 (mission analysis/needs identification) of a mission and transitions a bit to Phase A (feasibility) towards the end.

Project Management

This Section presents the organization structure of the Venus Research Station (VRS) project. It is separated into two main parts the mission and system team. Each of them has underlying work packages that are dedicated to one topic regarding the concept design of the VRS. Every work package is assigned to a project member. According to the ECSS a work package is defined as:

'A WP can be any element of the WBS down to the lowest level that can be measured and managed for planning, monitoring, and control. Control work packages are identified by the supplier at the level in the WBS where visibility and control is required, and for which reporting is to be performed. The control work packages represent the total work-scope and are agreed by the customer. The work of each supplier is explicitly identified in the work breakdown structure by at least one control work package.'[18]

In this work a work package represents a specific research aspect for the design of the station on a conceptual basis. The work packages are split into two teams with selected team leaders for a more efficient structuring of the project. Above the team leaders are the project manager and

the deputy project manager. Figure 1.2 depicts the project tree including the project members and their delegated work packages.

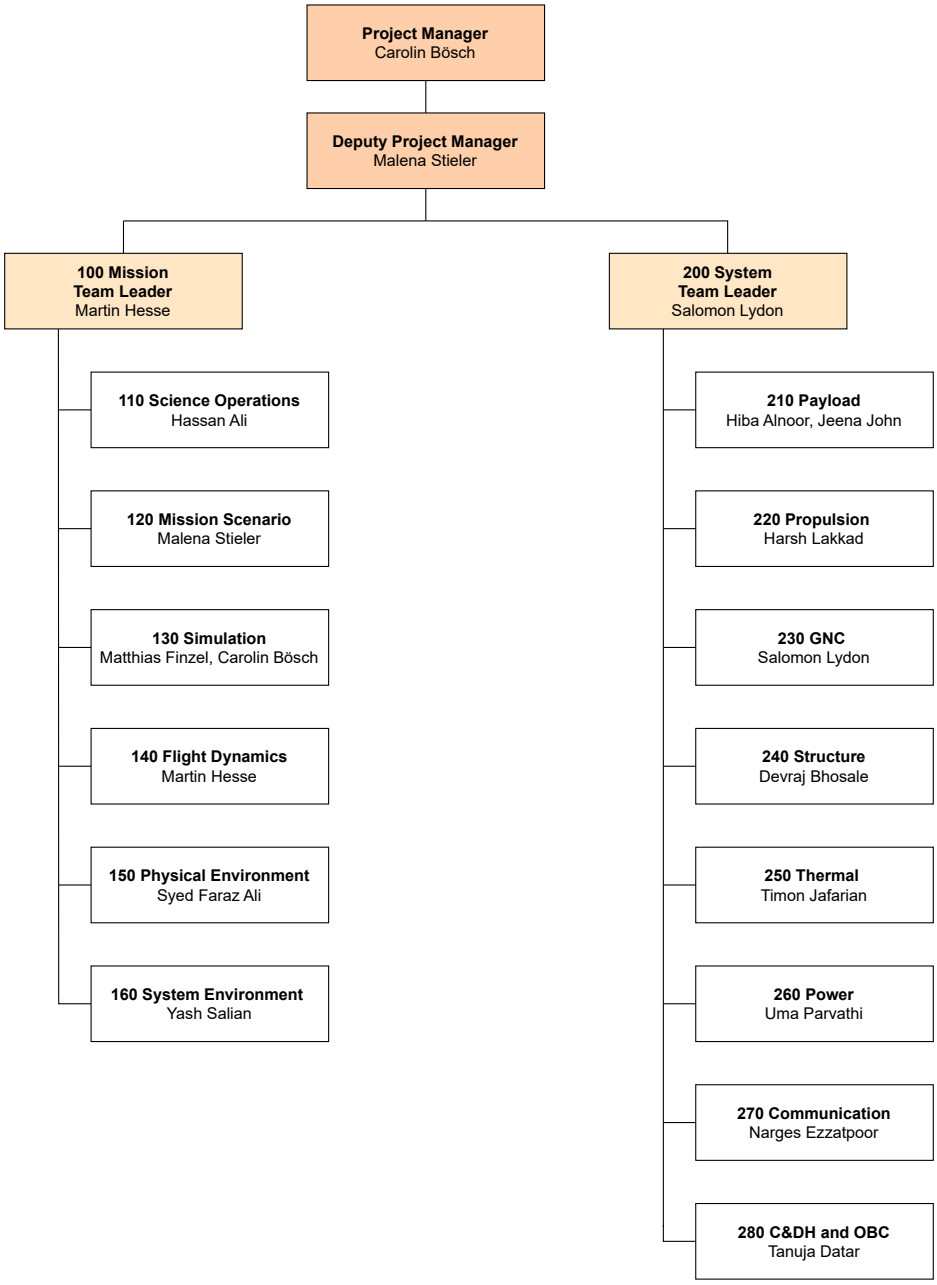

Figure 1.2: Project Organization Structure [Stieler].

The work packages within the mission team deal with mission planning and the surrounding elements of the Venus Research Station. Science Operation prepares the experiments to be performed to fulfil the objectives of the mission. The time schedule of the mission and Venus Research Station is planned by Mission Scenario. Simulation analyses and reviews the

interoperability of the VRS components and the performance in the Venus environment. The behaviour of the VRS operating in the Venus atmosphere and the deployment into it is covered by Flight Dynamics. Physical Environment focuses on environmental challenges and restriction the Venus Research Station has to cope. The mission parts and network beyond the VRS are described by System Environment.

The system team work packages are based on the subsystems a spacecraft typically has. They design the physical concept of the Venus Research Station. Payload is in charge of selecting and designing the instruments needed to fulfil the scientific objectives. Propulsion ensures the manoeuvrability of the station. Guidance, Navigation and Control (GNC) is responsible for stabilizing, tracking and directing the VRS. The model of the Venus Research Station is designed by the Structure work package and also the overall mechanical integrity is ensured. To outlast the extreme heat in the Venus atmosphere the Thermal work package is responsible for establishing a stable temperature inside the VRS. Power is planning the power generation, storing and supplying until the end of the mission. Communication is in charge of designing the reliable contact with the mission network and other components. Communication and Data Handling (C&DH) and On-Board Computer (OBC) work package defines the management of the Venus Research Station's activity by collecting, processing and forwarding of all information.

CHAPTER 2

The Physical Environment

by Syed Faraz Ali

The first and foremost step in designing such a mission is to know in detail and familiarise oneself with the environment in which the mission would be operating. Through this chapter, physical conditions of the planet Venus are elaborated on in order to help the reader paint a picture of the environment that the proposed Research Station would call home for its designated operational lifetime. This includes general and mission specific information on Venus' orbit, atmosphere and surface. Since mainly the domain of the atmosphere is pertained to for this mission and its design phase, the corresponding subsection on Venus' atmosphere (Section 2.2) is elucidated more. Besides a presentation of the overall description in this chapter, the challenges posed by the environment to designing such a mission are highlighted, the bounding parameters chosen while defining the mission objectives are justified and some scientific exploration and research gaps from previous missions are also explored. In addition to the in-text details, there are lengthy tables attached as appendix (Appendix A.1) at the end of this report that contain the values of several physical parameters measured by previous missions to Venus and analysed by researchers since the 1970s. Towards the end of this chapter, an understanding of Venus' physical environment, what makes it such an interesting space exploration site and the basis for this mission's scientific objectives and the mission scenarios, which will be discussed in further chapters, would have been gained by the reader.

2.1 Overview

Venus is often considered Earth's sister planet for its similarities in mass, size and composition and proximity. However, the exploration missions to Mars outnumbers those to Venus. This is majorly due to the planet‘s extreme environmental conditions. With surface temperatures going up to about 730 K, that can even melt lead, pressure almost ninety times that of Earth and a day lasting 234 Earth days, the reality of the planet named after the Goddess of Love is greatly ironical. Despite being in the Goldilocks‘ Zone of our solar system, Venus is highly inhospitable and very difficult to explore. However, it is believed that it was not always like this and that earlier at some point in its history, it contained vast oceans and could support life. This makes scientists more curious as to why Venus and Earth turned out to be so different in the course of time.

In the past, there have been more than 40 missions (including gravity assist flybys) to Venus, aimed at reaching our neighbouring planet, exploring it and understanding it better. F.W. Taylor et al. [8] list the past missions to Venus. Derived from that, Table 2.1 lists just the successful missions and a short remark on their findings.

Name	Country	Type	Launch/Arrival (DD.MM.YY)	Remarks
Mariner 2	USA	Flyby	27.08.62/14.12.62	IR and μ wave radiometers reveal hot surface
Venera 4	USSR	Lander	12.06.67/18.10.67	Atmospheric and magnetic data
Mariner 5	USA	Flyby	14.06.67/19.10.67	Particles and fields data
Venera 5	USSR	Probe	05.01.69/16.05.69	Confirmed high surface T,P
Venera 6	USSR	Probe	10.01.69/17.05.69	405 kg descent probe
Venera 7	USSR	Lander	17.08.1970	Returned data during descent and from
Venera 8	USSR	Lander	27.03.72/22.07.72	Returned data during descent and from surface.
Venera 7	USSR	Lander	17.08.1970	Returned data during descent and from surface.
Venera 8	USSR	Lander	27.03.72/22.07.72	Returned data during descent and from surface.
Mariner 10	USA	Flyby	04.11.73/05.02.74	Venus/Mercury—photos of Venus cloud patterns
Venera 9	USSR	Orbiter/Lander	08.06.75/22.08.75	First photo of surface; cloud structure
Venera 10	USSR	Orbiter/Lander	14.06.75/25.08.75	
Pioneer Venus 1	USA	Orbiter	20.05.78/04.12.78	Including IR radiometer
Pioneer Venus 2	USA	Probes	08.08.78/09.12.78	4 descent probes
Venera 11	USSR	Flyby/Lander	09.09.78/25.12.78	Reported observation of lightning & thunder
Venera 12	USSR	Flyby/Lander	14.09.78/21.12.78	As above
Venera 13	USSR	Flyby/Lander	30.10.81/01.03.82	First colour photo of surface
Venera 14	USSR	Flyby/Lander	04.11.81/05.03.82	Analysed basalt on surface
Venera 15	USSR	Orbiter	02.06.83/10.10.83	Radar mapping, IR observations of atmosphere
Venera 16	USSR	Orbiter	07.06.83/14.10.83	Radar mapping, IR observations of atmosphere
Vega 1	USSR	Lander/Balloon	15.12.84/11.06.85	Cloud-level balloon & nightside lander
Vega 2	USSR	Lander/Balloon	21.12.84/15.06.85	As above
Magellan	USA	Orbiter	04.05.89/10.08.90	Radar altimetry and imaging
Galileo	USA	Flyby	18.10.89/10.02.90	Jupiter orbiter (Venus Flyby)
Cassini	USA	Flyby	15.10.97/24.06.99	Saturn orbiter (Venus Flyby)
Venus Express	Europe	Orbiter	9.11.05/11.04.06	Polar orbit, apoapsis above South Pole
Mercury Messenger	USA	Flyby	03.08.05	Two Venus flybys: 24.10.06 & 06.06.07
Akatsuki	Japan	Orbiter	20.05.10/06.12.15	Equatorial orbit, focus on cloud tracking

Table 2.1: List of successful past missions to Venus with remarks on their aimed operation.

In order to understand the planet better, the following section shall delve into a detailed description of the Venusian environment. This information can be broadly classified as Atmospheric and Surface.

2.2 Atmosphere

Venus has a vast and dense atmosphere extending beyond 200 km from its surface. It is primarily composed of Carbon Dioxide (96%) and Nitrogen (3%), with trace amounts of Sulphur, Carbon and Hydrogen compounds, noble gases and water vapour. Moreover, there is a thick cloud layer between the altitude range of 45-65 km, composed of highly toxic sulphuric acid vapours. In between the cloud layers, there has been speculation of lightning, that has not yet optically been observed, but a number of other evidence certainly points to it. If confirmed, it could help scientists understand the atmospheric physics of Venus much better. Besides having a vast temperature, pressure and density profile, Venusian atmosphere is known for its extreme wind speeds that also give rise to its infamous 'super-rotation' phenomenon and its unique 'double-eyed' polar vortex.

Structure of the Atmosphere

Similar to the structure of the Earth's atmosphere, the Venusian atmosphere also has multiple layers, each with different characteristics. A comparison of the vertical temperature profile of Venus and Earth could also be drawn as the variation trends of atmospheric temperature with altitude are quite similar on both the planets, with the only major difference being the rise of temperature in the Earth's stratosphere due to absorption of UV radiation by the Ozone layer. This statement is however not meant to rule out the presence of Ozone in the Venus atmosphere. The Venus Express mission used the stellar occultation technique to detect the gas in the planet's atmosphere around the altitude of 90-120 km with a minimal concentration (about 1000 times less than that in Earth's stratosphere) that does not contribute a lot to the rise in temperature through UV absorption.

Since the atmosphere of any planet does not have defined boundaries, the consideration of altitude ranges to be categorised as part of a layer varies from researcher to researcher. In reality, the altitude range for a particular layer is of course not fixed as it varies slightly depending on various factors that might be local (wind speed and pattern), global (time of the day/position with respect to the Sun), or even cosmic (period of the Solar Cycle, changes in the space environment, etc.). F.W. Taylor, in his book 'The Scientific Exploration of Venus' [19] describes the mean vertical profile of the atmosphere in Figure 2.1 with different regions marked analogous to that in the Earth's atmosphere.

These regions of the atmosphere are defined by taking into account the major physical phenomenon occurring in the atmosphere at different altitudes – cloud properties, wind circulation, temperature variation, concentration of charged particles, etc. Hence, a better approach of describing the structure of the atmosphere would be to understand these various phenomena.

Clouds

The cloud cover in the Venusian atmosphere plays a pivotal role in its atmospheric dynamics and climate. The composition and thickness of the clouds dictate and influence the other physical parameters such as temperature distribution, wind patterns, etc. so greatly that the characteristics are defined based on the location of above, in between or below the cloud layer.

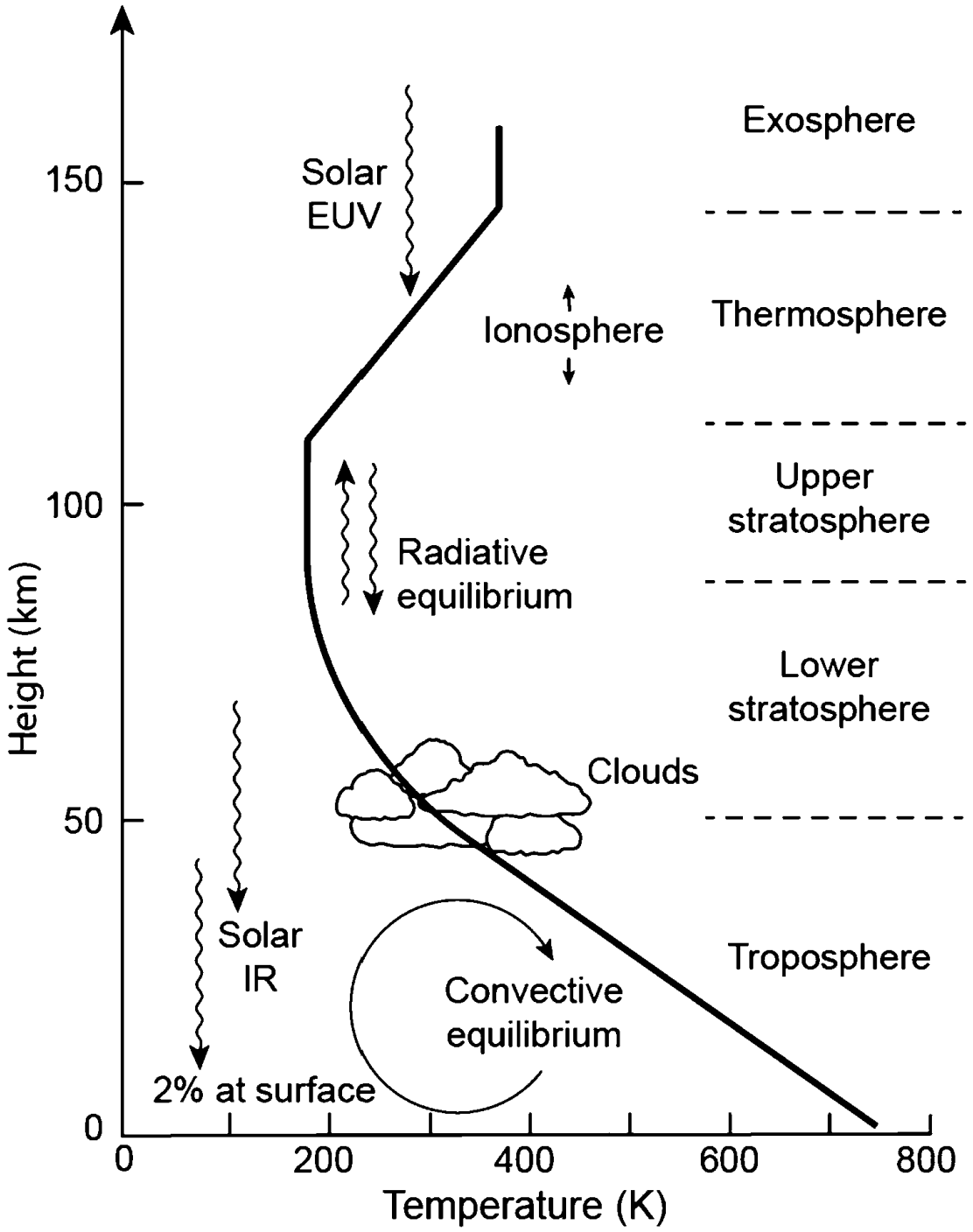

Figure 2.1: A diagram of vertical profile of the mean standard atmosphere of Venus indicating the major temperature balance processes with approximate locations of the cloud layers. [19]

The information gathered from several space missions, including Venera, Pioneer Venus, Vega, and Venus Express, has provided valuable insights into the vertical structure of Venus‘ clouds. These missions have utilized various entry probes, spectrometers, and imagers to explore the composition and distribution of aerosols within Venus‘ atmosphere.

The cloud layer is so thick that it could further be categorised as Upper, Middle and Lower layers, each with their own characteristics that are discussed further:

Upper Cloud Region (56.5-70 km) The upper cloud region of Venus is a crucial layer where photochemical reactions produce sulfuric acid from SO_2 and H_2O. Information from the Pioneer Venus Large Probe, Vega-1, and Vega-2 LSA aerosol particle size spectrometers has revealed a sharp increase in cloud extinction just below 50 km, suggesting an optically thick layer at 47-50 km. However, the presence of this feature varies among different descent probes, indicating strong variability in the deep cloud structure.

Furthermore, discrete cloud layers have been observed near 46 km and 43 km altitudes, distinct from the lower cloud. The Pioneer Venus Large Probe and Vega ISAV UV spectrometer have provided evidence for additional hazes extending down to 30 km altitude. Interestingly, these layers exist at altitudes below where liquid sulfuric acid would be expected to be in equilibrium, adding complexity to the understanding of the atmospheric composition.

Observations from VIRTIS, VeRa, VMC, and SPICAV-SOIR instruments on Venus Express have significantly advanced our knowledge of the upper haze. The mesosphere, located from the cloud top (around 70 km) to approximately 110 km, consists mainly of sulfuric acid particles. The haze has been probed through various techniques, such as polarimetry, limb scans, and spectroscopy, revealing a continuous distribution of aerosols.

The aerosol scale height in the upper haze region varies with latitude, indicating strong spatial variability. At high polar latitudes ($> 80°$ N), the scale height is larger, suggesting a complex aerosol distribution in these regions. Additionally, the upper haze exhibits considerable short and long-term variability, influencing the chemistry and radiative balance of the mesosphere.

Cloud Top Region The cloud top region of Venus is another critical layer that plays a significant role in the planet‘s atmospheric dynamics. Observations from VIRTIS and SPICAV instruments onboard Venus Express have enabled detailed characterization of the cloud top altitude and its variability. The cloud top altitude at 1.5 μm is approximately 72 ± 1 km in low and middle latitudes, decreasing poleward to 61–67 km in the polar regions.

UV markings, characterized by bright and dark mesoscale features, have been correlated with the cloud top altimetry maps, indicating a complex interaction between cloud top altitude and atmospheric dynamics. In the polar regions, the cloud top altitude decreases sharply, forming a lip into the polar region.

The cloud top sharpness, characterized by the aerosol scale height, also exhibits a latitude-dependent behavior. In low and middle latitudes, the upper cloud is more diffuse, while it becomes considerably sharper in the ‘cold collar’ and polar regions. The aerosol scale height in the cloud top region varies with altitude in the mesosphere, and its latitudinal trend further contributes to the complexity of the cloud structure.

Middle and Lower Cloud Region (47.5-56.5 km) The middle and lower cloud regions of Venus have been explored by the Soviet Vega missions in 1985. The aerosol properties measured by ISAV-A particle size spectrometer and nephelometer on Vega descent probes confirmed earlier findings but also revealed some differences. Two modes of aerosol particle distribution were identified, with mode 2 particles ($r = 1 - 2.5\,\mu$m) being significantly less numerous compared to mode 1 particles ($r = 0.25 - 2.5\,\mu$m).

Evidence of dense sub-cloud haze was observed in some regions, suggesting the presence of a haze layer down to approximately 35 km, especially during nighttime landings. However, some measurements from other missions did not fully support this finding, indicating the need for further investigation into the lower haze properties.

Indirect evidence for the cloud base altitude descending towards the poles has been derived from radio occultation experiments, indicating a presence of dense clouds down to approximately 45 km in the polar regions. Additionally, observations of the near-IR emissions have indicated greater total cloud opacity in the polar regions, supporting the idea of a more substantial cloud presence in these areas.

The vertical structure of Venus‘ clouds is a complex and dynamic system that exhibits significant variability with altitude and latitude. Information from Venera, Pioneer Venus, Vega, and Venus Express missions has shed light on the composition and distribution of aerosols within Venus‘ atmosphere.

The upper cloud region, with its photochemical processes and aerosol variability, is a critical area for understanding the planet‘s atmospheric dynamics and climate. The cloud top region‘s sharpness and altitude variations contribute to the complexity of Venus‘ atmospheric circulation. The middle and lower cloud region also contains intriguing features that require further investigation.

Solar Intensity and Temperature Balance

Venus, being closer to the Sun receives more solar energy than Earth with incoming solar irradiance at the top of the atmosphere being 2601 W/m^2, almost twice as much as Earth‘s 1358 W/m^2. However, it has been observed that the solar radiation reaching the surface is less than one percent of that value, being just about 25 W/m^2. This is due to the fact that Venus houses a very thick cloud layer, mainly situated in the middle atmospheric layer, that reflects most of this incoming radiation and emits thermal radiation back out to space. This high planetary albedo is one of the major reasons that make it so bright in the night sky. One would then wonder how the planet‘s surface experiences extreme temperatures. This can be explained by inferring from other physical conditions of the planet that the high surface temperature is primarily caused by the high atmospheric pressure and the greenhouse effect, rather than the net solar flux of the planet.

The solar intensity at a given location depends on the solar zenith angle, which changes very slowly due to the planet‘s long sidereal day period. Using NASA‘s Venus-GRAM software Section 16.2, values of solar zenith angle across the globe were derived by the simulation team and validated against the values from existing research. Schuler et al. [20] plot the different sources of atmospheric radiation as a function of SZA that changes with latitude. Two of those plots that help us understand the solar intensity variation on Venus are shown in Figure 2.2 and 2.3. It can be noted that the net solar flux increases from the poles towards the equator (which naturally faces the Sun direct) and with altitude. Whereas, the net thermal flux is highest near the surface and decreases with altitude as the IR radiation depends on surface temperature and emissivity due to the diffusion and reflection of radiation by the atmosphere that almost doubles the effect of direct radiation at all zenith angles.

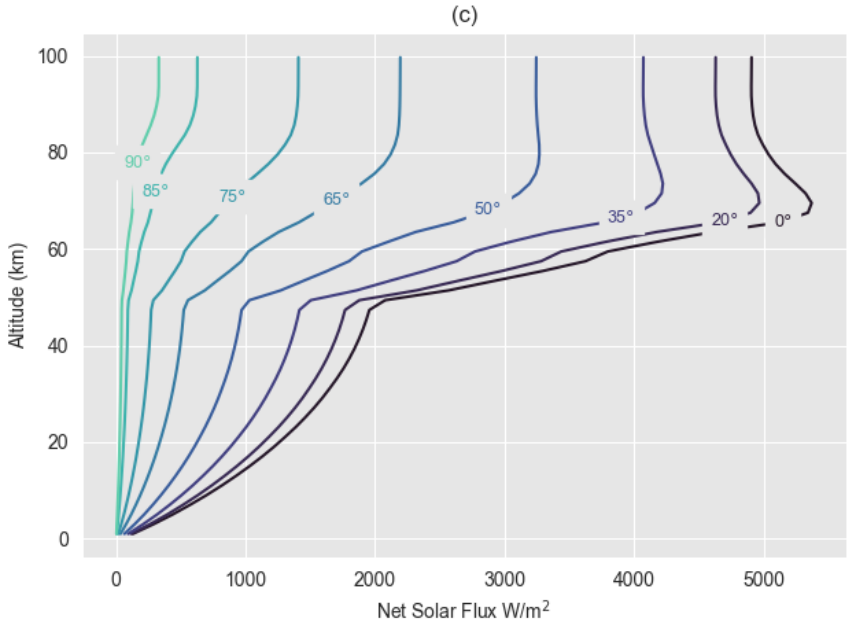

Figure 2.2: Net Solar Flux in the Venusian atmosphere as a function of solar zenith angle for different altitudes. [20]

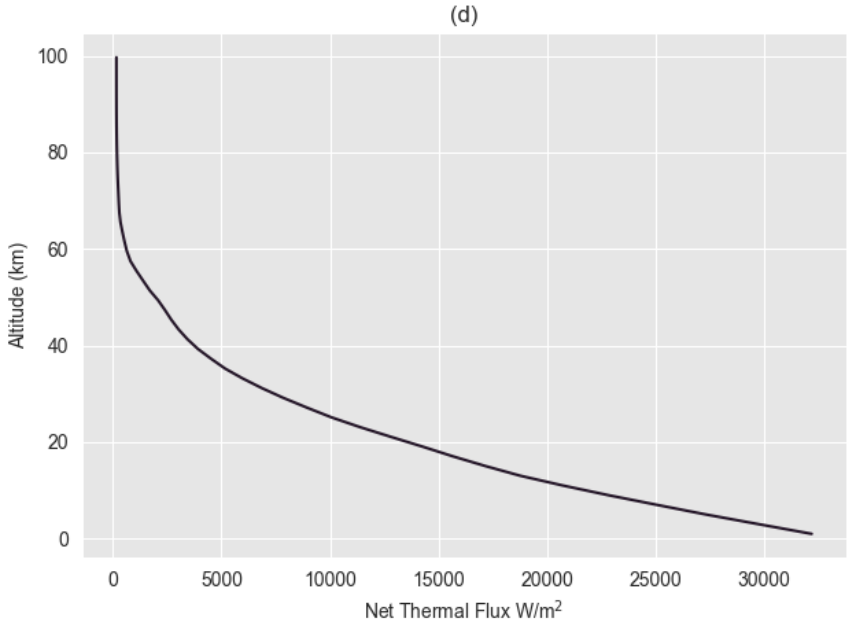

Figure 2.3: Thermal Flux in the Venusian atmosphere as a function of solar zenith angle for different altitudes. [20]

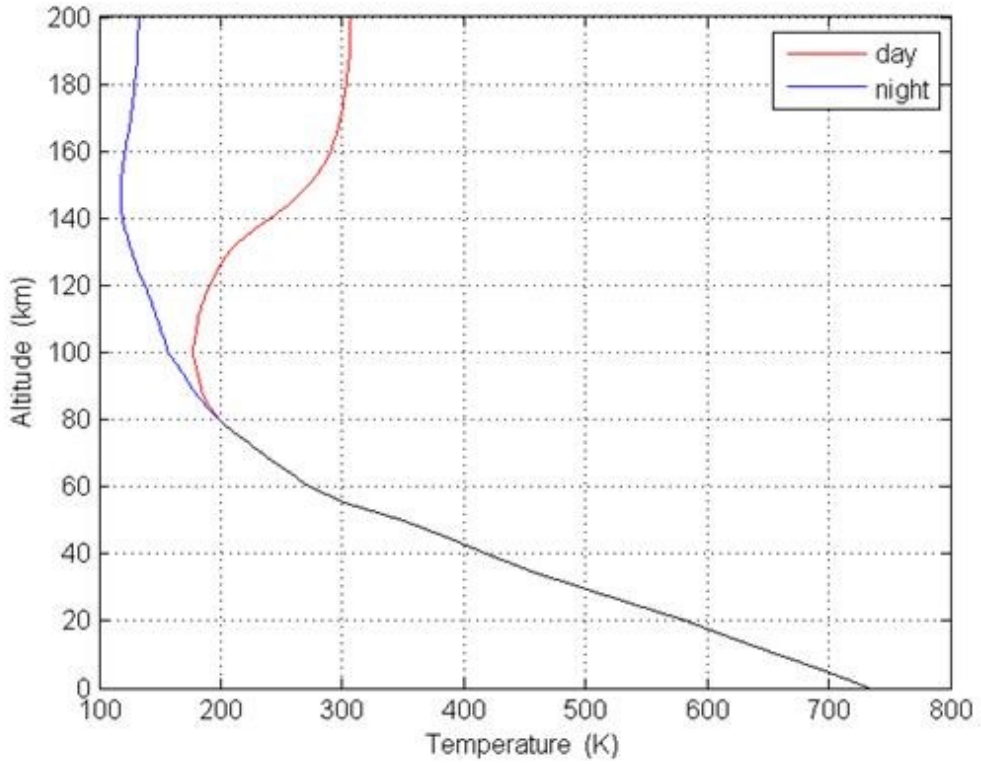

Figure 2.4: Diurnal variation of temperature in the Venusian atmosphere from VIRA model. [22]

Furthermore, it is interesting to note that at approximately 55-60 km altitude, most physical parameters on the Venusian atmosphere experience a significant change. The solar and thermal flux suddenly start increasing and decreasing respectively at around this altitude. This is also a result of the thick middle cloud layer. As a consequence, the diurnal variations of temperature occur significantly only above this layer and is negligible below it. This could also be corroborated from the VIRA (Venus International Reference Model) model of Venusian atmosphere developed by the Belgian Institute for Space Aeronomy (BISA), as shown in Figure 2.4, and from the research by Pätzold et al. [21], as shown in Figure 2.5. Between the range of 55-60 km, only a very slight difference is observed in the day and night temperature near the tropical region since it receives the highest direct solar radiation.

Colozza et al. [23] in their feasibility study of a solar powered flying station in Venus‘ atmosphere also develop equations to relate the solar attenuation with altitude, which is the ratio of solar intensity at a selected altitude to that above the atmosphere for a wavelength of $0.72\,\mu$m that falls around the middle of the spectrum. The resulting graph from these equations is shown in Figure 2.6. Above 65 km of altitude, there is practically no considerable attenuation. The table of physical parameters of the mean standard atmosphere of Venus Appendix A.1 is borrowed from the same study as well.

The distribution of particles such as aerosols and UV absorbers and the cloud structure also play a major role in defining the temperature variation and balance on the planet. The

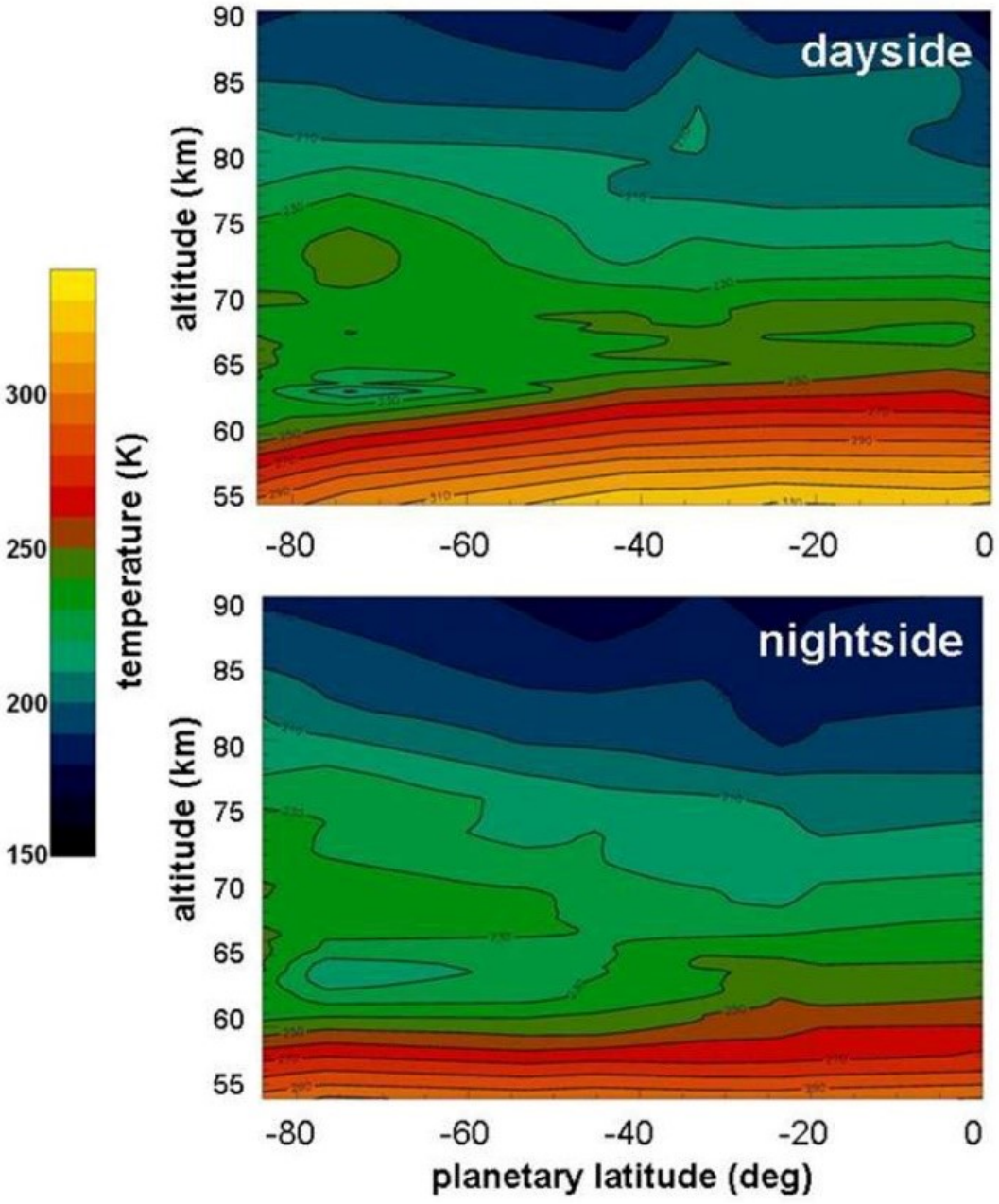

Figure 2.5: Day and Nightside temperature contour maps derived from VeRa radio occultation data. [21]

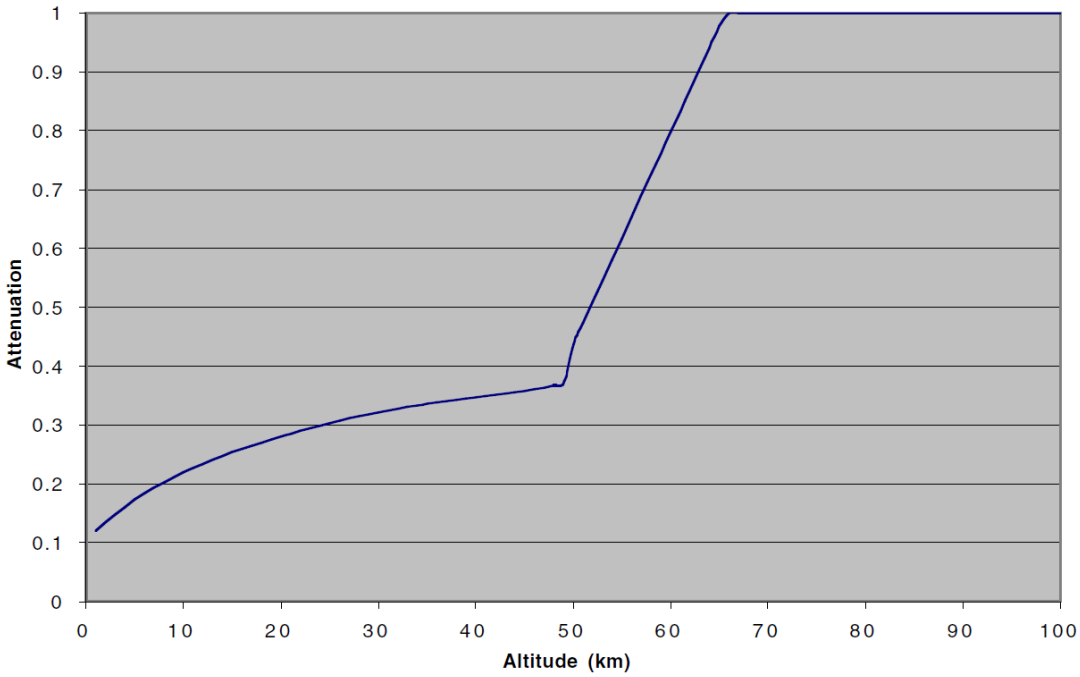

Figure 2.6: Attenuation of atmospheric solar intensity attenuation as a function of altitude at 720 nm wavelength. [23]

primary reflection of solar energy back to space through thermal emission happen from the cloud top region with the range of wavelength of the radiation being 10-50 μm [24]. Presence of an unknown mysterious UV-absorber has been confirmed by several researchers. This absorber is believed to be confined to the upper cloud layers at around the altitudes of 57-65 km, as suggested by Ekonomov et al. [25]. Since its absorption band is in the UV-blue range, in which the intensity of solar radiation is the highest, it absorbs almost half of the radiation energy that Venus receives from the Sun in the layers of upper cloud and beyond.

Schofield and Taylor [26] in their calculation on the thermal balance of the planet conclude that the cloud top temperature is in agreement with the net solar flux with a bolometric albedo of 0.762. It has also been observed that the outgoing thermal flux depends on factors such as the aerosol distribution and the temperature gradient. In fact, it also varies with latitude since studies by Zasova et al. and Lee et al. [27, 28], combined and compared by Titiov et al. [24] show that the aerosol and cloud scale heights decrease towards the poles (from about $\pm 50°$) and effect in a significant cooling peak rate at the cloud top near the poles. This gives rise to a 'cold collar' feature surrounding both the poles from around $\pm 75°$ latitude, while at the pole there is a warmer polar dipole feature, which is explained in the Winds section. Of course, the terms 'cold' and 'warm' here are relative and mean less or more than 200 K and 250 K respectively as the global mean temperature of this region lies between these two temperatures.

Below the clouds till the surface, the temperature of the atmosphere is directed by convection currents. There are spectral transparency 'windows' of near-IR band (0.6-2.5 μm), from which leaking of thermal radiation from the hot troposphere and surface has been observed. However, these emissions are quite weak in escaping the thick clouds and hence contribute little to the global radiative energy balance.

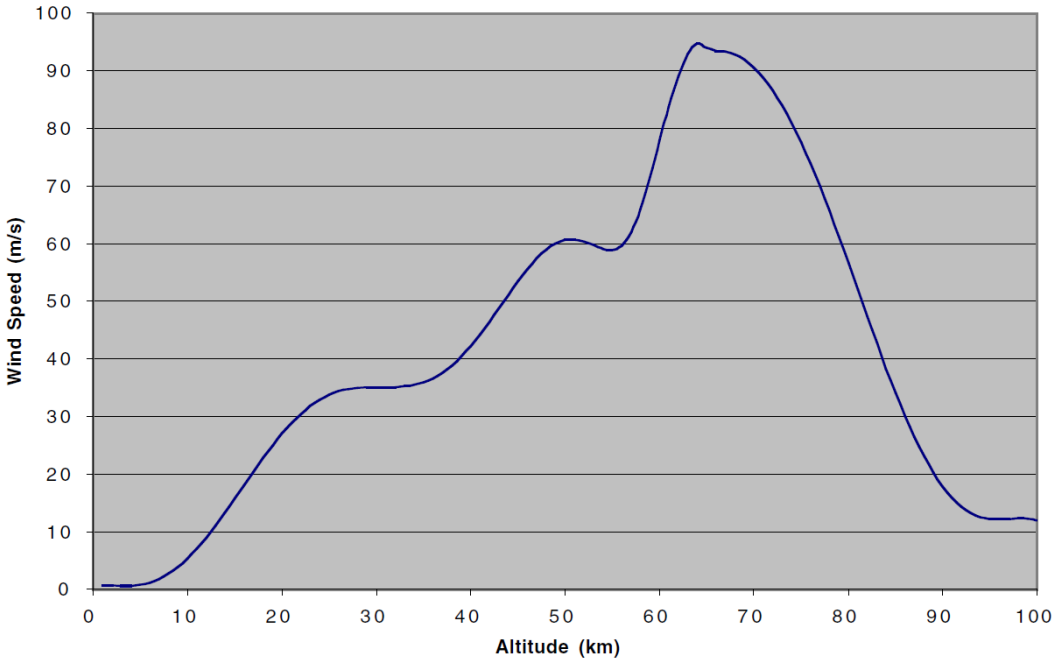

Figure 2.7: Variation of average wind speeds with the altitude. [23]

Winds

Venus has a fascinating atmospheric circulation phenomenon that makes it unique among other celestial bodies with an atmosphere. A glance at the values of wind speed for different altitudes in the Appendix A.1 and at Figure 2.7 from [23] would provide an outlook on how atmosphere behaves at different altitudes and can act as an extremity at certain locations. The research conducted by Sánchez-Lavega et al. [29] explains Venus‘ peculiar atmospheric dynamics very well.

Figure 2.8 from [30] shows the general circulation pattern of the planet‘s atmosphere. The three major features that govern the circulation are – Super Rotation; Hadley Circulation; and Polar Vortices. These features will now be discussed further.

Super-Rotation One of the most intriguing aspects of Venus‘ atmosphere is the phenomena of super-rotation. As the name suggests, super high speed winds circle around the globe parallel to the equator in the same retrograde direction (East to West) as the planet‘s rotation, but about 50 times faster. This corresponds to wind speeds of over 100 m/s, which means that the wind can travel around the whole planet in just four to five days (not Venusian days). This phenomenon is unlike anything found on Earth or other planets in our solar system. The origin of this super-rotation is not completely understood. Previous analyses suggest that unlike the usual momentum transfer from the solid planet‘s rotation (which is rather super slow in the case of Venus) to the atmosphere through friction and waves, these extremely high velocity winds are primarily a result of the solar tides and the temperature (and thus pressure) gradients in the relatively thin upper cloud and haze layers. Due to this, the super-rotation phenomenon is restricted to the aforementioned region. The wind decelerates steeply above the clouds, while the air density (and hence the drag) increases a lot below the clouds in the lower atmosphere,

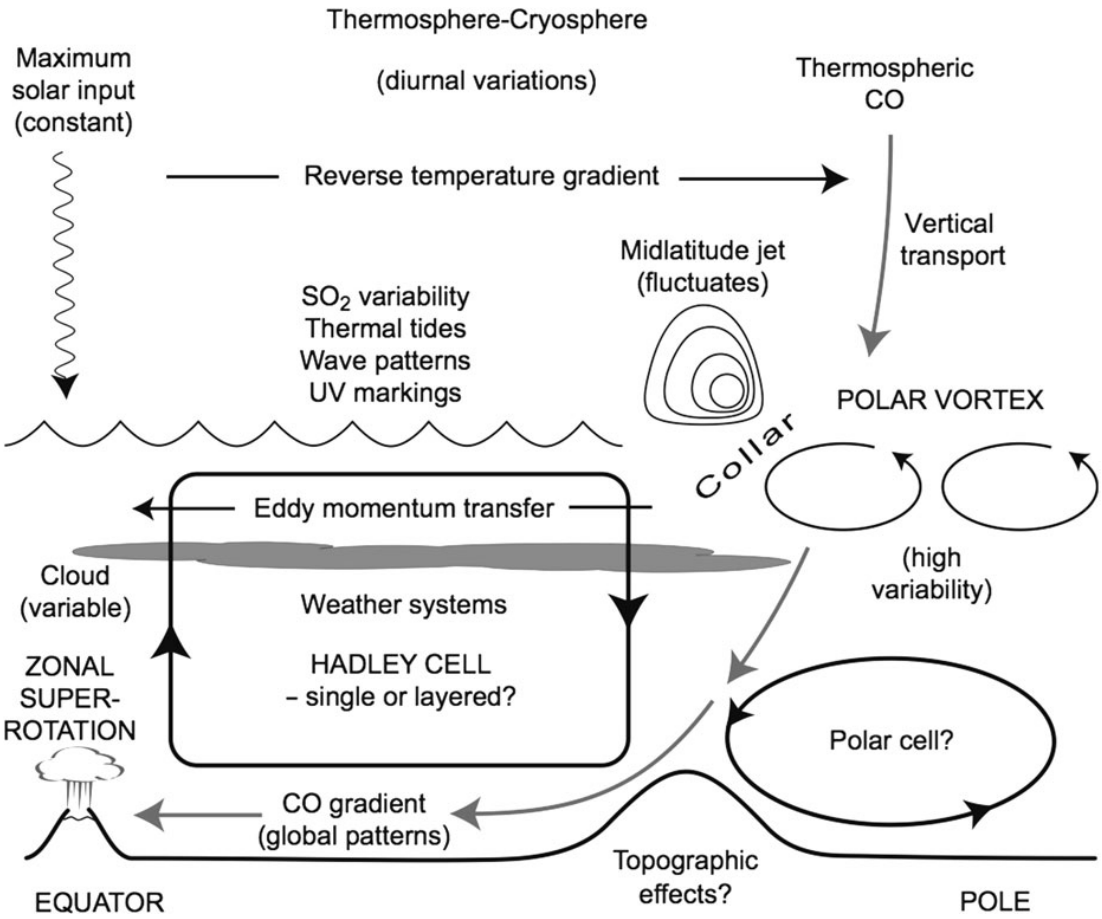

Figure 2.8: Diagram depicting the main features of atmospheric circulation. [30]

making the wind speed drop down to almost zero in both the regions.

Hadley Circulation This type of circulation is a common feature found in the atmospheres of other planets, including Earth. It involves the gradual overturning of the atmosphere between the tropical and high latitudes in the meridional direction. This kind of circulation plays a crucial role in redistributing the energy and heat within the atmosphere, influencing the weather and climate patterns. At approximately 65° latitude, the Hadley cell terminates with a critical transition in to the polar regime. Here, the strongest winds form a small midlatitude jet, and produces a circumpolar 'cold collar' that was introduced before.

Polar Vortex Venus' polar vortices are another riveting characteristic of its atmospheric circulation. All terrestrial planets with an atmosphere have polar vortices generally due to the sinking of cold and dense air at the high latitudes and the meridional flow. The small obliquity of the planet and super-rotation of winds produces an extreme version of vortices that occupy more than a third of each hemisphere by latitude. But what is unique about the polar vortices of Venus is the eye of the vortex, or rather, the 'two eyes' of each vortex, caused by a wavelike instability. The rotation rates of the polar vortices differ from what might be expected

if angular momentum were merely being conserved. This discrepancy has led to the suggestion that a double vortex, known as the 'polar dipole', may be more efficient in transporting angular momentum from the super-rotating equatorial regions downwards.

2.3 Surface

Venus has a mean density similar to Earth and Mercury, indicating a compacted core. The absence of a planetary magnetic field does indeed suggest against a liquid core, but the near resonance between Venus' spin and Earth's orbit suggests past frictional damping of a liquid core. Basaltic rocks found at landing sites of past missions indicate volcanic activity in the planet's history. An understanding of the Venusian surface features has been gained from studies by Taylor et al. and Smith et al. [8, 31] and attempted to be explained in this section.

Venus' surface appears flat compared to other planets, with 90% within a 3 km height interval. However, its surface is covered in various types of topographical features such as – Mountains; Volcanoes, Highlands, Lowlands, Craters, etc. Higher-resolution radar imaging and extensive coverage provided by the Venera 15 and 16 missions revealed Earth-like features on Venus, despite the fundamental difference in hypsometry. A global geological map of Venus developed by Ivanov et al. [17] is shown in Figure 2.9.

Highlands Elevated regions with varying topography and often characterized by mountainous terrain. They consist of ancient, highly deformed terrain called tesserae, with similarities to the earth's ocean floor. The highlands are relatively smaller in area compared to the plains. Highlands make up less than 8% and occur in three areas: Ishtar Terra, Aphrodite Terra, and Beta Regio. The highest mountain range on Venus and also the brightest on the radar, located in Ishtar Terra, is Maxwell Montes that rises approximately 11.1 km above the average planetary surface, making it one of the tallest mountains in the solar system. Whereas, the lowest point, Diana Chasma, is 2 km below the mean surface level. Gravity anomalies on the planet correlate with topography, with exceptions like Ishtar Terra not showing a corresponding anomaly. Linear features are interpreted as local or regional tectonic activity. Beta Regio is considered one of the youngest volcanic regions.

Lowlands Lowlands, such as Atalanta Planitia, are extensive basins, potentially representing basaltic lava flows. Tectonic features like ridge-and-trough systems and scarps are associated with various regions, indicating possible local or regional tectonic activity.

Volcanoes Venus is home to a vast and diverse volcanic landscape, indicating significant volcanic activity in its past. The planet's surface is dotted with various volcanic features, including large shield volcanoes, volcanic domes, and extensive lava plains.

- Shield Volcanoes: Shield volcanoes are widespread on Venus and are characterized by broad, low-profile structures with gentle slopes. One of the most prominent shield volcanoes is Maat Mons, which stands as one of the largest volcanoes in the solar system. These volcanoes were likely formed by the eruption of low-viscosity lava that spread out over large areas, contributing to the planet's smooth and flat surface.
- Volcanic Domes: These are small, steep-sided structures formed by the slow extrusion of highly viscous lava. Volcanic domes on Venus can be relatively young compared to other volcanic features, indicating that volcanic activity might still be ongoing in some areas.
- Lava Plains: The rolling plains on Venus, which constitute a significant portion of its surface, are believed to be vast lava plains resulting from massive volcanic eruptions. These

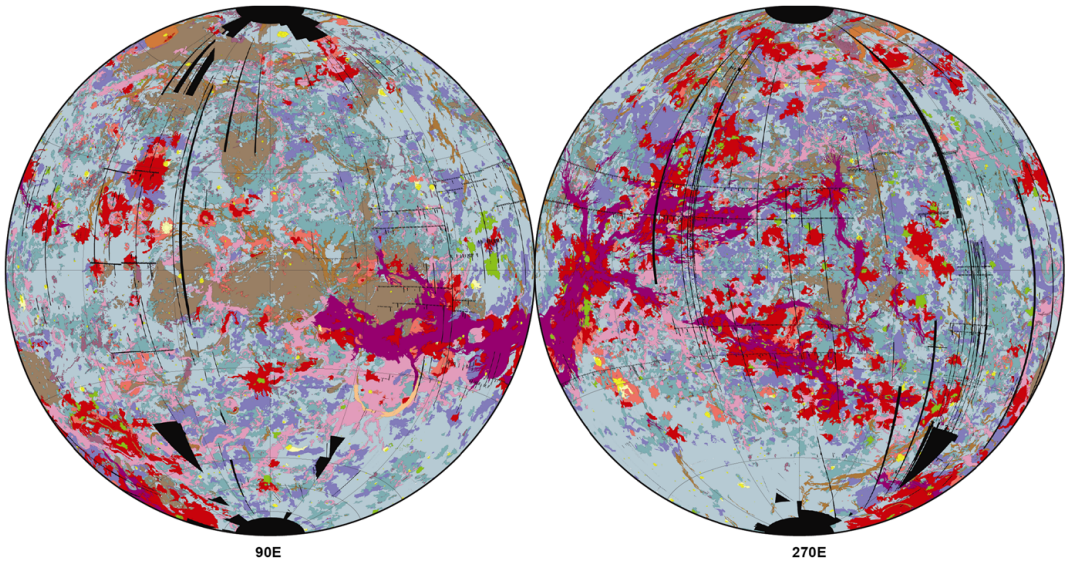

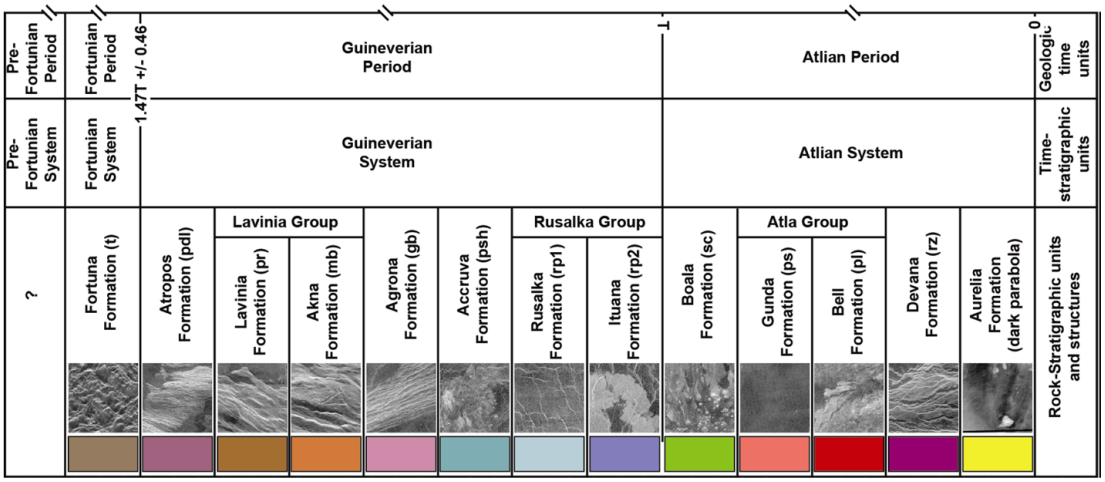

Figure 2.9: The global geological map of Venus compiled by F.W. Taylor et al. [8]

plains are thought to have erupted from extensive volcanic centres, contributing to the planet‘s relatively flat topography.

Craters Venus has a relatively young surface with limited cratering compared to other bodies in the solar system. The presence and distribution of craters provide insights into the planet‘s geological activity and surface history. Craters on Venus are relatively young based on crater statistics, suggesting ongoing geological activity. In situ observations by Venera landers show a rocky desert-like terrain with extreme weathering due to high temperatures, corrosion, and aeolian processes.

2.4 Conclusion

Venus stands as a unique celestial body with several fascinating features in its environment that pose all kinds of challenges for a mission aiming to study it better. Functioning in the extreme conditions that this seemingly beautiful planet present at a spacecraft is particularly difficult since different physical parameters tend to go to extremities while traversing from up the atmosphere down to the surface. Survival of a lander with scientific instruments on the surface is still an incredible challenge and hence mission designers are keen on conducting the science remotely from somewhere in the atmosphere. This mission aims to present a concept of a research station situated in Venus's vast and dense atmosphere. For a floating station to have mobility in its floating medium, it must have enough propulsive power to move faster than the movement of the medium itself. Thus, in order to move faster than the air on Venus, an appropriate region would be near the surface (to about 15 km) where the wind speeds are quite slow. However, near the surface, besides the extremely high pressure and temperature, the issue of power generation (considering solar arrays) could be faced as only minimal solar intensity is reachable in the lower layers of the atmosphere and on the surface.

In the region of upper atmosphere (beyond 100 km), the wind speeds drop down almost completely and enough solar energy is also available. However, keeping the station afloat and warm in that negligibly dense and cold environment would be a challenge. Moreover, the instruments aboard might face the problem of sensing through the particularly thick Venusian clouds and the operation from this altitude would practically be similar to operating from the orbit.

The middle atmosphere/cloud layers (45− 65 km) seem to be the most comparable to the standard conditions on Earth with comparable temperature, pressure and density. Sufficient solar radiation enables good amount of power generation in this range. The wind speeds are indeed quite high. But from the wind pattern, it can be observed that in these altitudes, it flows in a uniform retrograde direction between the latitude range of 55° N and 55° S. This could be used by a floating to its advantage by moving with the atmosphere, rather than moving through it. An additional propulsion system could aid with maneuverability and handling any gust speeds. Beyond this latitude range, the cold collar and the polar vortices could prove fatal to the station.

CHAPTER 3

Mission

by Carolin Bösch[1]

This Chapter gives an overview of the whole mission. First, the mission statement is defined, followed by the mission objectives. Then the requirements are stated, starting with the user requirements and leading up to the functional requirements. Finally, the boundary conditions are established. In this Chapter the objectives and requirements regarding the scientific questions and payload will not be further elaborated. This is done in the following Chapter, refer to Chapter 4.

3.1 Mission Statement

The mission statement (MS) sums up the mission‘s ultimate goal and purpose. It also serves to motivate contributors to achieve the mission‘s goal and convince investors of the mission‘s future. This mission‘s statement is given below.

Venus is not yet explored as much as Mars or Moon. This will probably change in the next 30 years. To support future research of Venus, a long term station within Venus atmosphere is to be established in this timeframe. The station will support future human presence in or around Venus as well.

3.2 Mission Objectives

The mission objectives elaborate on the ultimate goal stated in the mission statement. They are divided into scientific (SO) and technological objectives (TO). Table 3.1 lists all objectives of this mission.

SO5 and its derived requirements will not be pursued further in this work because it has been exported to another work. The technological objectives derive from the goal of a long term station, more accurately defined by TO3 as five years, and the support of future human presence. To ensure the future presence of humans, potential energy sources and resources including their on-site exploitation must be explored.

[1] established by entire team, written by Carolin Bösch

Nr.	Definition	Source
	Scientific Objectives	
SO1	Mapping of Venus‘ surface and gathering of compositional information of the planet	MS
SO2	Probing Venus‘ atmosphere at different altitudes for composition determination	MS
SO3	Accumulation of information about the climate and weather on Venus	MS
SO4	Investigation of effects of Venus‘ magnetic field and radiation in the atmosphere	MS
SO5	Search for life forms in Venus‘ clouds	MS
	Technological Objectives	
TO1	Investigation of feasibility and scalability of in-situ resource utilization	MS
TO2	Gaining information about possible energy sources	MS
TO3	Operation of the Venus Research Station for at least five Earth years	MS

Table 3.1: Mission Objectives.

3.3 Requirements

To ensure mission objectives are met, design (or product) requirements are established. Each requirement is usually assigned to a requirement category and given a corresponding numbering and description. The requirements of this mission are divided into four categories. It is also assigned the number(s) of its higher level requirement(s) as a source for requirement traceability. The requirement traceability allows showing the coherent flow of requirements[32]. The significance of a requirement is determined by specified phrasing rules. For this mission the phrasing of requirements follows the following rules.

- **‘Shall’** requirements are mission critical, i.e. the mission can not proceed without meeting these requirements.
- Requirements defined with **‘should’** must be fulfilled as long as they do not interfere with ‘shall’ requirements.
- Requirements with the lowest significance of being met (optional requirements) are defined with **‘may’**. They can improve the Venus Research Stations‘ (VRS) performance, but they are not necessary for mission success.

User Requirements

The user requirements (UR) are the top-level requirements set by the end user. Since there is no end user in this work, the work package science operations set up these requirements. They define the mission objectives more precisely, e.g. by physical parameters or regions of interest. Table 3.2 lists the user requirements of this mission. For further explanations refer to Chapter 4.

Comments The surface region of interest covers the entire planet (global coverage), whereas the region of interest within the atmosphere has been defined as 0 km to 130 km altitude. Harmful radiation in UR05 is defined as harmful to humans with ionizing properties (X-rays: wavelengths

Nr.	Definition	Source
UR01	The Research Station shall map Venus‘ topography with moderate resolution (5 m - 30 m) and geology with at least 10 cm penetration into surface.	SO1, TO1
UR02	The Research Station should map Venus with global coverage.	SO1, UR01
UR03	The Research Station shall investigate the atmosphere regarding presence and concentration of gases from 130 km to 0 km altitude at multiple different points around Venus.	SO2, SO3, TO1
UR04	The Research Station shall measure temperatures, wind speeds, and pressure from 130 km to 0 km altitude under day and night conditions.	SO3
UR05	The Research Station shall measure the magnetic field, as well as harmful radiation and electrical activity at operational altitude.	MS, SO4, TO1, TO2
UR06	The Research Station shall detect biosignatures in Venus‘ atmosphere.	SO5
UR07	The Research Station may incorporate technologically viable, but also sustainable solutions.	MS
UR08	All generated data should be sent back to earth.	MS
UR09	The Research Station should provide information regarding the solar intensity under different conditions.	TO1, TO2

Table 3.2: User Requirements.

between 0.01 - 10 nanometres), or harmful to the VRS (gamma rays: wavelengths less than 0.01 nanometres)[33]. UR06 derives from SO5 and is therefore not in detail pursued within this work. However to meet UR06, the following assumptions were made for the integration of the experiment as part of the VRS: mass of 5 kg, Power consumption of 10 W and a data generation rate of 100 kbits/s. This may involve one or more components. In regard of future human presence unnecessary pollution is to be avoided of Venus as stated by UR07. Since no other mission has taken place within the atmosphere of Venus for a longer period of time yet, the VRS shall send all data it generates back to earth as stated by UR08. This enables the complete monitoring of the VRS status over the mission to investigate the feasibility of such a mission and of course allows all generated scientific data to be evaluated. This work considers solar radiation to be an in-situ resource/energy source that is relevant to the maintenance of the VRS over its five-year lifetime (UR09). Further it might be exploitable for future human presence.

Mission Requirements

The mission requirements (MR) are in general describe the requirements for the entire mission, including which equipment and functionalities are needed to achieve the user requirements. These can be established jointly by all parties. Table 3.3 lists the operational requirements of this mission.

Comments MR02 ensures the mapping of Venus with a certain resolution, uniform atmospheric conditions and therefore also a uniform power generation for the VRS. To ensure the achievement

Nr.	Definition	Source
MR01	The mission shall start in the next 25 years.	MS
MR02	The Research Station shall operate within a fixed altitude range.	UR01
MR03	The Research Station shall be manoeuvrable at that altitude.	SO1, SO3, SO4, SO5, MR02
MR04	The Research Station shall maintain particular orientations during measurements.	SO1, SO2, SO3, SO4, SO5
MR05	The Research Station shall be equipped with a SAR.	UR01, SO3
MR06	The Research Station shall be equipped with multiple deployable atmospheric Scouts.	UR03
MR07	The deployable atmospheric scout should send all data to the Research Station.	UR03, MR06
MR08	The Research Station shall be equipped with infrared sounders.	UR04
MR09	The Research Station shall be equipped with an anemometer.	UR04
MR10	The Research Station shall be equipped with a barometer.	UR04
MR11	The Research Station shall be equipped with a magnetometer.	UR05
MR12	The Research Station shall be equipped with a dosimeter.	UR05
MR13	The Research Station should be equipped with an electrometer.	UR05
MR14	The Research Station shall have a communication connection to Earth through Relay Satellite/s.	UR08
MR15	The Research Station may have a redundant communication link directly with earth.	UR08
MR16	The Research Station should gather information on solar intensity with variation w.r.t. altitude.	UR09
MR17	The Research Station should gather information on solar intensity with variation w.r.t. atmospheric conditions.	UR09
MR18	The Research Station should gather information on solar intensity with variation w.r.t. electromagnetic spectral band.	UR09

Table 3.3: Mission Requirements.

of global coverage and precise measurements the VRS needs to be manoeuvrable within that altitude range and be able to hold certain poses as stated by MR03 and MR04. With the Research Station at a fixed altitude range it can not perform the necessary experiments in the altitude range of 0 to 130 km. Therefore the design is extended by multiple deployable atmospheric Scouts (MR06) that can determine the composition and the other physical parameters of the atmosphere from 0 to 130 km altitude. All data generated on the Scouts are to be transferred to the VRS, from where they can be processed, as well as compressed, and then sent towards Earth. This ensures that all data processing takes place onboard the VRS for simplicity of this design. Due to the atmospheric conditions a communication from within the atmosphere to Earth seems inefficient. The communication shall take place through Relay Satellites that are orbiting Venus (MR14). Nevertheless this design may incorporate a direct communication link to Earth if feasible (MR15). This would further present a redundancy for the communication

link from VRS to Earth.

Operational Requirements

The operational requirements (OR) can be described as the 'user manual' for this concept of a VRS. They elaborate further onto the mission requirements and answer the question of how the Research Station operates. Table 3.4 lists the operational requirements of this mission.

Nr.	Definition	Source
OR01	The Research Station shall operate autonomously between telecommands.	MS, TO03
OR02	The Research Station should perform instrument testing and carry calibration sources for the instruments.	TO03
OR03	The Research Station shall receive telecommands via Relay Satellites from Earth ground station.	MR15
OR04	The schedule of the Research Station shall be changeable with telecommands.	TO03
OR05	The modes of the Research Station shall be changeable with telecommands.	TO03
OR06	The Research Station On-Board Computer (OBC) shall be equipped with an On-Board Data Processing (OBDP) unit.	UR08
OR07	The OBDP unit should compress each payload's data separately into as small as possible packets while maintaining its quality.	UR08
OR08	The OBC shall have health monitoring and error reporting protocols.	TO3
OR09	The OBC shall include a recovery mode for each individual subsystem, ensuring independent restoration and recovery of specific subsystems in the event of failures or errors.	TO3
OR10	The Research Station should float passively to stay within the defined altitude range.	MR02
OR11	The Research Station shall be equipped with an active altitude control system.	MR03, MR04
OR12	The station shall operate between 45 km and 55 km altitude.	MS, MR02, OR10
OR13	The station should move with a constant speed relative to the ground.	MR03
OR14	The SAR should use L-Band.	MR05
OR15	The Research Station should use Long-Wave Infrared band (8 μm - 14 μm) and Mid-Wave Infrared band (3 μm - 5 μm) sensors.	MR09
OR16	The magnetometer shall be triaxial, and should be able to detect $\pm$0.6 Gauss magnetic flux density.	MR12
OR17	The Dosimeter should detect radiation up to 5.0 Sv.	MR13

(To be continued)

Nr.	Definition	Source
OR18	The deployable atmospheric Scout shall be equipped with an Infrared Spectrophotometer.	MR07, UR03
OR19	The deployable atmospheric Scout shall be equipped with an anemometer.	MR07, UR04
OR20	The deployable atmospheric Scout shall be equipped with a barometer.	MR07, UR04

Table 3.4: Operational Requirements.

Comments OR01, as well as OR03 through OR05 describe the degree of autonomy of the VRS and allow the operator a certain degree of influence during the mission. The changeability of the mission‘s schedule and the mode of the VRS via telecommand enables the operator to act if necessary, e.g switching into a recharging mode. OR02 states the requirement for autonomous testing procedures to ensure data correctness. With the generation of scientific data and receiving of telecommands the VRS is in need of an OBC with an OBDP unit (OR06). The OBDP enables the removal of unusable information, such as images that are obscured by clouds, corrupted files, incorrectly formatted information, or other useless data. To ensure a lower transmission rate the gathered data shall be compressed (OR07). OR08 implies that OBC must be equipped with mechanisms to monitor its own health status and report any errors or anomalies that it detects. This allows for proactive identification and communication of issues occurring within the OBC, enabling timely troubleshooting and resolution. So if there are any issues the research station will send some emergency telemetry to earth and then we can have a certain level of telecommands resolving that issue or at least we will know something wrong with some subsystem. And OR09 takes action in case of event upset and latch-ups.

The easiest approach to stay within a fixed altitude range under similar atmospheric conditions from a propulsion and power point of view is to apply levitation. A purely floating system would be uncontrollable, therefore OR10 is a should requirement supplemented by OR11 ensuring the controllability of the VRS. But due to the Hadley circulation of Venus, the polar regions (above approximately $\pm 50^\circ$ latitude) can not be reached by a mainly floating and wind-driven airship. OR12 defines the suitable altitude for a levitating VRS according to Chapter 2. The altitude of 50 km ± 5 km has further been chosen due to its Earth like atmospheric conditions and the regard of human future presence. The VRS will according to OR10 float along with the wind in the overall retrograde direction, but for accuracy of measurements the ground speed should be controlled to be constant. This expresses the need to overcome gust winds with the propulsion system.

Functional Requirements

The functional requirements (FR) describe the required functional capability of the concept design in terms of performances, interfaces and operations. Table 3.5 lists the functional requirements of this mission.

Comments Most of the functional requirements (FR01 - FR04, FR06 - FR08) stated below ensure the endurance of the VRS throughout the five-year period of the mission. Further FR04, FR06 and FR10 - FR14 ensure that all data generated onboard the Scouts or VRS are correctly transmitted to Earth and that sufficient storage until transmission is provided.

Nr.	Definition	Source
FR01	The Research Station shall provide sufficient power generation and energy storage throughout mission lifetime.	TO3
FR02	The Research Station shall maintain structural integrity throughout mission lifetime.	TO3

(To be continued)

Nr.	Definition	Source
FR03	The Research Station, instrumentation, and all auxiliary equipment should be resistant to environmental degradation.	TO3
FR04	The Research Station shall provide sufficient data storage between data transmissions.	TO3, MR15
FR05	The Research Station should have a variable power transmitter.	MR15
FR06	The Research Station shall ensure a sufficient link budget for communication links.	MR15
FR07	The Research Station shall provide sufficient thermal control for nominal operation of the station throughout mission lifetime.	TO3
FR08	The Research Station shall provide sufficient propulsion throughout the mission duration.	TO3
FR09	The propulsion system may use in-situ resources.	TO3, TO1
FR10	The deployable atmospheric Scout shall have sufficient backup data storage.	MR08
FR11	The deployable atmospheric Scout shall have sufficient link margin for uplink of data.	MR08
FR12	The deployable atmospheric Scout should have real-time communication with the research station.	MR08
FR13	There shall be more than one relay satellite to maintain a communication with the Earth.	MR15
FR14	The Relay Satellites shall have sufficient data storage.	MR15

Table 3.5: Functional Requirements.

3.4 Boundary Conditions

The boundary conditions (BC) for this mission, listed in Table 3.6, are pushing the European launch system development and provide self-reliance. The launch site is operated by Arianespace and has the compatibility with Ariane launch vehicles. Given the latitude of the launch site, there is a reduced energy requirement to reach a particular orbit suitable for this mission. The mass restrictions for the launch are from the Ariane 6 Manual, the currently biggest launch vehicle. For further information regarding the launch system refer to Chapter 6.

Nr.	Definition
BC01	The launch system shall be designed and manufactured by the members of the European Union.
BC02	The launch site should be the spaceport in French Guiana.
BC03	The total launch mass of the payload shall be less than 6900 kg.

Table 3.6: Boundary Conditions.

CHAPTER 4

Science Operations

by Hassan Ali

The purpose of this Chapter is to provide an overview of the science operations being carried out during Venus flagship mission. The science operations concept is presented, including an overview of the various mission phases. The specific science operations for the goals of the Venus Mission (VM) are:

I) Mapping of Venus' surface and gathering of compositional information of the planet,

II) Probing Venus' atmosphere at different altitudes for composition determination,

III) Accumulation of information about the climate and weather on Venus,

IV) Investigation of effects of Venus' magnetic field and radiation in the atmosphere,

V) Search for life forms in Venus' clouds.

More details on these goals and the objectives can be found further. To achieve these goals, our mission architecture relies on three collaborative platforms, a Venus Research Station, Scouts, and Relay Satellite(s) for communication, which house multiple instruments, many with heritage from prior missions, to elucidate from Venus interior to atmosphere, volcanic activity, weathering, atmosphere dynamics, cloud formation and atmospheric loss. Instruments on these platforms will assess at multiple scales with high precision. Through two launches, a research station entry vehicle, Relay Satellite(s), and Scout entry vehicles will be deployed to employ multiple Scouts to gather data on the exosphere, atmosphere, and surface at various scales with exceptional precision. Venus, as a complex planet with a highly interactive system, presents a unique opportunity for the Flagship mission concept to conduct complementary scientific measurements. To gain insights into surface weathering and chemical processes, measurements of near-surface atmosphere and rock composition will be crucial. These measurements will help determine the mineralogy, chemistry, and chemical sinks within the tessera, with data collected at depths of approximately 5 cm. The instruments on the Venus Research Station will provide valuable information on weather patterns, climate conditions, temperature, humidity, cloud cover, cloud top height, cloud top temperature, cloud phase, surface albedo, magnetic field, wind speed, and surface wind direction on Venus. Additionally, they will investigate the plasma environment, the interaction between the solar wind and Venus' atmosphere, gamma and X-rays, the composition of haze and cloud particles, and the transport of these particles through the mesosphere to the thermosphere. Furthermore, the instruments will assess the level of geological activity on the planet [34]. The Scouts, on the other hand, will contribute to the overall picture by measuring various gases in the atmosphere, capturing wind measurements, examining the interaction

between the solar wind and Venus, studying upper atmospheric photochemistry, and assessing the mass and heat transport characteristics of the atmosphere. Radiation and temperature measurements will also be conducted by the Scouts. These comprehensive measurements across different instruments and platforms will provide valuable data for a more complete understanding of Venus and its complex atmospheric and surface dynamics.

Tabular Matrix for Science Traceability (TMST)

The comprehensive objectives of the Venus Mission, including the necessary measurements to achieve them, are outlined in Figure 4.1, which presents the Tabular Matrix for Science Traceability. This matrix not only describes the scientific objectives but also provides insights into the operational requirements such as spectral and spatial resolution, sensitivity, and accuracy. It illustrates how these requirements are linked to the science measurements and details how each instrument performs the necessary tasks. The Tabular Matrix for Science Traceability sets the threshold performance requirements for the Venus Mission. Among the various measurements required, surface mapping and mineralogy assessments, conducted by instruments like synthetic aperture radar and others, are particularly challenging. The field of exoplanet research has advanced to a point where lessons learned from studying Venus have become indispensable for understanding all aspects of exoplanetary data interpretation, including orbits, formation, atmospheres, and interiors. Currently, exoplanet models heavily rely on the limited knowledge we have of terrestrial atmospheres within our own solar system. Hence, there is an evident and urgent need to characterize the atmosphere of Venus [35]. This characterization is vital for comprehending the evolution, dynamics, and surface of Venus, as well as providing crucial data to accurately interpret atmospheric models for terrestrial exoplanets. The Venus Mission is designed to fulfil this critical objective by providing comprehensive and highly targeted new measurements to further our understanding in this field [36, 37].

4.1 Science Operation/Goal A: Surface mapping & gathering of compositional information

To advance our understanding, an overview of techniques to get the Venus surface and compositional information is presented in this section separately.

Objective A.1: Surface mapping

In recent decades, significant progress has been made in our understanding of the Venusian landscapes. Findings from the Magellan mission have revealed that erosion processes are minimal under the current climatic conditions due to the high surface temperatures that inhibit fluvial activity [36]. Magellan images indicate the presence of wind streaks and a few dune fields, with spatial associations with impact craters suggesting that crater ejecta is likely the source of sediment [38]. Data from Venera lander missions and modelling studies suggest that surface winds on Venus are relatively low, below a few meters per second, partly due to the planet's slow rotation and dense atmosphere [39]. Large portions of the planet's surface consist of volcanic terrains that have experienced minimal erosion since their formation. However, tessera terrains, which are stratigraphically older than the plains, exhibit distinct deformation patterns such as folds, faults, and lineaments, indicating a dormant tectonic regime. The RADAR data also reveal roughness elements at the centimetre scale on the surfaces of tesserae. In some tesserae, RADAR data show patterns that could be interpreted as horizontal layering, suggesting the involvement of deposition and erosion processes in exposing these layers [40]. However, the

Goal	Scientific Objective	Science Investigation	Measurement approach	Measurement requirement	Performance requirements	Functional Requirement
To support future research of Venus exploration, a long term station within Venus atmosphere	Surface maping & gathering of compositional information	Mapping the land covers	Characterise the resolution	SAR mapper	L band, Medium Resolution(5mto 30m)	VRS
		Identyfying the volcanoes and direction of lawas	Characterise the area of interest	SAR mapper	L band, Medium Resolution(5mto 30m)	VRS
		Determine the compositional information	Characterisre the major suraface type	SAR mapper	L band, 5cm to 10cm penetration	VRS
	Accumulation of information about the climate and weather on Venus	Temperature, clouds and ozone Measurement	Characterise the ranges	sounding instrument	Infrared Radiation	VRS
		Pressure Measurement	Characterise the pressure range	Barometer	1-100bar	VRS
		Wind speed measurement	Characterise the wind speed range	Acoustic Anemometer	5 cm/s accuracy,	VRS
	Investigation of effects of Venus' magnetic field and radiation in the atmosphere	Magnetic field measurement	Characterise the B strength and	flux-gate magnetometer	± 0,5 Gauss,	VRS
		Radiation measurement	Characterise the radiations range	Dosimeter	0,01nm to 10nm for rays for xrays and less than 0,01nm for gamma rays	VRS
	Probing Venus' atmosphere at different altitudes for composition determination	Identifying the gases	Characterise the gases	Spectrophotometer	Infrared	Scout
		Wind Measurement	Characterise the wind speed range	drag-force anemometer	0.35 to 2,5m/s,	Scout
		Solar activity investigating	Characterise the ion concentration in atmosphere layer	Ion Mass Spectrometer	1 to 60 atomic mass units	Scout
		Radiation & Temperature measuremnet	Characterise the type of radiation and temperature range	Mercury Radiometer and Thermal Infrared Spectrometer	500m spetial resolution, 14 to 40 µm radiometer range	Scout
	Search for life forms in Venus' clouds.	----------				

Figure 4.1: Science Tractability Matrix.

resolution of Magellan data, at 100 m, is insufficient to determine the exact origin of these lineaments and roughness elements. On Earth and Mars, image resolutions of around 10 m or better have proven capable of revealing layered sedimentary sequences, drainages, small alluvial fans, and other erosional and depositional features that provide insights into different past climatic conditions. Detecting evidence of erosion in older terrains on Venus would indicate significantly different surface and atmospheric conditions, while evidence of past fluvial activity would strongly suggest past habitability. The Venus Research Station Synthetic Aperture Radar (SAR) will enable imaging of selected targets worldwide at a resolution better than 5-30 m. Additionally, during the descent, landing site and its immediate surroundings will be imaged by the Mercury Radiometer and Thermal Infrared Spectrometer (MERTIS at scales ranging from kilometres to centimetres at wavelengths of 0.9 and 1.02 μm. This will provide a comprehensive set of image data for the tesserae, spanning scales from meters to centimetres, allowing for a better interpretation of RADAR signatures in different terrain types, which can be compared to Magellan or other RADAR datasets.The side-looking imaging geometry of Synthetic Aperture Radar (SAR) improves the visualization of structural features such as folds and faults. These features are better enhanced when they are oriented perpendicular to the SAR's look direction. InSAR (Interferometric SAR) techniques are employed to accurately map volcano deformations [37, 41]. Additionally, polarimetric SAR has proven effective in mapping lava flows. In order to prepare raw SAR data for further analysis and interpretation, SAR pre-processing is necessary. Radar systems are utilized to acquire SAR data by emitting microwave signals towards the surface and receiving backscattered [42]. These backscattered signals contain valuable information about the surface properties and topography of the Venusian landscape, but they also include noise and artifacts. To extract the landscape features from the SAR data of the Venusian surface, various processing steps are applied. SAR pre-processing encompasses a series of procedures aimed at removing or reducing noise and artifacts present in the data, as well as enhancing the contrast and resolution of the features of interest. The key steps involved in SAR pre-processing include radiometric calibration, geometric correction, speckle filtering, and terrain correction. These steps collectively contribute to improving the quality and reliability of the SAR data for subsequent analysis and interpretation. By applying these pre-processing steps to SAR data, a cleaner and more accurate depiction of landscape features can be obtained. This enhances the quality of subsequent analyses, such as feature extraction, classification, image fusion, and change detection. After applying pre-processing techniques to enhance the SAR data and performing post-processing steps to refine the imagery, the data is ready for analysis [43, 34]. This analysis stage involves extracting the desired information from the SAR data in the form of various landscape features and their monitoring. To facilitate this analysis, specialized software packages such as ENVI, ERDAS, and ArcMap are utilized. ENVI, ERDAS, and ArcMap, an image analysis softwares, offers a range of tools and functionalities for processing and analysing remote sensing data. It provides capabilities for image classification, change detection, spectral analysis, and visualization, among others. Through the use of these software tools, analysts can delve into the data, exploit its rich information content, and derive meaningful insights about the landscape. The graphical representations produced by these software packages aid in visualizing and communicating the analysed information effectively. These representations could include thematic maps, feature classification results, change detection maps, and other visual outputs, allowing for a comprehensive understanding of the landscape features and their monitoring.

Objective A.2: Gathering of Venus compositional information

Our understanding of the formation, evolution, and structure of terrestrial planets, including our own Earth, as well as exoplanets, is hindered by our limited knowledge of Venus. At present, critical information about Venus, such as the size and state of its core, remains unknown. These data play a fundamental role in determining whether Venus and Earth share similar compositions, understanding the origin and sustainability of magnetic fields, unravelling the dynamics of the mantle, core, and crust, assessing heat flow patterns, and evaluating the condition of the lithosphere. By obtaining a more comprehensive understanding of Venus, we can gain valuable insights into the broader understanding of terrestrial planets, their formation, and their geological processes. Multiple remote sensing methods have been developed to acquire highly accurate geological information. Optical remote sensing is commonly employed for mineral mapping due to its ability to capture a substantial amount of spectral information in the visible, near-infrared, and shortwave infrared regions. This method effectively identifies minerals based on their reflectance spectra. However, optical images are susceptible to atmospheric conditions, and the presence of vegetation can interfere with the reflectance spectra used for analysing target materials such as soils, rocks, or minerals. To overcome these limitations, synthetic aperture radar (SAR) technology has been advanced for detecting geological targets on the ground based on the physical properties of the soil surface, particularly in tropical regions where atmospheric effects can be minimized. Full polarimetric SAR data enables discrimination of the target from the Earth's surface by measuring the type of scattering generated by the surface. While decomposition techniques have been widely utilized in the environmental field to classify polarimetric radar data related to surface scattering, their application in geosciences remains relatively uncommon. [44, 45] For instance, employed polarimetric decomposition techniques, specifically Cloude and Poittier's method, to extract the geomorphology and structure of active volcanoes by analysing surface roughness. By analysing the surface roughness, they successfully differentiated surface alterations, hot mud, and hot springs. The level of acidity (pH) on the surface can influence its roughness. Hydrothermal alteration, which involves changes in mineralogy, chemistry, and rock textures, occurs due to the interaction of hydrothermal solutions with rocks under specific chemical-physical conditions. Analysing alterations provides valuable insights for identifying mineral deposits in an area. By utilizing polarimetric Cloude-Poittier decomposition technique and surface roughness, it becomes possible to classify alteration zones in the studied region [46]. Decomposition methods have been introduced for analysing two or full polarimetric radar images to interpret the physical characteristics of objects based on their reflection properties. One of the recent techniques in polarization data decomposition involves employing eigenvalue analysis to obtain the physical attributes. Cloude-Pottier decomposition is a widely used algorithm for polarimetric data (covariance matrix or coherence shape). It can convert the highly complex full polarimetric data into three simpler units of analysis: entropy, alpha angle, and anisotropy. These units provide valuable insights into the physical characteristics and properties of the observed objects. Entropy (H) is a parameter that ranges from 0 to 1, representing the degree of randomness in object scattering on the Earth's surface. It serves as a measure of the relative intensity of the scattering process. When $H = 0$, it indicates a single, unique object or an object with low surface roughness. On the other hand, when $H = 1$, it suggests a random backscattering process without a dominant object or a surface with high roughness across the coverage area. Therefore, if an object on Venus's surface is singular, distinctive, or possesses low surface roughness, the entropy values will tend to approach zero. Another significant parameter is the angle alpha, which signifies the dominant type of backscattering observed in the pixels, regardless of the object. The value of alpha ranges from 0-90 °. A value of 0°indicates odd-bounce scattering from a flat surface, while even-bounce

scattering can be observed around $\alpha = 90°$. An alpha value of 45°indicates dipole scattering. Prior to the decomposition classification, the data must undergo several pre- and post-processing steps, including focusing and multi looking, followed by geocoding and terrain correction. The geocoding and terrain correction processes necessitate the use of digital elevation model (DEM) data. The subsequent step involves $H/alpha$ decomposition, which calculates the entropy (H) and alpha values. Once these two parameters are obtained, the polarimetric classification is carried out based on the $H/alpha$ values. The Cloude-Pottier polarimetry decomposition analysis generates the (H) and α values, as previously mentioned. The H value represents the degree of randomness in the surface scattering of an object, with surface roughness being influenced by H. It is worth noting that the surface of altered rock tends to be rougher compared to unaltered rocks. Additionally, rocks with a more acidic surface, characterized by a pH value lower than 7, exhibit higher surface roughness than rocks with a neutral pH or close to 7. The argillic alteration zone is distinguished by the presence of clay minerals such as kaolinite, and montmorillonite. This alteration occurs due to extensive cation leaching under acidic conditions, transforming plagioclase into kaolinite and eventually into montmorillonite in outer areas. The intermediate argillic zone displays minerals such as montmorillonite, chlorite, hydromicas, and locally kaolinite. The formation of these minerals is associated with limited availability of K, Ca, and Mg. Advanced argillic alteration refers to complete acid attack, leading to the formation of minerals such as kaolinite-dickite, diaspore, alunite, amorphous silica, slightly corundum, and pyrophyllite.

The Venus Research Station of the Venus mission utilizes SAR (Synthetic Aperture Radar) and NIR (Near-Infrared) radiance measurements, along with derived emissivity values, to capture distinct spectral signatures from the Venusian surface. These spectral signatures exhibit correlations with specific terrains and landforms. Notably, observations from Galileo NIMS and VIRTIS have revealed that the tesserae, compared to the surrounding plains, exhibit lower emissivity, suggesting a lower content of ferrous iron in the rocks of the region [47]. On the other hand, certain volcanoes display higher emissivity compared to the surrounding plains, indicating a greater presence of ferrous iron in silicates and suggesting lesser weathering in those areas [4, 48]. Ongoing development of high-temperature emissivity spectral libraries enables the correlation of these radiance variations with the specific mineralogy of surface rocks on Venus. These variations in radiance imply potential differences in magmatism, volcanism, climate regimes, and surface age over time. By incorporating improved spatial resolution SAR imagery with a target range of (5-30) m, as well as global multi-spectral measurements of NIR radiance (NIR-I) on the Venus Research Station and combining orbital observations with chemical measurements at the surface, it becomes possible to enhance the definition of volcanic units and potentially identify different types of sedimentary rocks. These data will provide insights into the history of volcanic volatile flux into the atmosphere, the cycling of volatile substances between the planet's interior, crust, and atmosphere, and changes in global weathering. These factors collectively influence the global climate of Venus. Radar back-scatter is influenced by the dielectric constant of the medium. An increase in moisture content in geologic materials leads to a higher dielectric constant, which in turn reduces the radar's penetration capability. However, the dielectric constant variations in most geologic materials, such as rocks and soils, are limited. Therefore, surface roughness is considered of greater importance than dielectric constant variations. [38]

Remote sensing spectral signatures of rock outcrops and bare in-situ soils can be used to determine their mineral composition. To discriminate between different minerals, subtle differences in the spectral signature across the visible, near-infrared, and thermal infrared regions can be utilized. Fine spectral resolution data are necessary to detect these subtle differences in the mineralogical composition. Additionally, high spatial resolution is advantageous to minimize spectral mixing effects from different land cover types. Imaging spectroscopy data,

such as AVIRIS and HyMAP, are well-suited for this purpose due to their high spatial and spectral resolution [49]. For instance, AVIRIS data has been employed to analyse variations in mineralogical and chemical compositions, mapping elements like SiO_2 and Al_2O_3 to estimate the degree of soil weathering [50]. Moreover, multispectral satellite data synergies, such as combining Landsat TM and ASTER data, have shown promising results in differentiating lithological variability based on Landsat TM and distinguishing different mineral groups based on ASTER [51].

The TIR region is particularly informative for identifying spectral features of typical rocks, including quartzite, carbonate, silicate, and mafic minerals. The analysis of mineralogy through spectral portable spectrometers (PS) has made significant advancements in recent years. Various institutes provide spectral libraries containing comprehensive collections of a wide variety of materials. One example is the ASTER spectral library version 2.0, which includes contributions from the Jet Propulsion Laboratory, Johns Hopkins University, and the United States Geological Survey. It offers over 2400 spectra covering minerals, rocks, vegetation, and manmade materials across the wavelength range of$[0.4–15.4]\mu$m. Additionally, the USGS Spectral Library provides a diverse range of mineral spectra [52, 53]. On the other hand, the PRISM and Tetracorder tools utilize a set of algorithms within an expert system decision-making framework for soil and terrain mapping. These expert systems compare the spectra of unknown materials with reference spectra of known materials to identify and characterize their composition. For instance, the USGS spectral library contains soil mineral properties and land cover types from various regions worldwide, enabling spectroscopic analysis to determine material composition . In traditional soil analysis, soil texture classes, such as silt, sand, or clay, are determined based on particle size distribution or physical texture. In remote sensing, soil texture is typically assessed by utilizing specific absorption features to differentiate between clay-rich and quartz-rich soils. Clay minerals exhibit a characteristic hydroxyl absorption at $2200nm$, while the presence of quartz can be detected using thermal bands between $[800$ and $9500]nm$, where the restrahlen feature (reflectance peak of silica) occurs. These bands correspond to bands 10 to 14 of ASTER. By combining ASTER SWIR bands 5 and 6 with TIR bands 10 and 14, it becomes possible to distinguish dark clayey soils and bright sandy soils from non-photosynthetic vegetation at a local scale, although organic matter can influence the results . Infrarad spectroscopy, which covers parts of the SWIR and TIR spectrum, provides more information on soil mineral and organic composition compared to the VNIR range, and its multivariate calibrations are generally more robust. The mid-IR range allows for the detection of defined molecular vibrations of soil components, whereas only their overlapping combination and overtone peaks can be detected in the NIR range. This combined signal results in numerous bands even for simple compounds. However, one limitation of mid-IR spectroscopy is the presence of distortions caused by specular reflection. Specular reflection leads to spectral distortions that depend on the concentration of the material and the specific band (frequency) under consideration [54–56].

4.2 Science Operation/Goal B: Probing Venus' atmosphere at different altitudes for composition determination

In this section, Venus atmospheric composition(presence and concentration of different gases), solar activity in atmosphere and wind, pressure, radiation and temperature profile determination through Scout probing is presented separately.

Objective B.1: Detection of Venus atmospheric composition

The composition of the Venusian atmosphere remains still poorly understood, despite its critical role in the Sulphur cycle and the formation of numerous trace constituents that have yet to be detected . Understanding the Sulphur cycle and the distribution of trace constituents is vital for comprehending the energy, mixing, and dynamics of the Venus atmosphere. Furthermore, it is likely that these factors play a key role in maintaining the atmospheric stability of Venus , especially considering the absence of the catalytic role of hydroxyl in CO_2 recycling due to the low water vapor abundance on Venus, in contrast to Mars. To investigate surface-atmosphere chemical interactions, measurements within the lowest few kilometres of the atmosphere are particularly crucial. A spectrophotometer shall be employed to determine the composition of the Venusian atmosphere [57].

Objective B.2: Detection of Solar wind interaction in Venus atmospheric

The highly elliptical orbit of the carrier vehicle was deliberately selected to enable simultaneous sampling of the Venusian atmosphere and the solar wind, facilitating a better understanding of the atmosphere's response to solar wind drivers. This orbit design also allows for dual sampling of specific regions behind the Venusian bow shock, providing valuable insights into temporal changes and fine-scale structures within the atmosphere. Each Scout module comprises ion and electron Electrostatic Analysers (ESA-i and ESA-e, respectively), which observe ions and electrons in both the solar wind and planetary environment within the suprathermal energy range 1 eV to 25 keV. These ion and electron observations play a crucial role in scientific investigations related to atmospheric escape, magnetic topology, reconnection, and the atmospheric response to solar wind variations and transient events. The ion mass spectrometer experiment provides measurements that offer valuable information about the interaction between the solar wind and Venus, upper atmosphere photochemistry, as well as the mass and heat transport characteristics of the atmosphere. Using a Bennett ion spectrometer similar to those flown on various Earth satellites and rockets, the concentrations of Venus' upper atmosphere ions will be measured in the mass range of 1 to 60 atomic mass units (u).

Objective B.3: Detection of wind, pressure, Radiation and Temperature profile in Venus atmosphere

To enhance our understanding of the atmospheric structure and dynamics on the surface of Venus and provide valuable input to climate models, it is crucial to measure parameters such as wind velocity and direction, pressure, radiation, and temperature profile. Accurate measurements of wind on the Venusian surface and tracking changes over an extended period are essential for gaining insights into the planet's atmospheric behaviour. Previous missions utilized different methods to estimate wind speed during descent and on the surface, including cup anemometers, acoustic microphones, and radio Doppler shifts. However, these measurements had significant uncertainties, reaching up to $\pm 50\,\%$ for the Venera missions. The Scout Instruments will directly measure wind velocities in various regions of Venus. During descent, the Scout will obtain a vertical profile of horizontal winds in the lower atmosphere. To disentangle vertical motions caused by buoyancy changes from those due to vertical winds and to enhance sensitivity to turbulence and atmospheric waves, an anemometer will be deployed. While winds in the upper atmosphere were previously determined indirectly from temperature structures, the Scout will directly measure line-of-sight winds using the anemometer. A miniature drag-force anemometer is being developed for this purpose, which offers advantages such as independence from variable heat transfer, maturity in harsh environments, and low mass and power requirements. Prototype drag-

force anemometers have demonstrated their capabilities in a simulated Venus surface environment, recording transient effects with integrated operational amplifiers. For multidirectional wind monitoring, the sensors can be deployed orthogonally as a three-dimensional array on a small arm. In addition to wind measurements, it is crucial to understand the near-surface atmospheric composition, radiation, pressure, and temperature to gain insights into Venus' atmospheric chemistry and the role of surface-atmosphere chemical buffering reactions. The Scout instruments, in collaboration with the Mercury Radiometer and Thermal Infrared Spectrometer (MERTIS), will determine these atmospheric parameters during descent and on the surface. MERTIS, designed for the BepiColombo mission to Mercury, will contribute to Venus exploration as well. With its thermal imaging dispersive spectrometer, MERTIS will study the global mineralogical composition, local temperature variations, and thermal surface studies. It operates in the range of (7 - 14) μm with 80 spectral channels, providing the ability to resolve and map low-contrast mineral bands at a nominal spatial resolution of 500 m. By integrating the capabilities of various heritage instruments, MERTIS ensures a comprehensive understanding of Venus' current state and evolution. Overall, the measurements obtained by the Scout Instruments and MERTIS will significantly contribute to our understanding of Venus' atmospheric dynamics, climate, and mineralogical composition, shedding light on its complex atmospheric processes and long-term evolution.

4.3 Science Operation/Goal C: Accumulation of information about the climate and weather on Venus

Detecting wind, pressure, and temperature profiles in the atmosphere of Venus poses unique challenges due to the planet's extreme conditions. Venus has a dense atmosphere primarily composed of carbon dioxide, with traces of other gases, and experiences high surface temperatures, high pressures, and strong winds at higher altitudes. Acquiring this information within the Venusian atmosphere is crucial for comprehending weather and climate dynamics on the planet, improving weather predictions, refining climate models, gaining comparative insights, and supporting future space exploration endeavours. Monitoring and analysing wind patterns on Venus provide valuable insights into the planet's atmospheric circulation, which drives weather systems, cloud formations, and atmospheric disturbances. By studying wind patterns, scientists can better understand short-term weather phenomena, enhance weather models, and make more accurate predictions about atmospheric conditions. Wind, pressure, and temperature profiles are interconnected and contribute to the overall atmospheric circulation and dynamics of Venus, influencing air mass movement, heat distribution, and energy transfer within the atmosphere. By studying the interactions between these profiles, scientists can deepen their understanding of the processes driving weather patterns and atmospheric behaviour on Venus. To ensure accurate climate modelling, comprehensive data on temperature, pressure, and wind profiles in the Venusian atmosphere are required. Climate models simulate long-term climate behaviour, including temperature variations and the impact of greenhouse gases. By incorporating observed wind, pressure, and temperature data, scientists can enhance the accuracy of climate models for Venus, leading to better predictions of long-term climate trends and variations. The study of Venus' weather and climate also provides valuable comparative data for understanding other planetary atmospheres, including our own Earth. Venus shares similarities with Earth in terms of size, composition, and the greenhouse effect. By comparing the atmospheric processes and dynamics of Venus and Earth, scientists can gain insights into commonalities and differences between planetary weather systems. This knowledge enhances our understanding of Earth's climate and aids in discerning the factors influencing weather patterns on both planets. As we continue to explore space and plan future missions to Venus, understanding the atmospheric

conditions is of utmost importance. Data on wind, pressure, and temperature profiles helps in designing spacecraft and instruments capable of withstanding the extreme conditions on Venus. Additionally, accurate knowledge of atmospheric conditions aids in mission planning, trajectory calculations, and overall mission success. To measure wind speeds on Venus, a proposed instrument called the Anemometer utilizes acoustic measurements. By analysing the acoustic wave signals, information about wind speed, turbulence characteristics, and atmospheric conditions can be extracted. In addition to wind measurements, the Infrared Sounder instrument is utilized to gather information on temperature, humidity, cloud cover, cloud top height, cloud top temperature, and cloud phase. This instrument operates in the thermal infrared region of the electromagnetic spectrum, detecting the infrared radiation emitted by Earth's atmosphere and surface. Its measurements contribute to weather forecasting, climate monitoring, and atmospheric research.

4.4 Science Operation/Goal D: Investigation of effects of Venus' magnetic field and radiation in the atmosphere

Multiple missions have confirmed that Venus currently lacks an intrinsic magnetic field, as demonstrated by measurements. However, there may exist remanent magnetism in the uppermost crust of Venus likely confined to a thinner layer compared to Mars due to the high temperatures. Previous spacecraft lacked magnetometers with the necessary sensitivity and proximity to the surface to adequately assess the presence of a remanent magnetic field [58, 59]. If sufficiently strong, permanent magnetism could potentially be observed from low orbit or a balloon. To investigate this further, the Venus mission will measure the magnetic field from multiple vantage points, including a magnetic survey conducted by the Mag instrument on the Venus Research Station. The Optical Magnetometer (OMAG) is an instrument specifically designed to measure the strength and direction of magnetic fields. It operates based on the principles of quantum mechanics and atomic physics, utilizing an optical detection technique. The Optical Magnetometer offers a precise and accurate means of measuring magnetic fields using the principles of quantum mechanics and the behaviour of atoms in an atomic vapor cell.The Venus Research Station's projected lifetime of 5 years will facilitate the mapping of the field strength across one hemisphere of Venus, extending from the equator to the pole. This mapping Endeavor aims to reveal the distribution, strength, and direction of any potential crustal magnetic sources. A comparable mapping effort conducted by the Mars Global Surveyor (MGS) in a low orbit around Mars uncovered robust magnetic fields with varying polarity in the ancient crust. This discovery enabled calculations of the magnetic layer's thickness, potential mineralogy, and suggested the existence of a core dynamo during Mars' early history, implying crustal spreading. The detection of remanent magnetism on Venus would constitute a significant scientific breakthrough, as it would imply the presence of a dynamo during a previous epoch. On Earth, a dynamo field has persisted for at least 3.5 billion years, as evidenced by the geological record. Earth's dynamo has played a crucial role in shielding organisms from harmful solar radiation effects. Furthermore, it is believed to have influenced the evolution of the atmosphere, although the precise mechanisms are not yet fully understood. The magnetic field affects the interactions between incident solar and cosmic particles and the atmosphere. Hence, understanding whether Venus exhibits any remanent magnetism is of great interest, both for comprehensive planetary comprehension and fundamental scientific inquiry. There are three potential explanations for the absence of a global field on Venus: The lack of an inner core, potentially due to Venus' smaller size and higher temperature. Many scientists propose that compositional convection resulting from inner core growth is responsible for sustaining Earth's dynamo. A transition in mantle convection within Venus triggered by a hypothesized resurfacing

event approximately 700 million years ago. Currently, Venus' mantle is not cooling at a sufficient rate to allow for core convection. The absence of a late giant impact during its formation. Such an impact may have facilitated the homogenization of Earth's core, enabling the terrestrial dynamo. It could also impact the likelihood of core-mantle interactions, such as the proposed magnesium precipitation on Earth. In this third scenario, unlike the other two, it is plausible that Venus never possessed a global field. Contrary to popular belief, the slow rotation of Venus does not hinder the possibility of core convection. Venus rotates at a speed sufficient for core convection, where the Coriolis force dominates the inertial terms in the equation of motion, despite its current 243 day spin period [49, 60–63].

Monitoring ultraviolet (UV) radiation in the Venusian atmosphere is essential for several compelling reasons: UV radiation is a valuable source of information concerning the composition and chemistry of the Venusian atmosphere. Various atmospheric constituents, such as Sulphur dioxide, sulfuric acid aerosols, and trace gases, possess the ability to absorb and scatter UV radiation at specific wavelengths. Through the analysis of absorption and scattering patterns, scientists can acquire insights into the composition and abundance of these atmospheric components. The role of ozone in the chemistry and dynamics of a planet's atmosphere is crucial. UV radiation governs the production and destruction of ozone molecules. By monitoring the interaction between UV radiation and ozone in the Venusian atmosphere, scientists can investigate ozone distribution and variations, thereby providing insights into atmospheric processes and photochemistry. UV radiation significantly influences a planet's energy balance and climate. On Venus, UV radiation contributes to the heating of the upper atmosphere and drives atmospheric circulation patterns. By monitoring the distribution and intensity of UV radiation, scientists can enhance their understanding of Venus' energy budget, explore climate variations, and investigate the processes that shape the Venusian climate system. The study of UV radiation also yields information about the properties of the Venusian surface and clouds. Through the examination of the reflection, scattering, and absorption of UV radiation by Venusian clouds and the surface, scientists can gain insights into their composition, structure, and optical properties. This knowledge enhances our understanding of the dynamics of Venus' thick cloud cover and its impact on the planet's radiation balance. UV radiation is of particular relevance when considering the potential habitability of a planet. Elevated levels of UV radiation can be detrimental to known life forms. By monitoring UV radiation in the Venusian atmosphere, scientists can evaluate the potential habitability of Venus and investigate the effects of UV radiation on the hypothetical biosphere of the planet. Overall, the monitoring of UV radiation in the Venusian atmosphere provides vital information regarding atmospheric composition, chemistry, climate, and potential habitability. It advances our comprehension of the intricate dynamics of Venus' atmosphere and contributes to our broader knowledge of planetary atmospheres, climate systems, and astrobiology. Monitoring x-ray and gamma radiation in the Venusian atmosphere holds significant importance for several reasons. By observing these high-energy radiations, scientists can gain valuable insights into the radiation environment present in the Venusian atmosphere. Understanding the levels and variations of x-ray and gamma radiation helps to characterize radiation hazards and assess their potential effects on spacecraft and future missions to Venus. The interaction of x-ray and gamma radiation with the Venusian atmosphere provides information about the composition and dynamics of the atmosphere itself. When high-energy radiation interacts with atoms and molecules in the atmosphere, it induces processes such as ionization and excitation. Monitoring these interactions enables the study of atmospheric constituents, their distribution, and their potential interactions with radiation. Venus is known to have active volcanoes, and monitoring x-ray and gamma radiation can aid in the detection and study of volcanic activity on the planet. Volcanic eruptions release high-energy particles and radiation, including x-rays and gamma rays. Analysing these

emissions provides insights into the nature and intensity of volcanic events on Venus. Studying x-ray and gamma radiation in the Venusian atmosphere contributes to comparative planetary studies. By comparing the radiation environment and its interactions with the atmosphere across different planets, scientists can enhance their understanding of fundamental processes and properties of planetary atmospheres and their evolution. The Venus Research Station is equipped with the dosimeter for the detection of UV, X and Gamma Rays.

The detection of UV, X and gamma rays in the Venusian atmosphere plays a crucial role in obtaining a comprehensive understanding of high-energy processes, atmospheric composition, and the radiation environment on Venus. UV rays provide valuable insights into atmospheric chemistry, the distribution of ozone, and the dynamics of the planet's climate. By studying UV radiation, we can gain knowledge about the composition of the atmosphere and its impact on climate dynamics. X-rays and gamma rays provide important information about energetic phenomena occurring in the Venusian atmosphere. They offer insights into processes such as volcanic activity, particle acceleration, and the presence of high-energy particles. By analysing these radiations, we can better understand the energetic processes shaping Venus' atmosphere and gain insights into phenomena like volcanic eruptions. The detection of UV, X and gamma rays holds significant importance for planetary exploration, atmospheric science, and comparative planetary studies. It provides crucial data for designing and planning missions to Venus, advancing our understanding of atmospheric processes, and conducting comparative studies with other planetary bodies. By studying these radiations, we can enhance our knowledge of planetary environments, atmospheric chemistry, and the broader field of planetary science.

CHAPTER 5

Mission Scenario

by Malena Stieler

This Chapter describes the pre-mission preparation before the start of the mission as well as the time planning and scheduling of the operations of the Venus Research Station(VRS). The mission is composed of four main phases:

1. Launch, Transfer and Deployment (LTD) Phase
2. Commissioning Phase
3. Science Operation (SO) Phase
4. Decommissioning Phase

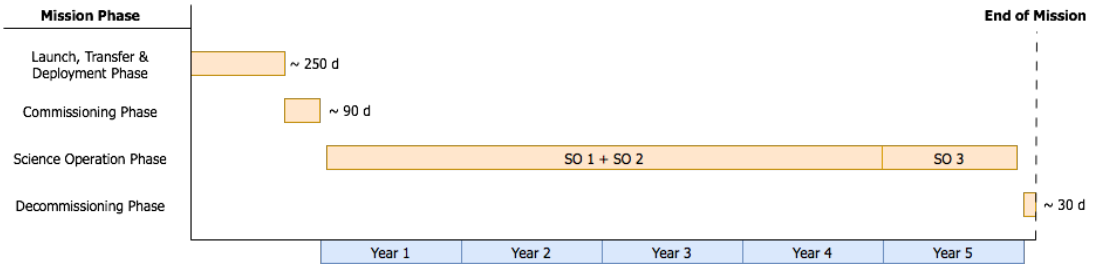

Figure 5.1: Mission Phases of VRS.

The LDT phase will have a duration of about 250 days, followed by the commissioning phase with an estimated span of 90 days and the SO phase of five years. In the final step the decommissioning of approximately 30 days will take place as depicted in Figure 5.1.

5.1 Preparation

The autonomy of the VRS stands in exchange with the preparations before the start of the mission. The user requirements listed in Table 3.2 demand a high level of independence.

The instrument and platform testing will be one segment of the launch preparations. To achieve calibration and validation of the instruments on board of the VRS concepts and procedures, that can be executed while operating, are defined. This ensures accurate and comparable data to past and future measurements.

Emergency procedures are defined to ensure the station can recover from various expected and unexpected situations. First possible error scenarios will be constructed and after that the reaction of the station is planned. For unexpected events default restoration sequences will be developed.

Finally, VRS as well as the other system components are transported to the launch facility at the French Guiana spaceport. The System is composed of the VRS, the Scouts, the Relay Satellites and the Carrier Vehicles. Which will be referred to as the system components in this Chapter.

5.2 Launch, Transfer and Deployment (LTD)

The first part of the mission incorporates the take off to orbit, the transit to Venus and the placement into the atmosphere. In this phase the system components will be exposed to a variety of mechanical, thermal, and electromagnetic environments. Therefore LTD puts the most pressure and stress on the structure and instruments. The global loads the system components have to resist include the static and dynamic loads that can origin from e.g. wind, gusts or buffeting at transonic velocity or from the propulsion systems. Random vibration occurs as well as acoustic vibration that can be caused by shock waves or turbulences [64].

The launches of the mission components will take place at the French Guiana spaceport with the Ariane 64 launch vehicle. Three separate launches are needed to take first the Relay Satellites plus their Carrier Vehicle and the Scouts plus Carrier Vehicle and last VRS with the Carrier Vehicle into Earth orbit. The escape out of the gravitational field of the Earth will take between 40 minutes and one-and-a-half hours [64].

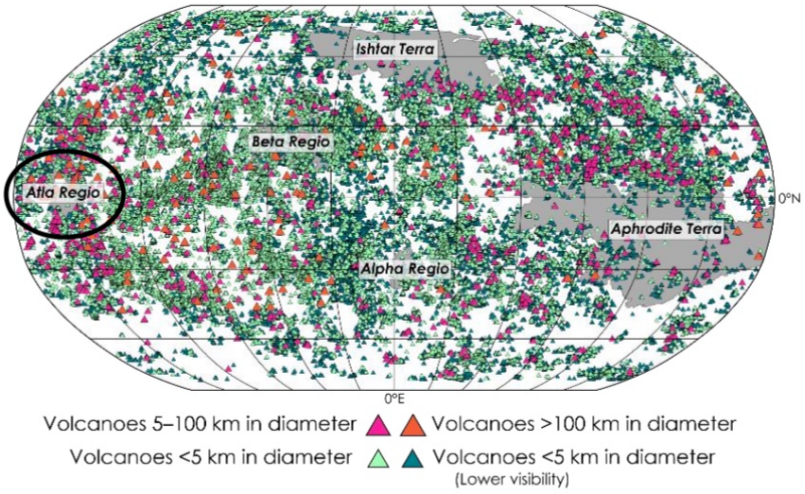

Figure 5.2: Map of Venus including volcanoes [65].

After the launch each Carrier Vehicle will get to the planet Venus via the planed interplanetary trajectory. The Transfer will take about 190 days. The Relay Satellites will be launched in advance of the VRS. This has the advantage that the build up of the satellite network can be started before the VRS reaches Venus atmosphere. Arriving at Venus the Relay Satellites will be deployed by the Carrier Vehicle in their dedicated orbits. The Carrier Vehicle equipped with

the Scouts is also assembled in an orbit around Venus. The VRS arrives and will be separated from the Carrier Vehicle and send to the initial location in the atmosphere of Venus at about 50 km height Chapter 6.

The Atla Region is chosen to be the deployment point of the VRS at 9S 199E. Figure 5.2 depicts the Venus topology and the existing volcanoes. For the localisation of the VRS the existing Venus surface maps will be used as mentioned in 11. Those maps have consistent resolution, but are more detailed at higher grounds. Also the mountains and volcanoes represent well recognisable features. The Atla Region has two of the highest elevation of Venus. The Maat Mons with about eight km and the Ozza Mons with five km height. The Aphrodite Terra, another highland, is also located in the equator area and has a variety of features that will be useful for localisation. The choice of the starting location is equally dependent on the fact, that the wind vertices are much less at the equator compared to the latitudes closer to the poles of the planet determined in Chapter 2. Therefore the VRS can be controlled with less effort.

5.3 Commissioning

The commissioning phase will begin immediately after separation from the Carrier Vehicle in case of the VRS and the Relay Satellites. The commissioning of the Relay Satellites is described in Chapter 6. The VRS will autonomously power on and put itself into Deployment Mode that is listed in table 5.1.

VRS is supposed to float with the winds of Venus while staying manoeuvrable as defined in MR03 of Table 3.3. This results in the VRS moving from east to west indicated in Chapter 2. Arriving at the desired altitude of 50 km the first contact to the Earth will take place as well as initial localisation and tracking will start. After that the subsystems are activated sequentially and the predefined calibration and validation procedures will be performed.

Guidance, Navigation and Control (GNC) described in Chapter 11 depends on the Synthetic Aperture Radar (SAR), the Inertial Measurement Unit (IMU) and the barometric altimeter (ALT). To ensure the stabilisation and localisation of the VRS the instruments will be initiated as first. The remaining equipment will start their commissioning procedures accordingly.

Part of the commissioning phase is a Scout drop at the Atla Region. The VRS will connect to the Scout an gather the data for testing purposes. The payload instruments on the Scouts can be activated after they reach a maximum velocity of 100 km/s. This will be possible at an altitude of about 76 km as specified in Chapter 9. Reaching the desired height, the Scouts turn on the instruments and perform a calibration procedure before starting their measurements.

5.4 Science Operation

The defined mission objectives in Chapter 3 state an operation time of five years. Therefore the plan of the VRS schedule also spans for five years.

The activities conducted by the VRS are describe by different modes. Table 5.1 depicts the defined modes, the used instruments as well as the experiments executed in the specific mode. The schedule of the science operations is constructed by lining up the different modes.
The Safe Mode describes the state the VRS only reaches, if a critical error occurs. Therefore the power consumption is reduced to a minimum. Every payload is switched off and only basic instruments are working to ensure a stable attitude and fast recovery.
After separation from the Carrier Vehicle the VRS will put itself into Deployment Mode. All instruments necessary for GNC are operating. The VRS is able to localise and determine the altitude to reach the initial position in Venus atmosphere. The Deployment Mode is also part of

the commissioning phase.
To establish connection with the Relay Satellites the VRS is set in the Data Transfer Mode. The antenna is pointing pointing in direction to the satellite. This state allows the transfer of Telemetry and Telecommands between the satellite and VRS.
The mapping of the surface of Venus is conducted in the Mapping Mode. The SAR is a shared instrument and operated as payload as well as GNC instrument. If the SAR is collecting surface data as payload instrument it is operated continuously. However, if it is only used for GNC purposes the instrument is only active periodically.
The Scout Mode of the VRS establishes a connection to a Scout to receive the data gathered while dropping. At the same time the VRS continues mapping Venus surface.
The experiments related to the Venus environment, weather and climate will take place in the Accumulation Mode. The magnetic field and radiation will be examined as well as wind, temperature and humidity measurements are taking place.
The Life on Venus (LoV) Mode is defined as placeholder for the experiment searching for life forms in Venus clouds. The experiment will be not part of this project as explained in Chapter 3.

Mode	**Description**	**Active Instruments**	**Executed Experiments**
Safe Mode	in case of mission critical error or failure	IMU, ALT	-
Deployment Mode	after launcher separation and while commissioning	IMU, ALT, SAR	-
Data Transfer Mode	connect to Relay Satellite	IMU, ALT, SAR	-
Mapping Mode	acquire Venus surface data	IMU, ALT, SAR	surface mapping
Scout Mode	receive data from Scout	IMU, ALT, SAR	Scout data and surface mapping
Accumulation Mode	acquire information of Venus environment, climate and weather	IMU, ALT, SAR, HIRS, MERTIS, IMA, UFFO, MAG, VAA	magnetic field, radiation, wind, temperature and humidity measurements
LoV Mode	acquire information of life in Venus atmosphere	IMU, ALT, SAR, LoV instrument	LoV experiment(s)

Table 5.1: Operation Modes of the VRS. BASED ON [66].

As pictured in Figure 5.1 and 5.3 the SO phase is composed of three sub-phases. Phase one (SO 1) is composed of the Data Transfer, Mapping and Scout Mode. The Accumulation Mode and the Data Transfer Mode will be executed in Phase two (SO 2). The VRS will start operating in SO 1 for one circumnavigation followed by the operation in SO 2 with the same circumnavigation. The alternating of those two phases will require about four years as evaluated in Chapter 16. Starting at the equator the VRS first moves south to -50° latitude and back to 0° and proceeds moving north until 50° latitude, after that returning to the equator. Finally the

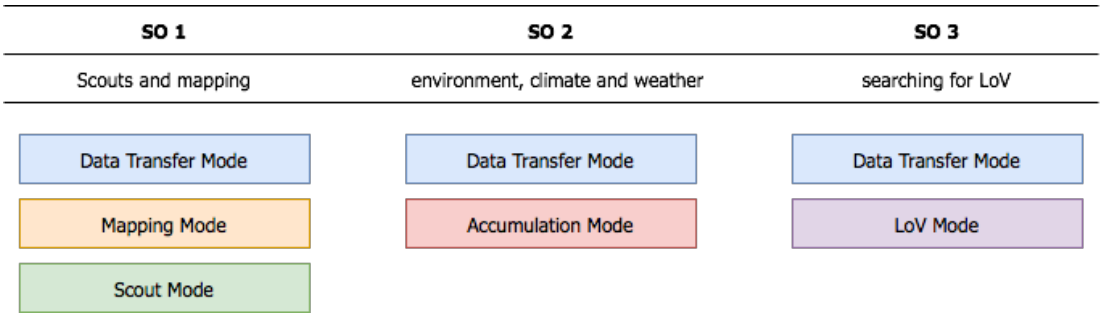

Figure 5.3: SO phases with assigned VRS operation modes.

phase three (SO 3) will be entered, which consists of the LoV Mode combined with the Data Transfer Mode. SO 3 is scheduled for one year also starting in the equator region.

The Scouts demand the VRS to be in communication range as it is expected that they only resist the harsh environment on the Venus surface for a short amount of time. This assumption is based on past missions with probes on the surface of Venus that would only last about two hours Chapter 2. The data transfer between Scouts and the VRS will take minimum one hour which is discussed in Chapter 14. While active the Scouts will be in the Dropping Mode where all the instruments are operating. After dropping one Scout in commissioning phase 14 Scouts are left to send them on their way to Venus surface. They will be deployed at $\pm 10°$, $\pm 30°$ and $\pm 50°$ latitude with respectively two Scouts at each latitude. One Scout will be dropped on the day side and the other one on the night side of Venus. This results in two Scouts being left as backup. They will be used if the connection to a Scout can not be established, the positioning of the station was faulty, the received data is abnormal and similar occasions. For the case that there are leftover Scouts they will be dropped at the equator region at towards the end of SO 1 and SO 2.

One scheduled circumnavigation at Venus is difficult to picture in one timeline because of the length of minimum 113 hours as determined in Chapter 9. Instead short schedule parts are displayed in 5.4.

Table 5.2 depicts the operation percentage of each payload instrument for one orbit for the different SO phases. The 13 % SAR operation in SO 2 and SO 3 result from taking one scan every hour for GNC. In SO 2 the other active instruments only stop data acquisition when the VRS is in the Data Transfer Mode which can also be deducted from the active instruments column in 5.1.

The operation of the payloads instruments will not change between day and night time. On one hand, the instruments are able to perform at night without the loss of data or quality. On the other hand, climate and weather analysis needs continuous data as stated by Section 5.4. Additionally, the Venus surface map should be complete. To gather complete surface data as well as environment, climate and weather information of the reachable area of $\pm 50°$ latitude the scheduled four years will be needed as simulated in Chapter 16. Therefore it is not feasible to differentiate the behaviour of the VRS between shadow and light times.

5.5 Decommissioning

The goal of the decommissioning phase is to restore the natural state of Venus environment. The mission objectives in Chapter 3 define that the mission should be performed with minimal

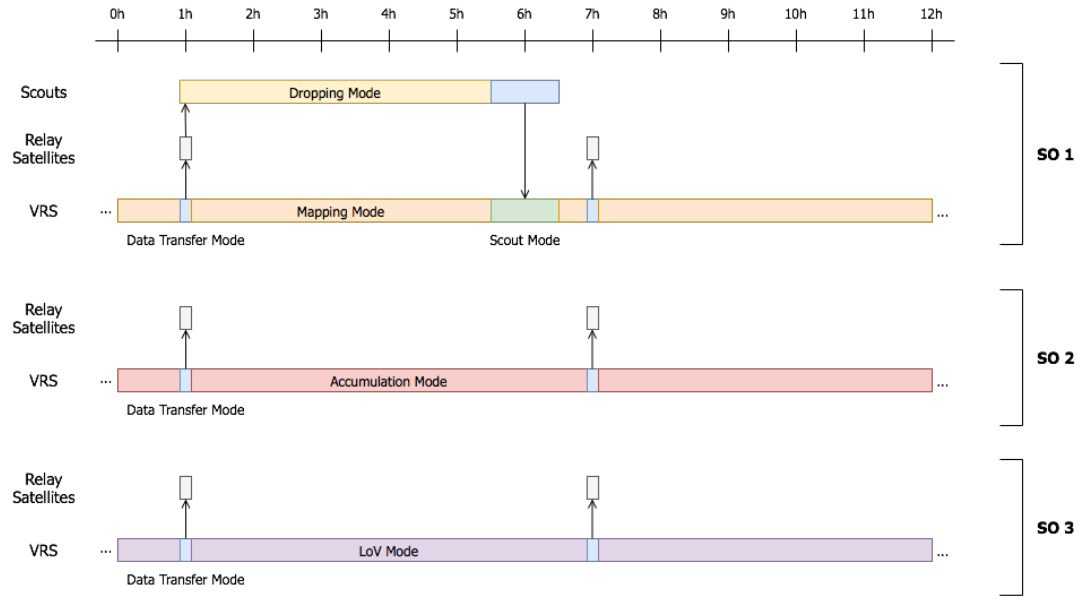

Figure 5.4: Schedule parts of system components categorised by SO phase.

Instrument	SO 1	SO 2	SO 3
SAR	100 %	13 %	13 %
HIRS	0 %	93.60 %	0 %
VERTIS	0 %	93.60 %	0 %
UFFO	0 %	93.60 %	0 %
IMA	0 %	93.60 %	0 %
VAA	0 %	93.60 %	0 %
OMAG	0 %	93.60 %	0 %
LoV instrument	0 %	0 % %	100 %

Table 5.2: Operation percentages of the payload instruments per circumnavigation and categorised by SO phase.

pollution of the planet. It is difficult to analyse the actual condition of the system components from Earth. If the operational lifetime is extended, the likely hood of failure increases.

In case of the Venus environment the burn-up approach is the most suitable. The high temperature at the surface ensures the destruction of all system components reaching the surface. The purpose of the Scouts is to hit the surface area. No further steps are needed and possible to perform the decommissioning. The VRS will also be intentionally dropped to the surface. This can be accomplished actively by utilising the propulsion system or passive by draining all the energy storage and causing the system to fail. The decommissioning of the Relay Satellites is described in Chapter 6.

CHAPTER 6

System Environment

by Yash Salian

This Chapter illustrates the critical significance that System Environment components have in the mission's success. Though not part of the system, these aspects have a significant impact on the mission's result, needing flawless coordination with the primary system to meet mission goals and requirements. This mission's primary System Environment aspects include Launch Systems, Earth-Ground Station Network (EGSN), and Relay Satellites. This Chapter further goes into interplanetary trajectory design and optimization, making use of cutting-edge software tools like pykep and pygmo [67]. Further investigation includes launch logistics, such as launcher type, launch site location, payload fairing constraints, and launch dates. Furthermore, the communication architecture used to facilitate data transfer between mission elements on Venus and Earth is described in depth.

From launch till the disposal of System Environment elements, a comprehensive Concept of Operations (Mission Scenario) evolves. Finally, the Chapter looks into the vital issue of Planetary Protection guidelines, highlighting the need of adhering to these criteria to protect the natural ecology of the target planet under research.

6.1 Launch Specifications and Near-Earth Operations

This Section brings forth the critical aspects of launch systems and Near-Earth operations which include the Launch and Early Orbit Phase (LEOP) followed by Rendezvous and Docking explained further in Section 6.4. These are the foundational phases that allow for a successful interplanetary mission. To boost the development of European launchers, maintain the European heritage of this mission, and follow the mission constraint BC01 in Table 3.6, the Ariane 64 launcher of the Arianespace Company, a subsidiary of the ArianeGroup was chosen. The Ogive-shaped fairing of the largest European launcher allows a maximum payload mass of 6900 kg to be launched at 2.5° declination with 2.5 km/sec of hyperbolic excess velocity (v_∞).[64] Considering the Hohmann Interplanetary Transfer, the hyperbolic excess velocity for departure comes to around 2.442 km/sec, thus further justifying the choice of the launcher. The size of the payload is constrained by the size of the fairing which is 20 m in height and has a maximum diameter of 5.4 m.[64] With its advantageous geographical location for space missions, the Spaceport *(5° 10' 8.4" N, 52° 41' 25.08" W)* in French Guiana emerges as the top launch site choice. However, a new location, ELA-4 *(5° 26' 46" N, 52° 79' 22" W)*, is being considered for further assessment.[64]

The launch vehicle integration sequence is rigorously planned by the experts to ensure a smooth and effective deployment operation.[64] Smaller antennae at Kourou[68] and NNO-2 (New Norcia 2, Australia)[69] are used for Near-Earth operations to provide efficient tracking

and telemetry downlink capabilities during the mission's vital early phases. Also, European Space Operations Centre (ESOC), headquartered in Darmstadt, will be the primary mission control centre during the Launch and Early Orbit Phase (LEOP) and scientific data gathering phase.

6.2 Communication Elements

This section focuses on the complex communication elements required for the interplanetary mission's success. The two main elements are the Earth-Ground Station Network (EGSN) and the Relay Satellites, both equally important to ensure the complete transfer of the highly crucial scientific data generated during the mission. These elements also allow the transfer of important telemetry and telecommand to-and-from multiple elements of the mission enabling the accomplishment of the mission requirements.

Earth-Ground Station Network (EGSN)

ESA's Tracking Station Network (ESTRACK) and NASA's Deep Space Network (NASA DSN) have been chosen as the main and the backup EGSNs, respectively, for this mission. The positioning of 35m antennas at Malargue, New Norcia, and Cebreros[70] assures the effective uplink and downlink of important scientific, telemetry, and telecommand data. The antennas at Cebreros and Malargue, in particular, provide Ka-Band downlink capacity for science data, supplemented by X-Band uplink and downlink capabilities for telemetry and telecommand data, considerably improving network dependability. Although the New Norcia 1 (NNO-1) presently only has X-Band downlink and uplink capability, plans are in the works to improve it to accommodate higher frequencies in the future.[71]

Relay Satellites

The Relay Satellites are critical components for improving communication between spacecraft and Earth. These satellites have Ka-Band downlink capabilities for Science Data, and they employ High Gain Antennas (HGAs) with precise pointing for efficient data transfer. The Relay Satellites are equipped with X-Band downlink and uplink capabilities, utilising Low Gain Antennas (LGA) or Medium Gain Antennas (MGA) combinations for telemetry and telecommand data transmission. Every relay satellite will have additional antennas, data storage components, and processing units to add resilience and redundancy.

For the level and extent of this project, the relay satellites have been considered as higher level systems with above mentioned necessary functionalities. This simplified the estimation of important parameters of these satellites such as mass, number of satellites, and orbital parameters at Venus. For mass estimation, the following approach was selected: From a database of 6718 satellites around the Earth, an average value of the mass of active communication satellites, with a lifetime of at least five years, and placed in a Low Earth Orbit (LEO) was chosen.[72] The estimated mass turned out to be 150 kg for such a satellite. The mass of the Relay Satellite was chosen to be twice this estimated value allowing some additional mass margin.

The second most influential parameter of the relay satellites was the orbit at Venus. A brute force technique was implemented using a simulation software known as Systems Tool Kit (STK) developed by Ansys[73] to fix the orbit, which was suitable enough to collect all the data from the Research Station and relay it to the EGSN while also providing polar coverage at Venus. In this technique, different types of orbits were simulated with the Relay Satellites. These orbits had different eccentricities, inclinations, and sizes. The Research Station was made

Parameter Name	Parameter Value
Orbit Type	Circular
Satellite Altitude	2000 km
Satellite Inclination	75 °
Number of Satellites	16 (14 + 2 back-up)
Mass of each Satellite	300 kg
Number of Contacts (per 24 hr)	59
Average Contact Time (per 24 hr)	1.35 hr
Time between contacts	0.42 hr
Average Contact Time with Earth GS	14.54 hr

Table 6.1: Relay Satellite Constellation parameter values.

to circumnavigate once around Venus at different latitudes such as 0°, 55°, and 75°. This can be clearly seen in Figure 6.1 as the red, green and yellow lines at different latitudes. Also, the inclination of the orbit was varied as 0°, 30°, 55°, and 90°(polar). The access times between the Relay Satellites and the Research Station was calculated from the above simulations. Also, the access times with the Earth ground station was evaluated. Keeping in mind the link margin restrictions from Chapter 15, the orbit with 2000 km orbital altitude above the surface of Venus, with an inclination of around 75° was chosen, as it provided the best trade-off between access time with the Research Station, polar coverage, and access time with Earth ground station.

The calculated access times were provided to Chapter 14, which in turn provided the minimum number of satellites required to successfully transfer all the scientific data generated during the mission duration. Thus the minimum number of satellites turned out to be fourteen, along with two extra satellites for redundancy, thus taking the total to sixteen satellites. Considering only fourteen satellites, it can be observed in Section 14.5 that the minimum transmission speed required by each satellite to transmit to Earth's ground station is around 3.5 Mbps. And the work by Dr. Leslie J. Deutsch, et al[74] provides the current minimum and maximum transmission speed possible from Venus, which turns out to be 5 Mbps, and 320 Mbps, respectively. Even the current minimum rate is higher than the required transmission rate, thus making Ka-Band very desirable in this mission. All the above parameters are crucial as they directly affect the mission scenario discussed further in Section 6.4.

The layout of the communication elements, as seen in Figure 6.1, is carefully designed to assure optimal data transmission during the interplanetary journey by utilising cutting-edge technology, carefully selected ground stations, and robust Relay Satellites. These efforts lay the groundwork for the successful transfer of priceless scientific data from the mission's trip to Venus, which will open up new horizons in space science and our understanding of the planet.

6.3 Interplanetary Trajectory Design and Optimization

The major goal of this part is to methodically design, optimize, and present the interplanetary trajectories required for the multiple launches described in Section 6.4. The section begins by delving into the processes and tools used for trajectory design and optimization. Following that, a detailed review of all the trajectories that meet mission criteria is offered. Finally, a short yet thorough summary of the chosen trajectory is produced, allowing the finalization of critical launch-related parameters such as launch dates and interplanetary phase time of flight.

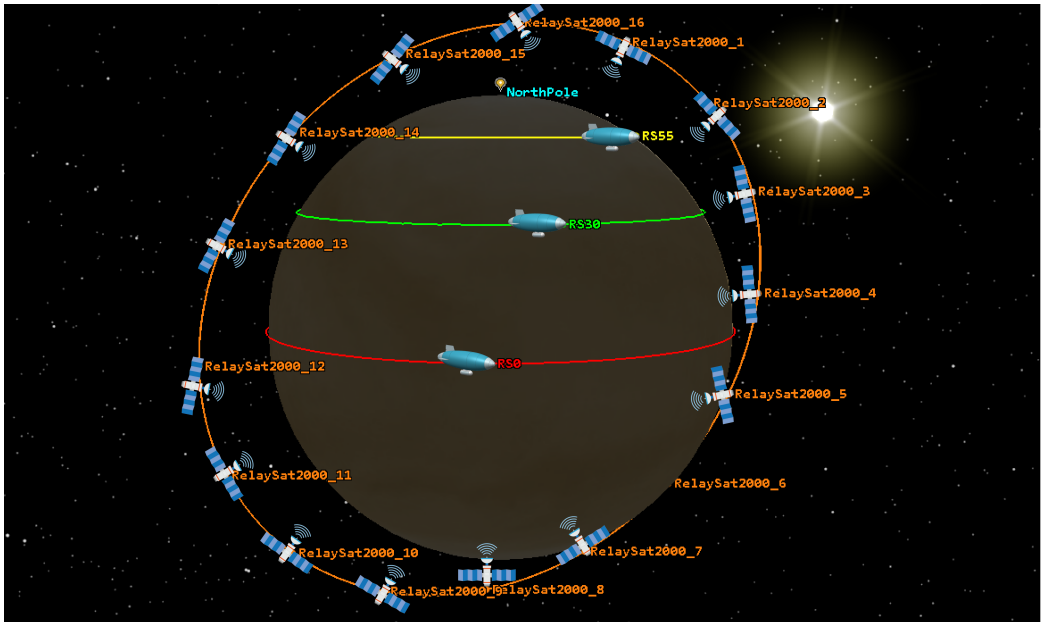

Figure 6.1: STK Simulation to evaluate the access times between Relay Satellites and the Research Station. Evaluation is done with single Research Station at different latitudes.

Methods and Tools

This section delves into the integration of the pykep and pygmo libraries for trajectory design and optimization. These key libraries were used to help with sophisticated computations and trajectory planning for interplanetary missions. The planets were instantiated using the Keplerian elements from the JPL Horizons System App[75] as the initial stage in the trajectory design process. The retrieval epoch for these planetary Keplerian Elements was June 21st, 2023. A User Defined Problem (UDP) with constraints and objective functions was created to accomplish efficient trajectory optimization. The planet-to-planet single leg with 'n' impulses problem structure from the trajopt module was utilized as a suitable UDP for the optimization process.

The UDPs included a plethora of critical characteristics, such as planet sequence, launch period, and allowed time of flight for each segment or the entire mission. Furthermore, target orbit factors such as perigee and eccentricity influenced the trajectory results. Using Hohmann Transfer to calculate flight duration, the number comes out to be roughly 150 days. This allowed the entire interplanetary trajectory's flight duration to be constrained between 100 and 200 days. Furthermore, the hyperbolic excess velocity (v_∞) was limited to 2 - 2.5 km/sec following the restrictions from launcher system as seen in Section 6.1

Finally, to get a more realistic delta-V budget, the maximum number of impulses permitted for each leg of the trajectory was set to five. After establishing a solid structure in UDP formulation, the next stage was to design and instantiate algorithms using the pygmo algorithm class. The construction of two islands, each with its own set of characteristics, was a key milestone in the trajectory optimization process. Each island used a unique algorithm to drive the development of many populations (initial random solution vectors) toward various optimized solutions. The optimization process was then initiated by executing the evolution of populations on each island using the evolve() method. The algorithms chosen were Particle Swarm Optimization Algorithm

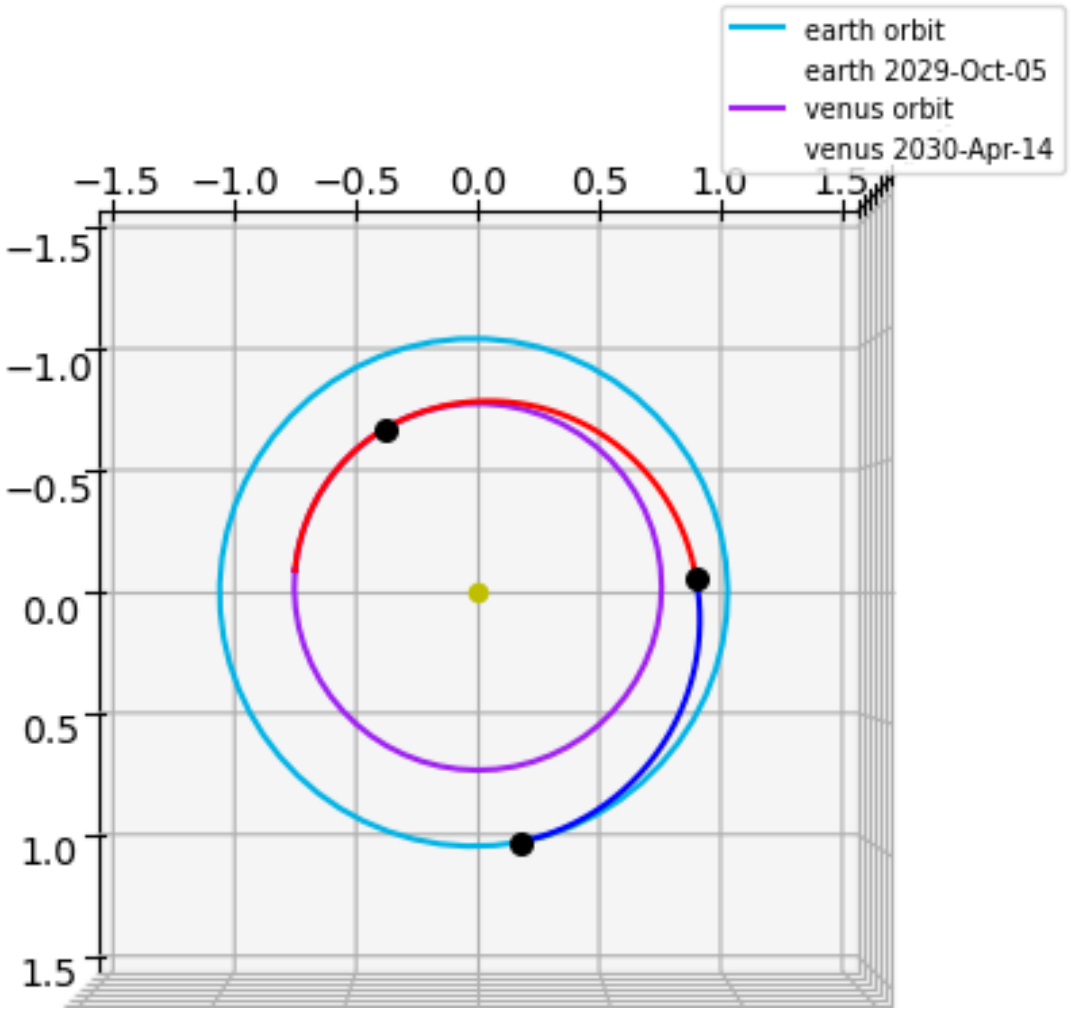

Figure 6.2: Interplanetary Trajectory from Earth to Venus for Launch 1.

and Simple Genetic Algorithm on each island. Finally, the Archipelago consisting of these two islands was optimized further using Simple Genetic Algorithm.

The optimization process was completed within the Archipelago, where the different populations were refined and optimized to find the optimum mission trajectory. The primary goal was to reduce the delta-V between 2025 and 2050, guaranteeing a trajectory that was perfectly consistent with the mission's objectives. The timeline was chosen following the Mission Requirement MR01 from Table 3.3.

Results

Following the aforementioned procedure, several trajectories for the 25 years 2025-2050 were discovered. The following Table **??** summarizes these trajectories. In this table, the green row indicates the best overall delta-V optimal trajectory, while the red row represents the worst trajectory with neither an affordable delta-V budget nor a quicker transfer time. The

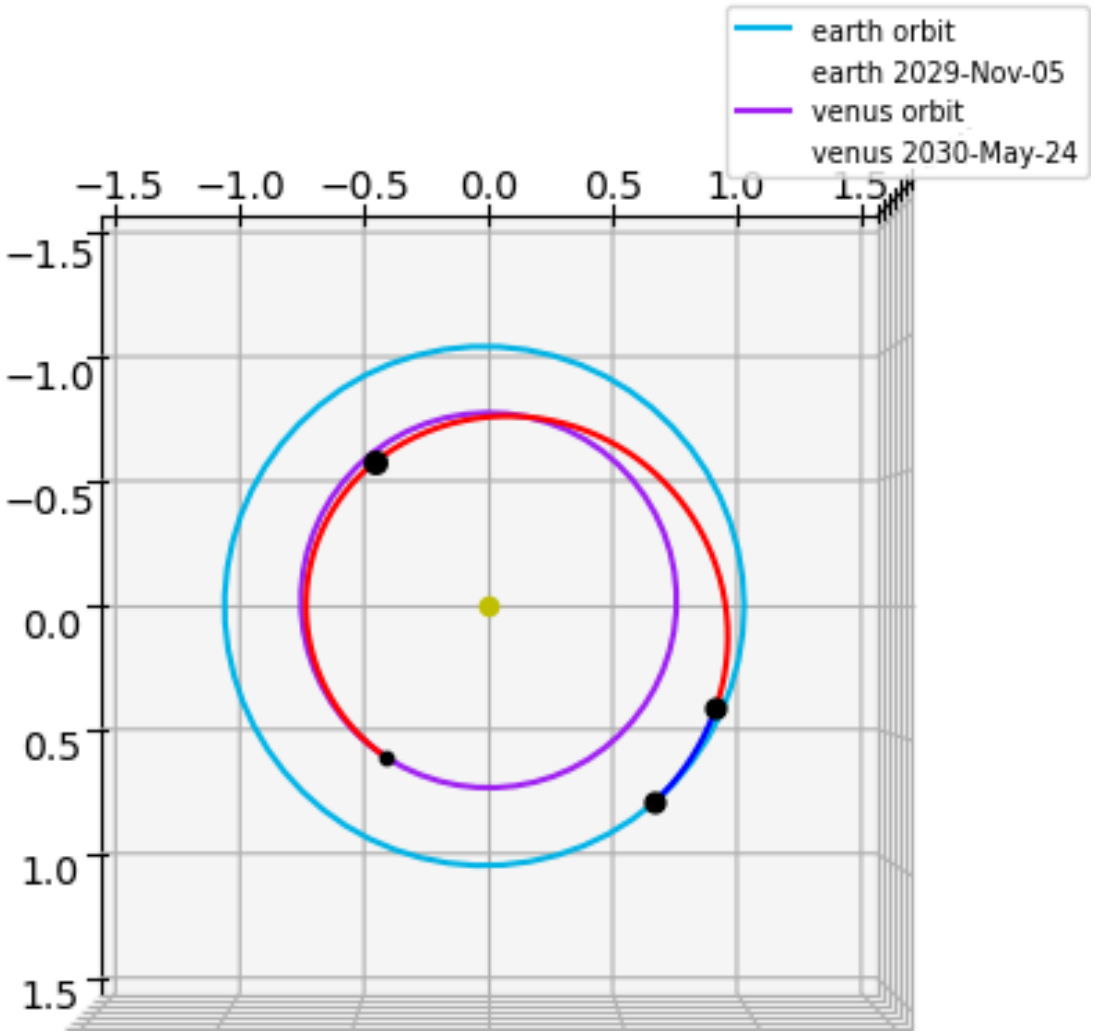

Figure 6.3: Interplanetary Trajectory followed post docking between Launch 2 and 3 elements.

yellow-colored trajectory represents a trade-off between delta-V and flight duration. It has the shortest transfer time, but the delta-V need is larger than in the green-colored trajectory. The delta-V optimal trajectory is chosen for this mission, however depending on the time required for system development, testing, and other logistical difficulties, any alternative trajectory with the appropriate trade-off between delta-V and transfer time can be chosen. The selected trajectory additionally provides opportunities for interplanetary and planetary capture manoeuvres.

Figure 6.2 and Figure 6.3 depict the Launch 1 (Phase 1) and Post Docking (Phase 2) interplanetary trajectories. Launch 2 occurs about ten days before the interplanetary departure, but Launch 3 occurs in five days after Launch 2. On-trajectory manoeuvres are shown by the black dots. The size of these dots indicates the magnitude of the manoeuvres. The use of a highly elliptical capture orbit decreases the planetary capture delta-V demand.

Sr No.	Departure Date	Arrival Date	Total Delta V [m/sec]	Transfer Time [days]
1	05-Oct-2029	14-Apr-2030	6252.619	190
2	11-Dec-2032	29-Jun-2033	6712.418	199
3	13-Jun-2034	30-Dec-2034	6913.188	200
4	22-Jan-2036	09-Aug-2036	7623.812	199
5	05-Sep-2037	24-Mar-2038	6486.980	200
6	07-Dec-2040	27-May-2041	6455.307	171
7	24-Jun-2042	10-Jan-2043	6761.043	200
8	06-Feb-2044	24-Aug-2044	7176.744	199
9	20-Sep-2045	29-Mar-2046	6461.900	190
10	11-Dec-2048	21-Jun-2049	6606.973	191
11	05-Jul-2050	21-Jan-2051	6706.106	200

Table 6.2: Optimized Interplanetary Trajectories between 2025-2050

6.4 Concept of Operations

The Concept of Operations section gives a thorough overview of the complexities involved in successfully coordinating an interplanetary trip to Venus. This section is separated into three major phases, each of which includes important components and activities that are critical to the mission's success. The deployment of Relay Satellites and Scouts in Phase 1 marks the start of this tremendous adventure. The deployment of the Research Station, a critical milestone in the mission's scientific objectives, is part of Phase 2. Finally, Phase 3 looks into all mission elements' End-of-Life Disposal (Decommissioning) processes. From launch logistics through End-of-Life Disposal, this section covers every facet of the interplanetary mission's successful execution.

Phase 1: Relay Satellites and Scouts Deployment

Launch 1 The ambitious interplanetary mission begins on October 5, 2029, with the launch of Ariane 64, which will transport 16 Relay Satellites and 15 Scouts to Venus. Each Relay Satellite weighs over 300 kg, while each Scout weighs around 30 kg. The launch consists of two carrier vehicles, each of which is responsible for capturing the assets in the required Venus Orbit, placing the Relay Satellites into an orbital constellation, and assisting the Scouts' atmospheric entry. These carrier vehicles are equipped with propulsion systems that allow them to perform interplanetary phase trajectory adjustment manoeuvres, planetary capture manoeuvres, orbit correction manoeuvres, and end-of-life atmospheric burn-up manoeuvres. They also have communication modules for telemetry and telecommand communication with Earth, on-board computing and processing units dedicated to telemetry and telecommand processing, and an elementary power system capable of supporting communication and on-board computing while potentially allowing recharging for relay satellites and scouts. A dispenser mechanism, similar to that used for multi-satellite deployment in Low Earth Orbit (LEO), aids in the deployment of the Relay Satellites. The Scouts, on the other hand, have been equipped with an Entry, Descent, and Deployment System (EDDS), that comprises heat shields, parachute deployers, parachutes, thrusters, and other components required to ensure successful atmospheric entry

and deployment.

Planetary Capture After the launch and the interplanetary phase, which lasts around 190 days as seen from Table **??**, the mission begins the Planetary Capture phase, which continues for roughly 30 to 45 days. During this phase, the mission crew performs essential manoeuvres to place the Relay Satellites and Scouts in the proper orbits. This time is critical for setting up and testing the relay satellite constellation, as well as ensuring that the assets are appropriately positioned before the Research Station arrives at its destination orbits. The Relay Satellite Carrier Vehicle and the Scouts Carrier Vehicle separate as the interplanetary phase comes to an end. Both spacecraft are captured in an initial capture orbit around Venus that is highly elliptical. They reach their target orbits after many days of manoeuvres and orbit adjustments. These capture orbits require minimum delta-V, and have the advantage of longer periods which can be utilized for initial set-up and testing. The Relay Satellite Carrier Vehicle has a 2000 km circular orbit with an inclination of 75°. The method and justification for the choice of such an orbit are provided in Section 6.2. On the other hand, the Scouts Carrier Vehicle is put in a polar orbit with dimensions of 300 x 15000 km, a configuration tailored to suit flight dynamics as mentioned in Chapter 9 and coverage requirements.

Relay Satellite Constellation Deployment The deployment of the Relay Satellites begins after the carrier vehicle is in its respective target orbits. The deployment procedure entails carefully placing the Relay Satellites to construct a resilient and efficient constellation orbiting Venus. At the end of this phase, the Relay Satellite Carrier Vehicle ascends to a higher orbit, strategically positioned to serve as a stable backup for telemetry and telecommand transmission. This enables continuous communication and control capabilities throughout the mission

Scouts Deployment After the Research Station has been successfully established, the Scouts will be sent. The Scouts are intended to remain in orbit at first with their Carrier Vehicle but can be manoeuvred into the Venusian atmosphere for scientific study. The Scouts additionally have an Entry, Descent, and Deployment System (EDDS) consisting of heat shields, parachute deployers, parachutes, and thrusters, which allows them to get deployed in the Venusian atmosphere after being ejected from their Carrier Vehicle in orbit. Their deployment procedures include accurate entrance into Venus's atmosphere, aerodynamic slowing with heat shields and/or aeroshells, parachute deployment to reduce the velocity, and a final descent for successful landings on Venus's surface. The Scouts continue to broadcast crucial information from the surface of Venus to the Research Station and back to Earth after landing. A more detailed evaluation of the deployment procedures can be found in Chapter 9.

Phase 2: Research Station Deployment

Launch 2 and 3 Launch 2 and Launch 3 play critical roles in Phase 2 of the interplanetary voyage, with a time gap of 10-15 days between them. Launch 2 is scheduled for October 27th, 2029, and will include critical components like the Gondola, Propulsion System, Antennas, Flight Control Systems, Balloon, and Helium Tanks. Launch 3, on the other side, is slated for November 1st, 2029, and will carry Cargo, Onboard Computers, Batteries, Air Tanks, and the Research Station Carrier Vehicle.

Parking Orbit Docking Following their flights, the systems from Launch 2 and Launch 3 will be placed in a circular orbit 200 to 500 km above Earth. The main advantage of choosing such an orbit is the availability of vast docking experience with the International Space Station

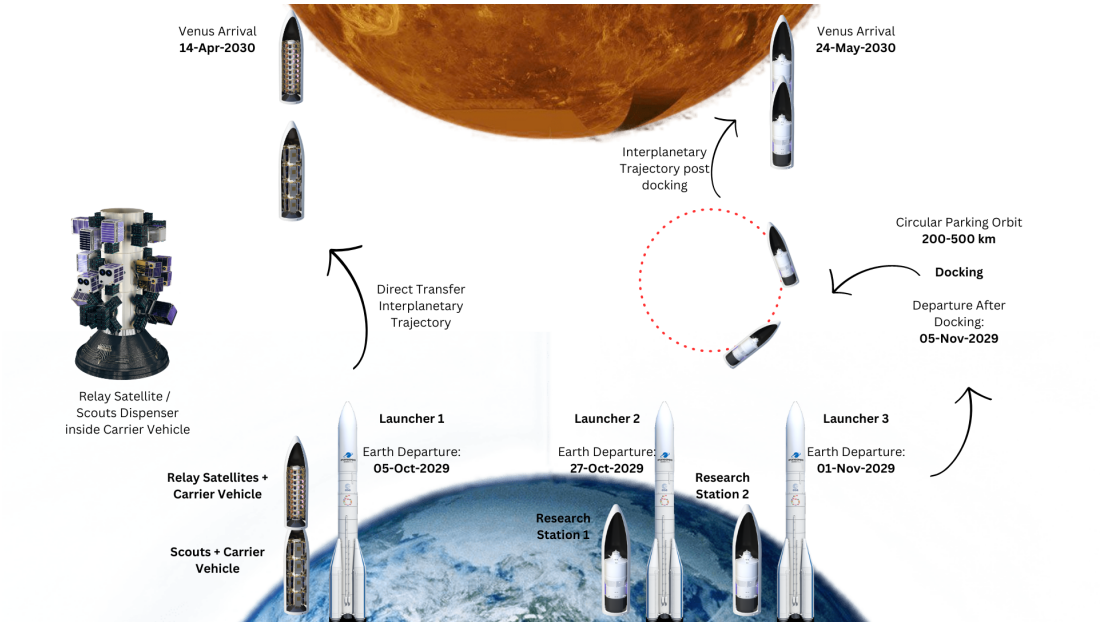

Figure 6.4: Concept of Operations of Phase 1 and Phase 2.

(ISS). With proximity to Earth, improved control, monitoring, and communication are possible, resulting in minimum communication lag throughout this stage. Once docked in the specified parking orbit on November 5th, 2029, the combined systems will begin the interplanetary phase, mapping a course toward Venus. During this phase, the Research Station Carrier Vehicle, which has capabilities comparable to those of the carrier vehicles for Scouts and Relay Satellites, ensures the Research Station arrives safely at its destination.

Planetary Capture On May 24th, 2030, the Research Station Carrier Vehicle gets captured in Venus's initial capture orbit, which has a high eccentricity and a prolonged orbital period. During this phase, connectivity with the Relay Satellites begins, enabling continuous telemetry and telecommand capabilities.

Research Station Deployment Precisely planned manoeuvres allow the carrier vehicle to be separated and the Research Station to enter the Alta Region at the specified periapsis point of 9S 199E as suggested in Chapter 5. This strategic decision maximizes mapping and scientific observations during the Research Station's mission in the Venusian atmosphere. Similar to the Scouts, the Research Station does not have a separate Entry Vehicle. Instead, it is outfitted with a sophisticated Entry, Descent, and Deployment System (EDSS) as described in Section 6.4. This precisely engineered system allows for precise entry and deployment into the Venusian atmosphere. This system allows peak heating and deceleration utilizing heat shields and/or aeroshells, parachute deployment to further reduce velocity, and balloon inflation during a more gradual descent in the thick atmosphere. Once the inflation process is complete, the Research Station can begin its scientific and navigation operations at the required altitude.

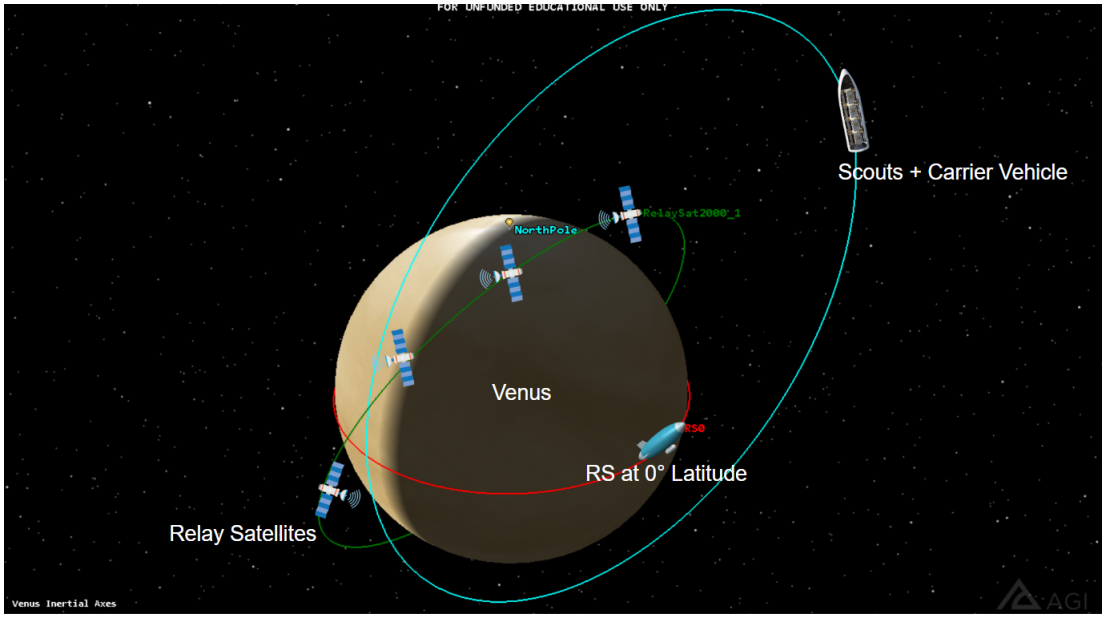

Figure 6.5: Final Arrangement of System Environment Elements after the successful completion of Phase 1 and Phase 2.

Phase 3: End-of-Life Disposal (Decommissioning Phase)

As the interplanetary mission to Venus approaches its conclusion, thorough End-of-Life (EOL) disposal processes are established to appropriately dispose of the project's numerous elements. Each component, including the Research Station, Scouts, Relay Satellites, and Carrier Vehicles, goes through a specialized EOL procedure to guarantee safe and regulated decommissioning while minimizing any potential influence on future exploration efforts. After completing its mission goals, the Research Station prioritizes the transmission of all relevant data back to Earth for assessment and future reference. To eliminate any potential risks during disposal the Research Station's onboard supplies, notably batteries, are completely exhausted to avoid explosions after a crash landing. The balloon's controlled depletion helps its steady entry into Venus's atmosphere. The landing site is carefully picked, to avoid damage to vital areas for future navigation and active sites like volcanoes, following planetary preservation requirements. Natural climatic factors cause the Research Station and its balloon to disintegrate over time, leaving no permanent traces on Venus.

Similarly, after relaying their critical data, the Scouts are instructed to avoid direct contact with significant active spots on Venus during their EOL period. The Scouts and their parachutes naturally dissolve over time due to climatic circumstances, leaving no substantial influence on the planet's surface.

The Relay Satellites' EOL procedure begins with the priority relay of critical data back to Earth. The Relay Satellites are designed to outlast the Research Station and Scouts, therefore all fuel and batteries are depleted to prevent explosions at atmospheric arrival. A regulated and managed decommissioning approach is used, with each Relay Satellite being deactivated and decommissioned sequentially to minimize danger during disposal. The satellites' hardware and architecture are meticulously adapted to minimize fragmentation during atmospheric entry,

guaranteeing that any remnant debris offers low risk to future missions. This technique is called Design for Demise practiced by European Space Agency (ESA).[76]

Carrier Vehicles, which play key roles in the operation, are likewise subject to particular EOL procedures. The first part to be discarded is the Research Station Carrier Vehicle. After the Research Station is successfully deployed, the carrier spacecraft reaches the Venusian atmosphere for controlled burn-up, assuring a safe and deliberate disposal process. The Scouts Carrier Vehicle and Relay Satellite Carrier Vehicle are both passivated and slated for atmospheric descent, with the sequence meticulously planned to guarantee optimal disposal.

Finally, the interplanetary mission's End-of-Life Disposal (Decommissioning) phase demonstrates appropriate space exploration procedures. Each aspect of the project is carefully managed to ensure the retrieval of vital data, safe disposal, and little influence on Venus's ecosystem. By following these precise processes, the mission leaves a record of successful exploration and scientific development while protecting the integrity of future missions to Venus and beyond.

6.5 Planetary Protection Guidelines

Exploration of celestial worlds such as Venus and Mars is followed by the necessity for planetary preservation to maintain their pristine habitats and avoid any contamination. While no particular guidelines have been created for Venus or Mars, worldwide scientific organizations such as COSPAR[77] have made proposals to regulate planetary preservation actions. Furthermore, in the publication ESSB-ST-U-001[78], the European Space Agency (ESA) has outlined its planetary protection standards.

The ESA's planetary protection strategy includes numerous critical factors to guarantee the confinement and sterilization of spacecraft and landers. Decontamination techniques[79] are an important component of these rules, focused on sterilizing or lowering the microbial load aboard spacecraft and landers to avoid forward contamination of future planets and moons. Cleanroom practices are also stressed, mandating tight requirements for maintaining sterile and controlled settings throughout spacecraft construction, integration, and testing to limit the entry of pathogens. Bio-burden reduction strategies are critical in lowering the number of germs on flying gear. To reduce the existence of microorganisms that may potentially hitch a ride on the spacecraft to another celestial body, methods like dry heat or hydrogen peroxide treatment are used. To ensure compliance with planetary protection criteria, microbial inspection processes are created to carefully test and monitor the cleanliness of spacecraft components and cleanroom environments.

Passivation processes are used to drain energy stores and prevent post-mission explosions or inadvertent biological material releases during spacecraft disposal. This guarantees that the disposal procedure is carried out appropriately and without harming the target planet or moon.

Additional safeguards are in place for Category 4 missions[77], which include probes and landers. These precise methods to protect against possible contamination are detailed in the ESSB-ST-U-001 publication. Containment precautions are put in place to treat and isolate any potentially dangerous elements that sample return missions bring back to Earth. This ensures that any possible biological or chemical dangers are appropriately controlled and handled.

The necessity of following planetary protection principles cannot be stressed as space exploration increases. The scientific community assures that the search for extraterrestrial life and the exploration of celestial bodies are undertaken responsibly and ethically by adhering to these rules. These safeguards are critical for ensuring the integrity of future missions and the possibility of groundbreaking discoveries beyond our planet.

CHAPTER 7

Payload

by Hiba Alnoor and Jeena John

This Chapter includes detailed information about payloads on Venus Research Station along with their work. Payload is a component on board that carries out the primary mission objectives of a spacecraft. They are mission specific and are designed, operated and delivered by the spacecraft or vehicle. These technological instruments vary in shape, size, properties and composition. A few examples are communication payloads, navigation payloads, payloads for measuring magnetic and electric fields and payloads for measuring temperature and pressure. They all observe different properties. For our mission, the payloads have been separated into two Sections. The ones that will be carried by Venus Research Station (main station) and the ones that will be carried by the scouts or probes. Payloads on the main station refers to the assortment of experiments, equipment, and provisions transported by spacecraft and connected to the station. These payloads encompass a wide range of items, including scientific instruments, research experiments, spare parts, and supplies for the crew. Whereas, payloads on scouts are the collection of scientific instruments, equipment, and tools that are carried by the space scouts to carry out a wide range of experiments and missions. These payloads are selected with utmost care and precision to suit the particular goals and objectives of each specific mission. Table 7.1 shows the distribution of payloads.

Payloads on VRS	Payloads on Scouts
SlimSAR	Venus Surface wind sensor
High Resolution Infrared Radiation Sounder/4 (HIRS/4)	Miniaturised Infrared Spectrophotometer
Orbiter Magnetometer (OMAG)	BIMS (Ion Mass Spectrometer)
Venus Acoustic Anemometer	Venus Radiometer and Thermal Infrared Spectrometer (VERTIS)
Venus Radiometer and Thermal Infrared Spectrometer (VERTIS)	MHP-3.80-001 Miniature Very High Pressure Sensor
Ion Mass Analyzer	
UFFO (Ultra-Fast Flash Observatory)	

Table 7.1: Payload overview for the mission.

7.1 Payload on Venus Research Station

In this Section, the payloads on Venus Research Station will be presented and discussed.

A) SlimSAR

SlimSAR will be used for mapping the Venus Surface but with some advancements. SlimSAR is an innovative, small and cost-effective Synthetic Aperture Radar that represents a significant advancement in high-performance SAR technology. It utilizes a unique design methodology, building on previous developments to achieve a compact and lightweight form while consuming less power compared to typical SAR systems. The mission requires a low mass SAR system which should operate at almost 50-60 km of altitude but SlimSAR is originally designed to operate at 2 km above ground level. One of the advantages of SlimSAR is that it is highly flexible which means that various advancements can be done according to the mission. It has a built-in power amplifier and an external power amplifier can also be added. Through this, the peak power can be increased which may further increase the range and altitude. It will still be a lightweight SAR system but with high peak power and altitude which will be designed according to our mission requirements. Also, for this mission, two SlimSARs will be used to improve the performance and range as shown in Figure 7.1 [80].

SlimSAR is an active payload. It sends out radio waves and microwaves toward the target. These waves bounce back after interacting with the target. By studying these reflected signals, radar instruments can extract important details about the target's characteristics, like the distance, speed and size. It operates in the L-band and the radar core of this instrument includes frequency block converters, making it a great fit for small Unmanned Aerial Systems (UAS's). It uses a linear-frequency modulated continuous wave (LFM-CW) signal, which maintains a high signal-to-noise ratio with minimal power consumption and pulsed mode. Direct Digital Synthesizers are used to generate two identical signals. One of these signals is delayed by the time it takes for the radar signal to travel to the nearest range of the area being imaged. When

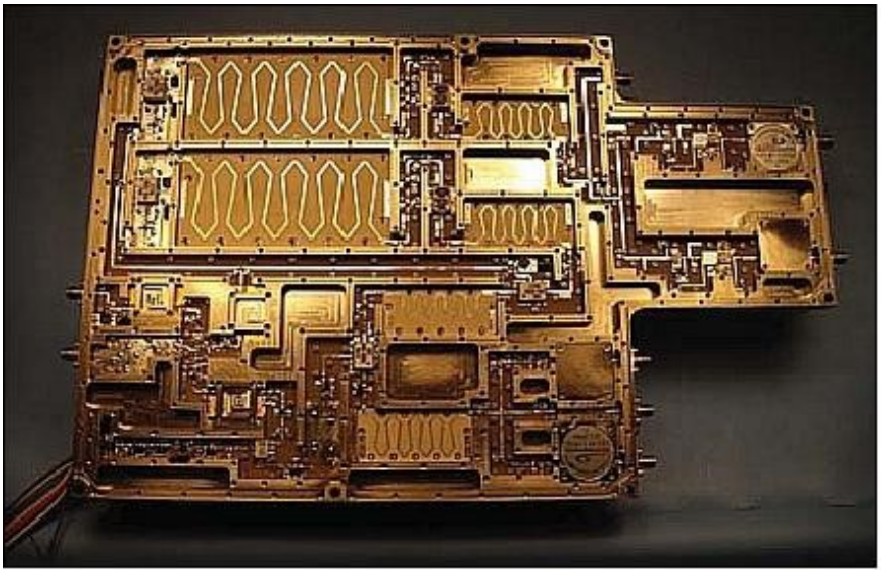

Figure 7.1: SlimSAR for mapping Venus Surface

the received radar signal is mixed with this delayed signal, the overall bandwidth is reduced, which helps to lower the sampling requirements. A delayed mix-down chirp is employed to increase the swath width allowing a wider coverage and more comprehensive imaging of the desired areas. It also has highly flexible control software which allows real-time adjustments to radar parameters during flight. It is equipped with a built-in high-quality GPS/IMU motion measurement solution, a small data link and a gimbal for the high-frequency antennas. It is a versatile instrument used in remote sensing and surfacing mapping of earth and other planets. It provides valuable data about topography, geology, agriculture and snow cover by analyzing differences in surface reflection. One of its applications is predicting snowmelt, while it can also be utilized to detect and monitor floods. Moreover, SAR data serves multiple purposes such as planetary observation, navigation and object detection and recognition.

B) High Resolution Infrared Radiation Sounder/4 (HIRS/4)

A High-Resolution Infrared Radiation Sounder shall be used in our mission as shown in Figure 7.2 [81]. It will serve as an atmospheric sounding instrument to measure various atmospheric properties such as temperature profiles, moisture content, cloud height and surface albedo. This instrument has an operating temperature range of $-40\ ^\circ$ to $+50\ ^\circ$ Celsius and a data generation rate of 2.88 kbps. It functions as a passive payload which means that it only detects and measures the infrared radiation that is naturally emitted by the target. It does not emit its signals or energy; instead, it relies on capturing existing natural radiation to gather valuable data and make important observations.

HIRS/4 utilizes seventeen specific spectral channels, which include a visible window around ($0.693\,\mu$m), a surface temperature window around ($3.71\,\mu$m), and a long wave window around ($11.1\,\mu$m). Among these channels, seven are dedicated to measuring CO_2 absorption for temperature sounding, two are used for water vapor sounding and five short wave channels provide data for temperature sounding related to NaO and COa. To perform this data collection efficiently, the instrument uses multiplexing, which involves three detectors and a single telescope.

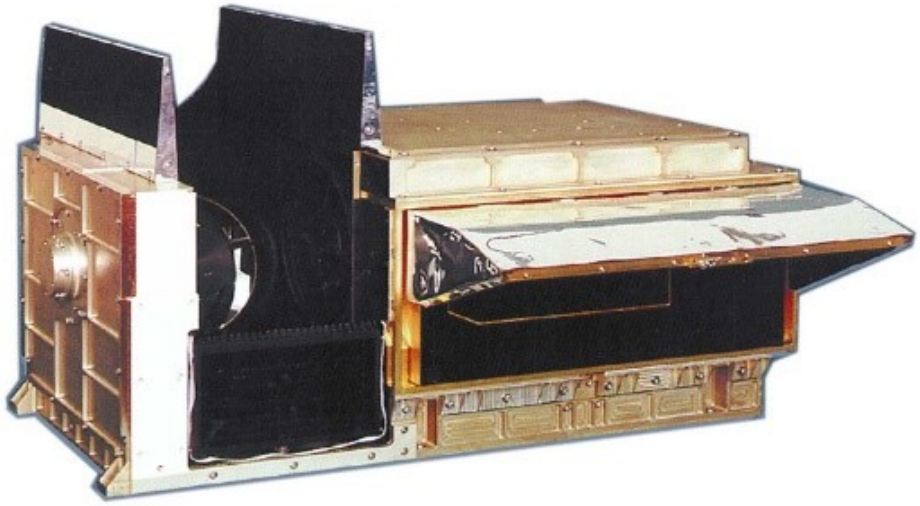

Figure 7.2: HIRS for Atmospheric Sounding

A filter wheel containing the seventeen spectral filters allows the instrument to switch between channels as needed for comprehensive data acquisition. A high-resolution infrared radiation sounder is primarily designed for atmospheric sounding purposes. It can measure various parameters such as water vapor, ozone, N_2O (nitrous oxide), as well as cloud and surface temperatures. It allows researchers and scientists to gain insights into atmospheric conditions and study various important atmospheric components. Major applications include; measuring ocean surface temperatures, cloud height and coverage and surface radiance.

C) Orbiter Magnetometer (OMAG)

For this mission, a magnetometer similar to an orbiter magnetometer (OMAG) will be used as shown in Figure 7.3 [82]. OMAG also known as Pioneer Venus Orbiter was used in the Pioneer Venus mission. The primary objective of the instrument was to measure the magnetic field. During the Venus orbit, the spacecraft experienced variations in sample rates allowing OMAG to capture data at different intervals depending on the specific region and phase of the spacecraft's orbit around Venus. It is a light weight instrument requiring an average of 2.2 W power only.

OMAG is a passive payload as it is used to measure the magnetic field of celestial bodies like planets and moon. It does not emit any signal or energy. It relies on detecting and analyzing the natural magnetic fields by observing how they interact with the sensor on the spacecraft. This payload has an atomic vapor cell which contains alkali metal atoms that possess unpaired electrons with inherent magnetic characteristics. These atoms are highly responsive to external magnetic fields. Through optical pumping, the atoms are pumped and using laser light, they are energized and elevated to higher energy levels. Electrons rotate around the direction of the external magnetic field which is proportional to the strength of the magnetic field. This leads to a change in the orientation of the atom's magnetic moments. As atoms return to their ground state, they can absorb and emit the polarized light which can be detected. A

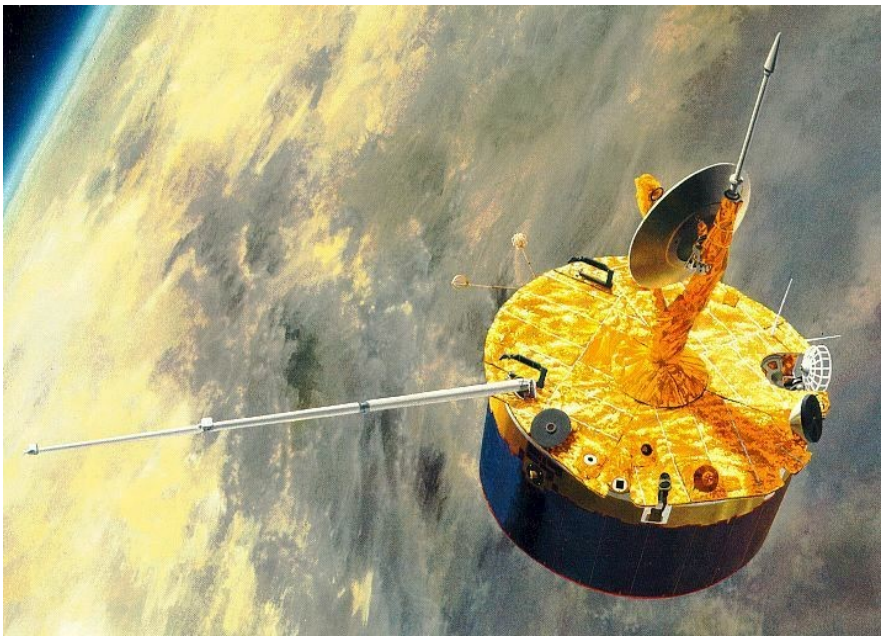

Figure 7.3: OMAG for measuring magnetic field

photodetector measures the intensity of the transmitted light. The variation in this transmitted light intensity is then used to determine the strength and direction of the external magnetic field which is used to investigate the magnetic properties of the observed celestial body. The major application of OMAG is to measure the magnetic field of a celestial body. It is used for the measurement of planetary and interplanetary magnetic fields. It is also used to investigate the nature of the magnetosphere's interaction with the satellite and examine the magnetospheric-ionospheric coupling. The data gathered helps scientists in studying the magnetic properties and characteristics of the body providing insights into its magnetic field and related phenomena.

D) Venus Acoustic Anemometer

It is a hypothesized instrument that comes from the idea of the Venus Wind sensor as shown in Figure 7.4 [83]. This instrument will specifically be designed for Venus's surface and will be able to tolerate harsh environments. It will rely on the measurement of acoustic waves generated by natural or artificially induced sound sources and their propagation through the Venusian atmosphere. By analyzing the acoustic wave signals, information about wind speed, turbulence characteristics, and atmospheric conditions can be extracted. It'll be a lightweight low power consumption instrument. Acoustic anemometers are categorized as active payloads. They actively produce ultrasonic sound waves and measure the time taken by these waves to travel between their transducers. This active probing helps the instrument to collect some valuable data. The instrument will consist of a sound source (e.g., a speaker) and a set of strategically placed receivers that will detect and measure the acoustic signals at various distances. Parameters such as Doppler shift, sound attenuation, and phase differences between received signals will provide insights into wind speed, turbulence, and atmospheric conditions. The instrument will consist of ultrasonic transducers which will be capable of emitting and detecting the sound waves at ultrasonic frequencies. The wind speed will be calculated based on the time taken by the waves to travel to the transducer. The instrument will collect data which will be then processed and converted into wind speed and direction values. Venus acoustic anemometer will be used to measure wind energy. Can also be used for meteorological research and environmental monitoring.

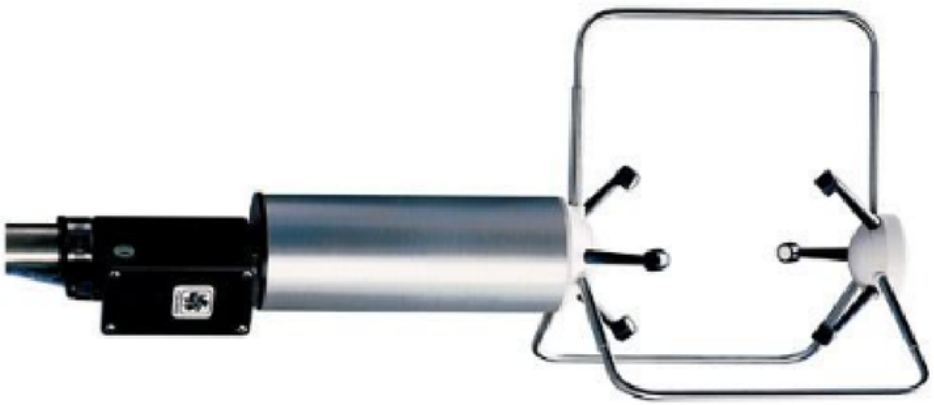

Figure 7.4: VAA for measuring wind energy

E) Venus Radiometer and Thermal Infrared Spectrometer (VERTIS)

Another proposed instrument for the mission is Venus Radiometer and Thermal Infrared Spectrometer which comes from the original instrument; Mercury Radiometer and Thermal Infrared Spectrometer (MERTIS) shown in Figure 7.5 [84]. MERTIS was specifically designed for Mercury but can also be used for our mission as it will be able to provide accurate measurements of the radiation and Temperature. VERTIS will be able to attain a high signal-to-noise ratio over 100 in a 7-14 μm wavelength range and will have a spectral channel width of 90 nm (same as MERTIS). These performance parameters are intended to be achieved even in the challenging thermal and radiation conditions present on Venus. It will be a lightweight instrument with an average required power 10 W. It is a passive payload as it is designed to detect and measure thermal infrared radiation naturally emitted by the surface. It does not emit any energy or signal itself. Its functional concept is based on the sequential illumination of four targets planet, deep space and two black bodies with temperatures of 300K and 700K. The instrument will be equipped with a monitored pointing system that will allow it to frequently observe in-flight calibration targets. The system will have a stepper motor and magnetic sensors which will be able to determine its zero position accurately. The radiometric component will measure the amount of infrared radiation emitted by the surface. Then the spectroscopic analysis will be done on the radiation which will be used to identify specific properties. To protect the blocking of incoming radiation, a cylinder can be used. The aluminum cover will isolate the device from the optical structure which will serve as the interface to the instrument's reflecting part ensuring efficient and precise observations. This instrument will have several important applications like water ice detection, calibration and instrument validation, surface composition analysis and temperature mapping.

Figure 7.5: VERTIS for radiation and temperature measurement

F) Ion Mass Analyzer

An ion mass analyzer is a hypothesized instrument shown in Figure 7.6 [85]. It will be designed especially for the critical Venus environment. It'll be able to collect data related to several aspects of Venus, including its interaction with solar wind, upper atmosphere photochemistry and characteristics of the atmosphere's mass and heat transport. It'll be a lightweight instrument with low power consumption requirement. They are considered an active payload. They directly interact with the analyzing sample by actively capturing and measuring the properties of ions. The instrument takes an active role in collecting and processing data from the sample. Their Working will be based on an ion mass spectrometer, similar to those used in Earth satellites and rockets, to measure the concentrations of ions in Venus's upper atmosphere within a specific mass range. It'll measure the concentration of thermal ion species, covering a range of ambient densities. The instrument's efficiency and mass discrimination will be accurately calibrated through laboratory and in-flight determinations, allowing direct conversion of measured ion currents to ambient concentrations. The initial step involves ionization, converting atoms into ions. The ions will be then accelerated and focused to form a concentrated ion beam. This beam is directed toward the mass analyzer for further examination. Inside the mass analyzer, the ions encounter electric and/or magnetic fields. These fields cause the ions to undergo deflection, dependent on their mass-to-charge ratio (m/z). They will be detected by a specialized detector which will record the time taken by each ion to reach there and also measures the ion current. The recorded data is then carefully analyzed and processed to construct a mass spectrum. The applications include: analyzing chemical composition, environmental monitoring, study of proteins and metabolites, space exploration and forensics and criminal investigations (by analyzing trace evidence like drugs and explosives).

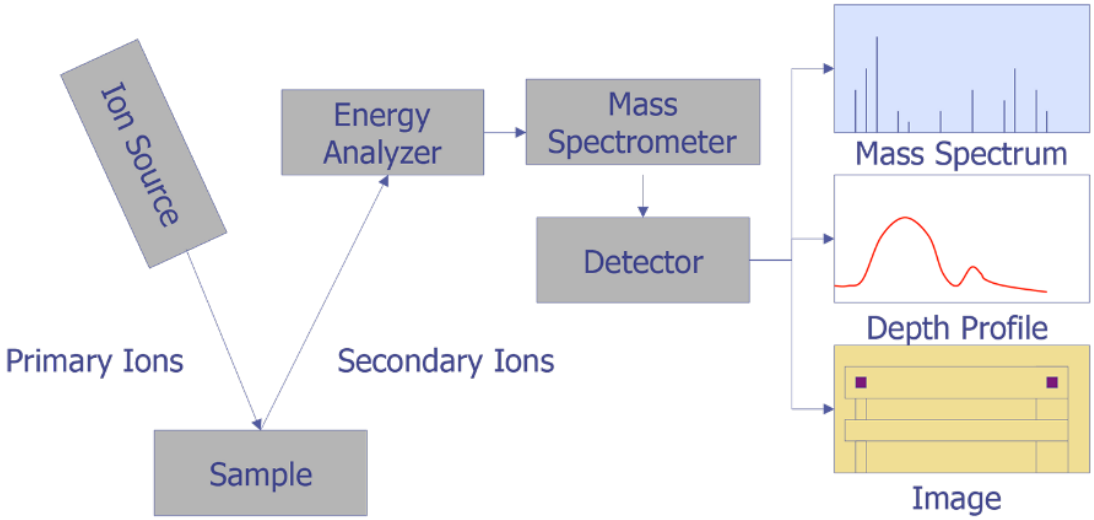

Figure 7.6: Ion Mass Analyzer for measuring mass-to-charge ratio of ions

G) UFFO (Ultra-Fast Flash Observatory)

UFFO (Ultra-fast flash observatory) is an instrument used for measuring Gamma and X-rays as shown in Figure 7.7 [86]. It has a slewing mirror telescope (SMT) capable of rapidly redirecting the optical beam without requiring the spacecraft to maneuver. This enables the UFFO to quickly

observe the early optical rise of Gamma-Ray Bursts with a response time of less than a second. UFFO is an active payload as it can redirect the optical beam enabling it to respond within a fraction of a second. This is an active mechanism that allows the instrument to accurately point its optical instrument at the precise location of a Gamma-ray burst without needing to adjust the spacecraft's orientation. UFFO is a dual-component observatory comprising the UFFO Burst Alert Telescope (UBAT) and the Slewing Mirror Telescope (SMT). UBAT operates in the gamma-ray energy range from 5-2000 KeV, collecting data on gamma-ray phenomena. It also provides point data to the SMT, which rapidly aligns itself to the location of the gamma-ray source, capturing UV/VIS imagery of the gamma-ray afterglow. UBAT utilizes a coded mask aperture camera with a wide field of view measuring 90.2 °x 90.2 °. Its detection system consists of an LSO-MAPMT Detector (Lutetium oxyorthosilicate Multi Anode Photo Multiplier Tube) with 48 by 48 pixels. Each pixel measures 2.88 by 2.88 mm and has a depth of 2 mm, resulting in an effective detector area of 191 cm^2. To capture the gamma-ray source's position in the sky, a pinhole mask is placed over the detector array. The shift in the shadow pattern is analyzed through a de-convolution procedure, encoding the X-ray source's location. The detectors in UFFO offer an energy resolution of 2 KeV and achieve an accuracy of approximately 10 arc minutes in localizing gamma-ray bursts. By capturing optical emission data from various GRBs, the instrument will offer valuable insights into the burst mechanism, transient event observations and space technology development Moreover, this data may lead to opportunities for exploring the universe beyond redshift z > 10, opening up new exciting frontiers in cosmological research.

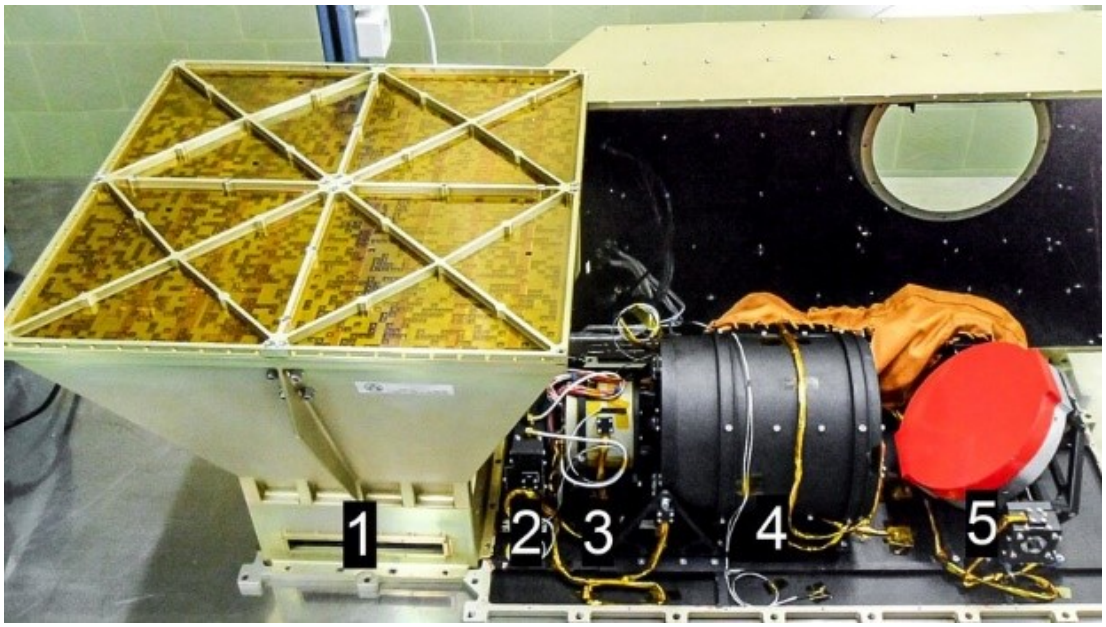

Figure 7.7: UFFO for measuring Gamma Ray Bursts

7.2 Payloads on Scouts

This Section provides an overview of payloads on scouts used for VRS mission which includes an array of specialized instruments like drag-force anemometer, pressure sensor, spectrophotometer, spectrometers and radiometers which are selected to withstand the harsh conditions and provide

valuable data about the Venusian atmosphere. The instruments were selected carefully through a competitive process, ensuring that they meet the stringent requirements of payload mass, data rate and power consumption. The instruments mentioned in this Section is a concept that serves as a demonstration of what is achievable in the formidable Venusian environment, providing concrete evidence that the mission's scientific goals can be realized. It should be noted that for the actual mission the payload instruments require a focused technology advancement for the VRM. Brief descriptions of the payloads selected on scouts are listed below. Table below provides a summary of the scout instruments, along with their mass, power, data rate and source. Table 7.2 provides an overview of the payloads on scouts.

Instrument	**Mass**	**Data Rate**	**Power Consumption**	**Source**
Venus Surface Wind Sensor	1 kg	5 kbps	10 mW	NASA
Miniaturized Infrared Spectrophotometer	0.5 kg	480 kbps	Milli joules	Scottish Universities Physics Alliance, Institute of Thin Films, Sensors and Imaging, University of the West of Scotland
VERTIS	3 kg	2-4 kbps	13 W	ESA
BIMS	1 kg	1498 bps	1 W	NASA
Miniature very high-pressure sensor	4.5 g	-	0.12 W	Althen Sensors and Controls

Table 7.2: Overview of payloads on scouts.

A) Venus Surface Wind Sensor

In order to gain a deeper understanding of the atmospheric structure and dynamics on the surface of Venus and to contribute valuable data to climate models, it is essential to accurately measure wind velocity and direction on the planet's surface and track these measurements over extended periods. In past missions, such measurements were achieved using various methods, including cup anemometers (Venera 9 and 10), acoustic microphones (Venera 13 and 14), and radio Doppler shifts (Venera and Pioneer Venus missions), which provided estimates of wind speed during descent and on the surface. However, these previous landers were short-lived, and now for VRM there is a need for advanced and durable wind measurement technology. For long duration missions on Venus, like the VRM, a significant challenge is to develop a wind-sensing technology that can withstand the harsh environment while minimizing mass and power consumption. Mechanical or spinning anemometers are susceptible to dust and corrosion, making them unsuitable for Venus' surface. Hot wire or film anemometers require additional power to heat the already hot ambient Venusian air. Acoustic and Doppler anemometers require electronics that are currently not viable for prolonged use in Venus' extreme 465°environment[87].

To address these challenges and enable long-term wind measurements under low power and mass requirements, a promising solution is a miniature drag-force anemometer as shown in the Figure 7.8[87]. Unlike other methods, a drag-force anemometer does not rely on a moving mechanical vane, allowing for use in an array configuration. This Section presents the working and application of a miniature drag-force anemometer, aiming to serve as a future Venus surface wind sensor for VRM.

To achieve valuable scientific data on the Venus surface, the objective is to measure both wind velocities and wind direction over an extended period while ensuring minimal impact on the power and mass. The sensor must be capable of operating under challenging conditions, including withstanding temperatures of 465°, in a high-pressure CO_2 supercritical atmosphere containing chemically reactive species like SO_2. Additionally, the sensor needs to be lightweight (less than 1 kg) and have low power consumption (less than $10\,mW$). The schematic diagram of a Venus surface wind sensor is depicted in the Figure 7.8b[87]. The Venus surface wind sensor utilizes a slender and rigid cantilever beam that extends from a fixed point. This beam is designed to be sensitive to the force exerted by the wind. Strain gauges are positioned near the bending point of the beam to measure any changes in its length caused by the wind's force which is shown in . As wind blows against the sensor on the Venusian surface, it applies a force on the cantilever beam, resulting in its bending. The strain gauges detect this bending and convert it into an electrical signal, allowing measurement of the force applied by the wind. By analyzing the strain measured by the gauges, the wind sensor can determine the wind velocity on the Venusian surface. Since the force on the cantilever is directly proportional to the square of the wind velocity, taking into account the specific atmospheric density on Venus, the sensor can accurately calculate the wind speed. To detect changes in wind direction, the sensor employs multiple cantilever beams arranged in different orientations. This arrangement enables the sensor to capture wind information from various directions, providing data on both wind speed and direction on the Venusian surface. By utilizing this miniature drag-force anemometer design, the Venus surface wind sensor can effectively and continuously measure wind velocity and direction on Venus over extended periods. This capability offers valuable insights into the atmospheric dynamics and climate of the planet.

The Venus surface wind sensor is classified as an active sensor. Active sensors require an external energy source to emit or transmit signals and actively interact with the environment to obtain measurements. In the case of the Venus surface wind sensor, it employs a miniature drag-force anemometer design, featuring a cantilever beam equipped with strain gauges to measure wind-induced forces. As wind flows against the sensor, the cantilever beam responds to the force applied, resulting in its bending. The strain gauges attached to the beam detect this mechanical deformation and convert it into an electrical signal. This signal is then utilized to determine both wind velocity and direction. The sensor's active operation involves continuous interaction with the wind to detect changes in force and translate them into useful data. This active nature enables the sensor to gather valuable information about wind conditions on the Venusian surface, contributing to a deeper understanding of the planet's atmospheric dynamics and climate.

The Venus surface wind sensor serves several critical applications. The wind sensor's continuous measurement of wind velocities over an extended period will help the mission to gain insights into the atmospheric structure and dynamics of Venus. The sensor's capability to measure wind direction enables the identification of prevailing wind patterns on Venus' surface. For VRM, some advancements should be made to improve its capabilities and performance in the challenging Venusian environment. Enhancement in the sensor's material and design to withstand even higher temperature, ensuring its reliable operation at the extreme temperature of 465°on the Venusian surface. Additionally, the sensor's capability should be expanded to

accurately measure wind velocities over a broad range, including both low and high wind speeds to capture a more comprehensive view of the Venusian wind patterns.

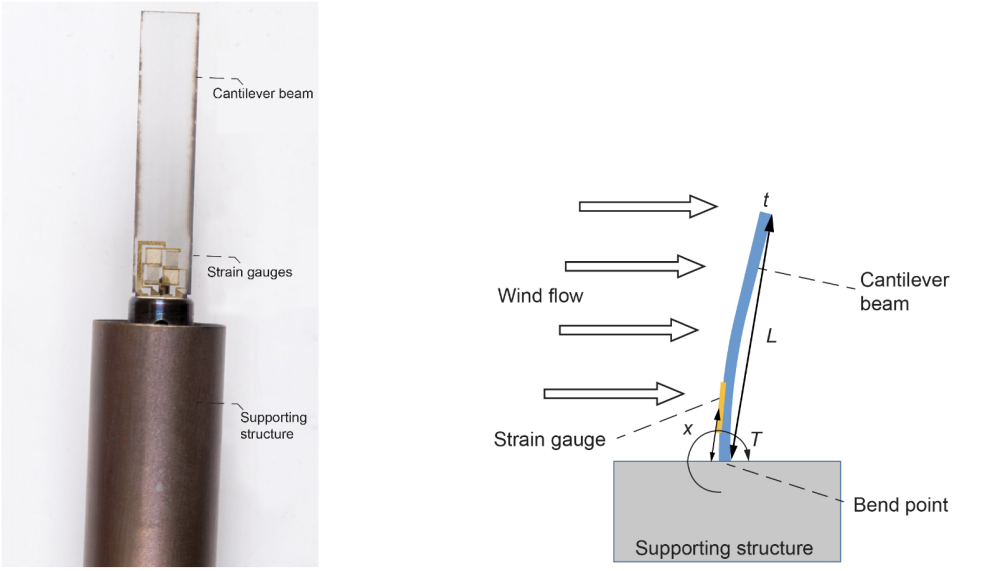

(a) Miniature drag-force anemometer.

(b) Strain analysis on drag-force anemometer cantilever.

Figure 7.8: Venus Surface Wind Sensor.[87]

B) Miniaturized Infrared Spectrophotometer

The Miniaturized Infrared Spectrophotometer is an advanced gas sensing technology designed for efficient power consumption and simultaneous detection of multiple gases. Operating in the mid-infrared range 2.9–4.8 μm, it can identify gases such as carbon dioxide, carbon monoxide, nitrous oxide, sulfur dioxide, ammonia, and methane. The device incorporates a lead selenide photo-detector array and a customized MEMS-based micro-hotplate for infrared detection. With its innovative design featuring short-time pulsed inputs for energy efficiency, the spectrophotometer can function independently as a stand-alone sensor, making it highly suitable for planetary missions and climate research.

The miniaturized infrared spectrophotometer as shown in the Figure 7.9[88]is an advanced gas sensing technology that revolutionizes multi-gas detection in a compact and low-power design that will be an valuable instrument for the VRM. Its working principle is based on infrared absorption spectroscopy, where gas molecules absorb specific infrared wavelengths of light, leading to changes in their vibrational or rotational energy levels. This principle enables the identification and quantification of multiple gases in the mid-infrared wavelength range 2.9–4.8 μm. At its core, the spectrophotometer comprises an infrared source emitting a broad spectrum of infrared light and a highly sensitive lead selenide photo-detector array. The gas sample is exposed to the emitted infrared light, causing specific wavelengths to be absorbed by the gas molecules present. As the absorbed infrared light passes through the gas sample, the lead selenide photo-detector array measures the transmitted light intensity. To ensure accurate measurements, the spectrophotometer incorporates a separate reference channel, providing baseline measurements without gas absorption. By comparing the intensity difference between

the gas-absorbed light and the reference light, the gas concentration is calculated using established calibration curves. The spectrophotometer also features a MEMS-based micro-hotplate acting as the infrared source, providing consistent and controlled infrared illumination. Additionally, its design includes short-time pulsed inputs for efficient energy consumption, optimizing power usage while maintaining the effectiveness of spectral measurements. The miniaturized infrared spectrophotometer functions as a stand-alone multi-gas sensor, making it highly versatile for various applications, including planetary missionslike VRM, environmental monitoring, and climate studies. With its combination of compact size, low power consumption, and capability to detect multiple gases simultaneously, this innovative gas sensing technology offers a powerful and efficient solution for precise gas detection in diverse scientific and environmental endeavors.

The Miniaturized Infrared Spectrophotometer functions as an active instrument, utilizing an external energy source to emit a broad spectrum of infrared light in the mid-infrared range 2.9–4.8 μm. This emitted light is directed towards the gas sample under analysis. The gas sample absorbs specific infrared wavelengths from the emitted light, leading to changes in its energy levels. The spectrophotometer's lead selenide photo-detector array actively detects the transmitted light after it passes through the gas sample. By measuring the intensity of the transmitted light, the spectrophotometer determines the gas concentration, enabling it to perform multi-gas detection. In summary, the Miniaturized Infrared Spectrophotometer actively interacts with the gas sample through the emission and detection of infrared light, making it an active instrument for gas sensing and spectroscopy.

The Miniaturized Infrared Spectrophotometer is a valuable instrument for VRM, providing critical data on the atmospheric composition and climate dynamics of the planet. It can be used to analyze the composition of the Venusian atmosphere. It can detect and quantify gases such as carbon dioxide, sulphur dioxide and other chemically reactive gases present in the thick atmosphere of Venus. The spectrophotometer's capability to detect multiple gases

Figure 7.9: Miniaturized Infrared Spectrophotometer.[88]

simultaneously allows for a comprehensive assessment of the Venusian atmosphere. The data obtained from the spectrophotometer can contribute to climate and weather studies on Venus. For the VRM, possible advancement in miniaturized infrared spectrophotometer can be made by improving the spectrophotometer's temperature resistance which will ensure its stability and functionality under harsh conditions, allowing it to operate reliably for extended periods. Additionally, by expanding the spectrophotometer's spectral range and resolution will enable it to detect a broader range of gases and provide more detailed spectral information for accurate gas identification and quantification.

C) Venus Radiometer and Thermal Infrared Spectrometer (VERTIS)

VERTIS is a hypothesized instrument for the VRM mission. Its primary objective is to measure the radiation and temperature of the Venusian environment. VERTIS is hypothesized from MERTIS which was a part of ESA's Bepi Colombo mission to Mercury, is an advanced imaging spectrometer designed for thermal infrared (TIR) range operation.

The VERTIS is an advanced imaging spectrometer specialized for the thermal infrared range depicted in the Figure 7.10[89]. Operating in the harsh Venusian atmosphere, it employs a push-broom scanning technique to capture thermal infrared radiation emitted or reflected by the planet's surface. Utilizing high spectral resolution and signal-to-noise ratio, the instrument identifies surface composition, mineralogy, and thermal properties despite the extreme conditions. By dividing the thermal infrared range into narrow spectral channels, the Venusian MERTIS distinguishes unique signatures of various materials and minerals on Venus's surface. Its precise nominal spatial resolution allows the creation of detailed mineralogical maps, aiding in the study of geological features and thermal variations of the planet.

VERTIS will be a passive instrument. By capturing and analyzing the natural thermal infrared radiation emitted by the planet's surface, it would provide crucial data about Venus's composition and thermal behavior. As a passive instrument, it would offer valuable insights into the geological features and atmospheric processes of Venus without emitting any signals of its own.

The VERTIS would be instrumental in studying the surface composition of Venus by analyzing the thermal infrared radiation emitted by the planet's surface. By measuring surface temperatures and variations across different regions of Venus, the instrument could contribute to studies of heat flow and thermal behavior of the planet's surface. The instrument's capabilities could potentially help in studying Venus's thick cloud cover and weather patterns. For VRM mission, potential changes and enhancements to the Venus Radiometer and Thermal Infrared Spectrometer (VERTIS) could include adapting it for operations in the extreme conditions of Venus's atmosphere, such as its thick atmosphere and high temperatures. This may involve reinforcing the instrument's thermal protection and incorporating materials capable of withstanding the harsh environment. Additionally, modifications to the spectral range and resolution may be required to suit the unique characteristics of Venus's surface and atmosphere. Upgrading the instrument's signal-to-noise ratio and spatial resolution would enable more precise measurements of Venus's surface composition, mineralogy, and thermal behavior. Integrating advanced data transmission and processing capabilities would facilitate real-time analysis, enhancing the instrument's scientific efficiency and yielding valuable insights into Venus's geology and atmospheric processes.

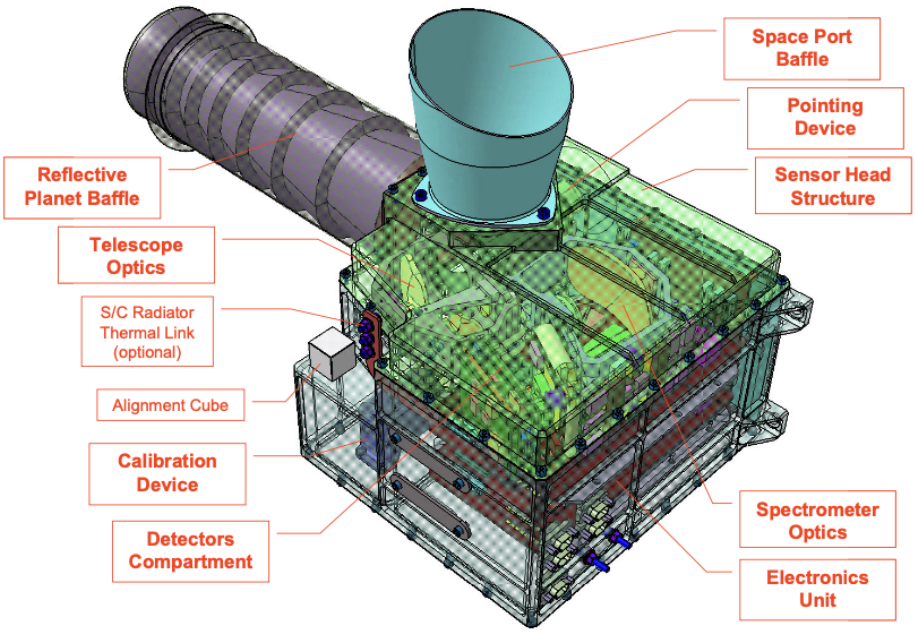

Figure 7.10: Venus Radiometer and Thermal Infrared Spectrometer (VERTIS).[89]

D) Ion Mass Spectrometer (IMS)

The Ion-Mass Spectrometer (IMS) as shown in the Figure 7.11[90] is an Instrument for investigating Venus's ionospheric plasma and the ionized gases in its atmosphere. By analyzing charged particles (ions) in the upper atmosphere, IMS provided essential data on Venus's atmospheric composition, ion density, and ion species. The instrument measured ion masses, which will help comprehend how different ions were distributed and behaved in the upper atmosphere. Through the study of the ionosphere, IMS can significantly help in understanding of Venus's atmospheric processes and its interactions with the solar wind.

The Ion-Mass Spectrometer (IMS) is a specialized instrument which is based on the original instrument Bennett Ion Mass spectrometer (BIMS) with the primary purpose of investigating Venus's ionospheric plasma and the ionized gases in its atmosphere. It functions by collecting charged particles, known as ions, from the upper atmosphere of Venus. These ions are then subjected to ionization, acquiring an electric charge. Next, the instrument propels these ionized particles through an electric field, which results in their separation based on their mass-to-charge ratios. This separation generates a mass spectrum that enables scientists to identify the various ion species present in the ionosphere. IMS' capability to measure ion masses and abundances provides crucial information about Venus's atmospheric composition, ion density, and ion species, significantly advancing our understanding of the planet's atmospheric processes and its interactions with the solar wind.

The Ion-Mass Spectrometer (IMS) is an active instrument. It actively collects and measures charged particles (ions) from the upper atmosphere of Venus. The instrument uses ionization techniques to give these ions an electric charge and then accelerates them through an electric field, causing them to separate based on their mass-to-charge ratios. This process allows IMS to

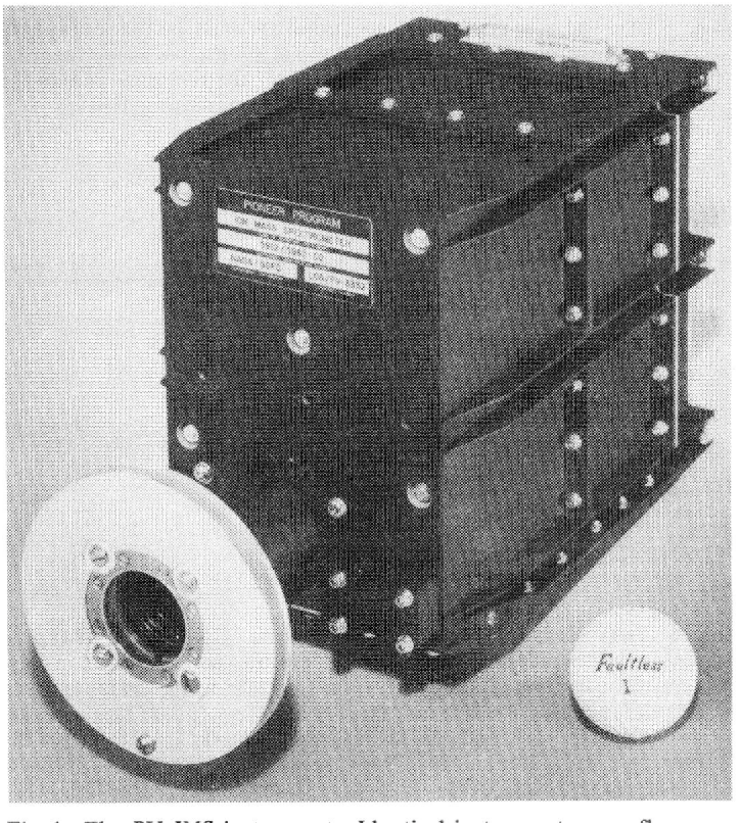

Figure 7.11: Ion Mass Spectrometer (IMS). [90]

create a mass spectrum and identify different ion species present in the ionosphere.

The Ion-Mass Spectrometer (IMS) on Venus plays a vital role in studying the planet's ionosphere and atmospheric composition. It provides valuable data on the types and abundance of ionized gases, allowing scientists to analyze the chemical makeup of Venus's upper atmosphere. By measuring ion density profiles at different altitudes, IMS contributes to a better understanding of the ionosphere's structure and dynamics. Moreover, the instrument aids in studying atmospheric escape processes, interactions with the solar wind, and atmospheric chemistry. IMS' observations help unravel the complexities of Venus's atmospheric processes and provide insights into ionospheric variability, advancing our understanding of the planet's atmospheric behavior and its interactions with the solar environment. For VRM mission, possible changes and improvements on the Ion-Mass Spectrometer (IMS) could include increasing sensitivity to detect lower ion concentrations, expanding the mass range to identify a wider range of ion species, and enhancing spatial resolution for more detailed ionospheric analysis. Implementing real-time data transmission would allow for faster data access and analysis, while deploying multiple IMS instruments on spacecraft or multiple spacecraft equipped with IMS would enable simultaneous measurements at different locations on Venus. Improving power management, reducing size and weight, and integrating IMS with other complementary instruments would enhance its scientific capabilities, enabling a deeper understanding of Venus's ionosphere and atmospheric dynamics, and enriching our knowledge of the planet's space environment.

E) Miniature very high pressure sensor

The miniature very high-pressure sensor is a compact and robust instrument designed for Venus missions. Its main function is to measure the extremely high atmospheric pressure on Venus's surface, which is about 92 times that of Earth. The sensor is specifically built to withstand the challenging conditions on Venus and provide essential data on the planet's atmospheric pressure at various locations. This information will help the VRM to better understand Venus's atmospheric behavior and its geological activities. Figure 7.12[91] shows a miniature very high pressure sensor that can be used for this mission.

The miniature very high-pressure sensor functions by utilizing strain gauges or piezoelectric materials to measure pressure. When exposed to Venus's extreme atmospheric pressure, the sensor undergoes deformation, resulting in a change in resistance or voltage output. This alteration is converted into pressure readings, enabling precise measurements of the high-pressure environment. The sensor's compact size and sturdy construction allow it to endure Venus's harsh conditions and provide accurate data, essential for studying the planet's atmospheric behavior and geological activities.

A miniature very high-pressure sensor is typically a passive instrument. Passive instruments, in the context of sensors, do not actively emit any signals or radiation themselves. Instead, they rely on external stimuli or environmental conditions to generate a response that can be measured. In the case of a miniature very high-pressure sensor, it responds to the high-pressure environment in which it is placed. When exposed to very high atmospheric pressure, the sensor undergoes deformation or a change in its physical properties (such as resistance or voltage output). This change is then converted into pressure readings, allowing the sensor to passively measure the pressure without actively emitting any signals.

The miniature very high-pressure sensor would be a critical component of a VRM, providing essential data on the extreme atmospheric pressure on Venus's surface. Its application would involve measuring and monitoring the atmospheric pressure at various locations on the planet. This data would help the VRM to understand Venus's atmospheric dynamics, weather patterns, and geological activities, as well as its interactions with the solar wind. Improvements to the Miniature very high-pressure sensor could include enhancing its measurement range to cover a wider range of pressures found on Venus. Additionally, optimizing the sensor's sensitivity and accuracy would allow for more precise pressure readings. The incorporation of advanced materials and technologies to ensure its durability and performance in Venus's extreme conditions would be essential.

Figure 7.12: Miniature very high pressure sensor.[91]

CHAPTER 8

Structure

by Devraj Bhosale

This Chapter addresses the conceptual design of an airship specifically tailored to endure and explore the Venusian atmosphere. Different aspects of materials for balloon, arrangement of subsystems in a compact structure are explored and a procedure that helps us conceptually design a conventional Airship as per our mission requirements is discussed. Finally the structure of the Venus Research Station is presented.

8.1 Introduction

The three phases of engineering design are conceptual, preliminary and detailed design. Of these, the conceptual design phase is the least in terms of total duration and investment; which is approx. 5% of the total. However, its importance and significance can be judged from the fact that decisions taken during this phase have a direct bearing and influence on the effort and investment in the phases that follow. One of the most important activities in the conceptual design phase are design studies that lead to the identification of the baseline requirements of the final product.

Several methodologies and procedures for obtaining baseline specifications of fixed wing aircraft are available, such as "Loftin"[92] for transport aircraft. However, no such methodology is available, at least in open literature, for conceptual design studies of airships. Further, there seems to be no standard procedure to identify the capabilities and limitations of an existing airship. For instance, to determine the payload capacity of an airship at a particular altitude, one has to either refer to the airship's performance manual or apply some simplistic thumb-rules.

With the help of below procedure in subs sections of 8.1, our mission of establishing a structure of Research station that would survive in Venus Atmosphere was accomplished.This methodology also enables the designer to carry out sensitivity studies related to the design parameters, as well as investigating the effect of incorporating certain design features, or choosing from among some possible design options.

Description of input parameters

The issues related to operation and design synthesis of airships are succinctly explained by various contributors in Khoury & Gillett[93]. Through a study of this literature, the key parameters that affect the operation and configuration of airships and performance requirements that strongly affect their design were identified. Such parameters, which constitute the list of inputs to the methodology, can broadly be classified under three categories, as listed in Table 8.1.

Operation related parameters	Performance Requirements	Configuration related parameters
Pressure altitude	Range	Fin layout
Atmospheric properties	Cruising altitude	No. of engines
Minimum operating altitude	Cruising speed	Envelope length to diameter ratio
Helium purity level	Pressure altitude	Ballonet volume for trim
Power off-take for engine driven accessories	-	Internal over pressure

Table 8.1: List of input parameters

The pressure altitude and atmospheric properties have a direct bearing on the volume of the airship envelope and the payload capacity. The difference between the pressure altitude and the minimum operating altitude determines the volume of the ballonets.The performance requirements listed in Table 8.1 directly influence the power-plant sizing and fuel requirements.

The methodology can be applied in either of the two modes; the design mode or the evaluation mode. In the design mode, which is relevant when a new airship is being designed, the envelope volume required to carry a user-specified payload is estimated. In the evaluation mode, which is relevant when the capability of an existing airship is being evaluated, the payload that the airship can carry for a specified envelope volume is estimated. Apart from this, the methodology also calculates the geometrical parameters of the envelope and the ballonets, and determines parameters such as max speed at cruising altitude, total installed power at 45km to 55km altitude conditions, fuel weight, the weight breakdown of major assemblies and empty weight.

Outline of methodology

In the design mode,the net lift available at the operating altitude is calculated. The next step is the estimation of geometric parameters of the airship, which include the dimensions of the envelope, ballonets and the fins. This is followed by the estimation of drag coefficient, and hence the installed power required and Helium weight. The last step is the estimation of weight breakdown of various components and hence the empty weight, through which the payload capacity is estimated. If this payload does not match the desired value, then envelope volume is adjusted and the calculation are repeated till convergence.

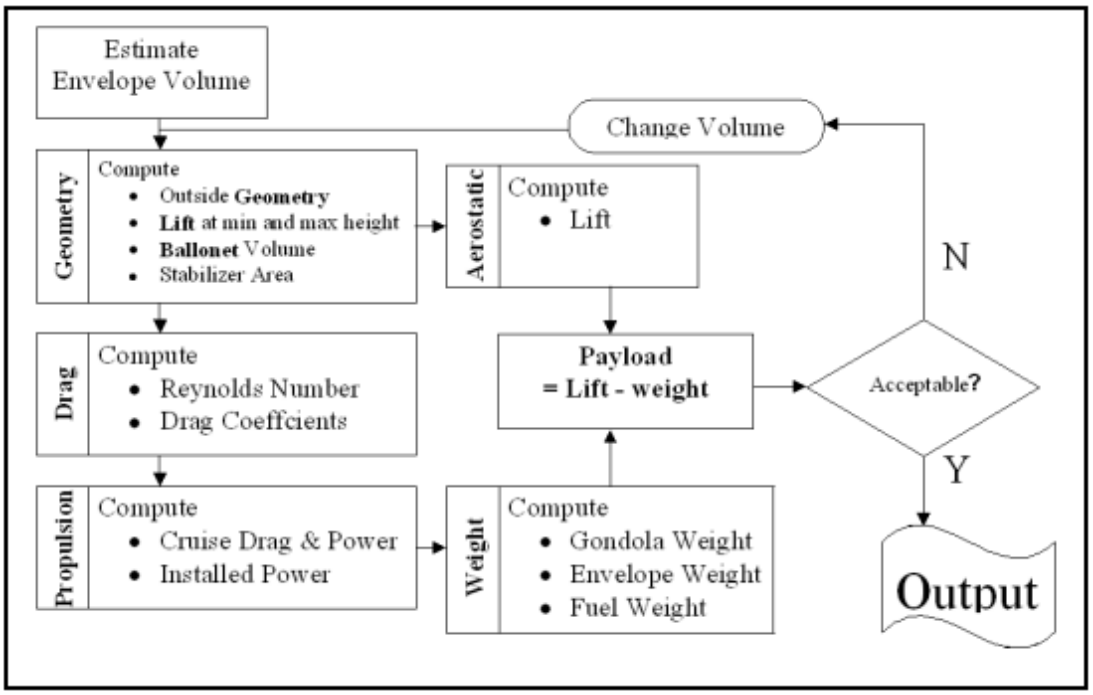

Figure 8.1: Flow chart of the methodology.

Details of methodology

Aerostatics Sub module The net lift of an airship is directly affected by the variation in the air pressure and temperature in the atmosphere and inside its envelope. The net lift reduces with increase in altitude, and is the minimum at pressure altitude. Using the methodology outlined by Craig in Khoury & Gillett[93], the net lift available at pressure altitude Hmax can be calculated as

$$L = V_e\,(1 - V_{\text{btr}}) \cdot \sigma_{aH_{\max}} \rho_{a0} - \rho_{h0} * \frac{1 + \Delta p}{P_{\text{Hmax}}} \tag{8.1}$$

Geometry sub-module In this sub-module, the length, maximum diameter, and surface area of the envelope and ballonets are estimated.Envelope geometry For airship envelopes of conventional shapes, it can be shown that the envelope volume and surface area satisfy the relations

Envelope geometry For airship envelopes of conventional shapes, it can be shown that the envelope volume and surface area satisfy the relations

$$\frac{V_e}{l_e^3} = \frac{k_v}{(l/d_e)^2} \text{ and } \frac{S_e}{l_e} = \frac{k_s}{(l/d)_e} \tag{8.2}$$

Young[94] has shown that for envelopes based on the R-101 airship shape,the factors kv, ks are 2.33 and 0.465, respectively.A study of existing airships with envelopes of double ellipsoid or similar shape was carried out, based on which these factors were estimated to be 2.547 and

0.5212, respectively.

Ballonet geometry The total ballonet volume is calculated by,

$$V_b = (V_{bpc} + V_{tr}) * V_e \tag{8.3}$$

Fin geometry The size and location of fins are a function of the desired control characteristics of the airship. Geometrical data related to fins of 15 airships was collected, analyzed and tabulated to standardize the fin geometry, as shown in Table 8.3

8.2 Airship Sizing

The envelope of airship is containing helium lifting gas. Due to the density of the Venusian atmosphere, helium provides more lift capability than an equivalent volume on Earth. Air and hydrogen are also viable lifting gasses to be considered for this concept, but the increased mass and volume of air required presents a significant burden for the transportation system and hydrogen presents issues with transportation from Earth to Venus.

For propulsion and control, solar panels on top of the envelope collect power and batteries to drive electric propellers. The power is also used by the payload attached to the bottom of the envelope in the gondola. For the mission, the gondola could consist of scientific instruments, any deployable probes,. The robotic airship, when fully inflated at 57 m long, is approximately the length of the Goodyear blimp. When packaged in the aero shell, the airship fits within a shroud diameter and length envelope of 4m diameter by 9m length.

Mass estimation

This sub-module estimates the weight of each major system and sub-system of an airship, viz. Envelope, tail, equipped gondola and other sub-systems, thus leading to the estimation of the empty weight

Gondola volume estimation

The volume of gondola is required to estimate its weight. It is reasoned that gondola volume will be proportional to the payload which itself will be proportional to the envelope volume. The gondola volume ratio i.e. ratio of apparent volume of gondola (length times breadth times height) to the envelope volume was obtained for 21 airships, and the average value was found to be 0.007. Since most airship gondola are rounded at the front and back for improved aerodynamic characteristics, the gondola volume is assumed to be lesser than the apparent volume by a factor of 1.4. Hence the gondola volume to envelope volume ratio is taken to be 0.005.

As per constraints quoted in system environment i.e maximum payload mass an Ariane 64 can carry is up to 6900kg.So weight breakdowns into two launch they are listed in Table 8.2 below,

1st Launch	mass (Kg)	2nd Launch	mass (Kg)
GNC	1.21	Payload	160
Antennas	23	some batteries	3509
Empty mass of balloon	2017	air tanks	9
Propulsion system	224	OBC & DH system	74
thermal system	209	-	-
some batteries	1491	-	-
Empty mass of gondola	2116	-	-
Total	**6082**	**Total**	**3753**

Table 8.2: Component weight breakdown

Balloon sizing

Balloon material Materials have made a huge leap forward in the development of airships, making them lighter, stronger, and more efficient.There are very particular demands on materials when it comes to airships construction. They need to exhibit proper properties of strength, weight, air-tightness, weather and UV stability, conductivity, and non-flammability. Therefore the material becomes a delicate balance between often competing demands.

Vectran™[95] offers a balance of properties unmatched by other high performance fibers. LCP polymer molecules are stiff, rod-like structures organized in ordered domains in both solid and melt states. These oriented domains lead to anisotropic behavior in the melt state, thus the term “liquid crystal polymer.”

For aerospace applications, materials are screened for outgassing and offgassing properties. Outgassing, the release of chemicals from non-metallic substances in vaccum conditions, and offgassing, the release of chemicals from materials at ambient or high pressure, are important in assessing the use of materials in these unique environments.

Vectran™[95]] fiber is resistant to organic solvents, some acids of 90% concentration, and bases of 30% concentration. It is unique in regards to other materials in that it provides a balance of properties rarely found in synthetic fibers: minimal moisture retention, thermal stability, and excellent impact resistance. Using the Dynatup Impact Test, Vectran™ performed far better than competitive materials.

Fin Sizing The size and location of fins are a function of the desired control characteristics of the airship. Geometrical data related to fins of 15 airships was collected in , analyzed and tabulated to standardize the fin geometry as per [96], as shown in Figure

Fin Parameter	Formula	Value
Area Ratio	$S_{\text{fin}}/S_{\text{env}}$	0.0594
Aspect Ratio	$4b^2/S_{\text{fin}}$	0.6585
Span to Chord Ratio	b/C_{r}	0.5625
Taper Ratio	$C_{\text{t}}/C_{\text{r}}$	0.7083
Location Ratio	$L_{\text{fin}}/L_{\text{env}}$	0.8000

Table 8.3: Parameters derived from statistical data

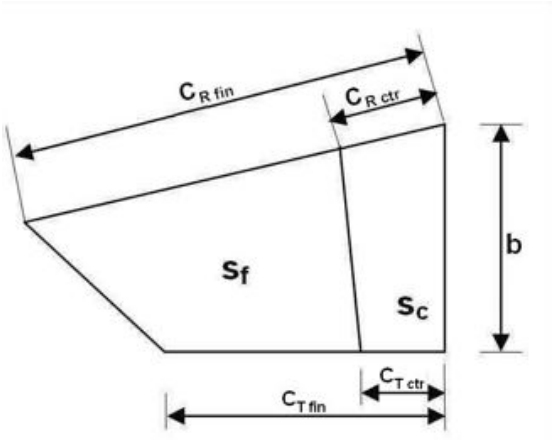

Figure 8.2: Schematic view of a fin.

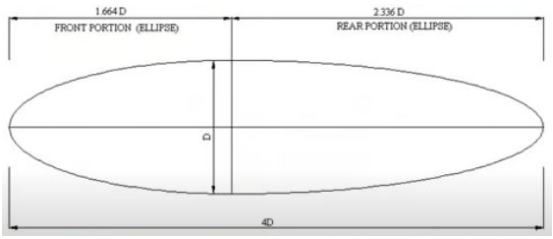

Figure 8.3: Schematic view of an Envelope.

Envelope sizing An airship balloon is combination of two Ellipsoid shapes, because having one symmetric ellipsoid can violet the conventional geometry of the blimp and can cause changes in various design parameters .Factors 1.664D and 2.336D are derived after studying multiple types of non rigid airship as per [96], so that we can have standardized formula for calculating envelope parameters which will help while designing in CAD software.

Gondola sizing

We design the gondola in such a way that we are able to fit everything and eject unnecessary components to full fill the mass constraints quoted in system environment So we divided the payload in two launchers as per Table 8.2. These two launchers will have a Docking and Ejecting mechanisms which will take place in a circular orbit in space and after completing the process we will commence towards planet Venus.

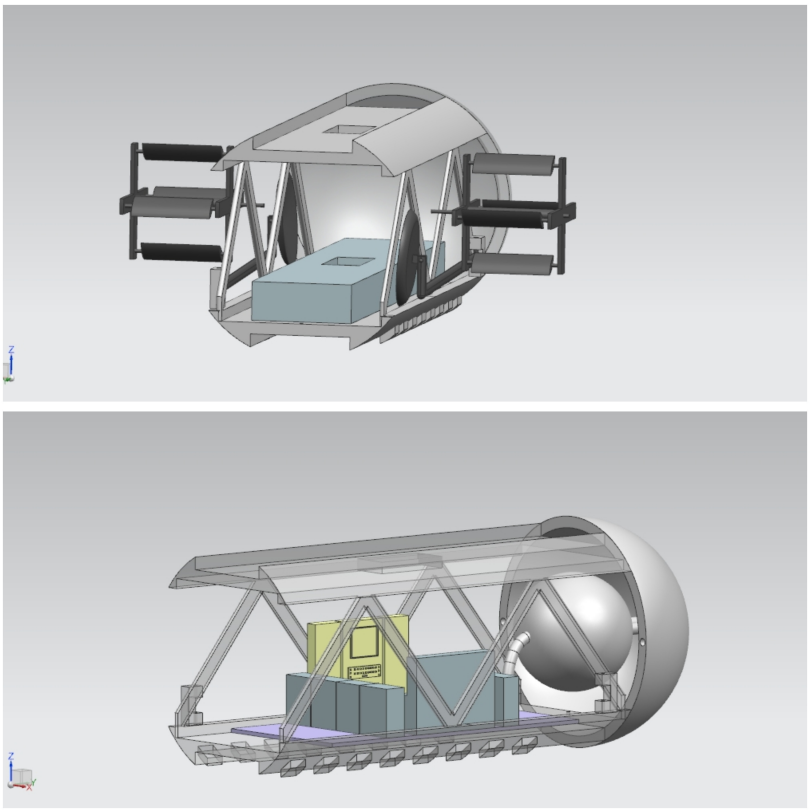

Figure 8.4: Payload divided in two launchers.

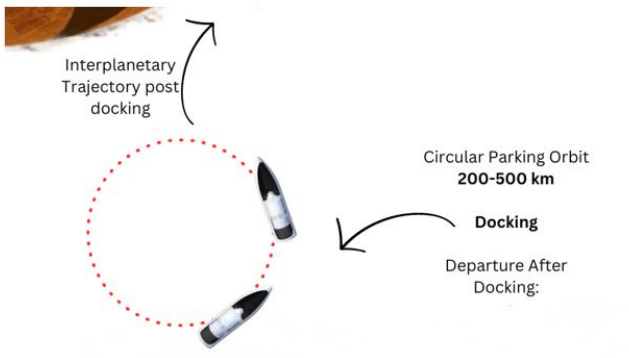

Figure 8.5: Docking phase.[Salian, original Figure 6.4]

The first half of payload will be in Launcher 1 and other half will be in Launcher 2 in the 8.4, both payloads will dock from opposite sides of spheres and will eject some unnecessary components in Docking phase, and then move on for the mission

8.3 Results

Though several empirical formulae and statistical data of existing airships have been used in the methodology. Following are the results achieved after multiple iteration.

- **Envelope Geometry:** length: 57m, Diameter:14.3m, Material : Vectran™
- **Fin size:** C_t = 10.07,Cr=7.736, b=5.30.
- **Gondola size:** length=9m, Outer Diameter=4m, Material:Aluminium 7050 & Carbon Fibre truss
- **Final designs** as depictec in Figure 8.6 to 8.11

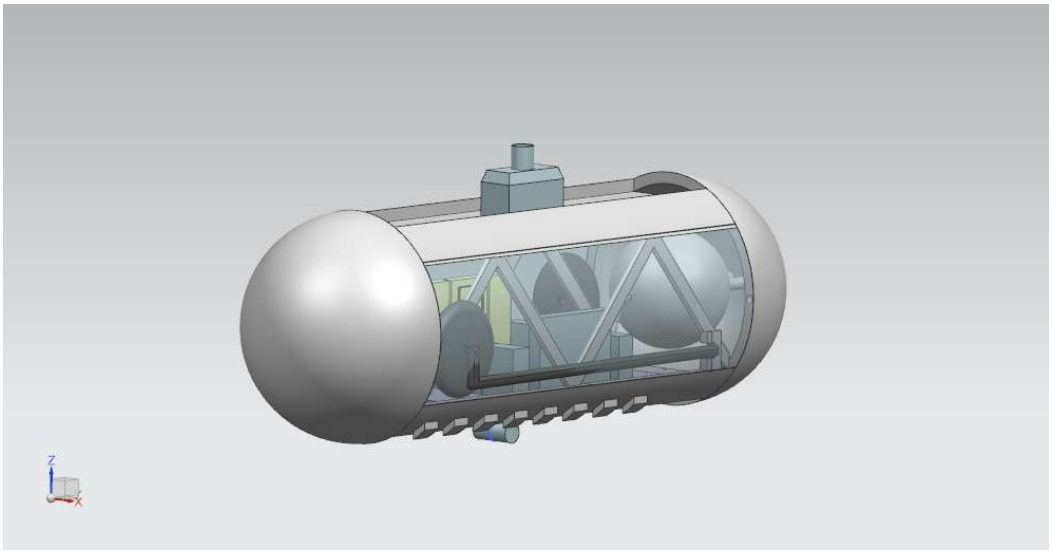

Figure 8.6: Final Output (g1).

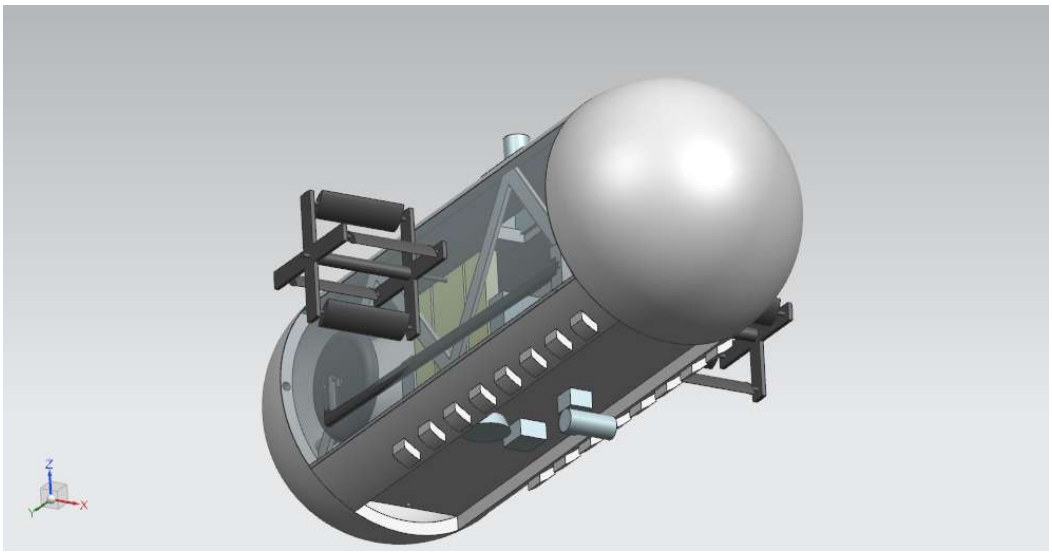

Figure 8.7: Final Output (g2).

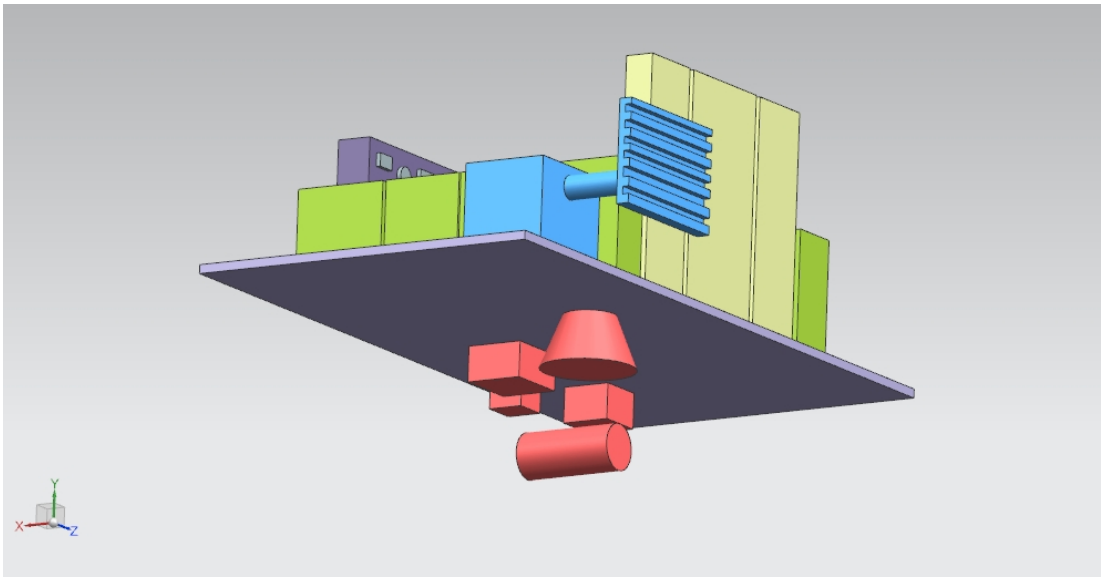

Figure 8.8: Final Output (p1).

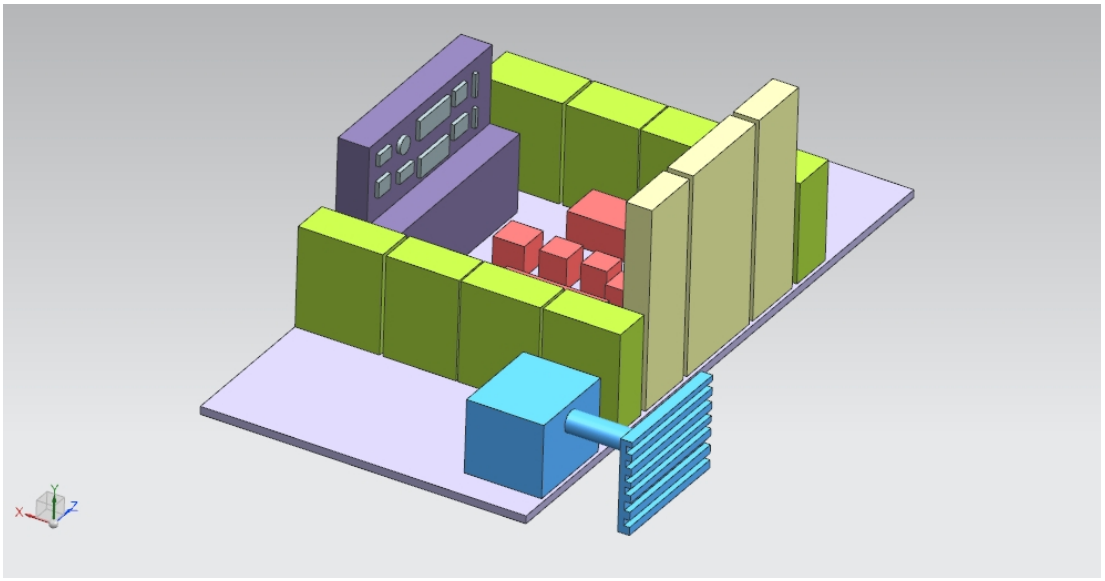

Figure 8.9: Final Output (p2).

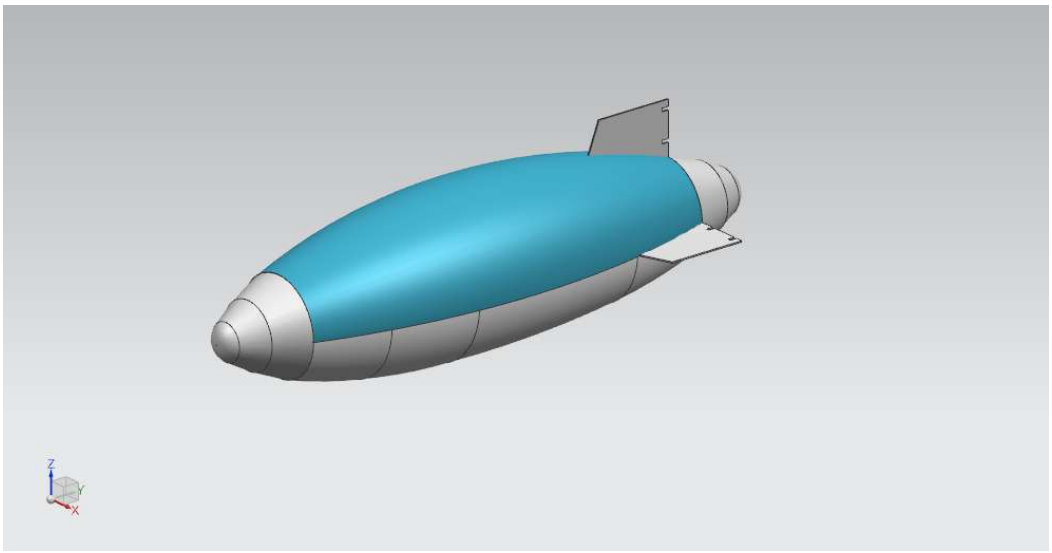

Figure 8.10: Final Output (b1).

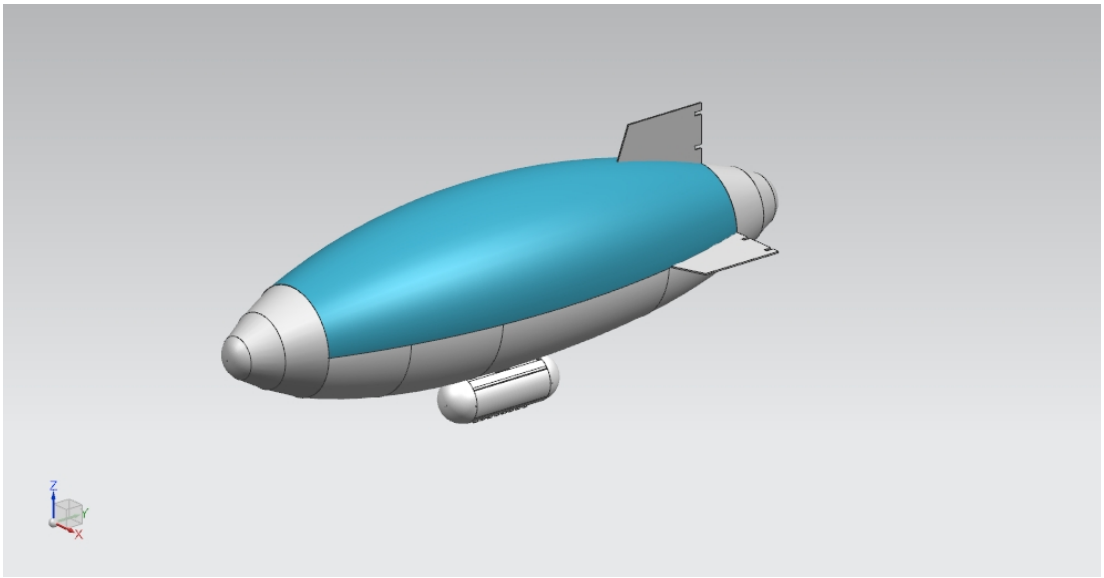

Figure 8.11: Final Output (D1).

CHAPTER 9

Flight Dynamics

by Martin Hesse

This Chapter discusses the flight dynamics of both the Research Station and the Scouts. For the Research Station this is focused on the steady-state case of it floating in the atmosphere at a certain height with controlled movement options. This also includes a discussion of different options for floatation as well as sizing of the relevant systems to achieve this.

For the Scouts the flight dynamics describes the entire lifetime of the Scouts. This starts as soon as they are released from the Carrier Vehicle 1. From there they will preform a de-orbit burn, to enter the atmosphere, through which they will fall and eventually touch down on the surface of Venus.

9.1 Venus Research Station

As stated by MR02 and MR03 (cf. Table 3.3) the Research Station has to float within a fixed altitude range and be manoeuvrable at that altitude. To achieve the floatation there has to be some force acting on the Research Station counteracting the gravitational force. This can either be done through lift or buoyancy. To create lift there are two options, either using a fixed wing, like on an aircraft, or a rotating blade, like helicopters or drones use. As long as the Research Station has some positive airspeed the wing will produce some lift, same as a rotating blade. But both of these options require a large continuous power usage. In case of a wing, the Research Station has to maintain a fairly high airspeed, same as an aircraft in Earth‘s atmosphere, which requires continuous forward propulsion. Using a rotor, there has to be a motor powering that rotor continuously. Both of these options are not able to use electric power, as this would far exceed the power generation capabilities of the Research Station. Therefore it would have to powered using a more traditional fuel. But this will run out after some time and will not be able to sustain the Research Station for the required lifetime of 5 years (TO3 from Table 3.1). All of this means the Research Station needs a system, that is capable to produce sufficient upward force completely passively (OR10 from Table 3.4). Consequently the Research Station will be fitted with a balloon filled with a gas, that has a lower density than Venus‘ atmosphere. Therefore the Research Station will float at the height, where the size of the balloon produces the same amount of buoyancy as the mass of the Research Station gravitational pull. Once set up the Research Station will, assuming no leakage, float at that height indefinitely, without any further input or power consuming system. In reality it can not prevented that the gas used in the balloon leaks, so it will have to be topped up once in a while, though this is not further considered in this concept study. Also, both for the orientation as well as the precise height adjustment of the Research Station, there will be an active control system, which is described in Chapter 11.

For various reasons an altitude range of 45 to 55 km was chosen, so the design altitude from now on is 50 km (cf. Chapter 3). Some of these reasons, like wind speeds and similarity to Earth's atmosphere are discussed in Chapter 2. But there are two more reasons for this height: Firstly, if the Research Station is any lower than this, the power production, which relies on solar energy, will drop considerably, so that the Research Station will run out of power (cf. Chapter 12). Secondly the density of the atmosphere decreases quickly as seen in Figure A.1, which would require a much larger balloon, so a lower altitude is favourable. This leaves us with the design altitude of 50 km.

For the lifting gas there are many options to choose from, the most common are helium and hydrogen [97, 98]. Hydrogen is the lightest of all gases and therefore produces the most buoyancy, but has many problems. The two largest are, that - other than helium - it is flammable and it also leaks very easily. Therefore helium is used as a lifting gas for the Research Station. With a density of $0.18\,\mathrm{kg/m^3}$ helium is still considerably less dense than the atmosphere of Venus at 50 km ($1.59\,\mathrm{kg/m^3}$), without the additional problems, that hydrogen has.

Mathematical model of the Research Station There are four relevant forces acting on the Research Station, three of which are external, that can be modelled, the forth one is the thrust generated by the propulsion system F_{prop}. The external forces are the gravitational force F_g, the buoyancy force F_b and force due to aerodynamic drag F_d. These are modelled as

$$F_g = mg \tag{9.1}$$

$$F_b = V_{station}\rho_{atm}g \approx V_{balloon}\rho_{atm}g \tag{9.2}$$

$$F_d = \frac{1}{2}A\rho_{atm}c_D v^2 \approx \frac{1}{2}A_{balloon}\rho_{atm}c_D v^2 \quad , \tag{9.3}$$

with m the total mass of the Research Station, g the local acceleration due to gravity at $8.87\,\mathrm{m/s^2}$, V the volume of either the entire Research Station or just the balloon, which is the significant part of the Research Station, ρ_{atm} the density of the atmosphere at $1.59\,\mathrm{kg/m^3}$, c_D the drag coefficient, estimated to be 0.3, and v the airspeed of the Research Station. As explained in Chapter 3, the Research Station will float along with the wind in a retrograde direction around Venus. As per OR13 from Table 3.4 the Research Station needs to maintain a constant ground speed, so small variations in the wind speed have to be adjusted for. In addition to the adjustment in the East-West direction, the Research Station also has to be manoeuvrable in the North-South direction. This requires the Research Station to overcome a total of 6 m/s of airspeed. The drag (Equation (9.3)) resulting from this airspeed v therefore has to be overcome by F_{prop}.

The two remaining forces F_g and F_b also have to be equal, for the Research Station to float at a constant height. Therefore

$$V_{balloon} = \frac{m}{\rho_{atm}} \quad . \tag{9.4}$$

Using a cylinder with a length l eight times as large as its radius r (cf. Chapter 8) as a model, the radius of the balloon is

$$r = \sqrt[3]{\frac{V_{balloon}}{8\pi}} \quad . \tag{9.5}$$

This now fully describes the necessary size of the Research Station and can also be used to calculate the necessary thrust of the propulsion system.

But there are two issues not yet addressed. Firstly this calculation starts of with a total mass of the Research Station, but that also has to include the mass of the balloon itself and the

Helium, for which the following estimates can be made:

$$m_{balloon} = \left(2\pi r^2 + 2\pi rl\right) t \rho_{balloon} \tag{9.6}$$

$$m_{He} = V_{balloon} \rho_{He} \quad , \tag{9.7}$$

with a balloon thickness t of 1 mm, a density of the balloon material $\rho_{balloon}$ of 1400 kg/m^3 (Chapter 8) and a density of Helium ρ_{He} of 0.18 kg/m^3. This adds additional mass to the Research Station which also has to be accounted for. Secondly the propulsion system of the Research Station also has to be operational during night time. At the equator the radius of Venus R_{Venus} is 6051.8 km and the average wind speed v_{GS} - and therefore ground speed of the Research Station - is 60 m/s, which means one full circumnavigation of Venus will take

$$T_{cir} = \frac{2\pi R_{Venus}}{v_{GS}} = 176 \text{ h} \quad . \tag{9.8}$$

As there are no seasons on Venus, as the rotation axis is tilted by almost 180°, half of the time for one circumnavigation - so 88 h - is spent without any sunlight. Consequently the batteries have to hold enough energy to power the Research Station over night. Both of these components (balloon and batteries) add more mass to the Research Station, which requires a larger balloon, increasing both the mass of the balloon and the required thrust from the propulsion system, which increases power usage, which once again increases battery mass.

This circular dependency is a key design challenge, which is solved iteratively. At first the total mass m is split in to two, m_{Bat}, which is only the mass of the batteries to power the Research Station over night, and m_{other}, which includes the rest (payload, structural mass of the Gondola and the balloon as well as the Helium). For the first iteration m_{other} is set to 2593 kg, 477 kg of which are the payload and 2116 kg are the structural mass of the Gondola. Using this the thrust is now only dependent on the mass of the batteries. The upper part of the thrust and power curves in Figure 10.9a and 10.9b can be linearized to:

$$\alpha = \frac{T_{prop} + 466.67}{66.67} \text{ and} \tag{9.9}$$

$$P_{prop} = 911.41\alpha - 8616.978 \quad . \tag{9.10}$$

Using Equation (9.4), (9.5), (9.3), (9.9) and (9.10) and other power demands of the Research Station $P_{other} = 3885$ W, the total necessary battery storage is calculated by

$$E_{bat,req} = \frac{T_{cir}}{2} \left(P_{prop} + P_{other}\right) \quad , \tag{9.11}$$

which is only dependent on m_{Bat}. The maximum potential energy stored depends on the specific energy of the batteries $E_{sp} = 300$ Wh/kg (cf. Chapter 12)

$$E_{bat,max} = E_{sp} m_{Bat} \quad . \tag{9.12}$$

Setting the Equation (9.11) and (9.12) equal to one another, m_{Bat} can be solved.

Adding the mass of the balloon and the Helium (Equation (9.6) and (9.7)) to the initial 2593 kg sets m_{other} for the next iteration, which requires a slightly larger balloon as the mass has increased. This process converges, where the values at the point of convergence represent the final system design, some of which are summarised in Table 9.1.

As described in Chapter 8 the chosen thickness for the balloon is only 0.5 mm, which is lower, than in the previous calculations. The difference will lead to a lower total mass, meaning the Research Station floats a little higher in the atmosphere, which is good, as this will lead to higher

m	13953 kg
$m_{Payload}$	477 kg
$m_{Gondola}$	2116 kg
$m_{Balloon}$	3940 kg
m_{Helium}	1554 kg
m_{Bat}	5866 kg
T_{prop}	1.33 kN
P_{prop}	15.65 kW
r	7 m
l	57 m

Table 9.1: The final design values for the size and mass of the Research Station.

power production and lower necessary thrust, as the density of the atmosphere decreases. This represents a safety margin in the final design. Assuming a maximum temperature of 400 K inside the balloon, which is well inside the estimations of Chapter 13, and a minimum temperature of 350 K, the outside temperature, the pressure difference between inside the balloon will not exceed

$$\Delta p = p_{outside} \left(\frac{T_{max}}{T_{min}} - 1 \right) = 15230 \text{ Pa} \quad . \tag{9.13}$$

Modelling the balloon as a thin walled cylinder the tensile strength of the material used has to be higher than

$$\sigma = \frac{\Delta p \cdot r}{t} = 0.213 \text{ GPa} \quad . \tag{9.14}$$

This is the case for the material used (cf. Chapter 8), so a thickness of just 0.5 mm is suitable.

To ensure stability of the Research Station the centre of gravity (CG) has to be below the centre of buoyancy, so that the Research Station does not flip upside down and the CG has to be in front of the centre of volume (CV) so it does not turn front to back. Both of these can easily be accomplished by placing the batteries at smart location inside the Gondola underneath the balloon (cf. Chapter 8).

Over the lifetime of the Research Station the balloon will leak some of its helium to the outside. Therefore there has to be some additional Helium kept in reserve, though this will not be enough to compensate for a hole in the balloon. If an event occurs, that creates a hole in the balloon, it would immediately result in mission failure. In further research it should be investigated, if splitting the balloon into multiple independent compartments, would help with redundancy. Although the overall size of the balloon would have to be increased, so that a loss of one of these compartments does not lead to mission failure. In this concept, even if the balloon would be split into multiple compartments and one of them fails, the Research Station would loose so much height, that power production would no longer we sufficient anyways.

9.2 Scouts

The Scouts will have a much shorter lifespan and will not have a steady-state case, at which they operate. They are designed to be one time use only vehicles, that probe the atmosphere at a single point at different heights. As per UR03 and UR04 from Table 3.2 the Scouts are responsible for the exploration of the atmosphere from a height of 130 km. This can be done

by either by lifting the Scouts from the Research Station up to a greater altitude and then letting them drop, or they can be deployed from orbit. The lifting process has two advantages, firstly the Scouts could be attached at the Research Station until they launch, which would simplify logistics, and secondly the lifting phase could be designed in a way, that they have zero speed at 130 km. To lift the Scouts up to the desired height there are two possibilities, either an active propulsion (rocket) or another balloon. Ignoring the aerodynamic drag and all other inefficiencies the rocket would need a Δv of at least

$$\Delta v > \sqrt{gh} = 950 \text{ m/s} \tag{9.15}$$

to reach 130 km with a launch from the Research Station, which is significantly too much to carry along for each scout, even though they will only have a mass of 30 kg. Using a balloon it would need a volume of at least

$$V > \frac{m}{\rho_{atm,130\text{km}}} = 0.4 \text{ km}^3 \quad , \tag{9.16}$$

which is much too large. Therefore both options to lift the Scouts up to 130 km from the Research Station are unfeasible, so they will be deployed from orbit.

This has the advantage, that it is actually feasible and it is more efficient. As ultimately everything has to be deployed from orbit anyways, it is obviously less efficient to first bring the Scouts with the Research Station down to 50 km, before lifting them back up to 130 km. The flight dynamics of the Scouts have to explain their entire lifespan starting in orbit to maximize the height, at which the instruments can start to work, which is at a certain speed, so the goal is to bleed of as much speed as possible as high up in the atmosphere as possible. This entire process is simulated, which is split up into multiple parts:

1. Detachment from the Carrier Vehicle 1 and de-orbit burn.
2. Coast phase to the upper atmosphere of Venus.
3. Aerobraking in the atmosphere.
4. Deployment and decent under a drogue parachute.
5. Deployment and decent under a main parachute.
6. Dismissal of the parachute and further decent.
7. Touchdown on the surface.

Detachment and de-orbit burn The orbit of the Carrier Vehicle 1 is an elliptical polar orbit with a perigee height of 300 km and an apogee height of 15000 km. An even higher apogee would decrease the necessary Δv of the de-orbit burn, but further increase the initial speed at which the Scouts hit the atmosphere, and vice versa for a lower apogee. As the orbit is a polar orbit the Carrier Vehicle 1 will pass over all parts of Venus after at most half a rotation of Venus. That and the exact timing of the deployment of the Scouts (slightly before or after they pass the apogee) gives the Scouts the opportunity to land at any point on Venus. In the simulation it is assumed the Scouts detach exactly at the apogee. After the detachment from the Carrier Vehicle 1 the de-orbit burn is preformed, which has a Δv of 32 m/s. This is just enough for the Scouts to enter deep enough into the atmosphere, so that they will not jump of it, any larger burn, would only further increase the entry speed. At this point the position and initial velocity $v = v_{orbit} - \Delta v$ are set and the simulation starts.

Coast phase During this part of the simulation only the acceleration due to gravity of Venus is simulated to update the position and velocity of the Scout.

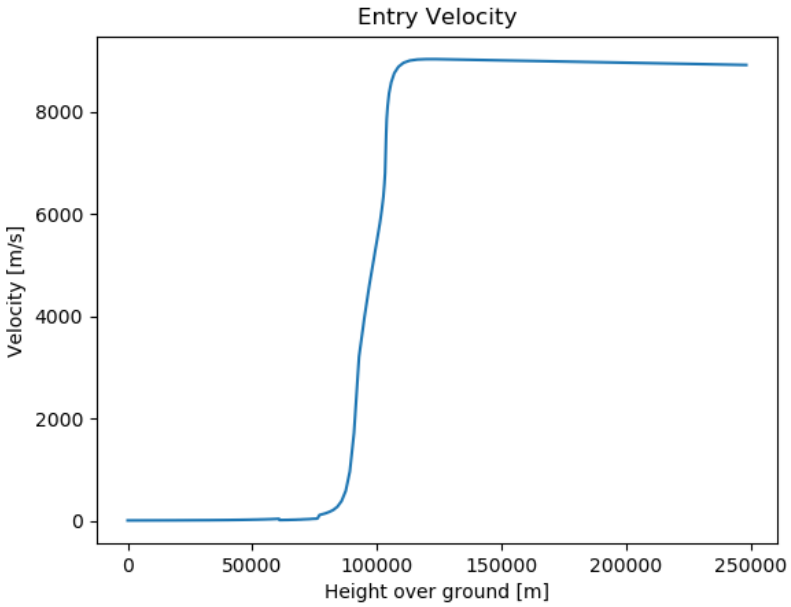

Figure 9.1: The velocity of the Scouts during atmospheric entry based on their height.

Aerobraking At a height of 250 km the next phase of the simulation starts. Besides gravity aerodynamic drag is now also taken into account, for which the density of the atmosphere is used as given by the NASA Software Venus-GRAM, explained in Section 16.2. In this phase braking is done using only the heat shield, which is modelled as a cone with a half vertex angle of 75° hence a drag coefficient of 1, as described in [99].

Drogue parachute At a speed of Mach 9 the drogue parachute is deployed, which has a drag coefficient of 0.3 [100]. It is assumed that the diameter is 3 m.

Main parachute As soon as the Scout falls short of Mach 0.3 the drogue parachute is cut and the main parachute is deployed. For the main parachute a drag coefficient of 0.55 with a diameter of 5 m is assumed [100].

Free fall Due to the very high density of the atmosphere at lower altitudes, the main parachute is cut at a speed of 10 m/s. From this point onwards the drag on the Scout itself is high enough to slow down the Scout, so no more parachute is necessary.

Touchdown As soon as a height of 0 m is reached the simulation is stopped, as the Scout has touched down. At this time the part of the Scouts lifespan relevant for the flight dynamics is over. The Scout will keep operating for another hour on the ground to transmit all the gathered data to the Research Station, but will eventually stop to operate, either when the power runs out, or the environment destroyed it, which ever comes first.

Results Running the simulation gives us the velocity of the scout at the different heights in the atmosphere. This is shown in Figure 9.1, from which it is clear, that almost all of the

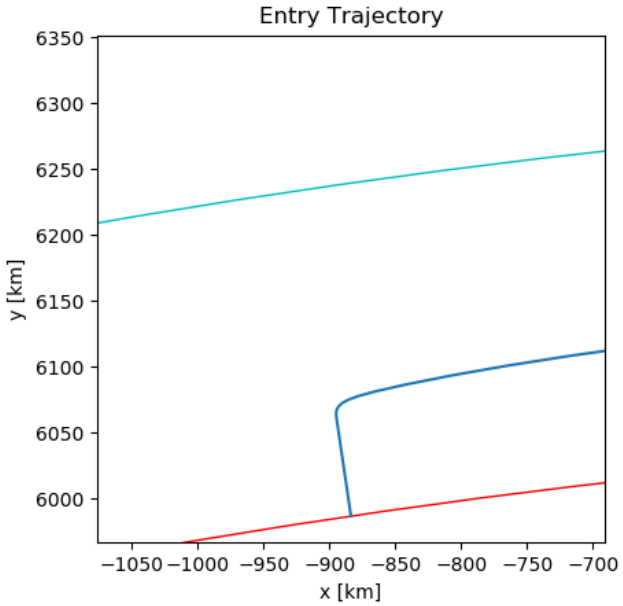

Figure 9.2: The trajectory of the Scouts during atmospheric entry. The blue line represents the trajectory, the orange line the ground and the cyan line a height of 250 km. The distances on the x and y axis are measured from the centre of Venus.

height above surface [km]	**fall time to surface [min]**
250	176
90	169
76	167
50	146
40	134

Table 9.2: The fall time through the atmosphere to the surface of the Scouts at various heights.

speed is dissipated over a short time period starting at around 90 km of height. This also can also be observed in Figure 9.2, in which there is a sharp bend in the trajectory. During this time is also when the maximum heat load of 8.833 MW (11.247 MW/m^2) occurs. This phase of large deceleration (heat load $>$ 80 KW) lasts for 280 s with an average heat load of 4.229 MW (5.385 MW/m^2) and is shown in Figure A.5. This also means that the Scouts do not reach a sufficiently slow speed fast enough to start the measurement process at 130 km. It is assumed from Section 7.2 that the payloads can start to work once the speed is below 100 m/s, which is only reached at a height 76 km. Further optimizations could be done, but will not significantly increase the height, at which 100 m/s is reached, as this is mainly limited by the extremely low density of the atmosphere above 90 km, which makes any aerobraking above that ineffective. Similarly the instruments could be redesigned to be able to work at higher speeds, but this would also only result in small improvements.

Time wise the lifespan of the Scouts are separated into three Sections. The coast phase up to the upper atmosphere (250 km) takes 141 min, the decent through the atmosphere takes 176 min, and finally an hour on the surface of Venus. More detailed times foe more heights can be seen in Table 9.2. Once at the surface the atmosphere is so dense, that the Scout has slowed down to 3 m/s, slow enough so that it can land without further considerations. Some of the further plots from the simulation can be seen in Figure A.2 to A.5.

As the Section 9.1 is focused only on the flight dynamics of the Research Station within the atmosphere, there is no Section about the deployment of the station. But the deployment of the Research Station will follow a similar pattern as the entry of the Scouts, so the simulation used for that could be slightly adapted to also simulate the entry and deployment of the Research Station. For this the main difference is the balloon, which will be filled with Helium during the entry, as soon as the Research Station is somewhat stabilized, which could be at around 70 km [101].

CHAPTER 10

Propulsion

by Harsh Lakkad

The Chapter presents usage of the Cyclocopter as propulsion for the Venus Research Station (VRS). The first section provides a summary of the selection considerations that lead to the parameters that must be taken into account while developing the propulsion system for space missions with the Mission's Feasible Propulsion Systems. The history of Cyclocopter propulsion and the inspiration behind its use are discussed in the next section. The part immediately adjacent to it describes the layout of Cyclocopter propulsion with material to be employed with its advantages on the VRS. The Chapter is ended with a possible improvement in efficiency.

10.1 Mission's Feasible Propulsion Systems

In the following, first important factors for a propulsion system are presented, and then feasible systems are analysed with pros and cons approach.

Factors of Choice

In general, the propulsion systems needed to establish an orbiting station on Venus depend on the mission's architecture and goals. The planned orbital height and inclination, the size and mass of the orbital station, the length of the mission, and the kind and quantity of scientific instruments and equipment that would be carried by the spacecraft are just a few of the important elements that would need to be taken into account. Here are some of the key factors that should be taken into account when designing a propulsion system for an outer space mission:

1. **Functional Requirement:** The propulsion system should be designed to meet the specific Functional Requirement, such as the destination, duration, and the required manoeuvrability of the spacecraft.
2. **Thrust and Specific Impulse:** The amount of thrust generated by the propulsion system and the specific impulse (i.e., the fuel efficiency of the engine) are key factors that determine the mission design and the amount of fuel required.
3. **Power Requirements:** The propulsion system should be designed to meet the power requirements of the spacecraft, which depend on the type and number of instruments, communication systems, and other subsystems onboard.
4. **Fuel and Propellant:** The choice of fuel and propellant is critical, as it affects the performance, efficiency, and mass of the propulsion system. The storage and handling of fuel and propellant also need to be considered.

5. **Environmental Considerations:** The space environment, including radiation, temperature, and vacuum conditions, can affect the performance and reliability of the propulsion system, and the system should be designed to withstand these conditions.
6. **Mass and Volume:** The propulsion system should be designed to minimize the mass and volume of the spacecraft, as these factors affect the launch vehicle requirements, the mission cost, and the overall performance.
7. **Low impact on the environment:** Any propulsion system used in the Venusian orbit must not create any significant environmental impact, such as the release of harmful gases or debris.
8. **Reliability and Safety:** The propulsion system should be designed to ensure reliability and safety during the mission, and the system should be tested and qualified before the launch.

Feasible Propulsion Systems for the mission are given in Table 10.1 with their benefits and drawbacks.

Type of Propulsion	Pros	Cons
Electrical		
Fuel Cell Power	• High Energy Efficiency • Environmentally Friendly • Reliable Power Generation • Versatile Fuel Options	• Limited Energy Density • Technological Maturity • Heat Management • Fuel Storage Handling Challenges
Battery-powered	• Environmental Compatibility • Simplified Fuel Supply • Reduced Heat Generation • Operational Flexibility	• Limited Energy Storage • Heavy weigh • Limited Power Output • Battery Degradation in Extreme Conditions
Solar based	• Long Endurance • Renewable Energy • High Efficiency • Precise Manoeuvrability	• Limited Power Generation • Power Storage Challenges • Limited Thrust • Atmospheric Hazards
Propeller-based	• Energy Efficiency • Simplicity and Reliability • Control and Manoeuvrability	• Limited Altitude Capability • Corrosive Environment • Temperature Challenges • Limited Thrust in Dense Atmosphere
Solid-state Aircraft	• Simplified Propulsion System • Higher Efficiency • Reduced Fuel Requirements • Lower Emissions	• Limited Power • Longer Flight Durations • Technological Limitations • Limited Operational Experience

(To be continued)

Type of Propulsion	Pros	Cons
Entomopter Concept	• Low Mechanical Complexity • Energy Efficiency • Manoeuvrability • Adaptability to Venusian Atmosphere	• Limited Payload Capacity • Flight Endurance • Complex Aerodynamics
Stopped-Rotor Cyclocopter	• Enhanced Manoeuvrability • Vertical Takeoff and Landing • Hovering and Station-Keeping • Adaptability to Harsh Conditions	• Limited Payload Capacity • Atmospheric Challenges

Table 10.1: Types of propulsion systems with pros and cons.

10.2 Cyclocopter

Conception and Scientific Research A rotating-wing system called a '**Cyclocopter**', also known as a '**Cyclorotor**' or '**Cyclogyro**'Figure 10.1a, has a blade span that is parallel to the axis of rotation. Each blade's pitch angle can be mechanically adjusted cyclically such that it encounters positive angles of attack at both the top and bottom of the azimuth cycleFigure **??**. As demonstrated inFigure **??**, the resulting time-varying lift and drag forces generated by each blade may be resolved into the vertical and horizontal directions. The amount and direction of the net thrust vector $T_{Resultant}$ produced by the Cyclorotor may be altered by varying the amplitude and phase of the cyclic blade pitch. This design allows Cyclocopter to manoeuvre in all directions, including vertical take-off and landing, hover, and potentially operate in dense atmospheric conditions. Moreover, it exhibits remarkable manoeuvrability, allowing them to operate in diverse flight regimes. The cyclic pitch control of the blades enables omnidirectional thrust, granting the ability to hover, manoeuvre vertically, and move in any direction. This versatility makes Cyclocopter well-suited for navigating challenging atmospheric conditions, such as those found on Venus.

Additionally, each spanwise blade element of a Cyclorotor operates at similar aerodynamic conditions (i.e., at similar flow velocities, Reynolds numbers, and angles of attack) compared to a conventional rotor, making it easier to optimize the blades to achieve the best aerodynamic efficiency. Furthermore, because the blades are cyclically pitched (1/rev), uneven flow processes may postpone the onset of blade stall, increasing the lift generated by the blades. Prior research has indicated that Cyclorotor may be able to achieve efficiencies like those of conventional rotor systems [102] and may also be able to generate significantly greater maximum thrust values.

$T_{Resultant}$ and Thrust phasor β are calculated from the values of T_Y and T_Z as shown in Figure 10.1b by using

$$T_{Resultant} = \sqrt{{T_Y}^2 + {T_Z}^2}\,, \tag{10.1}$$

Thrust Phasor

$$\beta = \tan^{-1}\left(\frac{T_Z}{T_V}\right)\,, \tag{10.2}$$

where, the angle β is calculated using $T_{Resultant}$.

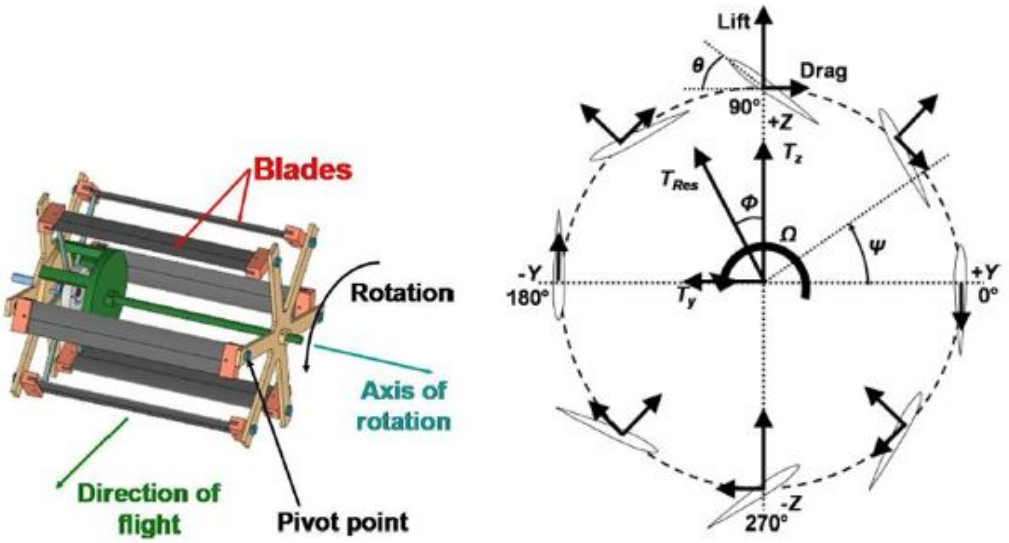

(a) Schematic of cycloidal rotor. (b) Blade kinematics and forces on cycloidal rotor.

Figure 10.1: Cyclodial rotor concept[102].

Scientific Research on Cyclocopter has been around for more than a century, although it's unclear who came up with the concept first. There haven't been any successful flying Cyclogyros, despite the fact that the viability of the Cyclorotor idea has been demonstrated both theoretically and practically by top aerospace researchers [103, 104]. The vast majority of prior attempts to construct a flying Cyclogyro/Cyclocopter lacked rigorous scientific research (theoretical or experimental) to fully comprehend the mechanics of such a device. This was the fundamental factor in the failure of all of these endeavors, which in many instances did not even make it through the design phase. The majority of the academic research on Cyclocopter from the 1920s to the present is included in this section.

In 1920s, Professor Kurt Kirsten of the University of Washington pioneered the research on cycloidal propulsion systems both for air vehicles and marine applications [105, 106]. Kirsten collaborated with Mr. W. E. Boeing and started conducting tests on the cycloidal propeller which he designed, known as the '**Kirsten-Boeing**' propeller. One of the primary benefits of the cycloidal propeller, according to Kirsten, is its nearly instantaneous ability to spin the thrust vector in any direction around the azimuth. The idea was to develop a '**cycloplane**' that could hover and move forward, as well as to use the cycloidal propellers' capacity to vector thrust for three-dimensional control of an airship. For airship control, it is feasible to direct the thrust in the required directions to rise, drop, or move forward and backward if the propellers are mounted with their axis of rotation perpendicular to the vertical plane of the airship. On the other hand, the airship can be propelled laterally if the axis of rotation is in the vertical plane.

During the period 1924–1933, Swedish-French engineer Strandgren carried out numerous experiments with cyclogyro models, first in aerodynamic laboratory in Saint-Cyr and subsequently with 'Lior-et-Olivier', a French aircraft manufacturer, where even real-size experiments were undertaken [107].

Motivation for Cyclocopter

Shenondoah In a series of papers spanning from 1944 to 2009, In 1934,American airship 'Shenondoah', as shown in Figure 10.2. It can be seen that the outer rim was left off so that the blades project directly into the open air. Six main propellers were thus designed with their axis 30 to the horizontal plane. The propellers were designed for a thrust of 1800 pounds each[105].

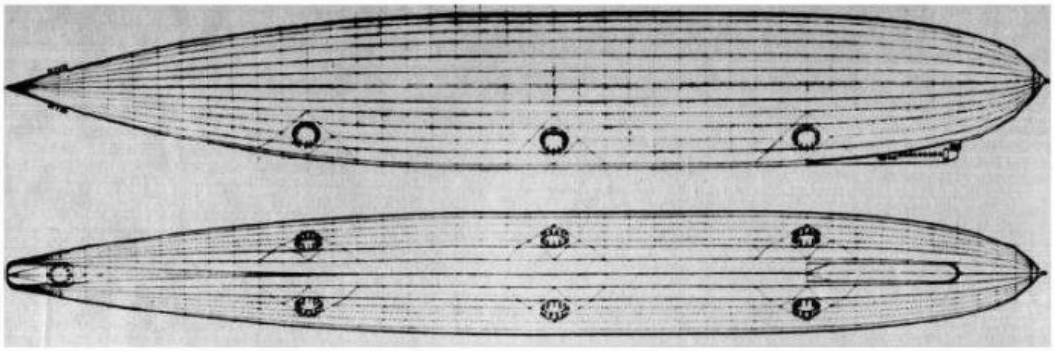

Figure 10.2: Side view and top view of an airship installed with Kirsten-Boeing propellers [105].

Nozaki In 2009, Nozaki et.al. conducted experimental studies on a cycloidal rotor to be used on a 20 meter airship as shown in Figure 10.3a andFigure 10.3b. The rotor used 3 blades with a rotor diameter of 2 meters, blade span of 1 meter, and chord of 0.3 meter. The blades used NACA 0012 airfoil profile[108].

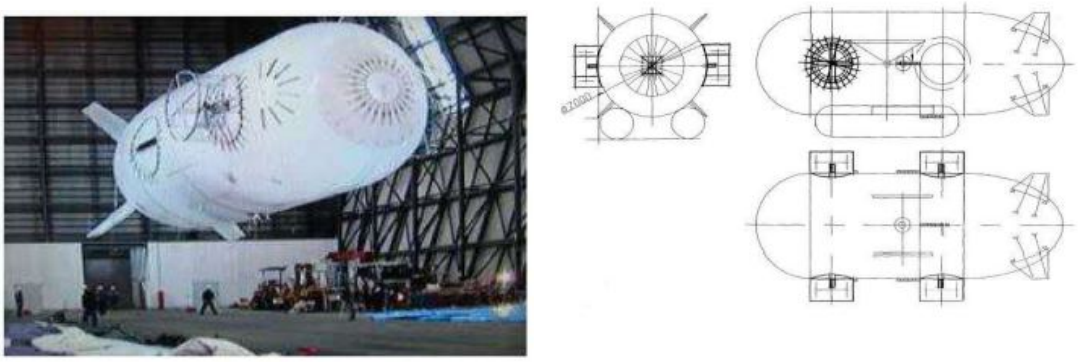

(a) Cyclocopter Installed on a 20 meter Airship. (b) Airship-type Aerial Base Robot.

Figure 10.3: Cyclorotor for Airship Control [108].

Blades Pitching Mechanism

Designing a straightforward, lightweight blade pitching mechanism is crucial if the Cyclorotor concept is to be used to a flying vehicle. The system designed to provide the necessary cyclic blade pitch is purely passive. As a result, the frictional losses caused by the moving parts are the sole power penalty experienced during operation. Two bearings made up the majority of the blade pitching mechanism, as depicted inFigure 10.4a. These bearings are positioned so that their axes are offset by L2 Figure 10.4b. The offset ring, which is put in place around bearing number 2, is attached to the pitch connections. The blade is attached to the opposite end of each linkage at point (B) behind the blade-pitching axis (A) seeFigure 10.4b. The system that resulted included a four-bar crank-rocker mechanism that could alter the blade pitch cyclically as needed. The offset length, L2 can be changed to adjust the pitching amplitude of the blades. The offset's size altered the pitching amplitude of the blades, which in turn altered the thrust generated.

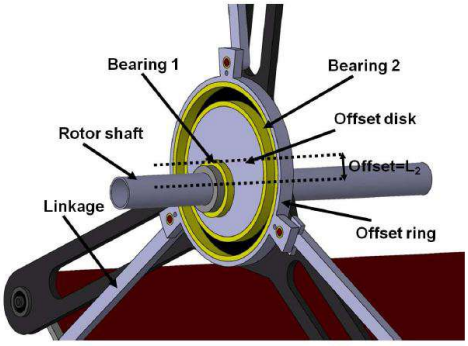

(a) Passive blade pitching mechanism.

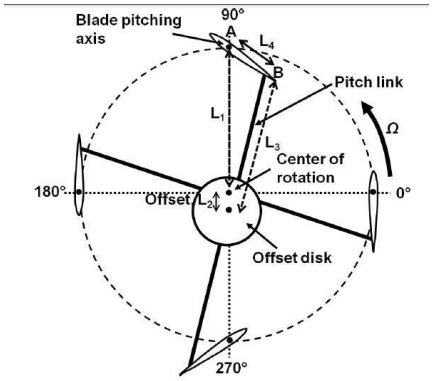

(b) Schematic showing the blade pitching mechanism.

Figure 10.4: Blade Pitching Mechanism [109].

Analysis and Performance

A computational fluid dynamics (CFD) study is done in addition to the modification of the current aerodynamic model to better pinpoint the properties of the cycloidal blades' system. Aerodynamic analysis may be performed using the commercial CFD programme FLUENT (ANSYS-Fluent, Inc., Lebanon, New Hampshire)[1]. Due to the cycloidal rotor blades' sinusoidal pitch angle fluctuations and the rotor's rotating motion, a moving mesh is required for this research. Thus, the FLUENT sliding mesh approach may be used. The produced mesh utilized in this investigation is seen in Figure 6. There are 79676 cells in this two-dimensional mesh, comprising four spinning blade domains and one rotating rotor domain. Using a 2.3 GHz CPU machine, the overall computation time for 20,000-time steps for unstable and transient simulations may take close to 12 hours. The flow field and thrust force of the cycloidal rotor may be determined using the studies.

[1]CFD : Computational Fluid Dynamics, ANSYS : Computational Analysis Software

	Specifications
Analysis type	Two-dimensional transient
Mesh type	Quadrilateral
Total number of cells	79,676
Rotating angle/time step	1.8 deg
Number of domains	6
Moving mesh type	Sliding mesh
Turbulence model	K-epsilon
Variables	Pitch angle
Number of time steps	20,000
Analysis time	12 h (at 2.3 GHz)

(a) CFD analysis conditions.

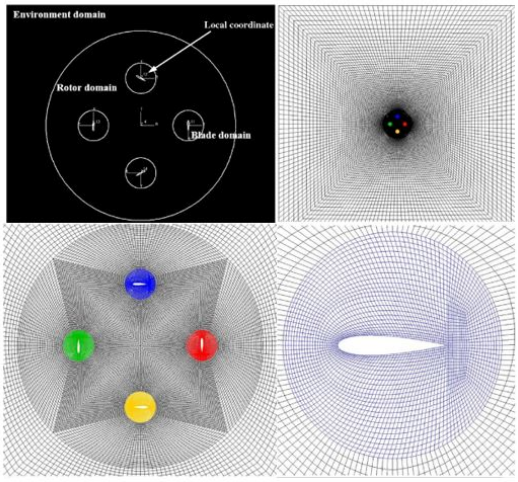

(b) CFD meshes of the Cycloidal Blades System.

Figure 10.5: Computational analysis [110].

10.3 Venus Resaerch Station's Onboard Cyclocopter

Designing the Cyclorotor with the least amount of weight and mechanical complexity was the primary difficulty in the Cyclocopter' s construction. The cyclorotor system employed for our expedition is depicted in Figure 10.6.

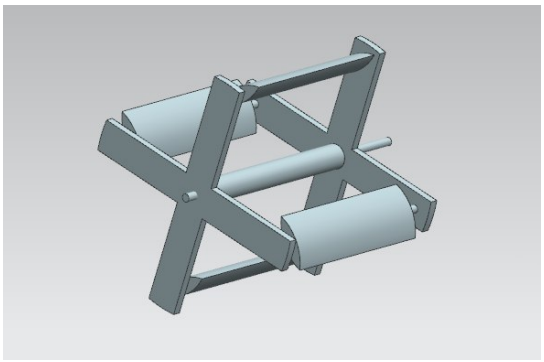

(a) Propulsion system architecture.

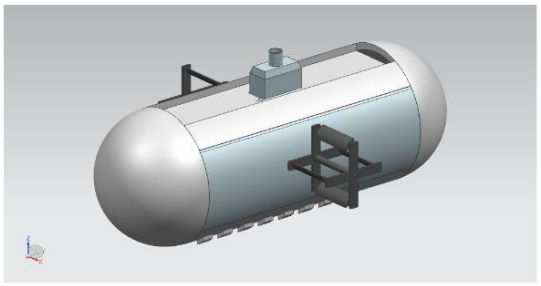

(b) Position on the Gondola.

Figure 10.6: Design overview of the propulsion component.[Bhosale]

Layout Including Benefits

The constraints of the propulsion system are illustrated in the accompanying Figure 10.7. Figure 10.8 shows the materials utilised for various Propulsion system components.

No.	Subsystems	Total Mass (KG)	Dimensions (m)	Volume (m^3)	Description of Components
1.	Rotors blades	32.6	1.5(L)*0.247(B)*.044(T)	0.016302	NACA0018
2.	Blade winglets	7.8	0.3(L)*0.260(B)*0.050(T)	0.0039	Winglets to reduce Induced drag
3.	Rotor Shaft	21.36	1.7(L)*0.20(Dia.)	0.053407	connected to motor via bearing mechanism
4.	Rotor (Hollow cylinder)	5.18	0.15(L)*0.50(Dia.)	0.01295	connected to shaft
5.	Blade-Rotor shaft linkage	21.6	1.8m(L)*0.20m(B)*0.15m(T)	0.054	linked to rotor shaft and blades
6.	Blade Tip linkage (off-set) to main Rotor	3.6	0.6m(L)*0.15m(B)*0.10m(T)	0.0090	to change pitching of blades
7.	Motor+Servo	20	0.20m(L)*0.15m(B)*0.15m(H)	0.0045	-
	Total Mass (Two Rotor)	**224.28**	**Total Volume (Two Rotors)**	**3.80146**	

Figure 10.7: Estimation of construction parameters and mass.

No.	Components	Made of	Temperature Sustainability	Density(g/cm^3)
1.	Blades	Foam Core+ Carbon composite Prepreg wrapped	250°C to 400°C	0.020
2.	Winglets	Foam Core + Carbon composite Prepreg wrapped	250°C to 400°C	0.020
3.	Rotor Shaft	Aluminum Foam	330°C	0.4
4.	Blade-Rotor shaft linkage	Aluminum Foam	330°C	0.4
5.	Blade Tip linkage	Aluminum Foam	330°C	0.4

Figure 10.8: Details on fabrication.

Benefits of Employing These Materials like foam core and aluminium foam in Cyclocopter propulsion system offers several advantages in certain applications. Some of the advantages are:

1. Light weight,
2. High Strength-to-Weight Ratio,
3. Energy Absorption and Impact Resistance,
4. Thermal Insulation,
5. Design Flexibility.

10.4 Results and Efficiency Improvement

A figure derived by CFD analysis from applied mesh and computational data is shown in Figure 10.9 below.

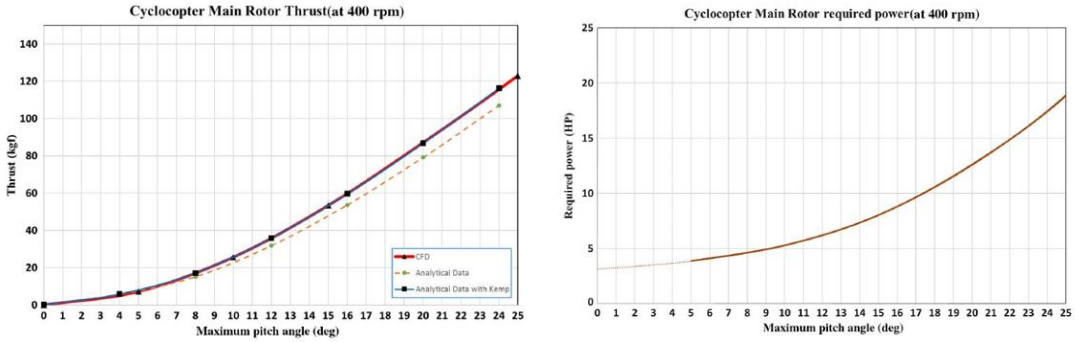

(a) Thrust vs pitching angles.

(b) Power required vs pitching angles.

Figure 10.9: CFD results obtained for thrust end Required power of the cyclocopter main rotor[110].

According to Section 9.1, maximum Thrust and Power requirements for manoeuvring The Research Station are $T = 1.33\,\text{KN}$ and $P = 15.65\,\text{Kw}$. Under the linearity assumption after a 22-degree pitching angle and using the graphs (Figure 10.9), the blades must pitch at 28-degree angle. At 28 degree, $T = 135.71\,\text{kgf}$,[2] $P = 2\,\text{Hp}$.[3] This is equivalent to the mission's necessary thrust and power.

Efficiency Improvement

The revolving blades of cycloidal propellers experience a variety of drags. These drags consist of profile drags of the drags and driving arms brought on by blade tip vortices. The main goal of these inspections is to lessen these two different types of drags.

Fairing Effects The drag reduction fairing effect is a term that describes the aerodynamic advantages gained by adding streamlined fairings or covers to exterior structures, such as cars or other objects. The resistance that an item experiences when travelling through a fluid medium like air or water is known as drag, and these fairings are made to lessen it.

The following methods can explain the drag reduction fairing effect:

[2]Kgf to KN: 1kgf = 0.0098KN
[3]HP to KW: 1HP = 0.7456KW

- Streamlined Shape,
- Minimization of Cross-Sectional Area,
- Smoothing of Surface Irregularities.

Winglet Effects Winglets are frequently added to wings to prevent wing-tip vortices. It is well known that winglet effects can increase the lift coefficient of three-dimensional wings. Increased thrust and thrust/power consumption rates are therefore possible.

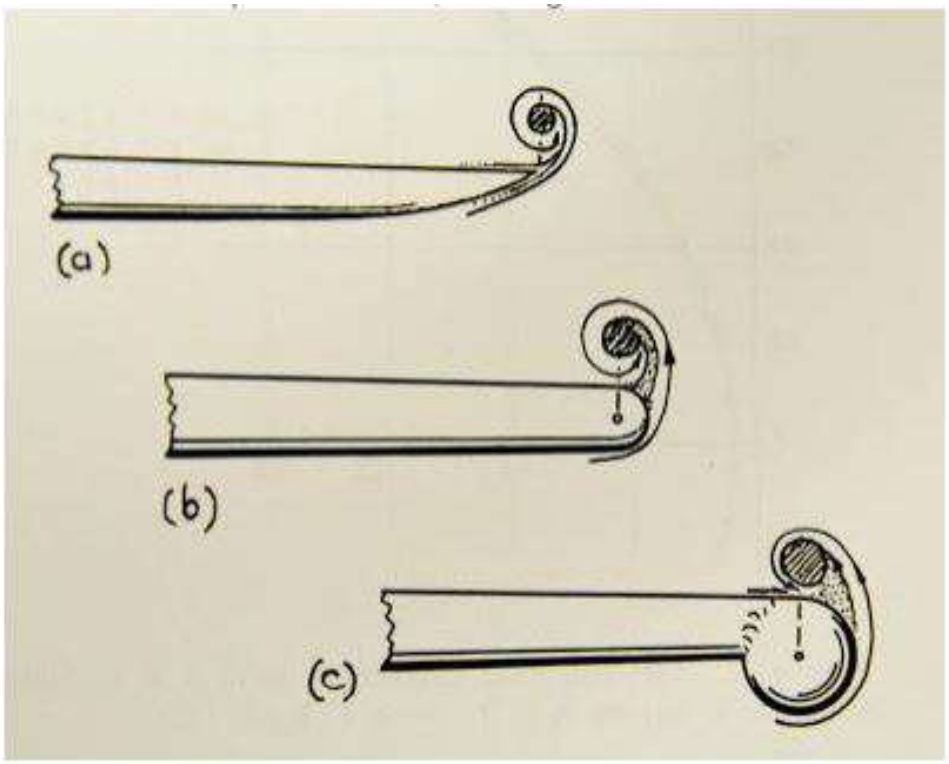

Figure 10.10: Vortices size with different winglets[111].

CHAPTER 11

Guidance, Navigation, and Control

by Salomon Lydon

In this Chapter, the development of the guidance, navigation, and control (GNC) subsystem of the Venus Research Station (VRS) is presented. The GNC subsystem is an integral part of any autonomous, mobile platform, and the unique challenges presented by the Venus environment further accentuate the necessity of a robust, reliable GNC subsystem. This Chapter is divided into sections discussing guidance, navigation, and control, respectively. In each section, the main challenges are presented and briefly analyzed, and the final concept design solution is presented.

11.1 Guidance

In order to meet all requirements and fulfill the mission objectives, the VRS must be capable of investigating regions of Venus that are of particular scientific interest. This includes regions on the surface of Venus as well as regions within the atmosphere. Due to the significant time delays involved in communication between Earth and Venus, remote control of the system is not feasible. Therefore, a certain level of autonomy must be realized. The first step in achieving autonomous navigation is relaying information about regions of interest from Earth to the VRS. This is achieved via the network of communication relay satellites in orbit around Venus. Telecommands are sent from mission control on Earth to the relay satellites, which then transmit this information to the VRS.

As discussed in Section 9.1, the VRS will primarily float passively within the atmosphere. Due to the rotation of the atmosphere relative to the surface of Venus, the longitude of the station changes at a roughly constant rate. This operational concept simplifies the guidance portion of this subsystem greatly. Since the East-West motion of the station is realized passively, target longitudes need not be assigned, and only target latitudes and altitudes must be relayed to the Research Station. This effectively limits the position control to two dimensions. Furthermore, changes in latitude and altitude have little to no impact on each other, thus allowing them to be treated independently. This further simplifies the guidance problem to two independent one-dimensional states. The primary benefit of this is that complex trajectories are unnecessary to complete the mission. Rather, straight-line paths can be used to update the VRS position in each of the control dimensions.

Important to note is that the guidance concept described thus far does not consider short-time-scale perturbations and atmospheric fluctuations. Furthermore, attitude control of the VRS is not taken into consideration when discussing guidance because the attitude of the system is not directly relevant to the completion of the mission, and therefore requires no explicit command. However, attitude control is essential to the survival of the system in the Venusian

atmosphere and is therefore crucial to the completion of the mission. These issues will be considered further in the control section of this Chapter.

In summary, the guidance portion of the GNC subsystem is concerned with how the VRS updates its target state (i.e., latitude and altitude) and generates internal commands to which the controller and actuators must react.

11.2 Navigation

Before closed-loop control can be achieved, the controller must have some way of measuring the state of the Station, and thus generate an error signal to be corrected by the actuators. This is the problem addressed by the navigation section of the GNC subsystem. In general, an aircraft in flight has three translational and three rotational degrees of freedom. The three translational degrees of freedom correspond to the problem of localization of the station, and the three rotational degrees of freedom correspond to the problem of attitude determination. These problems will be dealt with separately in the following subsections.

Localization

In this paper, localization refers to the process of determining the position of the VRS relative to Venus. This includes determining the longitude, latitude, and altitude of the Station as it moves relative to the surface. Therefore, reference points along the surface of the planet must be selected (either prior to the mission or in real-time) to maintain a precise estimate of the position of the Station. Without precise location estimates, the maps created from the SAR instrument data will decrease in accuracy. The method by which the VRS determines its position is discussed in the following section.

Localization Method In modern terrestrial airships, the primary method of navigation is satellite based navigation via a global navigation satellite system (GNSS). However, satellite navigation services are not available on Venus, nor is it currently feasible to establish such a system. Therefore, the VRS cannot determine its position in the Venus-fixed coordinate system with satellite based methods. In the absence of global positioning capabilities, the VRS must employ other methods of localization using the resources available. One such resource is the SAR instrument, which can be used, along with on-board data processing, to recognize and track features on the surface of Venus as it scans. Through this process, the station is simultaneously determining its position relative to some surface features and generating a map of the surface of Venus. This process is called simultaneous localization and mapping (SLAM). Several algorithms for this process exist and can be employed to track the position of the VRS while simultaneously completing its mission to map the surface of the planet. [112] The benefit of this approach is that prior surface maps exist, to varying degrees of resolution, for some regions of Venus. Therefore, the Station can determine its initial position using the SAR instrument based on the identification of surface features derived from existing surface maps. However, as the VRS moves relative to the surface of the planet, different surface features will come in and out of view of the SAR instrument. It is for this reason that SLAM algorithms must be employed. The station must be able to identify and keep track of new features throughout its circumnavigation in order to ensure precise, reliable localization.

A drawback of this approach is the high computational cost of processing large amounts of SAR data onboard the VRS. Therefore, inertial measurement units (IMUs) can be used to estimate the position of the VRS on short timescales, and those estimates can be periodically updated by SAR measurements using stochastic methods such as Kalman filtering. A similar

approach is often employed in military submarines, wherein the body of water above the submarine makes GNSS localization impossible for long periods of time. Thus, the submarines often must estimate their location via inertial navigation until they can safely surface and update their position estimates with precise GNSS data.

Important to note is that the navigation concept cannot be based solely on inertial navigation with IMUs due to their tendency to accumulate errors over time. Therefore, periodic updates from more precise localization techniques (e.g., the aforementioned SLAM algorithms) are necessary to mitigate the inaccuracies introduced by IMU integration error propagation.

The above discussion has focus primarily on determining the longitude and latitude of the VRS. The SAR measurements also provide altitude data, however, they cannot be the sole source of altitude measurements. Therefore, barometric altimeters are used in conjunction with SAR measurements to determine altitude.

Localization Instruments The localization instruments follow logically from the localization described above. A combination of SLAM and inertial navigation will be used for localization, therefore necessitating a mapping instrument and an IMU, respectively. The VRS is already equipped with a SAR payload instrument for mapping the surface, which can be used for navigation via SLAM as well. To minimize the effects of error propagation from integration of IMU measurements, low random-walk, low bias-drift IMUs have been selected. Tactical grade IMUs, such as those used on military submarines, are characteristic examples of those required for this mission, e.g., SDI500 Quartz MEMS Tactical Inertial Measurement Unit. [113] Furthermore, barometric altimeters such as the HDI series amplified pressure sensors from First Sensor can be used for altitude measurements. [114]

The above-mentioned localization instruments are intended to be representative examples of the types of instruments that could be employed for a mission such as this. However, to determine whether these specific models or merely instruments with similar characteristics should be used, further detailed analysis is required, which is beyond the scope of this paper.

Attitude Determination

The attitude determination aspect of the GNC subsystem shares many similarities with the localization aspect. The primary challenge facing this subsystem is finding reliable references relative to which the orientation of the station can be determined. Typically, space-based systems will use distant stars, the Sun, other celestial bodies, the magnetic field of the Earth, etc. as attitude references. However, Venus has no permanent magnetic field, and its atmosphere drastically reduces the amount of light that reaches the VRS. Therefore, using celestial objects for attitude determination is not possible. The only remaining viable reference is Venus itself. The specific method employed is discussed below.

Attitude Determination Method As with the localization method, which uses the SAR instrument to identify surface features that can be used as position references, measurements from the SAR can be used to determine attitude. In its simplest form, two vector observations (e.g., the position vectors of two distinct surface features in the VRS frame) can be made, which are then compared to known representations of those vectors in the base reference frame (e.g., the position vectors of those same surface features in the Venus-fixed reference frame) in order to determine the transformation matrix between the observation (VRS) frame and the base (Venus-fixed) frame. There are various algorithms which solve this problem, the earliest of which being TRIAD. The two-vector observation problem, and in particular the TRIAD solution, is a special case of the more general n-vector observation case, wherein each observation is given a

weight, and an optimization problem must be solved. [115] The number of vector observations available to determine attitude at any given time depends on the number of visible surface features and available computational resources. Therefore, the algorithm employed must be flexible with respect to the number of observations.

This n-vector observation method is the cornerstone of accurate attitude determination in this concept design, however, it cannot be the sole source of attitude estimation. As mentioned above, continuous onboard processing of the SAR data is a large computational undertaking, and is not ideal for our system. Therefore, measurement of rotation rates and the local gravity vector by the IMUs will be used for short timescale attitude estimation. Attitude estimates will then be periodically updated by the more precise SAR attitude measurements. In this way, accurate, robust attitude determination can be ensured.

Attitude Determination Instruments The attitude instrument suite is largely the same as the localization instrument suite. However, altimeters are not necessary for attitude determination. Therefore, they are omitted here. Thus, the attitude determination instruments include the aforementioned IMUs and the SAR payload instrument.

11.3 Control

The guidance and navigation concepts discussed thus far support the primary aim of the GNC subsystem: control. As in Section 11.2, the control concept will be split into attitude and position control. However, position control relies heavily on attitude control. Therefore, attitude control will be discussed first.

Attitude Control

The choice to operate an airship in the Venusian atmosphere introduces unique attitude control challenges that space-based systems need not consider. For example, the complex, highly non-linear aerodynamics involved in flight within the atmosphere can be ignored for most orbital spacecraft. However, some unique characteristics of fluid mechanics can be exploited to reduce the energy required to achieve attitude control. The following paragraphs investigate these phenomena further.

Passive Stability In Figure 11.1, the roll, pitch, and yaw axes are depicted. They are the x-, y-, and z-axes, respectively. The definition of these axes is important to the following discussion. Due to the relatively high concentration of mass in the gondola below the balloon, the center of gravity (CG) is below the center of volume (CV), which is also assumed to be the center of buoyancy (CB). It is about the CB (and, therefore, the CV) that the airship rotates.

As the CG lies below the CV, if the roll or pitch of the VRS is perturbed, the buoyancy force acting on the CV and the gravity force acting on the CG generate a force couple. Clearly, if the CG and CV lie on the same line (i.e., the airship is not perturbed), no force couple is generated. In the absence of external forces, this represents an equilibrium state of the attitude of the VRS. It remains to determine whether this is a stable or unstable equilibrium. For this, we consider only the roll axis of the VRS.

Let us consider the simplified free-body diagram of the VRS roll axis depicted in Figure 11.2. The rolling moment about the CV generated by the force couple is given by equation Equation (11.1), where $\mathbf{M}$ is the moment, $\mathbf{G}$ is the local gravity vector acting on the CG, and $\mathbf{d}$ is the displacement vector of the CG relative to the CV. Note that $\mathbf{G}$ is positive according

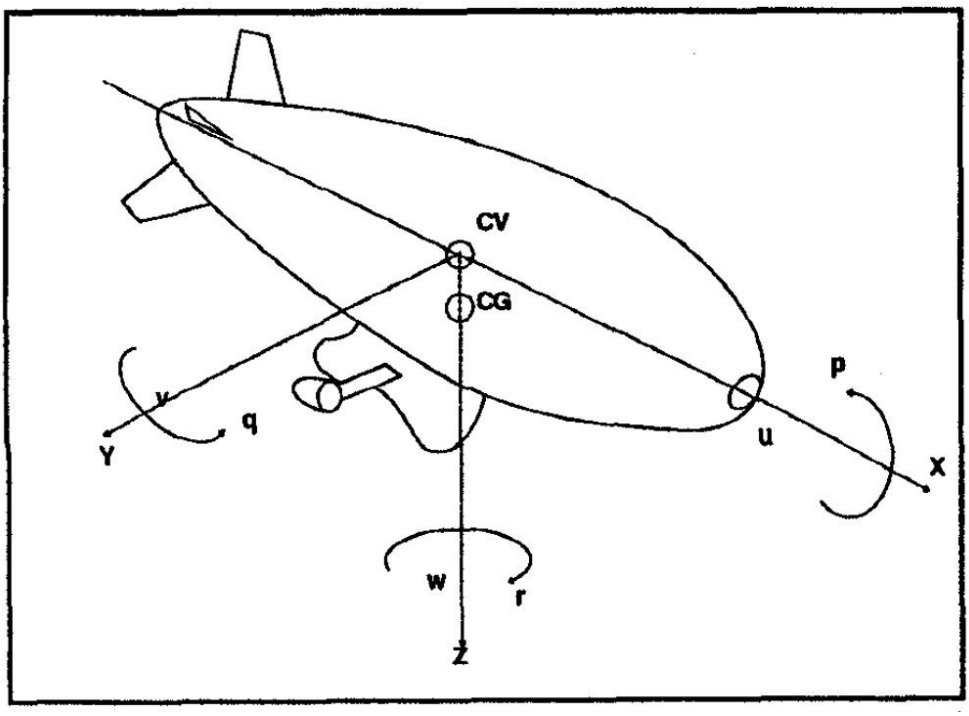

Figure 11.1: Airship body axes, including roll (x-axis), pitch (y-axis), and yaw (z-axis). [116]

to the defined coordinate frame. Therefore, the sign of $\mathbf{M}$ depends on the sign of the component of $\mathbf{d}$ perpendicular to $\mathbf{G}$.

$$\mathbf{M} = \mathbf{d} \times \mathbf{G} \tag{11.1}$$

From this, we can see that a perpendicular displacement of the CG along the y-axis relative to the CV generates a rolling moment that works to decrease that perpendicular displacement, i.e., the system tends to return to equilibrium. Therefore, this is a stable equilibrium. The caveat of this statement is that the CG is below the CV. There also exists an unstable equilibrium when the CG lies directly above the CV. In this case, perturbations cause the system to diverge from that equilibrium point and return to the stable equilibrium. However, for the purposes of this paper, the CG is always below the CV.

The same line of reasoning can be followed to assess the stability of the pitch axis. One can find that the pitch axis is also passively stable. However, in order to ensure level flight, an additional constraint must be applied, which is that the CG should not be displaced relative to the CV along the x-axis of the VRS.

It remains to assess the stability about the yaw axis. However, as the yaw axis and local gravity vector lie on the same line, the no moment about this axis is generated do to displacement of the CG. The passive stability of the yaw axis instead depends on the center of area of the VRS. In order to ensure passive aerodynamic stability, the center of area of the airship as a whole must lie behind the CV. This requires that the cross-sectional area of the VRS (as projected onto the x-z plane) behind the CV (in the direction of travel) must be greater than that in

front of the CV. This necessitates the addition of aerodynamic control surfaces to the rear of the VRS. The sizing of these control surfaces will be discussed in a later section. For the sake of brevity, the proof of this is omitted here. The reader is encouraged to consult textbooks regarding aerodynamics and aircraft yaw stability.

From the above discussion, we can conclude that all three axes are passively stable, albeit to varying degrees. This is beneficial for the Station as a whole, as it reduces the amount of power required by the GNC subsystem for active stabilization.

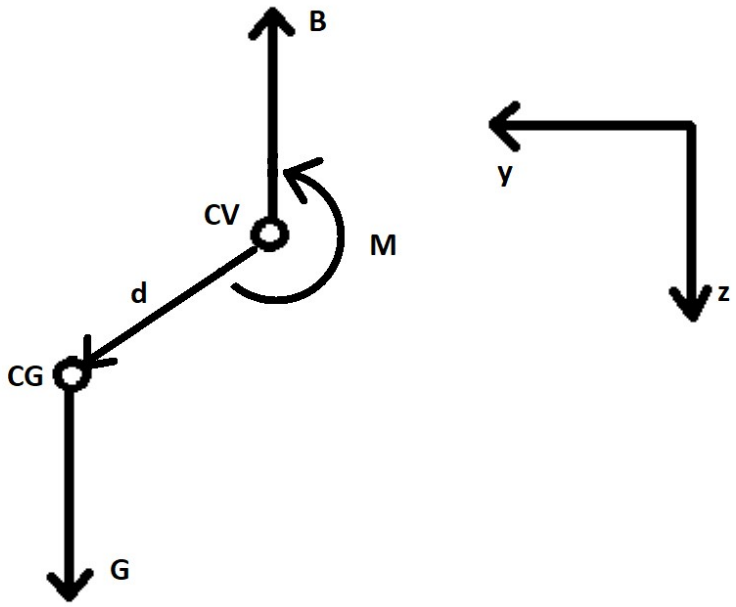

Figure 11.2: Free-body diagram of the perturbed roll axis. The coordinate system is depicted in the top right.

Aerodynamic Control As mentioned above, the aerodynamic control surfaces located at the rear of the VRS allow the Station to achieve passive stability on the yaw axis. However, these surfaces are also useful for active attitude control. Figure 11.3 shows the aerodynamic surfaces used by the VRS. The vertical control surface acts as the rudder and can be actuated (i.e., deflected) for yaw control of the Station. The horizontal stabilizers act as elevons, i.e., they act as both elevators for active pitch control and ailerons for active roll control.

Unfortunately, there is no one-size-fits-all method to choosing the size and shape of the aerodynamic surfaces, as many different factors must be considered in this process. Therefore, for the purposes of this concept design, simplicity and generality were prioritized. For this, the method presented in [117] was used to design the aerodynamic control surfaces. From the previous discussion regarding yaw stability, one can see that the most important parameter in the control surface design is the surface area. The shape of the control surfaces is thus secondary.

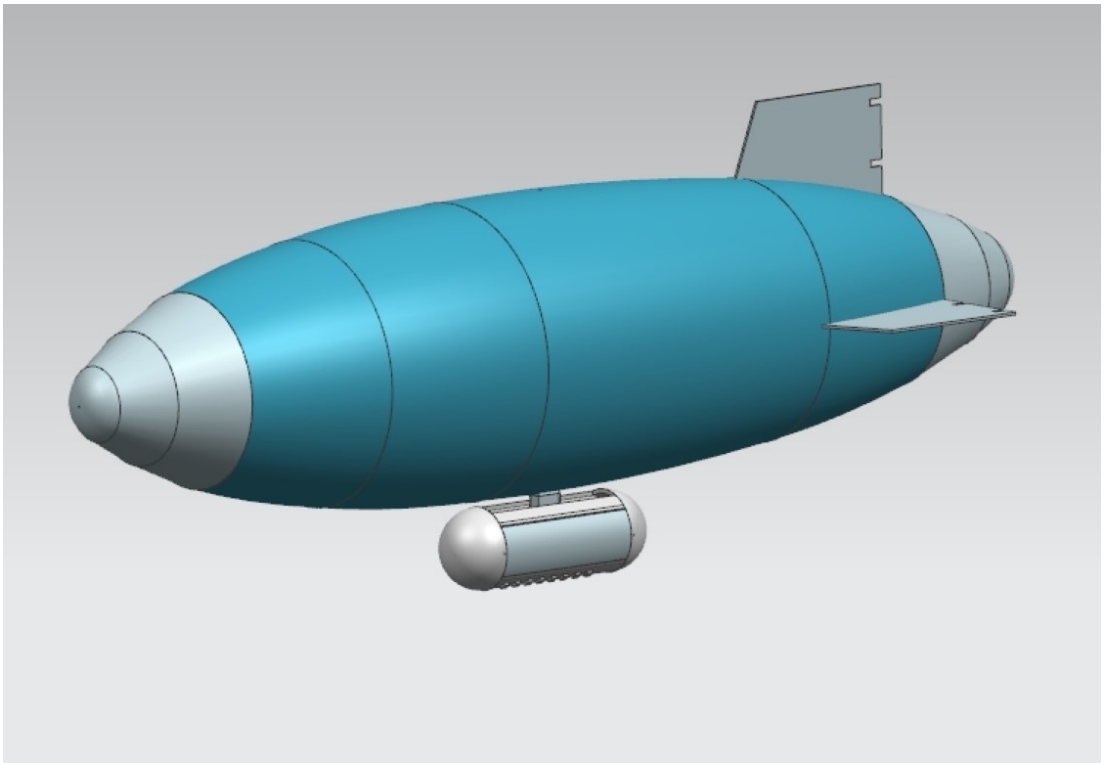

Figure 11.3: Complete VRS system including balloon, gondola, and aerodynamic control surfaces.[Bhosale]

Therefore, the shape of the control surfaces were chosen to be trapezoids in the interest of simplicity. The relevant equations for the dimensions of the control surfaces with a, b, and c as depicted in Figure 11.4 are summarized below.

$$S_f = S_b \cdot r_{fA} \tag{11.2}$$

$$a = c \cdot TR \tag{11.3}$$

$$b = \sqrt{\frac{AR \cdot S_f}{4}} \tag{11.4}$$

$$c = \frac{b}{SCR} \tag{11.5}$$

In the above equations:

- S_f is the surface area of the control surfaces.
- S_b is the surface area of the balloon.
- r_{fA} is the area ratio of control surfaces to balloon.
- TR is the taper ratio of the trapezoid.
- AR is the aspect ratio of the trapezoid, i.e., the ratio of span to average chord.
- SCR is the ratio of span to root chord.

These parameters were derived from Table 3 of [117]. From these equations, the dimensions $a = 7.737\,\text{m}$, $b = 5.302\,\text{m}$, and $c = 10.07\,\text{m}$ were calculated.

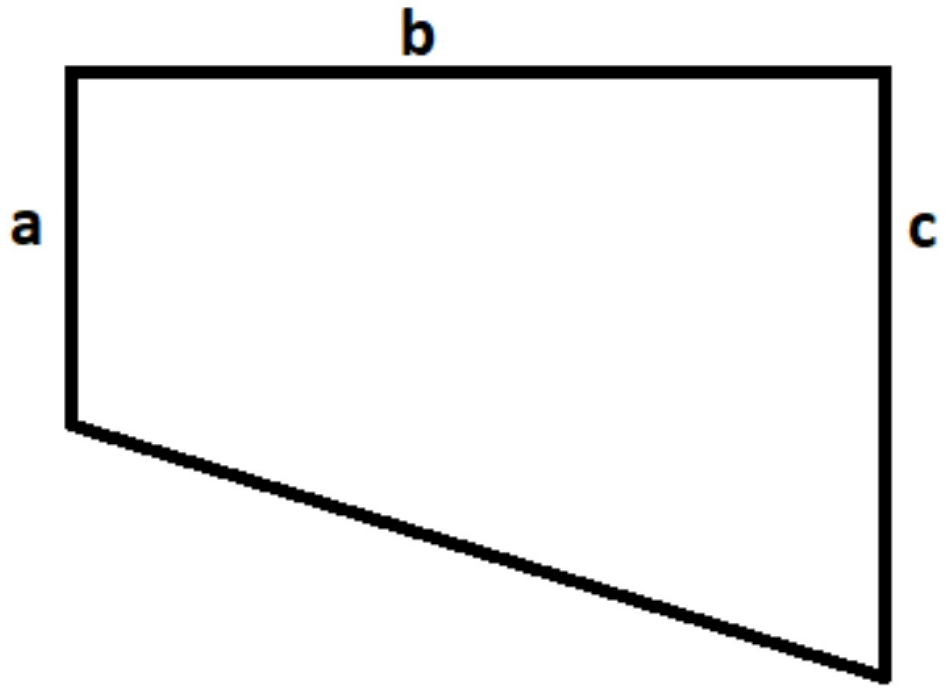

Figure 11.4: Control surface dimensions as calculated in accordance with [117].

Thrust Vector Control As described in Section 10.2, the chosen propulsion system has the benefit of thrust vectoring, thus enabling the use of thrust vector control (TVC) in the GNC subsystem. The concept is straightforward. A propulsion unit is mounted on either side of the payload gondola. Referring to Figure 11.1, each propulsion unit is capable of vectoring its thrust in the x-z plane. Therefore, by adjusting the thrust vector up or down on either side of the VRS, a roll moment can be generated, thus achieving roll control via TVC. Similarly, differential thrust can be used to achieve yaw control.

Unfortunately, this configuration is not well suited to pitch control. Although it is possible in a limited capacity, pitch control relies on rapid acceleration of the VRS relative to the atmosphere, which is not feasible for this design. However, as discussed above, the VRS is passively stable on the pitch axis. Furthermore, due to its elongated shape and large surface area, the pitch axis has a large apparent moment of inertia and significant aerodynamic drag. These effects combined result in greater natural resistance to pitch perturbations, as well as greater damping of oscillations. For these reasons, TVC on the pitch axis is neither feasible nor necessary.

The inclusion of TVC in the attitude control scheme ensures that the VRS is capable of maintaining control even in unfavorable weather conditions. Importantly, it also provides a level of redundancy in case one of the aforementioned control methods fails. The drawback of using this approach is the increased demand of power from the propulsion subsystem. This reduces the power available for forward propulsion, thus limiting the maximum controllable airspeed of the VRS, thereby indirectly reducing its operating domain in the Venusian atmosphere. For this

reason, TVC is only to be used when absolutely necessary, e.g., in case of aerodynamic control failure or stronger than average wind gusts.

Position Control

Position control of the VRS is, once again, relatively straightforward. The primary challenges revolve around changes in atmospheric conditions, namely changing winds and atmospheric density. The former pertains in particular to latitude control, while the latter pertains to altitude control. These two control modes will be discussed individually in the following paragraphs.

Note that longitude control was not mentioned here. This is because the VRS will circumnavigate primarily Venus by floating within the atmosphere, which rotates relative to the surface of Venus in the East-West direction. Therefore, the VRS achieve an approximately constant speed in the East-West direction by entirely passive means.

Latitude Control AS discussed in Section 11.1, the VRS will receive a target latitude via telecommand to which it must navigate. To achieve this, it must be able to overcome local flow irregularities in the atmosphere. This is done entirely via the propulsion subsystem. The aerodynamic forces generated by varying winds in the atmosphere are estimated by the onboard IMUs and compensated by the propulsion units.

Altitude Control Altitude control of the VRS is somewhat more challenging. As the altitude of the station is maintained entirely by buoyancy, which is dependent on the ambient atmospheric density, any changes in atmospheric density will alter the altitude of the Station. Therefore, in order to maintain altitude control, the buoyancy of the station must be manipulated. From Equation (9.2) in Section 9.1, it can be seen that the force balance between the weight of the VRS and its buoyancy depends on its mass and the volume of the balloon. Altitude control via buoyancy manipulation is typically accomplished in terrestrial airships through the use of ballonets, which operate by changing the volume of the lifting gas inside the balloon.[116] However, this is somewhat mechanically complex. Therefore, in the interest of robustness and mechanical simplicity, an alternative method was chosen.

Once again, we draw inspiration from submarines. Submarine hulls are rigid, and therefore do not lend themselves easily to changes in volume. Instead, water is pumped into and out of ballast tanks to change the mass of the submarine, thereby swaying the balance between weight and buoyancy. A similar approach is applied to the VRS.

Inside the gondola sit two high-pressure tanks of carbon fiber composite material. The material was chosen to minimize the empty mass of the tanks while still guaranteeing their strength. One such tank is shown in Figure 11.5. The spherical shape chosen for the tank minimizes the amount of material required to withstand the 15 bar pressures chosen for this design. The use of high pressure tanks allows the VRS to store more atmospheric gasses in a smaller volume, thus reducing the overall size and mass of the altitude control system.

The operation of this system proceeds as follows. During the day, solar radiation heats the atmosphere, thus reducing its density, causing the VRS to lose buoyancy and altitude. When this happens, gasses stored in the ballast tanks are released into the atmosphere, thus lowering the total mass of the VRS. This reduces its weight, thereby causing it to ascend until the buoyancy force is once again canceled out by the weight of the Station.

At night, the opposite occurs. The Sun no longer heats the atmosphere, so the ambient temperature drops, and the density increases. This causes the Station to rise due to the increased buoyancy. More gas is pumped from the atmosphere into the ballast tanks to increase the total

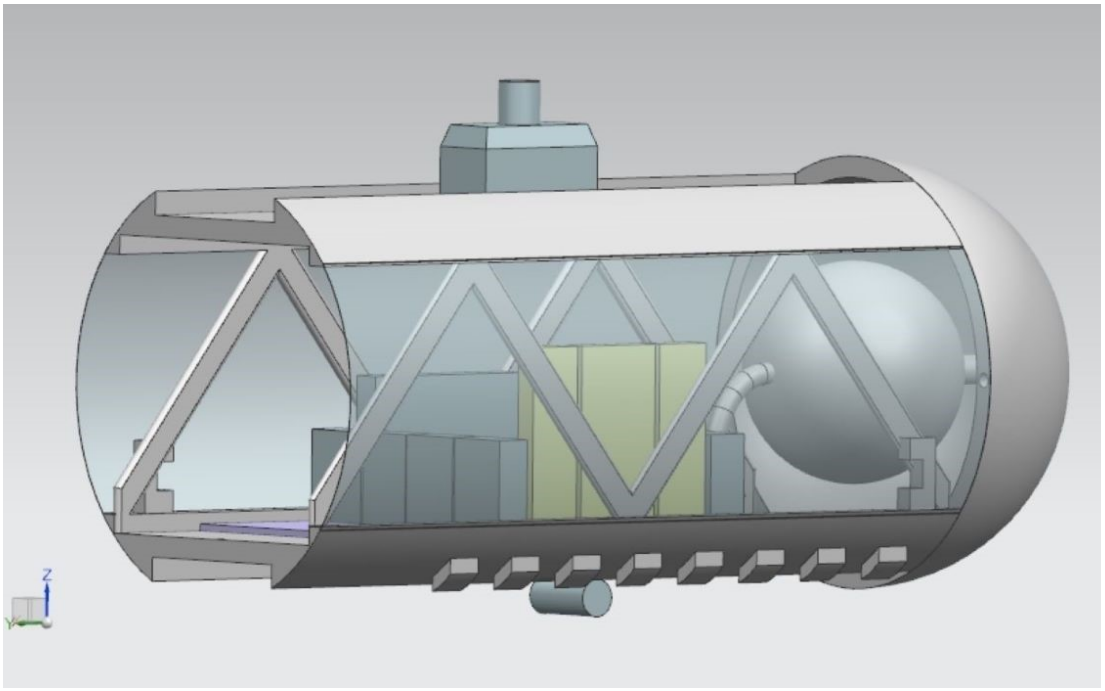

Figure 11.5: Ballast tank for altitude control located inside the gondola.[Bhosale]

mass and weight of the VRS, thus cause it to decrease in altitude. This process is repeated as necessary.

The necessary volume of the tanks can be determined by considering the difference in atmospheric density between 45 and 55 km, which are the operational altitude limits as defined by OR12 in Table 3.4. The derivation of the relevant equation is omitted here.

$$V_{tank} = \frac{R \cdot T \cdot V_b \cdot (\rho_{45} - \rho_{55})}{p} \tag{11.6}$$

In Equation (11.6), R is the gas constant of the atmospheric gasses (primarily carbon dioxide), T is the ambient temperature, V_b is the volume of the balloon, p is the internal tank pressure, and ρ_{45} and ρ_{55} are the atmospheric densities at 45 and 55 km altitude, respectively. The minimum necessary tank volume was calculated to be 2.19 m^3.

While this design concept does reduce mechanical complexity, it is not without its drawbacks. The gondola of the VRS must be designed to withstand the added weight of a full ballast tank.

11.4 Conclusion

The guidance, navigation, and control subsystem is vital to any autonomous, mobile system. Due to the unique operating environment of the VRS, extra care must be taken to ensure that the GNC subsystem reliably execute the commands of scientists on Earth. For this, methods derived from several disciplines such as computer science, aerodynamics, control engineering, and mechanical

engineering were employed to produce a robust GNC system capable of supporting the system as a whole to complete its mission. A combination of SAR payload data processing via SLAM and n-vector observation attitude estimation algorithms alongside high fidelity IMU measurements were selected to achieve accurate localization and attitude estimation. Aerodynamic control surfaces, thrust vector control, and ballast tanks for buoyancy control were chosen to achieve full position and attitude control within the operational constraints of the system. All GNC instruments and actuators are redundant, thus eliminating any single point of failure.

Naturally, this GNC concept design requires more analysis and testing before it can be applied to any practical application. However, it can serve as a starting point to those interested in designing such a system in the future.

CHAPTER 12

Power System

by Uma Parvathi

Power system is a crucial part of the research station. All the other systems are dependent on the power system to perform its function throughout the mission. The primary objective entails designing a resilient power supply and distribution system infrastructure capable of meeting all the demands and thus ensuring a smooth workflow of the research station. The designing process of such a power system starts with an in depth analysis of the peak and average power demand, as well as the energy consumption of the Venus research station. Subsequently we delve into studying various viable power sources. Following the study, a suitable source that meets the power demand of the station is selected. Simulations are done, allowing for a comprehensive evaluation of the power source design. After the designing of the power source, possible energy storage technologies are studied and the one which meets the requirement is singled out. The process of designing a robust power system involves a process of iterative refinement.

12.1 Layout of Power System

Figure 12.1 illustrates the general layout of the power system. The energy consumers are the payload and all other subsystems in the research station. These systems are fed with requisite power from the energy source and energy storage unit. This is facilitated by the power distribution unit which encompasses a power conditioning and distribution module. Energy storage is used in situations where the primary source of power proves insufficient to meet the demand, thus ensuring an uninterrupted operation of the research station.

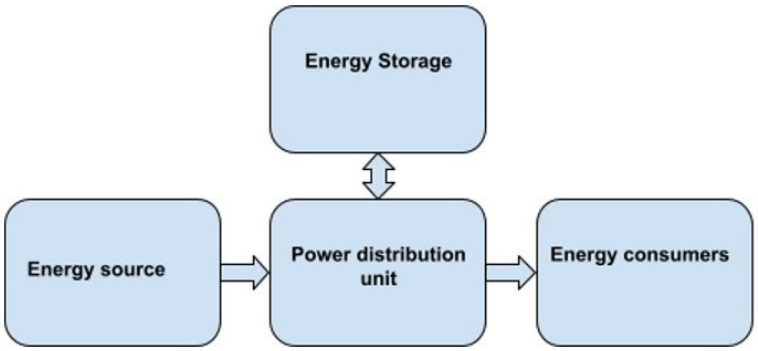

Figure 12.1: General layout of the power system.

12.2 Power Demand of The Research Station

This includes the comprehensive identification of the energy consumers within the research station and calculation of the energy consumed during each distinct mission phase. The estimation of peak and average power required by the research station was taken as the pivotal foundation for sizing of the power system. The initial step involved compiling a list of all devices that require power. Each system contributed to this list, thus enabling the determination of the peak power demand of the research station. Table 12.1 below represents the peak power demand of the research station.

System	Power [W]
Payload	719.2
GNC	1135.63
Communication	600
OBC and C&DH	264
Propulsion	16000
Thermal	1500
Payload	719.2

Table 12.1: Peak power demand of the research station.

A latitude range of $-50°$ to $50°$ from Chapter 3 was selected to calculate the peak energy consumption. Given that Venus experiences equal day and night as mentioned in Chapter 2 the circumnavigation time at each latitude is halved to estimate the day and night periods. Subsequently, the energy consumption during day and night was derived. The energy consumed during day and night period were equal. Table 12.2 shows the instantaneous energy consumption at $-50°$, $0°$, and $50°$ latitude. The estimation of peak values of both power and energy

Latitude	Energy consumed [MWh]
$-50°$	1.12
$0°$	1.75
$50°$	1.12

Table 12.2: Peak energy required by the research station.

requirement of the research yields valuable insight into the requisite power generation necessary for smooth operation of the research station. Thus providing a criterion for selecting the appropriate power source.

The mission of the research station unfolds through well defined phases as elaborated in the Chapter 5 The average power demand and the average energy consumption of the research station were estimated based on these phases. These were estimated for the longest circumnavigation time which is 176 h at $0°$ latitude (refer to Section 9.1). The operating time for payload and Command and Data Handling and On-Board Computer (OBC and C&DH) is contingent upon the mission phases whereas all other systems work continuously, irrespective of the mission phase. Propulsion and thermal system of the research station works with the peak power throughout the entire circumnavigation time. Conversely, the communication system requires the peak power only for three hours during the whole circumnavigation time. The rest of the time it

operates at a reduced power of 180 W. Guidance, navigation and control system (GNC) works with the peak power only for two hours in the entire circumnavigation time. The rest of the time the pump is turned off, resulting in a decrease in the power requirement. The average power demand from these systems are summarized in Table 12.3.

Parameters	Communication	GNC	Propulsion	Thermal
Peak power [W]	600	1135.6325	15650	1500
Peak power time [h]	139.5	2	176.04	176.04
Energy consumed at Peak power [Wh]	83700	2271.265	2755026	264060
Nominal power [W]	180	855.6325	NA	NA
Operating time [h]	36.54	174.04	NA	NA
Energy consumed at Nominal power [Wh]	6577.2	148914.2803	NA	NA
Total consumption [W]	90277.2	151185.5453	2755026	264060
Average power [W]	512.83	858.8135952	15650	1500

Table 12.3: Average power demand of systems except payload and OBC and C&DH.

Payload and OBC and C&DH work with their peak power during the entire operating time. The operating time for all payloads, OBC and C&DH payload supporting unit and other instruments that work with payload depend on the mission phases. The rest of the OBC and C&DH instruments that are necessary for the successful operation of research station works the entire circumnavigation time.

1. In mission phase SO1, The payload instrument SlimSAR works for the entire circumnavigation time and all other payloads are turned off. In this phase only the OBC instrument that supports SlimSAR works full time and other payload supporting instruments are deactivated.

2. In mission phase SO2, the payload instrument SlimSAR works only for 13 percentage of the circumnavigation time whereas the rest of the payload instruments work for 97.99 percentage of the time. Consequently OBC instruments for SlimSAR works only for 13 percentage of the time and the payload supporting unit of OBC works the complete circumnavigation time.

3. In mission phase SO3, the SlimSAR works for 13 percentage of the circumnavigation time whereas the instrument necessary for conducting experiments to find life on Venus works for the entire time.The power required for this instrument is stated in Chapter 3. The OBC instrument for SlimSAR works for 13 percentage of the circumnavigation time and all other OBC instruments works for the entire time.

   Table 12.4 summarizes the average power demand of Payload and OBC and C&DH.

Table 12.5 summarizes the average power and energy demand of the station during all the three phases, combining the average power demands from all the systems.

Phases	Payload Power [W]	OBC and C&DH Power [W]
SO1	18.75	221
SO2	65.57	210.93
SO3	12.43	202.93

Table 12.4: Average power demand of payload and OBC and C&DH for different mission phases.

Phases	System	Avg. Power [W]	Shadow Time [h]	Avg. Energy [Wh]
SO1	Payload	18.75	88.019	1650.372432
	OBC	221	88.019	19452.38974
	Prop.	15650	88.019	1377510.857
	GNC	858.81	88.019	75592.33859
	Thermal	1500	88.019	132029.7946
	Comm	512.83	88.019	45139.22637
	Total	**18761.39**	**88.019**	**1651374.979**
SO2	Payload	65.57	88.019	6032.881414
	OBC	210.93	88.019	18566.02972
	Prop.	15650	88.019	1377510.857
	GNC	858.81	88.019	75592.33859
	Thermal	1500	88.019	132029.7946
	Comm	512.83	88.019	45139.22637
	Total	**18801.11**	**88.019**	**1654871.128**
SO3	Payload	221	88.019	19452.38974
	OBC	221	88.019	19452.38974
	Prop.	15650	88.019	1377510.857
	GNC	858.81	88.019	75592.33859
	Thermal	1500	88.019	132029.7946
	Comm	512.83	88.019	45139.22637
	Total	**18744**	**88.019**	**1649844.313**

Table 12.5: Average power and energy demand of the station

12.3 Power Source

This section explores a wide array of all possible power sources suitable for the Venus research station. Venus presents an immensely harsh environment with numerous challenging factors as discussed in Chapter 2. These challenges impose significant constraints on the selection of power sources. The pro's and con's of each power source were evaluated to select the suitable source that can withstand the environment and can provide uninterrupted supply for the research station.

Wind Energy

Using wind energy presents significant challenges for the Venus environment. Conventional terrestrial wind turbines cannot be used on a floating airship. One potential solution is the use of airborne wind turbines, although this has never been used in any of the space exploration missions and terrestrial airships. A study explored the approach of using a Venus lander powered with an airborne turbine [118]. The research station floats at an altitude range of 45 to 55 km as stated in Chapter 3. Airborne turbines float at higher altitude than the research station. This increases the complexity of the system and will be hard to control. The critical limitation is the density of the atmosphere, it is significantly low at higher altitude. Consequently the output of the wind turbine becomes minimal and inconsistent in this context.

Radioisotope Thermoelectric generator (RTG)

RTG's are proven to be an efficient power source in many long term missions like the Curiosity rover. One of the benefits of RTG is that it can provide consistent power throughout the mission, independent of the surrounding environment. There are very few critical impacts of the harsh Venusian environment on an RTG system.However, incorporating an RTG system in the research station comes with certain challenges. One of those being the complexity in thermal control. RTG systems can pose challenges in maintaining structural integrity. For instance, the output power of one Multi-mission radioisotope thermoelectric generator (MMRTG) [119] is 110 W and the mass is 43.6 Kg. This would mean the research station would require at least 182 of such an RTG to meet the demand of 20 kW. This would mean a total mass of 7936 kg, which increases the structural complexity. While RTG's provide sufficient power a trade-off has to be made between the thermal and structural complexity and the power generation.

Primary Battery

Primary batteries are more suitable for a low power system. However for the research station the high power demand and substantial the energy storage requirements, primary batteries prove to be inefficient. Batteries with very high capacity and specific energy density are required to meet this demand. The batteries currently available that are being used in missions do not meet these requirements. For instance, a primary battery cell studied in the venus flagship mission [120], lithium-thionyl chloride (Li-SOCl2), the main concern of using this battery is life cycle and the self discharging of the cell after one year [121]. This drastically reduces the power output. Given these limitations, primary batteries are not suitable as a power source for the research station.

Solar Energy

Venus atmosphere experiences a higher rate of solar intensity attenuation. But only within the cloud layer which extends up to 45 km , this is detailed in Chapter 2. However the Venus

research station operates at an altitude higher than the cloud layer, where the solar intensity is sufficient for generating power. The altitude range 45 to 55 km is well-suited for a solar powered airship [122]. The solar intensity at these altitudes can go up to 1613.560 W/m^2. One potential drawback is the degradation of solar cells due to corrosion, but this can be mitigated effectively by using proper surface coatings. With proper consideration of the operating conditions of the research station. Solar power emerges as a considerable source of power for the research station.

Result

From the comprehensive comparative study of potential power sources, wind energy and primary batteries turned out to be inefficient source of power, thus a trade-off is made between RTG and solar power. Although RTG can generate power more consistently than solar, it introduces considerable complexity to the system. Whereas solar is still able to provide sufficient power without adding any complexity. The constant change in sun angle with time can reduce the power output, Nevertheless sufficient power can be generated by choosing the suitable altitude of operation from the given range. Therefore, it is concluded that solar power is the optimal choice for the Venus research station. This would mean that the research station should be equipped with a suitable energy storage system for uninterrupted operation during night time. The quantitative evaluation of the power source and the sizing of the power system is done in Section 12.5

12.4 Energy Storage

In the comprehensive study of various energy storage technologies, it becomes evident that several of them can be ruled due their unsuitability to the harsh Venusian atmosphere [123]. Primary batteries, as stated in Section 12.3 are not suitable for a high power system that operates for a long time. Fuel cells, while a viable option, can increase complexities, including the necessity to carry sufficient fuel. This will significantly increase the mass of the entire station. As a result, it is concluded that secondary batteries are suitable for the research station. The advantage of batteries is their simple design, robustness and easy availability. However, despite the merits, secondary batteries pose some challenges, especially due to the high energy required by the research station. This means the station requires secondary batteries with high specific energy density. Among the secondary batteries, Lithium ion batteries (Li-ion) batteries are found to have higher specific energy density. With recent advancement in Li-ion batteries achieved a high specific density of 300 Wh/kg. Additionally ongoing research in this has led to the development of lithium sulfur batteries with specific energy density of 450 Wh/kg [124]. All these show a promising potential of secondary batteries in effectively storing substantial amounts of energy [125]. To summarize, Li-ion secondary batteries with high specific energy density is a potential energy storage system for the Venus research station.

12.5 Design of Power System

This section entails a quantitative evaluation of the solar power source. It includes the estimation of the instantaneous power generated at $-50°$, $0°$, and $50°$ latitudes for a specific solar zenith angle (SZA). Subsequently the average power generated from the solar power source through the latitude range for every SZA was estimated. These were simulated for an altitude range of 45 to 55 km. The detailed process is elucidated in Section 16.4. The results of the simulations were then compared with the power demand of the station. The next steps involved the size of the solar array to generate the requisite power. Finally the energy storage system was sized

to ensure adequate energy storage. This evaluation provides insights into the feasibility of the selected power source.

Power Generation Estimation

This subsection provides an outline of the procedure of estimating the instantaneous and average power that can be generated.

1. Calculation of Solar intensity attenuation The mean solar intensity of Venus above the atmosphere (Io) is 2613 $\mathrm{W/m^2}$ [122]. The attenuation in the solar intensity in the altitude range of 45 to 55 km is calculated to finally estimate the power output. The power output or the generated power is influenced by this attenuation. This is calculated using [122]

   For 0 to 550 km

   $$\frac{I}{I_o} = 0.10306 + 0.17383h - 7.99\times10^{-4}h^2 + 2.752\times10^{-5}h^3 - 5.2011\times10^{-7}h^4 + 3.874\times10^{-9}h^5 \tag{12.1}$$

   For 50 to 65 km

   $$\frac{I}{I_o} = -1.3639 + 4658h \tag{12.2}$$

2. Calculation of projected area

   Due to the continuous variation in the sun angle, the incidence of sunlight on the solar panel area changes accordingly. This angle of incidence is determined by the solar zenith angle, leading to incomplete illumination of the entire surface area Therefore it is necessary to calculate the projected area based on the sun angle. The length [l] and diameter [d] of the airship was given in Section 9.1. The value of solar zenith angle were derived from simulation Section 16.4. Based on these the projected area was calculated as [126]:

   $$\text{Projected area: } Ap = \frac{\pi d^2}{4}\sqrt{\cos^2 B + n^2 \sin^2 B} \tag{12.3}$$

   $$n = \frac{l}{d} \tag{12.4}$$

3. Efficiency of Solar cell E_{ff}

   The efficiency of the solar cell has great influence on the power generated, especially in the challenging environment of Venus, which can severely impact its performance. The conventional solar cells used in space missions cannot withstand the Venusian environment. Hence a conceptual solar cell specifically designed for Venusian conditions is considered for the research station. A study was conducted on the solar cells and certain results were generated, the research station will use one such solar cell for the design. The efficiency at various altitudes altitudes are presented in the study.[127]

4. Calculation of power generation

   For the initial estimation, the instantaneous power generated at the specified latitudes, corresponding to the instantaneous solar zenith angle, was calculated. This was calculated for altitudes 45, 50 and 55 Km. The equation used for calculating the power is [122] :

   $$\text{Power : } P = I_o(\frac{I}{I_o})A_p E_{\mathrm{ff}} \tag{12.5}$$

Latitude	P at 45Km [W]	P at 50Km [W]	P at 55Km [W]
0°	43808.20	70972.69	159799.83
−50°, 50°	29391.03	47615.76	107210.12

Table 12.6: The instantaneous power generated at the three altitudes for fixed latitude and SZA

Table 12.6 depicts the generated power. The average power generated from the solar power source through the latitude range for every SZA for altitude range of 45 to 55 km was simulated. Further elaboration on the calculation methodology can be found in Section 16.4. The plots generated are shown below in Figure 12.2.

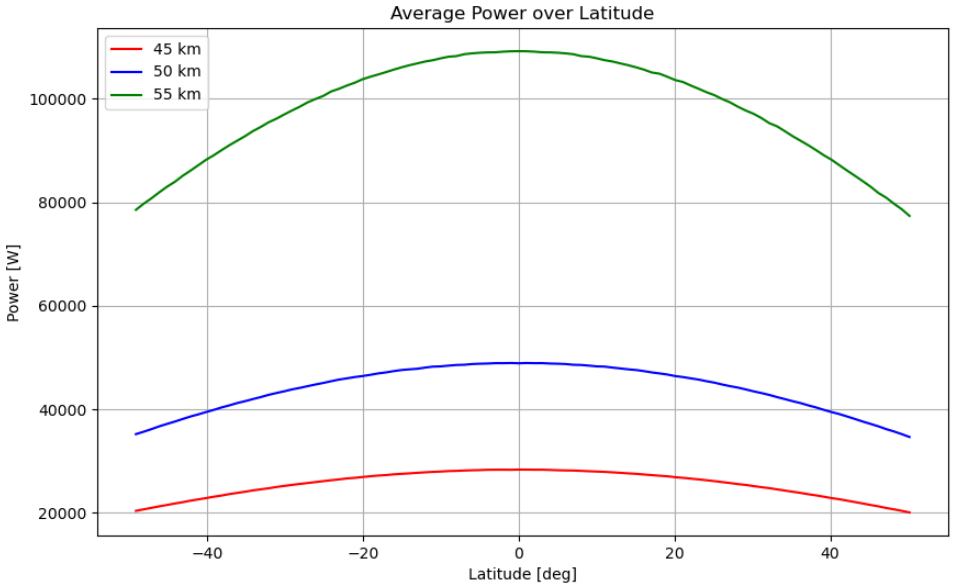

Figure 12.2: Plot of Average power generation throughout the latitude range for altitudes 45, 50 and 55 Km.[Finzel]

Comparing the result from simulation and the power demand calculated, it is evident that at an altitude of 55 km, sufficient power is generated across the entire latitude range to meet the demand of the station as well as to store required energy for night time operation. However at 50 km, there is limitation on the latitude range, the range should be confined between −20° and 20° for sufficient power generation to meet the demand of the station as well as to store required energy for night time operation. Additionally, It is also noted that 45 km is not suitable for the station's operation. Thus a more strict range of operation is deduced from this result.

Sizing of Energy source

As mentioned in earlier section, conventional solar cells are not suitable for Venusian environment. Thus the solar cell considered for the research station is a triple junction solar cell which was studied and showed promising result [127]. To provide an approximate estimate of the power

source size, a basic calculation is performed. This includes calculating the total number of solar cell that will be included in the surface area. From the study conducted output power of this solar cell for various altitude ranges are given in [127]. Table 12.7 depicts the output power for 45, 50 and 55 km As a basis for calculation, a conventional triple junction solar cell is considered

Altitude [km]	Output Power [W/m^2]
45	181.4
50	256.0
55	404.4

Table 12.7: Output of solar cells at various altitudes

[128]. The total number of solar cells required for generating this power was estimated to be 114 covering an area of approximately 79 m^2.

Sizing of Energy Storage

The energy storage system is designed to meet the worst case scenario. The maximum shadow time and the peak energy demand is considered. The battery considered here is a Li-ion pouch cell [129], as it exhibits the highest specific energy density. The estimation is summarised in Table 12.8.

With this battery, the research station can operate effectively and reliably throughout its mission, providing the necessary power for all systems and instruments. The careful consideration of battery technology and sizing ensures the station's successful operation in the challenging Venusian environment. Simulation of battery capacity was done and the results are discussed in Section 16.4.

12.6 Power System for Scouts

A general overview of scouts is provided in Chapter 3. This section focuses on the power system required for a successful operation of the scouts. To determine the power requirement, the energy consumers were identified, this includes payload instruments, communication system and Command and Data Handling & On-Board Computer. The power requirements of each system were documented. The operating time for scouts was specified as three hours Section 9.2, a safety margin of one hour was added to the operating time, considering the harsh environment conditions. Thus the operating time was set as four hours. Based on these parameters the power system was designed.

Max energy consumed	1748851.916 Wh
Li-ion battery Specific Energy Density	300 Wh/Kg
Total mass of battery	5829.506387 Kg
Cell dimension	94.8 x 102.0 x 6.8 mm
Volumetric energy density	700 Wh/L
Total Volume of battery	2498.35988 L

Table 12.8: Mass estimate of battery based on specific energy density

Given the low power requirements and short operating time, primary batteries are chosen as power source. However a primary battery suitable at high surface temperature has not yet been developed. Research in this area holds a promising potential for the use of primary batteries [130]. Solar power cannot be used as the surface temperature is too high, rendering solar cells to be inefficient.Similarly, wind energy is also not a suitable option because the size of scouts are small making wind turbines impractical. RTG could supply the required power, but it will increase the mass of the scouts and this can have a negative impact on the launch and movement of the scouts. RTG also adds complexity to the thermal control of scouts, as scouts lack active thermal control. Hence a primary battery is proposed as the power source for scouts.

1. Total power required by scouts 55.14 W
2. Time of operation 4 h
3. Energy consumed approximatley 220.56 Wh
4. The primary battery chosen here as a reference to estimate the size of the power system is lithium-thionyl chloride (Li-SOCl2) [121], this battery was proposed in the venus flagship mission study [120].
5. Each cell provide 13 Ah of current at 3.6 V for 47.7 Wh
6. No of cells required - 10
7. Total mass ˜[1]kg; mass of each cell 100 g

CHAPTER 13

Thermal Control System

by Timon Jafarian

This Chapter outlines the design of the thermal control system. Given Venus's extreme heat, a reliable cooling system is crucial to maintain the continuous operation of the research station. In Section 13.1 all the heat sources that may affect the station are explained and the formulas for their calculations are provided. The possible options for thermal hardware are compared in Section 13.2. It is stated which ones were decided on to use for this project and for what reasons. In Section 13.3 the thermal balance of the Venus Research Station (VRS) is determined. It is looked into which heat sources affect which part of the station in its environment and which are negligible. The calculation of the inside temperature of the balloon is described and how the cooling of the gondola is achieved.

13.1 Thermal Analysis

The temperature of the VRS is influenced by various heat sources. Heat is transferred via either radiation, conduction, or convection. In this section, the heat sources that affect the station will be explored, with a focus on radiative and conductive heat loads. Different radiation sources emit thermal energy towards the VRS at a height of 50 km, and the VRS itself radiates heat back to the outside. Additionally, the hot atmosphere causes a conductive heat transfer to the inside of the gondola of the VRS. To determine the station heat balance the heat flow coming from all those sources and the VRS must be considered. In the following, it will be explained how those values are determined.

Solar Heat Load

The solar heat load refers to the amount of radiated solar energy absorbed by the surface of the VRS within sunlight A_{surf}. It depends on the effective area hit directly by sunlight A_{eff}, the absorptivity of the surface material α and the solar intensity at the station's height I_{sun}.[20]

$$q_{solar} = A_{eff} \cdot \alpha \cdot I_{sun} \tag{13.1}$$

The gondola of the VRS is unaffected by the solar heat load for the most part of the mission‘s duration. Due to it being located directly under the balloon and their size differences, the station will be within the balloon's shadow for most of the time. Only if the sun‘s elevation is below a certain angle, parts of the gondola be within sunlight. But this also means that the effect of the solar power will be diminished. The Sunlight that hits the gondola at a low elevation angle has to travel a longer distance through Venus's thick atmosphere, where it is being attenuated.

On the other hand, the solar heat load always influences the temperature of the balloon while the VRS is on the day side of Venus. The maximum amount of solar heat load for the balloon is calculated for the case that sunlight hits the balloon directly from above.

Albedo Heat Load

The albedo heat load is determined by the amount of sunlight that is reflected by the surface of Venus and sent upwards, where it is absorbed by the station. It depends on the amount of solar flux that is reflected back up to the height of the VRS at 50 km I_{albedo} and the view factor F which depends on the angle of orientation of the surface area towards the direction of the reflected sunlight.[20]

$$q_{albedo} = A_{surf} \cdot \alpha \cdot I_{albedo} \cdot a_{venus} \cdot F \tag{13.2}$$

The view factor has a value of 1 for the case where a given surface is hit directly by the reflected sunlight. The effect of the albedo heat load on the VRS can be neglected due to the attenuation of sunlight in the atmosphere of Venus. At the top of the atmosphere the solar flux amounts to $I_S = 2613.9\,\mathrm{W/m^2}$, which is reduced to only $25\,\mathrm{W/m^2}$ at the surface of Venus. The part that is reflected back up from the surface is then attenuated even further.

Infrared Heat Load

Objects emit thermal radiation as electromagnetic waves depending on their temperature. Therefore the amount of infrared radiation being emitted by Venus must be determined for the calculation of the heat balance of the VRS. Due to the intense solar radiation and the effects of the atmosphere, Venus has a surface temperature of 457 °C. The thermal radiation emitted by a body is calculated using the Stefan-Boltzmann Law,

$$q_{IR} = \epsilon \cdot \sigma \cdot A \cdot T^4 \tag{13.3}$$

where ϵ is the emissivity of the body that relates how much radiation is being emitted relative to a black body with the same properties, σ is the Stefan-Boltzmann constant and the surface area of the object. With this formula, the infrared radiation near the surface of Venus can be determined. For the calculation of the amount of heat being transferred to the VRS by this effect the attenuation caused by the atmosphere must be considered.

Not only does the VRS absorb the infrared radiation coming from Venus, but it also emits infrared radiation itself. This heat flow to the outside must be considered when determining the station temperature.

Heat Conduction by the Atmosphere

At a height of 50 km the atmosphere on the outside of the VRS has a temperature within the range of 84.29 °C and 67.4 °C. Furthermore, the outside temperature does not change depending on whether the research station is on the day or night side. If the inside of the station is at a different temperature than the atmosphere then this will cause a conductive heat exchange. The VRS is to be cooled to a temperature suitable for the operation of all the components. This causes a heat flow from the outside to the inside. The rate of conductive heat flow can be determined using Fourier‘s Law. It depends on the thermal conductivity of the wall material k, the area through which the heat flows and the temperature gradient.[131]

$$q_{cond} = -k \cdot A \cdot \frac{\mathrm{d}T}{\mathrm{d}x} \tag{13.4}$$

The gondola of the VRS has a cylindrical shape and uses different types of material in its walls. For this case, the rate of heat flow can be approximated as a combination of the thermal conduction through the cylindrical wall of the gondola and the thermal conduction through the two flat-end parts of the cylinder. This is done using the formula for heat conduction in long multi-layer cylinders and the one for thermal conduction through planes. When considering multi-layer cylinders, the radii of the different layers, as well as their thermal resistances, must be taken into account. The gondola has an outer wall consisting of carbon fibre and an inner layer of insulation. Solving Equation (13.4) for multi-layer cylinders yields:[131]

$$q_{cyl} = \frac{T_{outside} - T_{inside}}{R_{total}} \tag{13.5}$$

$$R_{total} = R_{inside} + R_{insulation} + R_{cf} + R_{outside} \tag{13.6}$$

$$R_{inside} = \frac{1}{2\pi r_1 l_g k_{inside}} \tag{13.7}$$

$$R_{insulation} = \frac{\ln \frac{r_2}{r_1}}{2\pi l_g k_{insulation}} \tag{13.8}$$

$$R_{cf} = \frac{\ln \frac{r_3}{r_2}}{2\pi l_g k_{cf}} \tag{13.9}$$

$$R_{outside} = \frac{1}{2\pi r_3 l_g k_{outside}} \tag{13.10}$$

The distance from the centre of the gondola to the inner edge of the insulation is denoted as r_1, the distance to the point where the insulation and the carbon fibre are connected to each other by r_2 and the radius of the gondola is r_3. The values of the thermal conductivity of the outside atmosphere, the carbon fibre structure, the insulation layer and the air on the inside are described by k and the length of the gondola by l_g. The thermal conductance through the circular end parts of the cylinder is calculated using the following formula:

$$q_{side} = \frac{T_{outside} - T_{inside}}{\frac{l_{cf}}{A_{side} k_{cf}} + \frac{l_{insulation}}{A_{side} k_{insulation}}} \tag{13.11}$$

The conductive heat flow of the balloon is calculated under the same assumptions, with the only difference being that there is no insulation layer. Therefore the calculations for the heat transfer into the cylinder simplifies. Instead of R_{total} the following term for the thermal Resistance is used in Equation (13.5):[131]

$$R_{balloon} = \frac{\ln \frac{r_2}{r_1}}{2\pi l_b k_{balloon}} \tag{13.12}$$

13.2 Thermal Hardware

In order to keep the temperature of the VRS in an acceptable range for all the devices thermal control hardware is used. During the design of the thermal control system different hardware options were considered and the ones most suitable for the environment of the VRS were chosen. The two types of thermal control methods are passive and active. A thermal control system should rely on passive methods as much as possible. Their advantage over active methods is that

they use no power to maintain the temperature within the VRS. Also, they are more reliable because active components, like for example coolers, degrade over time and require redundancy.

Due to the atmosphere outside the research station being higher than the required inside temperature, it is not possible to utilize passive control hardware alone. An active system is needed to cool the inside of the VRS and reject the excess heat to the atmosphere. Passive systems can be used to minimize the heat flow to the inside as much as possible.

Passive

The VRS is affected by conductive and radiative heat transfer. Passive options for thermal control that reduce these effects are insulation and applying paint to the surface of the station with a low absorptivity α.

Insulation has a low thermal conductivity and therefore reduces the thermal flow from the hot atmosphere on the outside to the cooled inside the VRS. A thick layer of insulation material is installed on the inside of the shielding of the VRS. That way it is protected from the corrosive effects of the atmosphere. Many types of different insulation materials exist with varying properties. One that is commonly used for the Venus lander mission is Microtherm.[132] It is a ceramic-based insulation material that is easily available and cost-effective. Another option that was explored is Aerogel.[133] It has similar values for its thermal conductivity but the advantage of a lower density. One downside is that it is more fragile.

Material	**Thermal Conductivity [W/mK]**	**Density [kg/m^3]**
Microtherm	0.023	260
Aerogel	0.020	5 - 200

Table 13.1: Properties of different insulation materials

For this mission, it is necessary to keep the mass of the insulation layer to a minimum. Otherwise, it would only increase the load on the balloon. Therefore Aerogel was chosen as the insulation material. It has the lowest density out of all considered options and good thermal conductivity.

The amount of radiative thermal energy absorbed by the VRS depends on the properties of the surface material. By using a white, matte paint with a high albedo value the radiative heat flow into the VRS can be reduced. Furthermore, the thermal radiation emitted by the VRS depends on the emissivity ϵ of the paint that is applied to the surface. For this mission, it is planned to use a paint with an absorptivity of $\alpha = 0.05$ and emissivity $\epsilon = 0.91$[134]. This will cause the VRS to have a low absorptivity for incoming radiation and also increase the thermal energy radiated back to the outside.

The same amount of heat that flows into the VRS must be transported back to the outside. Heat pipes are a passive method of thermal transport. Heat is absorbed at one end of the pipe, causing the working fluid to evaporate and move to the cooler end, where it condenses and releases the heat. This creates a continuous cycle that allows heat transfer. Heat pipes are used for this mission to transport the heat that is lifted by the active cooler to the heat sink on the outside of the station.

This heat sink is used to reject the excess heat back into the atmosphere. The temperature that the heat sink needs to be at to reject a given amount of heat can be calculated using the following formula:

$$T_{hs} = R \cdot q + T_{outside} \tag{13.13}$$

Here T_{hs} is the temperature at the flat end of the heat sink that is connected to the heat pipe, q is the rate of heat flow from that point to the outside and R is the thermal resistance of the heat sink. A heat sink with properties suitable for this mission is the Alutronic PR 264. It has a size of 40 cm by 40 cm for the base, a fin length of 13.2 cm and a mass of 18 kg. The thermal resistance for this heat sink is 0.0105 K/W[135].

Active

While passive thermal control hardware can be used to reduce the heat flow to the inside, active thermal control is needed to reject the remaining heat flow back to the atmosphere. The outside atmosphere is at a higher temperature than the required inside temperature and heat can only flow from a hot temperature reservoir to a cold one. Therefore a heat sink with a higher temperature than the ambient one can be used to create a heat flow to the outside.

Heat pumps create a temperature gradient along their hot and cold end. The temperature of the hot end can then be chosen in a way that causes a heat flow to the outside of the same amount as the heat flow to the inside. This creates an equilibrium state in which a stable inside temperature is achieved.

The heat pump used for this mission needs to have good efficiency, as the power generation on the VRS is limited. Thermoelectric coolers were briefly considered. They are solid-state heat pumps that use the Peltier effect, in which an electric current passing through a junction of different materials transfers heat from one side to the other, creating in a hot and cold end. They have the advantage of being lightweight and reliable due to not having any moving parts, but the downside of low efficiency. The power consumption for the thermal control system would be too great if Thermoelectric were to be used. The option that was chosen for this mission is Stirling cycle cryocoolers. They use the cyclic compression and expansion of a working gas to lift heat from a cold side to a hot one, creating a temperature gradient. The temperature for the cold end is chosen as the required inside temperature of the VRS of 30 °C and the heat that is lifted to the hot end is transported to a heat sink on the outside of the VRS using heat pipes.

Stirling cryocoolers have already been used in a wide range of Venus missions. They have the advantage of a high cooling capacity, long operating life and high efficiency. Their downsides are their higher mass compared to Thermoelectric coolers. Missions using Stirling coolers with a cooling system comparable in terms of temperature ranges to this mission have achieved a cooling efficiency of 50 % Carnot efficiency. The Carnot efficiency is the maximum possible efficiency for a heat pump as stated by the second law of thermodynamics. It can be calculated using the temperatures of its cold and hot ends.

13.3 Thermal Balance

Now that it has been established how the heat flow to the inside and outside of the VRS can be calculated and what thermal hardware is used to improve the system, the thermal balance can be determined. The balloon and the gondola of the VRS will be considered separate from each other.

Balloon

Inside the balloon, there is no hardware to control its temperature. Due to its size, it would consume too much power. It has been designed to function at ambient temperature. The inside temperature of the balloon depends on the total radiative heat transfer to the inside, the conductive heat exchange to the atmosphere and the radiated heat to the outside. According to

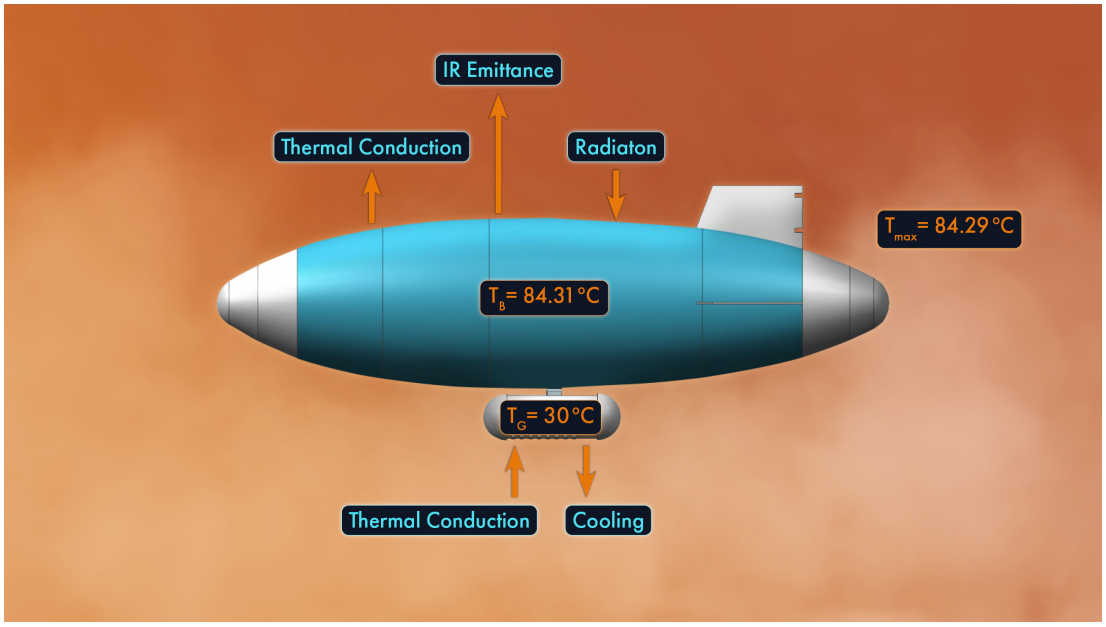

Figure 13.1: The effect of different heat sources on the Venus Research Station

[20] the net thermal flux affecting the station at a height of 50 km has a value of 2000 W/m^2. This is also the value for the direct solar flux, meaning that all other radiation sources like the solar reflected heat load and the infrared heat flux are attenuated by the atmosphere and have no effect at 50 km. Therefore the radiative heat load into the balloon can be calculated using Equation (13.1) with the absorptivity of the surface paint of $\alpha = 0.05$ and the surface area of the balloon. For the worst case in which the highest amount of radiative heat flow is received, the radiation is absorbed from above the balloon with an incident angle of 0 °. Assuming a cylindrical shape for the balloon with a length of 50 m and a radius of 7.13 m the effective surface area that is affected by the solar flux has an approximate value of 713 m^2. Using Equation (13.1) yields a value of $q_{rad} = 71.3$ kW.

The infrared radiation that is being emitted by the balloon is calculated using the Stefan-Boltzmann Law Equation (13.3). The total approximate area of the balloon is 2559.4 m^2 and the emissivity has a value of $\epsilon = 0.91$. The radiative heat flow to the inside is greater than the emitted heat flow of the balloon. Therefore the balloon heats up to a temperature higher than the ambient one. This causes a conductive heat flow from the inside to the outside.

The steady-state temperature of the balloon can be determined by considering all the radiative heat flow that enters it, the conductive heat flow to the atmosphere and the infrared heat flow emitted by the balloon.

$$q_{rad} = q_{cond} + q_{emit} \tag{13.14}$$

$$0 = q_{cyl} + 2 \cdot q_{side} + \epsilon \cdot \sigma \cdot A_{gondola} \cdot T^4 - A_{eff} \cdot \alpha \cdot I_{total} \tag{13.15}$$

If the sum of these heat flows reaches a value of zero, thermal equilibrium is achieved. This is the case for a Temperature of 84.3069 °C. The heat flows that result from this temperature on the inside are $q_{cond} = 70.89$ kW and $q_{emit} = 407.3$ W. The increase of temperature of the inside of the balloon due to radiation effects compared to the ambient temperature has a value of 0.0169 °C and is therefore negligible.

Gondola

The inside of the gondola is to be cooled to a temperature of 30 °C. This causes a conductive heat flow from the atmosphere to the inside of the station. There is no radiative heat flow from the sun towards the gondola, due to it being in the shadow of the balloon. Also, the heat emitted to the outside by infrared radiation is negligible in this case. Therefore there is only the conductive heat flow to the inside of the gondola. It is calculated using Figure 13.2 and Equation (13.11). Figure 13.2 shows the heat flow to the inside of the gondola depending on the thickness of the aerogel insulation.

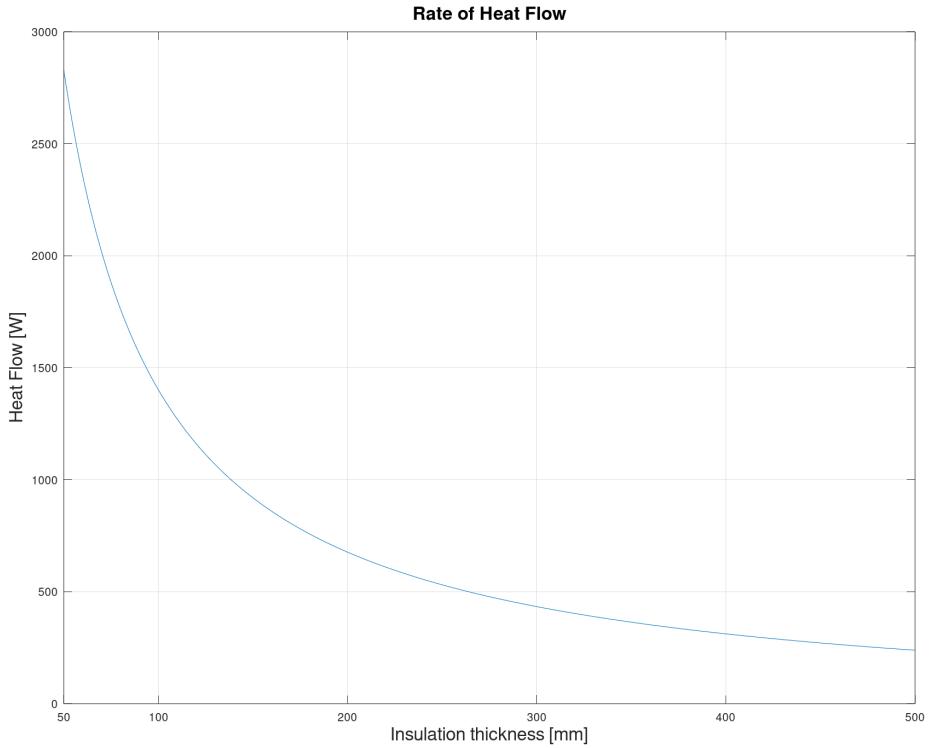

Figure 13.2: Heat flow from the outside of the gondola to the inside, depending on the thickness of the insulation layer

It can be seen that a thicker insulation layer greatly reduces the conductive heat flow. An insulation thickness of 30 cm was chosen, as it reduces the heat flow to a value of $q_{cond} = 433.5W$. This is an acceptable amount to comply with power consumption requirements while still adding a reasonable amount of mass. Figure 13.3 visualizes how the amount of conductive heat flow to the inside relates to the mass of the insulation layer.

For the design of the thermal control system, the trade-off between power consumption and mass is crucial, as both are limited under the given conditions. For an insulation layer of 30 cm thickness the total mass is 180.6 kg. This shows how important it is to have a low-density insulation material. In the case of using Microtherm, the mass for an insulation layer with the same thickness would be 8.7 tons.

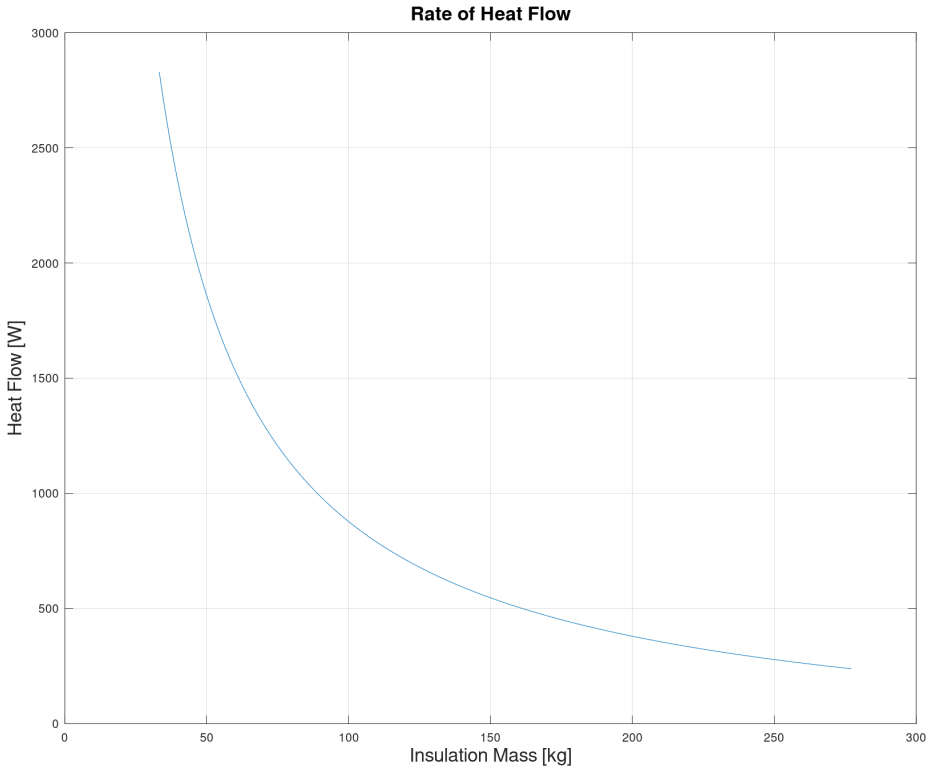

Figure 13.3: Heat flow from the outside of the gondola to the inside, depending on the mass of the insulation layer

To keep the inside temperature of the gondola at stable temperature, the same amount of heat that flows into the station must be rejected back into the atmosphere. This is done using a Stirling cycle cryocooler in combination with a heat sink as described in the earlier sections. For the given conductive heat flow to the inside of 433.5 W, the temperature of the heat sink on the outside is determined using Equation (13.13). This yields a temperature of 88.84 °C which is 4.55 °C above the ambient temperature.

This means the Stirling cooler needs to lift the heat from a temperature of 30 °C to 88.84 °C. The power consumption of a Stirling cooler depends on its efficiency, the amount of heat that needs to be lifted from the cold end to the hot one and their temperatures.[134]

$$W_{cooler} = \frac{q_{rejected} \cdot (\frac{T_{heatsink}}{T_{inside}} - 1)}{\eta} \tag{13.16}$$

The power consumption is calculated assuming a Carnot efficiency for the Stirling cooler of 50 %.[136] The Carnot efficiency is the maximum possible efficiency for a heat pump and depends on the temperature of the cold side from which the heat is lifted and the hot one.[134]

$$\eta_{carnot} = 1 - \frac{T_{cold}}{T_{hot}} \tag{13.17}$$

For this system, the Carnot efficiency has a value of 16.3 %. The calculation of the power consumption for the Stirling cooler to lift 433.5 W from 30 °C to 88.84 °C then yields 1035.2 W. With this amount of power, the temperature of the inside of the gondola will stay at a stable temperature for the worst case of the outside temperature. For the lowest outside temperature of 67.4 °C the conductive heat flow reduces to 298.6 W and the power consumption to 677.1 W.

Some systems need to be cooled to a temperature lower than 30 °C. For example, the communications system requires an operating temperature of 200 °K. For this purpose, an insulated volume of 1 m^3 is added inside of the gondola. It is equipped with a separate Stirling cooler that lifts heat from a temperature of 200 °K to the inside of the gondola. Aerogel is also used as the insulation material for this cold box. The thickness of the insulation layer is 10 cm. The heat flow from the inside of the gondola at 30 °C through the side walls of the cold box is calculated using Fourier´s LawEquation (13.4). It has a value of $q_{cond} = 123.8W$. The cooling of the cold box is done in the same way as the cooling of the gondola. A Stirling cooler lifts heat from the cold side to the hot side that is connected to a heat sink outside of the cold box using heat pipes. A smaller version of the same heat sink with dimensions of 20 cm by 40 cm for the base plate is used to reject the heat to the inside of the gondola. The temperature required by the heat sink to do so is 31.92 °C and is calculated using Equation (13.13). The power needed for the Stirling cooler to keep the cold box at a temperature of 200 °K under the same assumptions is then 377.61 W. The total power consumption of the thermal control system is then the sum of the power consumption of both cooling cycles and has a value of 1364.5 W. By having a two-stage cooling system for the components that need to be at a lower temperature than 30 °C power can be saved. If the heat would instead be lifted from 200 °K to the temperature of the atmosphere, more power would be consumed by the cooler to create a greater temperature gradient.

13.4 Thermal control of Scouts

The thermal control for the scouts is handled by passive methods only. It is not feasible to have an active cooling system given the limitations of mass and power. The initial inside temperature of the scouts before entry is 30 °C. During the entry phase, the scout will experience heat load averaging 4.23 MW over a duration of 280 seconds according to Chapter 9. It is planned to use a heat shield that absorbs the heat during entry and is discarded afterward. Furthermore, a thick layer of aerogel insulation can be used to minimize the heat flow from the atmosphere to the inside of the scout. This should guarantee that the temperature rises inside the scouts remains within an acceptable range, enabling all components to operate throughout the duration of their mission.

In this Chapter, the thermal control system was designed in a way to meet all the mission´s requirements. By integrating a combination of passive and active cooling methods a stable inside temperature within the station is achieved.

CHAPTER 14

Command and Data Handling (C&DH) and Onboard Computer (OBC)

by Tanuja Datar

This Chapter focuses on the Command and Data Handling (C&DH) and Onboard Computer (OBC) systems, which are essential to mission operations. This Chapter investigates the primary requirements and operations for the Data Handling (DH) system, including data collection, processing, storage, classification, and transmission.To build a thorough data budget, the sources of data generation are identified, and the amount of data produced is estimated. With a focus on real-time processing considerations for handling substantial amounts of data in real-time scenarios, the data flow is discussed through the system's architecture. The main features and parameters of the OBC's performance matrix are discussed along with an analysis of it.

In addition, the Chapter includes a market survey on the components needed for C&DH and OBC systems to ensure optimal performance and dependability. To ensure mission continuity in the case of system failures, redundancy and backup options are rigorously analyzed. The Chapter also includes the overview to the assigned priority level for receiving or transmitting data and commands signifying the importance and urgency of the data.

14.1 System Architecture

This Section gives in detailed information of the entire C&DH and OBC system architecture which includes the purpose of each component use, their interconnections with each other, redundancy and backup options. This architecture was thoroughly developed following an extensive analysis of multiple research publications, with important references provided for the essential papers [137],[138],[139] and [140] that had a significant effect on its development.

Overview of the C&DH and OBC System Architecture

The complicated connection between multiple subsystems and components are shown in detail in Figure 14.1 of the system architecture. The Onboard Computer (OBC), which serves as the system's brain and controls and coordinates all of its operations, is a vital element of the architecture. The Payloads are considered into two separate sections, with SAR acting as the primary component. A backup SAR is also used in cold redundancy. SAR has a dedicated Smart Onboard Data Processors (SOBDP) and Clock Monitoring and Control Unit (CMCU), which allows for smoother and more effective operations. The GNC system receives input from the SAR-CMCU-SOBDP interface for precise localization. Other payloads have dedicated Onboard Data Processors (OBDP) and their corresponding payload support unit. With its more than six

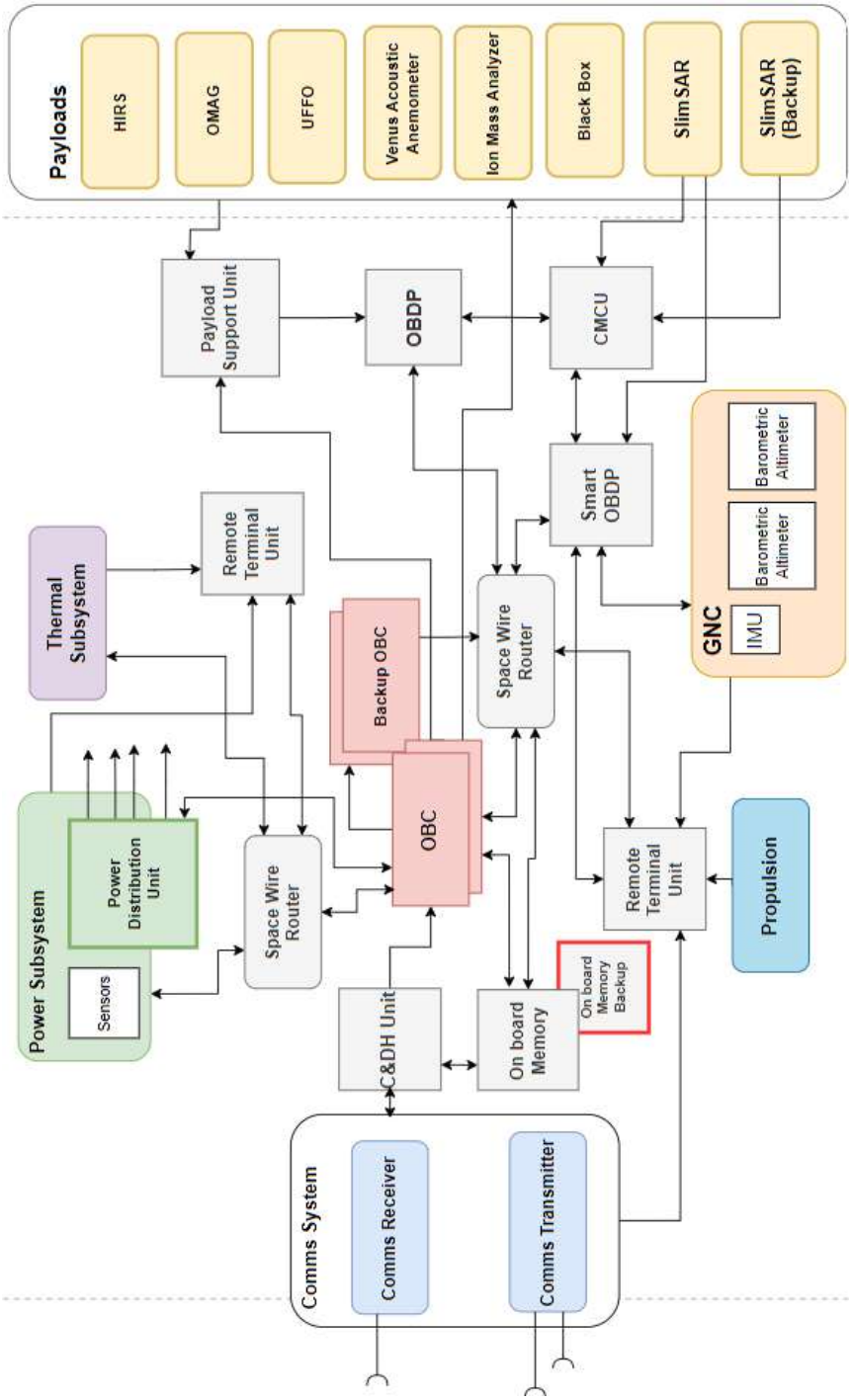

Figure 14.1: Block Diagram of C&DH and OBC System Architecture

Component	Producer	Mass [kg]	P [W]	OT Range [°C]
ICDE - NG OBC[142]	Airbus	13.6	35	-25 ∼ +50
OBC NG [143]	Beyond Gravity	9	38	-55 ∼ +40
C&DH Unit[144]	Magellan Aerospace	10	34	-35 ∼ +65
CMCU[145]	Airbus	5.2	21	-15 ∼ +45
NEMO-2-2120[146]	Airbus	14	66	-25 ∼ +60
Mk25-133[147]	Star Dundee	1.5	1	-25 ∼ +60
PLSU[148]	BST	1	8	-20 ∼ +40
RTU Type B[149]	Beyond Gravity	17	15	-65 ∼ +60
Smart OBDP[150]	Kp Labs	5	40	-15 ∼ +40
OBDP[151]	–	∼5	∼ 35	-25 ∼ +45

Table 14.1: Market Research Findings - Verified Components. P: Power Consumption [Watts]. OT: Operating Temperature [°C].

ports, the Spacewire Router acts as an interface connector and improves the effectiveness of data exchange. The Communication subsystem is connected with Command and Data Handling (C&DH) unit and the on-board non volatile memory which also has a cold redundancy backup for increased robustness. This complex network of connections and components is the effective and reliable system architecture to precisely and dependably achieve its goals. Entire architecture and component selection procedure is as per ESA standards mentioned in [141].

14.2 C&DH and OBC Components

This Section focuses on the Market research which is essential to stay updated with the latest advancements and trends in the industry. By analyzing the current market offerings and understanding the parameters and characteristics of existing components, we can make informed decisions about the components used in the mission's architecture. Additionally, forecasting the future versions of these components can help in planning for upgrades and improvements as technology evolves. Some verified components can be found in Table 14.1.

Each component is selected according to the particular requirements of the mission, taking into account its functionality and the essential function it plays in the mission's success. If the certain component does not possess the exact parameters required, something similar can be customized, manufactured and tested (considering as long as base functions remain the same). Also, all the products considered in this analysis are sourced exclusively from European companies.

Overview of the Components and Their Functions

In this Section, detailed justifications and explanations are provided for the selected components in the mission's architecture.

Remote Terminal Unit (RTU) RTU is used to collect analogue and digital telemetry from sensors and different subsystems. It also monitors Temperature, Pressure, Digital Status of

AOCS actuators and sensors, Solar Array Drive Equipments, and heater/cooling lines. For a research station, having a distributed RTU can be beneficial as it will result in an essential decrease in harness, operational segregation, and improved integration performance[152]. A dual set of modules can be built as two independent units that can operate in either cold redundancy or hot redundancy, or they can be built as one unit incorporated into the same backplane module.

To achieve OR08 and OR09 from Table 3.4, which specifies that if any problems or defects develop in a particular individual subsystem (such as power, thermal, communications, GNC, etc.), that specific subsystem should be able to recover on its own without compromising other subsystems or requiring their shutdown.To improve failure robustness and operational segregation, every unit provides as much autonomy as feasible while sharing only a few transparent interfaces spread over the linked subsystems via a backplane module.

Clock Monitoring and Control Unit (CMCU) The research station must be localized precisely, which can be accomplished by appropriately georeferencing and interpreting SAR data (which will be carried out by a SOBDP). The CMCU can offer precise time information for synchronization between the station's processor and SAR for accurate localization. By maintaining a very precise master clock generator, the CMCU can help in timestamping the SAR data correctly and synchronizing it with data collection and processing systems. By using the exact timing information from the CMCU to timestamp SAR data, it is able to correctly localize and align the captured SAR images.

Payload Support Unit (PLSU) PLSU is used as an assistance / backup system to manage the payload data and commands received for a certain payload. Additional functions are to control the payload temperature (Heat) and operate a focus mechanism (FOCM).

Command and Data Handling (C&DH) unit C&DH unit ensures the seamless transfer of data and precise execution of commands, performs a crucial role in the DH system design. Before transmitting commands to the appropriate subsystems and payloads, it decodes and validates the commands it receives from the Earth via Communication Subsystem. Additionally, the C&DH unit efficiently does the packaging engineering for telemetry and scientific data generated by various payloads and subsystems.

On board Data memory NEMO-2 It provides superior mass memory capacity and performance. Its scalable, modular architecture with certified building blocks in a slice form factor guarantees adaptability and flexibility. NEMO-2 ensures effective data handling with its simple and simultaneous record and replay capabilities using Flash technology. It consists of two to eight identical slices with memory slices and dedicated DC/DC redundant converters. The storage required memory is later decided using the data budget which is 16 Tbits.

On Board Data Processor (OBDP) OBDP is used to compress the other payloads and telemetry and telecommand data (TMTC) by 50%, and is essential for managing data. Furthermore, it effectively compresses data from every other payload besides SAR for the best data management. The SOBDP filters the SAR data by 50% and further compresses it by 50%. The Smart OBDP offers 100-fold reduction in data volume, which is remarkable given the considerable amount of data generated by SAR's continuous operation. The Smart OBDP is crucial to the success of the mission because it allows SAR data analysis for exact localisation while retaining image quality at 50% [153]. Additionally, the OBDP ensures data

processing redundancy by acting as a dependable backup processor when SAR data is lower than anticipated.

Redundancy and backup strategies

A backup component or alternative interconnect is provided for each component that is essential to the operation's success, ensuring redundancy and mission continuity. The architecture includes a fully redundant On-Board Computer (OBC) with cross-stacking capabilities and various slices for data transmission. To handle data compression SAR, the SOBDP has a distinct interconnection provision with OBDP for redundancy.

Data dependability is further secured by the NEMO-2 mass memory system's simultaneous record and replay capabilities, which use Flash technology and also, another memory in cold redundancy to avoid strain on mission power requirements. With these fail-safe systems in place, the mission is well-equipped to withstand potential setbacks and guarantee the successful completion of its goals for C&DH and OBC systems.

Overview of OBC

The On-Board Computer (OBC) is required to have systems in place that allow it to keep track of its own and other subsystems' state of health and report any problems or irregularities it notices. This enables prompt troubleshooting and resolution by providing proactive identification and sharing of issues occurring within the OBC or any other subsystem. Therefore, if there are any problems, the research station will broadcast some emergency telemetry to Earth, which will allow mission control to issue some level of telecommands to fix the problem, or at the very least, let mission control know that a subsystem is malfunctioning[141].

The OBC selected ICDE-NG (Integrated Control and Data Equipment - Next Generation) is made for multipurpose applications in satellite systems but similar versions can be used onboard Research Station[142]. Its architecture features an in-flight programmable EEPROM, a CPU module with an ERC32 processor, and substantial memory capacity. It can uplink and downlink ESA standard TC/TM packets that are processed quickly and effectively by the Telecommand/Telemetry module which will be functioning complimentary with the C&DH unit.

14.3 Performance Matrix

Performance Matrix summarizes the computer and data handling characteristics. It helps to analyze the degree of activity that needs to be assigned to parameters of different subsystems. It is based on concept given by [154]. The allocation of low, medium, or high for various aspects reflects the characteristic's level of involvement and significance in performing its designated tasks.

Key functions and Parameters explained

The High, Medium and Low in Performance Matrix Table 14.2 indicates

High: Indicates a significant or intense level of the parameter, which may require more resources, processing power, or precision.

Medium: Represents an intermediate level of the parameter, indicating moderate resource usage or performance requirements. It may not be as demanding as "high" but still requires adequate attention and resources.

Low: Refers to a relatively lower level of the parameter, implying minimal resource usage or less demanding performance requirements.

The following information aims to provide a comprehensive understanding and justification of the role and significance of the characteristics for each Subsystem in the overall mission. It provides an explanation for why each characteristic is assigned a priority level of high, medium, or low.

1. **Payload Subsystem**:

   OBC Utilization **(OBC U)**: High - Due to complex data processing tasks performed by SAR and other payloads.

   Throughput Estimation **(TE)**: High - To handle the large volume of data generated by SAR and other payloads efficiently.

   Non-Volatile Memory Allocation **(NVMA)**: High - To store collected data for later processing and analysis.

   RAM Allocation **(RAMA)**: Medium - For temporary data storage during data processing.

   Real-time Precision **(RTP)**: Medium - To ensure timely and accurate data acquisition and processing.

   Update Rate **(UR)**: High - To handle frequent data updates from SAR and other payloads.

2. **Communication Subsystem**:

   OBC U: Medium - Primarily handles data transmission and reception between the research station and external entities.

   TE: Medium - To manage data transmission and reception tasks efficiently.

   NVMA: Medium - For storing communication protocols and network configurations.

   RAMA: Low - Mainly focuses on data routing and management.

   RTP: Low - Primarily deals with data transfer and routing.

   UR: Medium - To maintain efficient communication links with external entities.

3. **Power Subsystem**:

   OBC U: High - Involves controlling power flow and distributing power to various components.

   TE: High - To manage power flow, track energy levels, and optimize power distribution.

   NVMA: Low - Focuses on real-time power management and control.

   RAMA: Low - Involves immediate power calculations and control operations.

   RTP: Medium - Accurate monitoring and control of power generation and distribution.

   UR: High - Continuous monitoring and adjustments for optimal power operation.

4. **Thermal Subsystem**:

   OBC U: Medium - Involves monitoring and controlling temperature sensors and thermal management systems.

   TE: Medium - To manage thermal sensors and control cooler operations.

   NVMA: Low - Focuses on real-time temperature monitoring and control.

   RAMA: Low - Involves immediate temperature data processing and sensor readings.

   RTP: Low - Deals with temperature monitoring and control with slower dynamics.

UR: Medium - Periodic measurements and adjustments for maintaining desired thermal conditions.

5. **G&C Subsystem (Guidance and Navigation Control)**:

   OBC U: Low - Basic guidance and navigation functions with no extensive computational requirements.

   TE: Low - Processing sensor data and basic navigation algorithms with no high data throughput.

   NVMA: Low - Real-time monitoring and control of navigation parameters.

   RAMA: Low - Immediate processing of sensor data and navigation algorithms.

   RTP: High - Accurate positioning and maneuvering of the spacecraft.

   UR: Medium - Periodic measurements and adjustments for accurate guidance and navigation.

6. **Structures Subsystem**:

   OBC U: Medium - Controls the deployment mechanism and monitors its status.

   TE: Medium - Manages the operation of the deployment mechanism.

   NVMA: Low - Real-time monitoring and control of the deployment mechanism.

   RAMA: Low - Immediate monitoring and control commands for the deployment mechanism.

   RTP: High - Accurate and timely deployment of structures.

   UR: High - Frequent measurements and control actions for proper deployment operations.

7. **C&DH Subsystem (Command and Data Handling)**:

   OBC U: High - Processes commands, manages data handling functions, and coordinates communication.

   TE: High - Manages data handling and communication for optimal data transfer rates.

   NVMA: High - Stores critical data and software for reliable system operation.

   RAMA: High - Buffers and processes real-time data during system operation.

   RTP: Medium - Timely response and efficient data handling for command execution and communication.

   UR: Medium - Periodic data handling and control actions for reliable communication and data exchange.

8. **Propulsion Subsystem**:

   OBC U: Medium - Controls thrust and monitors RPM (Rotations Per Minute).

   TE: Medium - Monitors and controls thrust and RPM data.

   NVMA: Low - Real-time control and monitoring of propulsion parameters.

   RAMA: Low - Immediate processing and control of thrust and RPM data.

   RTP: High - Accurate control of the spacecraft's propulsion.

   UR: High - Continuous monitoring and control of thrust and RPM parameters.

Subsystem	Components	OBC U	TE	NVMA	RAMA	RTP	UR
Payload	SAR	High	High	High	Medium	Medium	High
	Other Payloads	Medium	Medium	Medium	Medium	Low	Low
Comms	Transmitter	High	High	Low	Low	High	High
	Receiver	Medium	Low	Low	Low	High	Low
Power	PCDU	Medium	Medium	Medium	Low	Low	High
	Battery	Medium	Low	Low	Low	Low	Medium
Thermal	Sensors	Medium	Low	Low	Medium	Medium	Medium
	Cooler	Medium	Medium	Low	Low	Medium	High
GNC	FRS	High	Medium	Low	Low	Low	Medium
	IMU	Medium	Medium	Low	High	Medium	High
C&DH	C&DH Unit	High	Medium	Low	High	Low	Medium
	RTU	Medium	Medium	Low	Medium	High	High
Structures	Deployment	High	Medium	Low	Low	High	High
Propulsion	RPMS & TMS	High	Medium	Low	Low	Low	Medium

Table 14.2: Performance Matrix

14.4 Data Budget for Research Station

In this Section the in detailed Data Budget for both the operation phases is provided. For the purpose of analysis and calculations, only Ka band data transmission is considered, as it exhibits a significantly higher transmission rate compared to X band, which was not compatible with data rate requirements and is not taken into account in this study. Table 14.8 presents the Data Budget for the Subsystem Components during SO Phase one of the mission in which SAR is operating continuously. Table 14.9 presents data budget for SO Phase two, in which all the payloads except SAR are working and the remaining SAR data from phase one is transmitted. SO Phase 3 will have a single working payload to find life on Venus mentioned in Chapter 3 and all other subsystems is shown in Table 14.10. All the data budgets includes columns namely the subsystem, Components that generates any type of data (TMTC or Payload), the Data rate of specific component, Operating time for one circumnavigation (e.g.176 hrs), Amount of Data to Transmit after Data processing to Relay Satellite, Operating Time between two successive contacts with Relay Satellite (e.g.0.42 hr 24 mins), and Data generated (filtered and processed) between two successive contacts with Relay Satellite.

14.5 Data Budget Trade off and Analysis

After a significant iterations of trade off and analysis the final values were decided to ensure the transmission of all the data generated. A quick view for trade parameters and it's effects on other parameters can be found in Table 14.3

Trade of Parameter	Action	Affected Parameter	Affect
Payload DR	Decrease	Coverage%	Decreases
VRS Transmission DR	Increase	Link Margin	Decreases
Compression Ratio	Increase	Image Integrity	Decreases
Data Storage	Increase	Power Consumption	Increases
No. of Relay Satellites	Increase	Launcher Mass, No. of Launches	Increases

Table 14.3: Impact Analysis of Trade Parameters.

The most difficult parameter to trade off is the data generation rate of SAR (50 Mbits/s) which is almost six times the data transmission rate (8 Mbits/s) of Research Station. Hence, to decrease the data volume filtering and compression is necessary for SAR data, to maintain data integrity only 50 % of each is possible. All generated Data TMTC or from any other component is compressed by 50 %. Even with compression SAR data decreases by a significant amount but still not sufficiently low enough to achieve the complete data transmission.

The average access time per circumnavigation of Research Station with single Relay Satellite is about 35872 Sec which gives the required data rate of 222 Mbits/s (Possible achievable data rate 8 Mbits/sChapter 15). As the number of Relay Satellites increases the required data rate decreases. By not affecting number and mass of launches much the trade off analysis gives the conclusion to use 14 Relay Satellites which gives required data rate of 16 Mbits/s which is clearly double of achievable data rate. The detailed analysis can be found in Table 14.4. It can be concluded as for each 176 hrs SAR is turned on it should be turned off for next 176 hrs.

No. of RS	Data Rate required in SO1[Mbits/s]	Data Rate required in SO2[Mbits/s]	Data Rate required in SOP3[Mbits/s]
1	222.00	110.81	1.83
5	44.34	22.16	0.61
10	22.17	11.08	0.26
14	15.84	7.91	0.18

Table 14.4: Analysis on number of Required Relay Satellites

Parameters	SO Phase 1 [Gbits]	SO Phase 2 [Gbits]	SO Phase 3 [Gbits]
Data Generated per Successive contact	19	9	0.17
Data Transmitted per Successive contact	9	9	90
Data Generated per Circumnavigation	7953	3968	65
Data Transmitted per Circumnavigation	4017	4017	4017
Remaining Data per Circumnavigation	3935	ALL DATA SENT!	

Table 14.5: Data Transmission Summary for VRS. The values in this table are approximated to whole numbers for clarity, though they are based on accurate calculations with several decimal digits.

Considering the storage of 16 Tbits. as the total data generated in a single circumnavigation is around 8 Tbits hence, considering the safety margin, the storage is considered double that of amount of data generated. The mission operation phases were fixed dependent on data transmission while ensuring sufficient amount of Venus coverage. The mission's success can be considerably impacted by balancing data rates, transmission capacities, compression effectiveness, storage capacity, and number of relay satellites. A concise, summarized version of the successful trade-off, backed by numerical evidence, can be found in Table 14.5

To identify and analyze data rates or total amount of data generated two methods were used; First Method is to calculate the amount of data that can be transmitted by the communication system basically depends on the achievable data rate by transmitter. Second method gives the required data rate considering the number of relay satellites functioning. More graphical representation of above study can be found in this report under Section 16.5.

Formulas used for calculations:

$$D_{Total} = R \times t_o \tag{14.1}$$

$$D_{Ka} = R_{Ka} \times t_A \times X_{RS} \tag{14.2}$$

$$R_{required} = \frac{D_{Total}}{t_A \times X_{RS}} \tag{14.3}$$

$$D_t = D_{Total} - D_{Ka} \tag{14.4}$$

Where;
D_{Total} - Total Amount of Data generated
R - Data generation rate
t_o - Operating time
D_{Ka} - Amount of data that Ka band can transmit
R_{Ka} - Data rate of Ka band
t_A - Access time with Relay satellite
X_{RS} - No. of Relay Satellite
D_t - Total Amount Data needs to be transmitted
$R_{requiredX}$ - Required Data rate with X no. of Relay Satellites

14.6 Command and Data Priority

In this Section, we categorize and prioritize the various types of data and commands relevant to the mission operations. The table below outlines the descriptions and priority levels assigned to different data types and commands based on their criticality and time sensitivity. This Priority study was developed out of an extensive analysis of many research articles, with the key ones being duly referenced here [155],[156].

Type	Description	Priority Level
Time Critical Command from Earth	To do any timely changes in the mission operations, To change mission parameters, To Fix any Error	HPC 0
Mission Critical Telemetry	In case of mission failure, If more than two subsystems are not working as predefined or failing simultaneously	HPD 0
Component Telemetry Data	Flagged by OBC, In case of Failure of component/s	HPD 1
Data from other Payloads	Just 0.22 % of the whole payload data generated compared to SAR, If time-critical situation this should be prioritized	HPD 2
Mission Support Data	Health Monitoring and TMTC data from each subsystem	LPD 0
Data from Scouts	Timely analysis, scheduling changes can be made	LPD 1
Data from SAR	SAR data is crucial for mission objectives, it does not require immediate action in time-critical scenarios	LPD 2

Table 14.6: Assessment of Priorities and Descriptions

The Table 14.6 provides an essential framework for understanding the priority levels assigned to different data types and commands in the mission. The priority levels (HPC - High Priority Command, HPD - High Priority Data, and LPD - Low Priority Data) help in efficiently managing and responding to various scenarios and mission conditions. This satisfies OR04 and OR05 from Table **??**.

Due to its size and the prevalence of time-sensitive occurrences, SAR data is classified as low priority. Smaller critical data is prioritised in these situations to allow for immediate response. SAR data, which is crucial for mission goals, is frequently used for long-term planning and

post-analysis, making it less time-sensitive during crucial situations. This method reduces the possibility of losing all data in time-critical situations by ensuring that essential information is handled promptly suggested in [157]. The relevance of each data type and command can be clearly defined, ensuring prompt and suitable responses that contribute to the mission's overall success and effectiveness.

14.7 Data Budget and storage for Scouts

This Section provides essential information about data transmission for Scouts, including the onboard data storage unit and the data budget (Table 14.7). The maximum operational time for the Scouts is 3 hrs, and in determining their limitations, a minimum transmission time of 1 hr is taken into account assuming survivability on the Venus surface. The data storage on board Scouts is Kryten M3 developed by AAC CLYDE SPACE which has 8 MB MRAM for code storage and execution as well as 4 GB flash memory and a mass of just 61.9 g. It consumes maximum power of one watts[158].

Components	**Data rate [Kbits/s]**	**Operating Time [h]**	**Amount of Data [Mbits]**
Payloads			
VSWS	5	3	54
MIS	2	3	21.6
BIMS	1.498	3	16.18
MERTIS	4	3	43.2
Total Data parameters			
Total Data Generated			134.98
With Worst scenario	13	1	46.8
With Best scenario	54	1	194.4
Data Rate Required to transmit all the data	37.494		

Table 14.7: Data Budget for Scouts.

Two approaches are used to evaluate the data rate; first, the communications team determines the best-case and worst-case achievable data rates which depends on the transmitters capabilities and link margin; second, the required data rate is calculated. The data budget analysis shows that the required data rate is much lower than the best-case scenario. Hence it can be said that in most of the cases all the data generated can be successfully sent to VRS.

Subsystem	Components	Data rate [kbits/s]	Operating time [h]	Data to Transmit [Mbits]	Time between Contacts with RS [h]	Data to Transmit [Mbits]
Payload	SlimSAR	50000.00	176.00	7920000.00	0.42	18900.00
GNC	IMU	22.40	176.004	7096.32	0.42	16.93
	BA	1.28	176.00	405.50	0.42	0.97
	FRS	0.160	2.00	0.58	0.068	0.02
	Pressure Sensor	0.320	176.00	101.38	0.42	0.24
Power	PCDU	15	176.00	4752.00	0.42	11.34
	PDIO	10	176.00	3168.00	0.42	7.56
Thermal	Coolers	18	176.00	5702.40	0.42	13.61
	Temperature Sensors	12	176.00	3801.60	0.42	9.07
C&DH and Comms	TM Data	1.00	176.00	316.80	0.42	0.76
	Data Receive	200.00				
Propulsion	DPAS	0.6	176.00	190.08	0.42	0.45
	RPMS	2	176.00	633.60	0.42	1.51
	TMS	1	176.00	316.80	0.42	0.76
	Current Sensor	20	176.00	6336.00	0.42	15.12
Total Data Generated by all components of VRS [Gbits]			7952.821		18.978	
Amount of data still needs to be transmitted [Gbits]			3935.1298			

Table 14.8: Data Budget for VRS SO Phase 1.

Subsystem	Components	Data rate [kbits/s]	Operating time [h]	Data to Transmit [Mbits]	Time between Contacts with RS [h]	Data to Transmit [Mbits]
Payload	SAR (Data from SO Phase 1)			3935129.80	0.42	8925.00
	HIRS	2.88	176.00	912.38	0.42	2.18
	OMAG	2.048	176.00	648.81	0.42	1.55
	UFFO	11.57	176.00	3665.38	0.42	6.12
	VAA	1.20	176.00	380.16	0.42	0.91
	MERTIS	4	176.00	1267.20	0.42	0.84
	IMA	0.08	176.00	25.34	0.42	0.06
GNC	All Combined	24.16	176.00	7603.78	0.42	18.16
Power	All Combined	25.00	176.00	7920.00	0.42	18.90
Thermal	All Combined	30.00	176.00	9504.00	0.42	22.68
C&DH and Comms	TM Data	1.00	176.00	316.80	0.42	0.76
Propulsion	All Combined	23.60	176.00	7476.48	0.42	17.84
Total Data Generated for VRS				3974850		9015

Table 14.9: Data Budget for VRS SO Phase 2. All the components combined for each subsystem are as same in SO Phase 1

Subsystem	Components	Data rate [kbits/s]	Operating time [h]	Data to Transmit [Mbits]	Time between Contacts with RS [h]	Data to Transmit [Mbits]
Payload	LoV instrument	100.00	176.00	31680.00	0.42	75.60
GNC	All Combined	24.16	176.00	7603.78	0.42	18.16
Power	All Combined	25.00	176.00	7920.00	0.42	18.90
Thermal	All Combined	30.00	176.00	9504.00	0.42	22.68
C&DH and Comms	TM Data	1.00	176.00	316.80	0.42	0.76
Propulsion	All Combined	23.60	176.00	7476.48	0.42	17.84
Total Data Generated for VRS				65806.27		172.84

Table 14.10: Data Budget for VRS SO Phase 3. All the components combined for each subsystem are as same in SO Phase 1.

CHAPTER 15

Communication

by Narges Ezzatpoor

Venus exploration involves sending probes to its surface and using orbiting or flyby satellites. Past missions like Mariner 10, Pioneer Venus 2, Venera 4-14, and Vega 1 and 2 successfully delivered probes to Venus, providing valuable data about its atmosphere and physical properties. Future missions can benefit from this information to increase their chances of success and explore new scientific avenues. An essential aspect of mission planning is establishing a reliable Radio Frequency (RF) communication link between the atmospheric descent probe, the flying Venus Research Station, and Orbiting Relay Satellites. This is crucial for effective mission planning and communication equipment design.

15.1 Introduction

The communication link between the probe and the Venus Research Station (VRS) and then with the Relay Satellites faces significant challenges due to Venus's thick and harsh atmosphere. Transmitting data from the surface to the VRS or back to The Relay Satellites becomes difficult because the atmospheric constituents, such as carbon dioxide and sulfuric acid clouds, absorb and weaken radio signals.

Several factors impact the RF communication link, including atmospheric absorption, the length and geometry of the signal path, antenna design, and orientation. The relative motion between the probe and the VRS also causes a Doppler shift in the communication signals. Moreover, choosing RF frequency is critical to overcome atmospheric interference and ensure reliable communication.

To address these challenges, previous missions have employed high-gain antennas, used orbiters as Relay Satellites, and implemented data compression techniques. Future missions can build upon this knowledge and advancements in communication technology to plan more robust RF communication links. This will increase the likelihood of mission success and enable further scientific exploration of Venus's atmosphere and surface. In this Chapter, Communication Links and their frequencies were explained, as well as the Communication Architectures, Atmospheric Losses, and Link Budget in each Communication Link.

15.2 Communication Links

The communication links require efficient data transformation, encompassing the connection between the Scouts and the Venus Research Station and between the Venus Research Station and the Relay satellites. Finally, data transmission occurs from the Relay Satellites to the ground station. As is shown in Figure 15.1 shows the *Communication Links*. The Scouts' main

task involves gathering information about the atmospheric properties of Venus, utilizing probes as payloads. Subsequently, this information is transferred to the Research Station using UHF Band frequency. An essential payload called the Synthetic-aperture radar (SAR) plays a crucial role in the surface mapping of Venus. SAR boasts a high data rate to achieve the best resolution. After processing some of the data onboard, the stored data is transferred to the Relay Satellites using Ka- and X-Band. For communication purposes, both high-gain and middle-gain antennas will be employed.

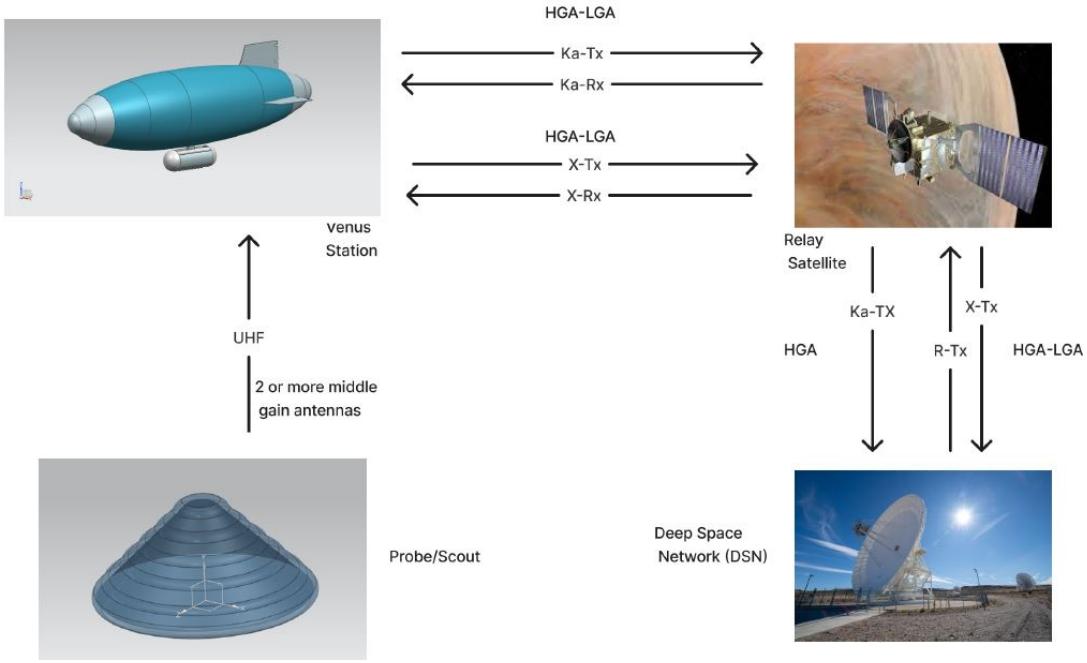

Figure 15.1: Communication Links between the Scouts and VRS as well as the VRS and Relay Satellites

15.3 Communication Architectures

Satellite communication architecture has become an indispensable component of modern telecommunication systems, enabling seamless connectivity across the globe. As the demand for high-speed data transmission and real-time communication continues to grow, satellite communication technology has evolved to meet these needs. This Chapter is providing an overview of its key components and their roles in facilitating efficient and reliable communication.

X-Band and Ka-Band

As depicted in Figure 15.2, the architecture for X-Band and Ka-Band encompasses both the transmitting and receiving parts. This representation aims to explain the key components of satellite communication in a simplified manner.

In the transmitter section, the process commences by employing a digital-to-analog converter to transform digital data into an analog signal. Once the analog signal is generated, it undergoes modulation using an ultra-stable oscillator to achieve the desired frequency. Subsequently, a converter and a local oscillator are utilized to synchronize the signal and adjust the carrier frequency. Following this, a bandpass filter is implemented, and a high-power amplifier is used to achieve the desired transmitting power. Afterward, the signal is sent to the circulator to protect the hardware from reverse power. Furthermore, a duplexer is employed to switch between transmission and reception modes. Additionally, an RF switch is utilized to switch between high-gain or medium-gain antennas.

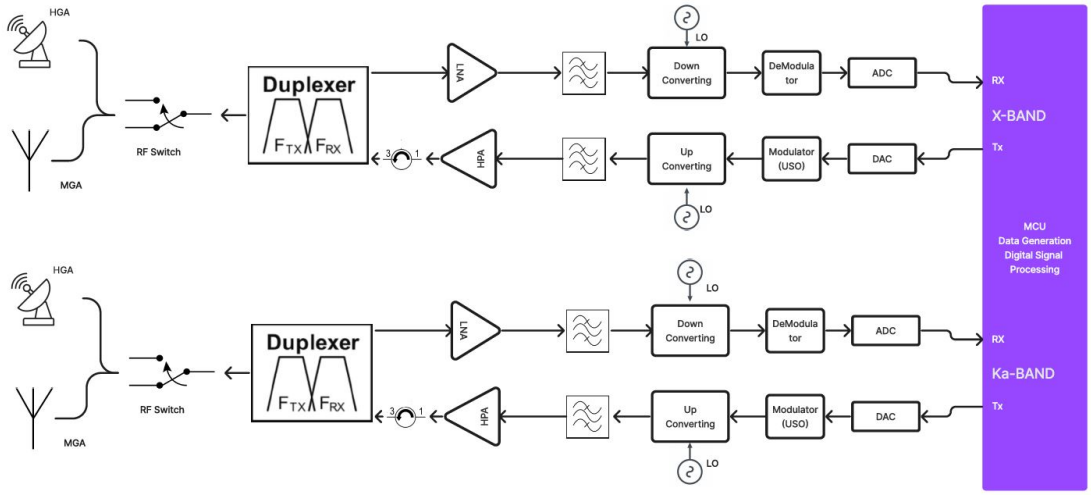

Figure 15.2: Communication Architecture in X- and Ka-Bands

On the other hand, in the receiver mode, the output switch facilitates the selection between the high-gain or medium-gain antennas. Subsequently, the receiver mode is chosen, and the signal is directed to the low-noise amplifier. By utilizing a bandpass filter, the desired signals are filtered out. Afterward, the signal is down-converted to a lower frequency, achieved with the assistance of a local oscillator that aids in selecting the desired signal and synchronizing the signal using a synthesizer.

Using the modulator, the data is extracted, and then the digital converter ensures precise data acquisition. It is important to note that this architecture represents a simplified receiver signal process, and additional steps may exist with different filters and frequencies or employing multiple amplifiers in each stage to enhance signal amplification.

UHF Band

For the receive signals in the Venus research station, a specialized setup has been developed utilizing two helical antennas to capture UHF frequencies from the Scouts, as shown in Figure 15.3. Each antenna receives and amplifies the signal independently using a low-noise amplifier. Subsequently, the signal undergoes filtering before going through a mixer and local oscillator for down-conversion to lower frequencies.

In the following step, another amplifier is utilized, and a second local oscillator is employed for further down-conversion, allowing synchronization of the signal's frequency and phase. This synchronization is crucial due to the Scouts' movement during transmission, leading to frequency

shifts and atmospheric changes affecting the signal. To achieve precise synchronization, two steps of synchronization are used, ensuring the proper extraction of data.

The reason for using two antennas is that each of them is positioned differently in the research station. This way, at least one of the antennas will capture the signal from the Scouts effectively. Additionally, if both of the antennas receive a signal with a very low signal-to-noise ratio, the output signals from both antennas are compared using comparators to determine the accurate signal.

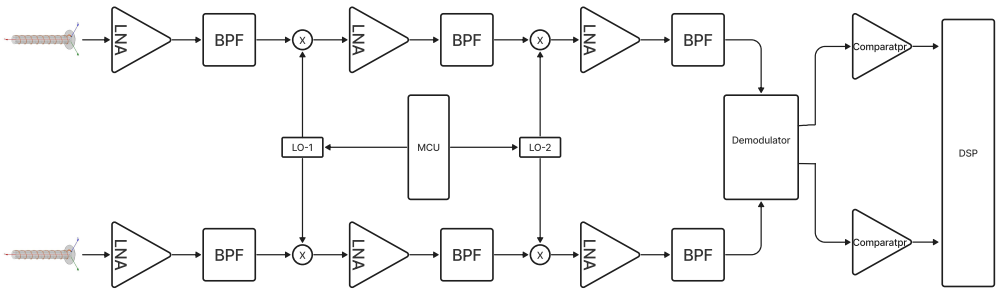

Figure 15.3: Communication Architecture in UHF Band

15.4 Atmospheric defocusing and absorption Loss

The absorption in the Venusian atmosphere is determined by the attenuation parameters linked to the dominant gases present in the atmosphere, as well as the physical properties such as pressure, temperature, density, and gaseous concentration content. Knowledge about the attenuation caused by individual gases is derived from past laboratory experiments, while empirical models of relevant atmospheric properties as functions of altitude were constructed based on observations from previous missions to Venus. Using these models, the atmospheric attenuation due to absorption can be determined as a function of altitude. After establishing the ray path between the spacecraft and a descent probe, the total absorption attenuation can be determined through integration along this path. Slight deviations from the nominal path can be employed to identify any defocusing or focusing effects.

UHF-Band Losses

To achieve a better understanding of the defocusing and absorption losses in the UHF Band, one must consider the ray path. For this purpose, two scenarios are considered. The best-case scenario(BCS) occurs when the scout is directly under the VRS. On the other hand, there is another scenario where the VRS is at the horizon of the scout, which still lies within the line of sight but at the maximum distance.

According to [159], the defocusing loss will vary with θ. For the BCS, θ, is equal to zero degrees, representing a 0.15 dB loss. On the other hand, in the WCS, θ, is equal to 90°, representing a 5 dB loss.

Despite the defocusing loss, the absorption loss varies with the frequency. Other missions have used the S-Band and X-Band for communications. In our mission, to have a good estimation

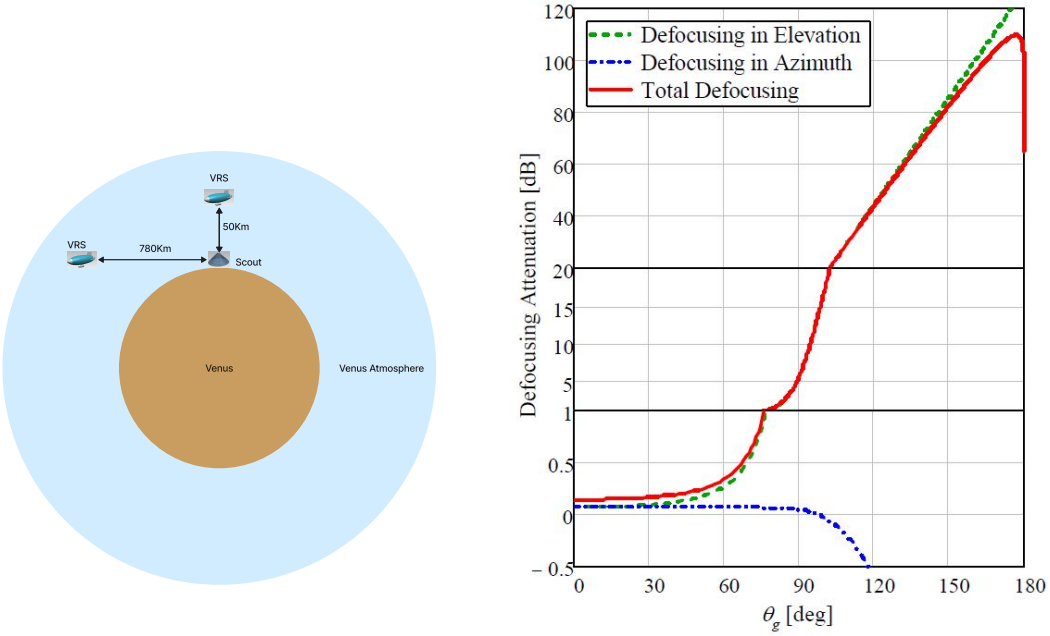

(a) Ray path for two scenarios

(b) Defocusing Loss from the [159]

Figure 15.4: Defocusing Loss in UHF Band

of the absorption loss, we plotted the relationship between the frequency and absorption loss. As expected, there is a linear relationship between the frequency and absorption loss, providing valuable insights into optimizing communication strategies for our mission. According to the results from [159] the predictable absorption loss for UHF frequency is achieved, as it is clear in Figure 15.5 the relationship between the frequency and absorption loss can be considered to be linear.

$$\text{Absorption Loss(UHF)} = 0.00452\,\text{dB/Km} \tag{15.1}$$

X- and Ka-Band Losses

Considering that defocusing loss varies with the angle of the ray path and depends on the mission's manoeuvres at each time, it can be accounted for in the link budget calculation with a value of 2 dB. This value will be adjusted autonomously for both the X- and Ka-bands, taking into account the changing conditions during the mission.

$$\text{Absorption Loss(X-Band)} = 0.00928\,\text{dB/Km} \tag{15.2}$$

$$\text{Absorption Loss(Ka-Band)} = 0.03017\,\text{dB/Km} \tag{15.3}$$

For calculating the absorption loss, an altitude of 120 km is considered as the altitude where there is no atmosphere. This assumption allows us to establish a baseline for the absorption loss at its minimum level, providing a reference point for further calculations.

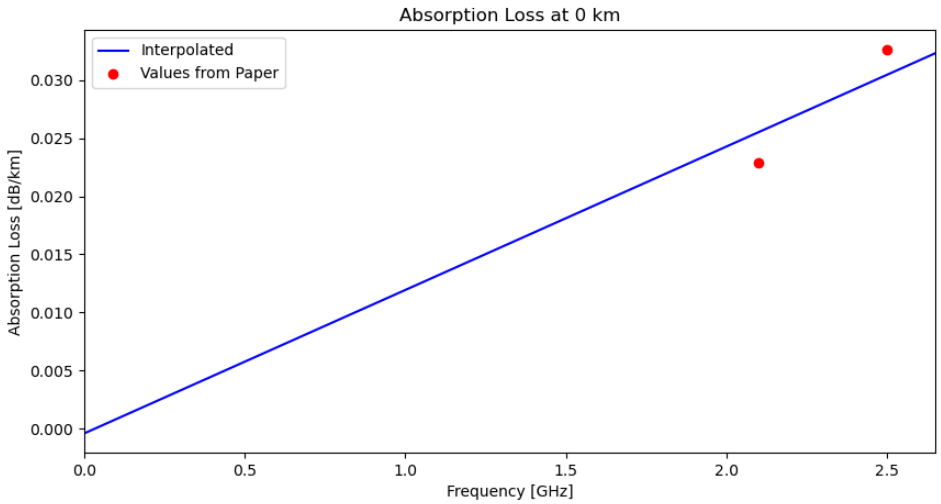

Figure 15.5: Relation between absorption loss and frequency for UHF at the altitude of $0[Km]$.[Bösch]

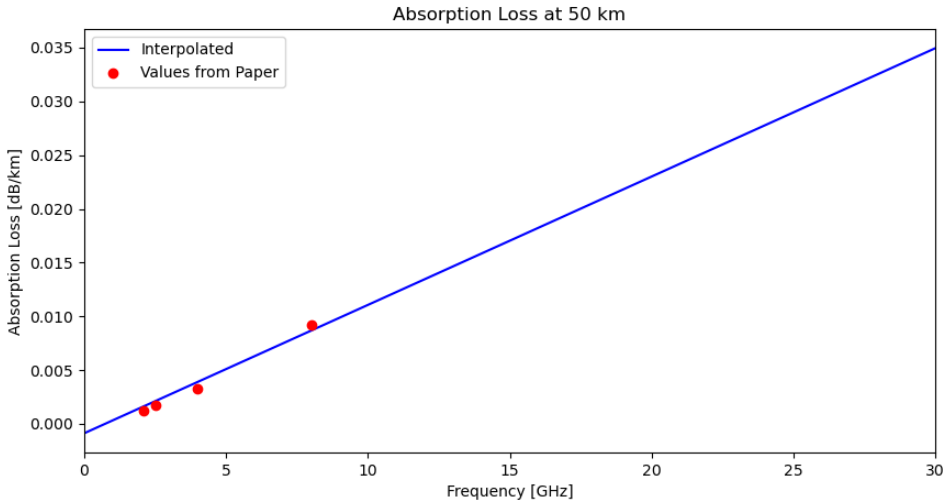

Figure 15.6: Relation between absorption loss and frequency for X- and Ka-Bands at the altitude of 50 km.[Bösch]

15.5 Link Budget

After having considered and calculated the significant losses, the link budget calculation can now be initiated. It is noticeable that the transmitting power is chosen carefully, adhering to the maximum limitation in power. GaN HEMT(Gallium Nitride-High Electron Mobility Transistor) amplifiers are being used, considering an efficiency of 60%.The maximum power output can vary with factors such as distance, data rate, and power consumption, for example, in a save power mode, autonomously. This adaptive approach allows the communication system to efficiently utilize resources and adapt to varying requirements during the mission while adhering to specified limitations and operational conditions.

UHF-Band

The preceding section covered the consideration of absorption and focusing losses. Now, in the free space path loss calculation, both the best and worst-case scenarios will be taken into account.

$$\text{FSPL[dB]} = 92.4 + 20\log f\,\text{GHz} + 20\log d\,\text{Km} \tag{15.4}$$

$$\text{BCS-FSPL[dB]} = 92.4 + 20\log 0.4 + 20\log 50 = 118.4306\ \text{dB} \tag{15.5}$$

$$\text{WCS-FSPL[dB]} = 92.4 + 20\log 0.4 + 20\log 780 = 142.2931\ \text{dB} \tag{15.6}$$

	Worst Case Scenario	**Best Case Scenario**
Absorption Loss [dB]	3.5256	0.226
Defocusing Loss [dB]	5	0.15
FSPL [dB]	142.2931	118.4306
System Noise Temperature [K]	200	200
Antenna Gain of VRS [dBi]	15	15
Antenna Gain of Scout [dBi]	6	6
Transmitter Power [dB]	16.5	-3
N0 [dB]	-205.59	-205.59
S/N0 [dB]	92.2716	104.7834
BER	10e-4	10e-4
SNR(BPSK) [dB]	7	7
Data Transmission Rate[kB/S]	13	54
Margin [dB]	44.13	50.46

Table 15.1: The link budget of the UHF-Band in VRS encompasses all losses in both the Best Case Scenario (BCS) and Worst Case Scenario (WCS)

X- and Ka-Bands

In the earlier section, we discussed the analysis of absorption and focusing losses. Now, during the calculation of free space path loss, we will include both the X- and Ka-Bands in our considerations.

$$\text{FSPL[dB]} = 92.4 + 20\log f[\text{GHz}] + 20\log d[\text{Km}] \tag{15.7}$$

$$\text{X-Band-FSPL[dB]} = 92.4 + 20\log 8 \ + 20\log 2000 \ = 176.492 \text{ dB} \tag{15.8}$$

$$\text{Ka-Band-FSPL[dB]} = 92.4 + 20\log 26 \ + 20\log 2000 \ = 186.73 \text{ dB} \tag{15.9}$$

Taking into account the maximum allowable mass for the antennas, it has been decided to utilize reflector antennas with a diameter of 2 meters for both the X-Band and Ka-Band high gain antennas. Additionally, the Relay Satellite antenna will boast a diameter of 3 meters. The reflector antenna gain can be calculated using the following equation. It is assumed that the efficiency of all the antennas (η) is 0.55.

$$\text{Aeff} = \eta\,(\pi\left(\frac{D^2}{4}\right)) \tag{15.10}$$

$$\text{Gain} = Aeff(\left(\frac{4\pi}{\lambda^2}\right)) \tag{15.11}$$

With the VRS having a 2-meter antenna and the Relay Satellites featuring a 3-meter antenna, for the antenna with a 2-meter diameter in the X-Band, the gain can be calculated using the efficiency (η) of 0.55 and the appropriate formula for antenna gain calculation.

$$\text{Aeff(X-Band)} = \eta\,(\pi\left(\frac{2^2}{4}\right)) = 1.7274[\text{m}^2] \tag{15.12}$$

$$\text{Gain(X-Band)} = 1.7274(\left(\frac{4\pi}{\lambda^2}\right)) = 15505 \tag{15.13}$$

$$\text{Gain[dB]} = 10\log(15505) = 42[\text{dBi}] \tag{15.14}$$

Now for the antenna with a 3-meter diameter:

$$\text{Aeff(X-Band)} = \eta\,(\pi\left(\frac{3^2}{4}\right)) = 3.8877[\text{m}^2] \tag{15.15}$$

$$\text{Gain(X-Band)} = 3.8877(\left(\frac{4\pi}{\lambda^2}\right)) = 3.4741e+04 \tag{15.16}$$

$$\text{Gain[dB]} = 10\log(3.4741e+04) = 45[\text{dBi}] \tag{15.17}$$

For the 2-meter diameter antenna in the Ka-Band, considering a frequency of 26 GHz:

$$\text{Aeff(Ka-Band)} = \eta(\pi\left(\frac{2^2}{4}\right)) = 1.7274[\text{m}^2] \tag{15.18}$$

$$\text{Gain(Ka-Band)} = 1.7274(\left(\frac{4\pi}{\lambda^2}\right)) = 1.6309e+05 \tag{15.19}$$

$$\text{Gain[dB]} = 10\log(1.6309e+05) = 52\text{[dBi]} \tag{15.20}$$

And for the antenna with a 3-meter diameter:

$$\text{Aeff(Ka-Band)} = \eta(\pi\left(\frac{3^2}{4}\right)) = 3.8877[\text{m}^2] \tag{15.21}$$

$$\text{Gain(Ka-Band)} = 3.8877(\left(\frac{4\pi}{\lambda^2}\right)) = 3.6695e+05 \tag{15.22}$$

$$\text{Gain[dB]} = 10\log(3.6695e+05) = 56\text{[dBi]} \tag{15.23}$$

	X-Band	Ka-Band
Absorption Loss [dB]	0.6496	2.1112
Defocusing Loss [dB]	2	2
FSPL [dB]	176.492	186.73
System Noise Temperature [K]	100	110
Antenna Gain of VRS [dBi]	42	52
Antenna Gain of RS [dBi]	46	56
Transmitter Power [dBW]	18	23
N0 [dBW]	-208.6	-208.18
S/N0 [dB]	135.45	148.34
BER	10e-4	10e-4
SNR(BPSK) [dB]	7	7
Data Transmission Rate [kB/S]	1800	8000
Margin [dB]	65.9	72.3

Table 15.2: The link budget in both X- and Ka-Bands of the VRS comprehensively considers all losses involved. RS = Relay Satellites

As per the information presented in Tables 15.1 and 15.2, the achievable data transmission rates are as follows: 54 kbits/s for the UHF Band, 1.8 Mbits/s for the X-Band, and 8 Mbits/s for Ka-Band.

15.6 Conclusion

In conclusion, effective communication in the Venus exploration mission poses significant challenges due to atmospheric absorption and defocusing loss. However, employing 14 Relay Satellites can overcome these limitations and ensure reliable data exchange between the Scouts, Research Station, and Relay Satellites.

While Free Space Optical Communication (FSOC) shows promise with its high data rates and compactness, the atmospheric conditions on Venus, including cloud cover, high wind speed, sun intensity, and turbulence, make optical communication impractical at this stage.

As the mission progresses and technology advances, it is essential to keep an eye on future developments that may address these atmospheric challenges and open up new possibilities for optical communication in Venus exploration.

The Chapter has shed light on the complexities and potential solutions for establishing robust communication systems for this extraordinary mission. By considering various communication methods and understanding the unique conditions of Venus, we can work towards enhancing data transmission capabilities and achieving success in this ambitious venture.

CHAPTER 16

Simulation

by Carolin Bösch and Matthais Finzel

In this Chapter the simulation of the Venus Research Station (VRS) is presented. The simulation is based on research carried out in the previous chapters of this report. It is a Python based program, which allows the direct plotting of the results. First the general structure of the simulation is introduced. This is followed by the simulation of the atmosphere, which is based on the National Aeronautics and Space Administration (NASA) software Venus Global Reference Atmospheric Model (Venus-GRAM) [1]. Subsequently, the individual modules of the simulation are presented and their results for the developed concept. These include propulsion and position of the VRS, power and communication and data handling.

16.1 General Structure

The code for the simulation was written in a modular manner. This principle is beneficial, as it improves flexibility, maintainability, and efficiency. It promotes better organization and structure, as each module encapsulates a specific functionality, which reduces the complexity of the system. Changes can be made to one module without affecting the others, enhancing system stability. Modules can be reused across different parts of the application, which saves development time and computing resources. Furthermore, modular software enables parallel development for the simulation team. Two major simulation modes were implemented that calculate most of the overall results, as well as several minor simulation modes intended to be used for in-detail calculations of different scenarios.

Time Step Manager

The Time Step Manager is the core of the simulation. It is implemented inside the main file, where it can interact with the software blocks. Its primary role involves invoking the update functions of these interconnected blocks. Before the time step manager begins operation, the total number of time steps is determined based on the total mission time and the time interval of one time step. During each time step, the update functions are called, which then perform the calculations for updating the simulation model. The results of these calculations are stored in arrays and in text files at each time step. Following the completion of all time steps, the Time Step Manager is exited and the results are plotted for visual representation and analysis. The sequence of software blocks accessed by the Time Step Manager follows a specific order, as there are certain dependencies between those software blocks, starting with 'Atmosphere', followed by 'Position', 'Venus Body', and finally, 'Power'.

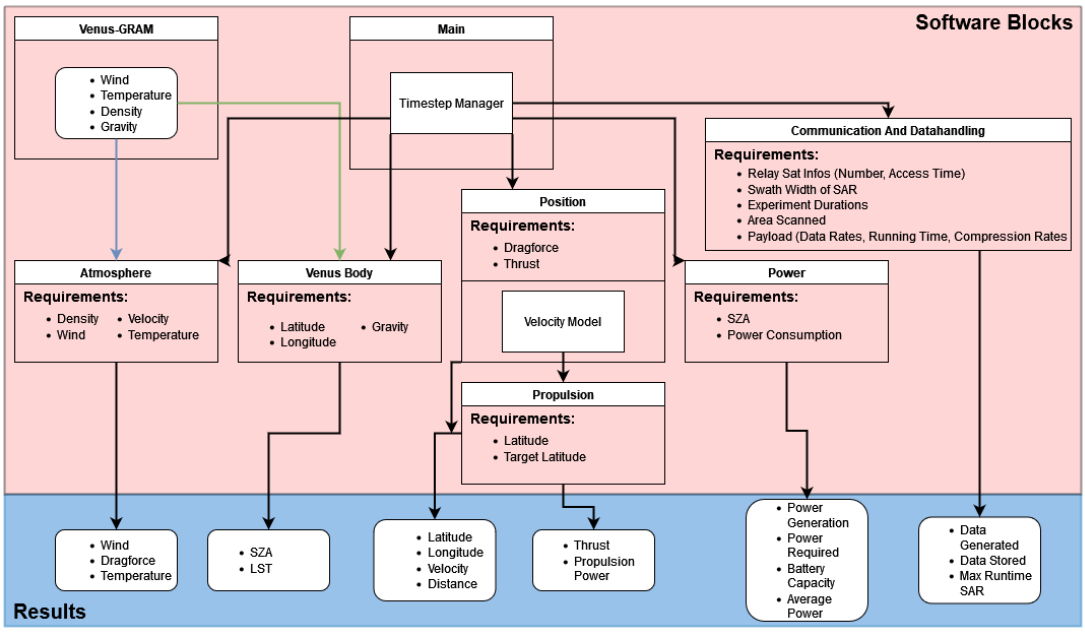

Figure 16.1: The Simulation consists of several Software Blocks working together. The Software Blocks exchange data that is required for the calculations of the Simulation. The outputs are saved in arrays as well as in a text file, to be plotted later.

Software Blocks

The Atmosphere software block calculates the drag force, and reads out the current wind speed, atmospheric density and temperature for a given latitude and altitude. It requires the velocity of the VRS as data input. The Venus Body software block calculates the solar zenith angle and local solar time. These computations require inputs of latitude and longitude. This block is used to determine how the position of the sun relative to the station affects light exposure and thus, energy generation. The Propulsion software block calculates the thrust and required propulsion power. This requires the current latitude, the target latitude of the VRS and the drag force acting on the VRS. The drag force helps determine how much thrust power is needed to reach or maintain a desired position. This module is essential for maintaining and changing the station's course as necessary. The Position software block calculates the latitude, longitude, velocity of the VRS, and the travelled distance. This block requires inputs on the drag force and thrust of the propulsion system. This aids in tracking the current position and speed of the VRS, which could be vital for course corrections, and calculating the distance travelled, important for tracking progress. The Power software block calculates power generation, power required, battery capacity, and average power. This block requires the solar zenith angle to calculate potential solar power generation and the power consumption of the modules on the VRS to calculate the power demand. This information allows for effective power management and planning, ensuring the station has enough energy to operate effectively. Finally, the Communication and Data Handling block, calculates the data generated and transmitted for the overall mission, as well as the data budget including data generation, storage and transmission for certain circumnavigations. This block requires details about each sensor and payload that generates data, compression and filter factors, and information about the communication architecture, e.g.

number of Relay Satellites and transmission rates. This block helps to ensure that all compressed generated data sent to the Relay Satellites without occupying more storage than available. The results calculated by the software blocks are saved in arrays and plotted immediately after the end of the simulation calculations. The results are also saved in text files so that the plots can be configured and replotted or new plots can be generated without having to re-run the whole simulation.

Simulation Modes

The first major mode is the average calculation mode, used to provide mean values which are required as the basis of calculations by the system's work packages. In this mode, the VRS starts at the latitude $\Phi = +50°$ and performs a circumnavigation around Venus at the respective westbound wind speed of the current latitude provided by the atmospheric model. After completion, the VRS is instantly moved to the next lower latitude by one degree. For each latitude, average calculations for power generation, power balance, thrust and velocity. Once the Station reaches $\Phi = -50°$, the simulation ends and the results and plots are generated. The second Simulation mode is for performing a full simulation of the mission scenario with a minimum mission time of 5 years. The initial position of the VRS is at the equator and longitude $\lambda + 0°$ at noon local time. From there, the VRS will again perform full circumnavigations at each latitude to mimic the SAR scanning operation, with the exception that the latitudes will be provided as target values that the VRS will have to reach using its propulsion system.

16.2 Atmosphere

The NASA Software Venus-GRAM 2005 [1] is used as the database for the simulation of the atmosphere. Access to the NASA Software can be requested under [2]. The results of the software are output as text files which can be loaded and used in the simulation. Venus-GRAM takes an input trajectory and an input date and simulates for the different points within the atmosphere at that point in time the following parameters based on atmospheric data files from Kliore et al. [160]:

- Radial distance [km], planetary centre of mass to spacecraft position (planet radius plus height),
- Local planetary radius [km],
- Local acceleration of gravity [m/s^2],
- Density [kg/m^3], including low, average, and high density values,
- Temperature [K], also including low, average (also available in [°C]) and high temperatures,
- Wind speed [m/s], in east and north direction, including mean wind speeds, perturbations and total wind speeds (mean + perturbed),
- Mean pressure [N/m^2] and [mb],
- and others.

For the mission's purposes the points to simulate the atmosphere were chosen to be at altitudes h from 45 to 55 km with a step size of 1 km and latitudes Φ from -90 to $+90°$ with a step size of 5°. Since the longitude λ has no influence on the results of Venus-GRAM and in

order to limit the size of the database, the points were only chosen at $\lambda = 0°$. This leads to a total of 407 entries for the database of Venus‘ atmosphere. The input date only has an influence on solar parameters, such as solar zenith angle, or planetocentric longitude of the sun. These are either not needed for this simulation or are self-computed. Therefore, 1st January 2035 was randomly chosen as the input date.

Temperature In order to be able to reliably calculate the thermal requirements for the VRS, Venus-GRAM was used to gather and calculate temperature information dependent on latitude and altitude. Consequently, the minimum and maximum temperature values were extracted from the dataset and the mean temperature over all latitudes and altitudes were calculated. Additionally, the temperature at the current altitude and latitude was plotted during the run of the full simulation mode. The temperature range over the different altitudes can be seen in Figure 16.2. At an altitude of 45 km the maximum temperature was 385.4 K, the minimum temperature was 380.4 K, thus the temperature range was only 5 K. The average temperature was 384.5 K, indicating that the VRS spent most time in the upper temperature ranges. At 50 km altitude, the maximum and minimum temperatures were 350.5 K and 347.4 K respectively. Thus, having an even smaller temperature range of 3.1 K. The average temperature was 350.2 K. Finally, at an altitude of 55 km the recorded temperature was the lowest with a maximum value of 302.3 K, a minimum temperature of 299.1 K and thus a temperature range of 3.2 K. The average temperature was 302 K.

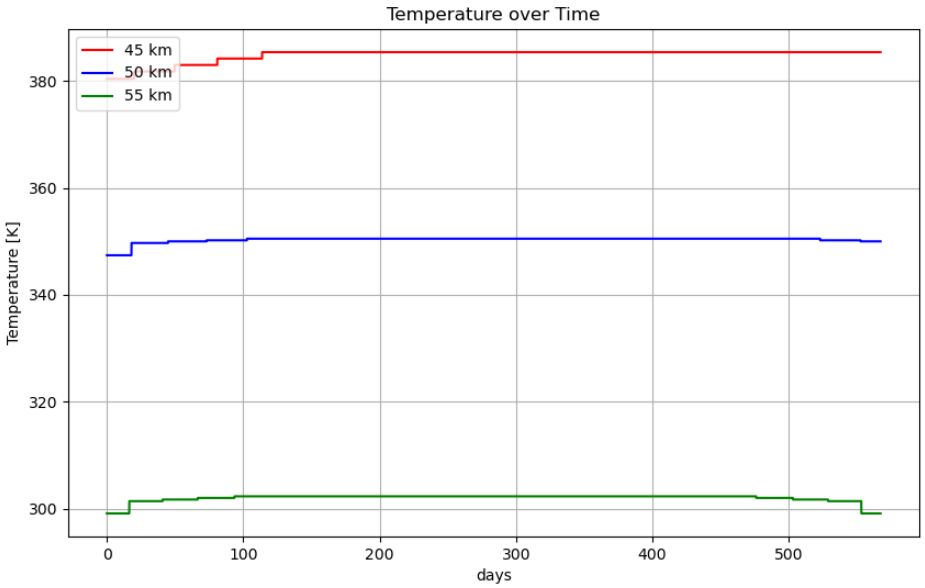

Figure 16.2: The recorded temperature over time during the average calculations. Three altitudes were considered for temperature comparison. At higher altitudes, the temperature decreases. The temperature range also decreases at higher altitudes.

Drag Force The wind induced drag force that acts on the VRS is calculated separately for the north and the east component by using the basic drag equation[161].

$$F_{Drag} = c_D \cdot \frac{\rho \cdot v_{diff}^2}{2} \cdot A \tag{16.1}$$

Where v_{diff} is the difference between the current velocity component of the station and the respective component of the wind speed. c_D is the drag coefficient estimated by Section 9.1, ρ is the atmospheric density at the current latitude and altitude of the VRS and A is the reference area. It is assumed that the VRS always points toward the north-south component of the wind, as this is the only drag component that it needs to compensate during station keeping. Thus, the area for the calculation of the north-south component of the drag force $F_{Drag,N}$ is reduced to a circle and the area for the east-west drag force component $F_{Drag,E}$ has the shape of the ellipse projected by the side of the balloon of the VRS.

16.3 Propulsion and Position of VRS

In order to calculate the acceleration of the VRS, the drag force is equated with Newton's Second Law.

$$F_{VRS} = m_{VRS} \cdot a = c_D \cdot \frac{\rho \cdot v_{diff}^2}{2} \cdot A = F_{Drag} \tag{16.2}$$

The acceleration is integrated over the time to get the resulting change in velocity Δv of the VRS. For this purpose, the time step needs to be chosen as small as possible such that the Δv is not overestimated. Decreasing the default time step of 10 minutes to a necessary interval of one second would increase the total number of time steps by a factor of 600 and thus, greatly increase the simulation time. Instead, the velocity model was introduced that only iterates through the calculations that are relevant for the propulsion and velocity calculations with a time resolution of one second. The change of velocity is summed up during each velocity model iteration to get the current velocity of the VRS. The distance travelled is then the sum of all velocities over the course of one time step. Due to the small step sizes and consequently small distances, it is assumed that the travelled distance is equal to the angular distance travelled over the surface of Venus. The angular distance δ is the first information that is necessary for the calculation of the position of the VRS. The second information is the heading θ, which is calculated using the arc tangent of the north and east components of the velocity. By setting an initial Position at the beginning of the simulation, every successive position on the surface of Venus can now be calculated using the following formulas[162]:

$$\phi_2 = \arcsin\left(\sin\left(\phi_1\right) \cdot \cos\left(\delta\right) + \cos\left(\phi_1\right) \cdot \sin\left(\delta\right) \cdot \cos\left(\theta\right)\right), \tag{16.3}$$

$$\lambda_2 = \lambda_1 + \arctan\left(\frac{\sin\theta \cdot \sin\delta \cdot \cos\phi_1}{\cos\delta - \sin\phi_1 \cdot \sin\phi_2}\right). \tag{16.4}$$

A simple P-controller was implemented to control the thrust of the propulsion system and thus perform station keeping. A target latitude is set, and the latitude error is converted to an angular distance before being multiplied with the proportional constant of the controller. The result is used as the thrust value for the propulsion system, while also being used to estimate the power demand of the system. A P-controller is a very simple and non-ideal controller for most applications, but in this case, the maximum possible thrust is relatively low compared to the large distance errors and the time resolution is high enough so that the system does not oscillate. Furthermore, the error is never zero and usually it converges towards 2 km where there is an equilibrium between the calculated thrust and the drag force. This behaviour is typical for a simple p-controller. This value is acceptable considering that one degree of latitude

difference on Venus translates to roughly 105 km distance, which results in a relative error of under 2%. Finally, as the wind acts as a constant force on the VRS, there would be no benefit of eliminating the error in terms of power consumption of the propulsion system. Figure A.6 shows a typical thrust curve during the full simulation mode. It can be compared to the latitude trajectory in Figure A.7 to study the behaviour of the station keeping function. Negative thrust means that the thrust vector is pointing south, while positive thrust values indicate that the thrust vector is pointing north. Thus, when moving towards the South Pole, the propulsion system utilizes maximum negative thrust to quickly reach the target latitude while also having a smaller positive thrust force that compensates the wind once the target latitude is reached. Vice versa, if the VRS is moving north the maximum thrust is positive with smaller, latitude dependent negative thrusts to compensate the wind. Figure A.8 shows a typical velocity curve during full simulation mode. The velocity curve shows in which direction the VRS is moving during operation. The average speed over all latitudes and altitudes is a necessary information for the data handling part of the simulation. After each circumnavigation, the mean of the total velocity of the VRS for the given latitude was calculated and saved into an output file. This process was repeated over the three altitudes 45 km, 50 km and 55 km. Finally, by calculating the average of all mean total velocities of all three output files, the complete average speed was estimated to be $61.5 m/s$.

16.4 Power

The equations for calculating the generated power were provided by Section 12.5. The equation for calculating the effective area requires the solar zenith angle SZA to determine the projected surface area that is illuminated by the sun. The general formula[163] for the calculation of the SZA is

$$SZA = \arcsin\left(\sin\left(\phi\right) \cdot \sin\left(\gamma\right) + \cos\left(\phi\right) \cdot \cos\left(\gamma\right) \cdot \cos\left(LST\right)\right) \tag{16.5}$$

with γ being the declination and LST the Local Solar Time. The axial tilt of Venus is relatively low with only 2.64° thus it is neglected in further calculations. This simplifies the above equation, as the sine term becomes zero and the cosine of γ equals one. The LST is calculated by taking the current angular position H of the sun vector and subtracting the longitude of the VRS. The angular position relative to the prime meridian is set to zero initially and then from there on the position is updated iteratively with the following formula.

$$H = \sum_{i=0}^{T} \left(2 \cdot \frac{\pi}{d_{venus}} \cdot T_{res}\right) \tag{16.6}$$

Where T is the current time in the simulation, d_{venus} is the duration of one synodic rotation period, which is 116.75 days[164]. T_{res} is the time step of the simulation. The capacity of the battery is calculated in each time step by calculating the power balance, which is the difference between the generated power and the total power demand of the VRS. The power demand is the sum of all module power requirements and dependent during a mission phase. The power balance is then multiplied with the time step and divided by one hour in seconds to yield the energy difference during one time step. The energy is added to the current battery capacity, which charges or discharges it depending on the sign of the power balance. The average generated power per latitude is calculated at the end of each circumnavigation. The results are stored in a text file and at the end of the simulation they are plotted. Figure A.9 shows how the required power changes over time during the full simulation mode. Once the mission phase SO1 is completed, the SAR module will switch to low-power mode, which results in a drop of

the total required power visible in the figure just after 250 days of operation. Another small drop can be observed after 4 years of operation, where the other instruments for measuring the Venus weather are switched off after the completion of mission phase SO2. This graph shows that while the changing power demands over time due to the changing mission phases are still noticeable, the major part of the power requirement still comes from the propulsion system with a maximum power requirement of 16.5 kW.

16.5 Communication and Data Handling

This part of the simulation serves to first give an overview of all data generators. Subsequently, the communication with the Scouts is simulated and analysed. In addition, it is determined how long the SAR has to operate for this mission. Furthermore, the required number of Relay Satellites is determined based on the necessary and possible data transmission rate. Then the data generation, data transmission and storage capacity for two circumnavigations are examined. Based on this, the total mission data budget is verified.

In addition, linear interpolations of values for estimating the absorption loss were carried out by the simulation. Figure 15.5 and Figure 15.6 show the results in Chapter 15.

Data Generators

Figure 16.3 and 16.4 give an overview of the data generation. The generated data over one circumnavigation was calculated to compare the individual subsystems and components. The max. duration of one circumnavigation of 176.0 h, refer to Chapter 9, is used for all following calculations and storage considerations. The total generated data is the data rate times the operating time per circumnavigation, whereas the compressed generated data also takes the compression factor into account. Only exception for the calculation of the compressed generated data is the SAR instrument, which is additionally filtered. The compression factor for all instruments including payload and Scouts is 0.5. The SAR filter factor is also 0.5. All values, including data rates, operating times per circumnavigation, compression and filter factors, etc., are from Chapter 14.

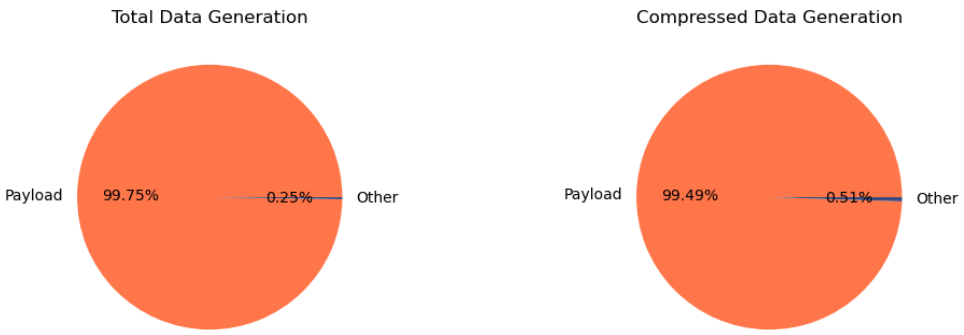

Figure 16.3: Data generators overview - Comparison Total and Compressed. Total (left) vs. compressed (right) data generation by subsystem (with Other including GNC, Thermal, Propulsion, Power and Scouts).

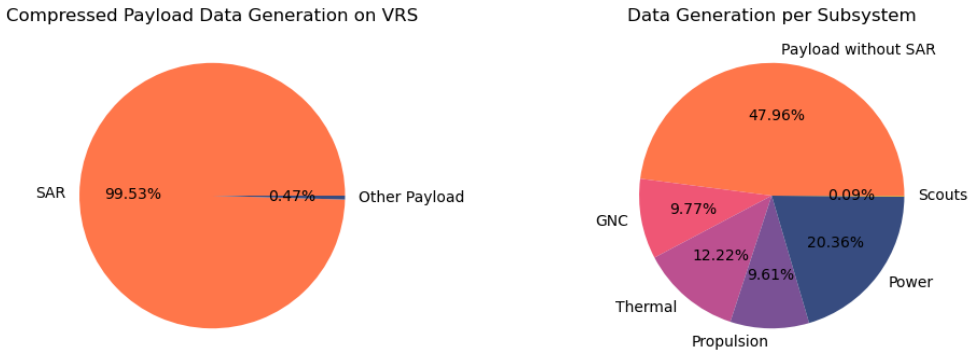

Figure 16.4: Data generators overview - Payload and Subsystem without SAR. Left: closer look at compressed payload data generation. Right: data generation (total and compressed) by subsystem without SAR.

Figure 16.3 shows that the payload onboard the VRS generates the most data before and after filtering and compressing all data. A closer look into the payload subsystem, refer to Figure 16.3, (not considering payload on Scouts) reveals that the SAR is the biggest data generator by far. Considering the subsystems without the SAR, each sensor and instrument is compressed by 50 %. This results in the same percentages of the subsystems for total and compressed.

Communication with Scouts

The following assumptions were made for the simulation of the Scouts' communication with the VRS. The Scout can only generate data from an altitude of about 76.0 km. This results in about 2.783 h of data generation which is rounded up to 3 h of data generation for a maximum value. The Scouts have a data rate of 10.0 kbits/s in the worst case transmission scenario and 37.0 kbits/s in the best case. The Scout transmits as soon as it is below the VRS and survives a maximum of one hour on the ground. For a minimum transmission time, transmission starts at 40 km altitude and the Scout immediately stops transmitting as soon as it hits the ground. This leads to a minimum transmission time of 2.2 h rounded off. In contrast, for maximum transmission time, the Scout transmits from an altitude of 50 km and survives one hour on the ground. With a fall time of 2.4 h, this results in a transmission time of 3.4 h. All values regarding transmission rates are from Chapter 15 and regarding duration of the fall of the Scouts are from Section 9.2. Figure 16.5 illustrates the data transmission from the Scouts to the VRS. The max. data generated on the Scouts amounts to approximately 135 Mbits and the average data generated to 125 Mbits.

As can be seen from Figure 16.5 in the vast majority of cases the entire amount of data is transferred. Only in the worst cases that need to be avoided, where the VRS sees the Scouts permanently on the horizon, is it not possible to transmit the complete amount of data.

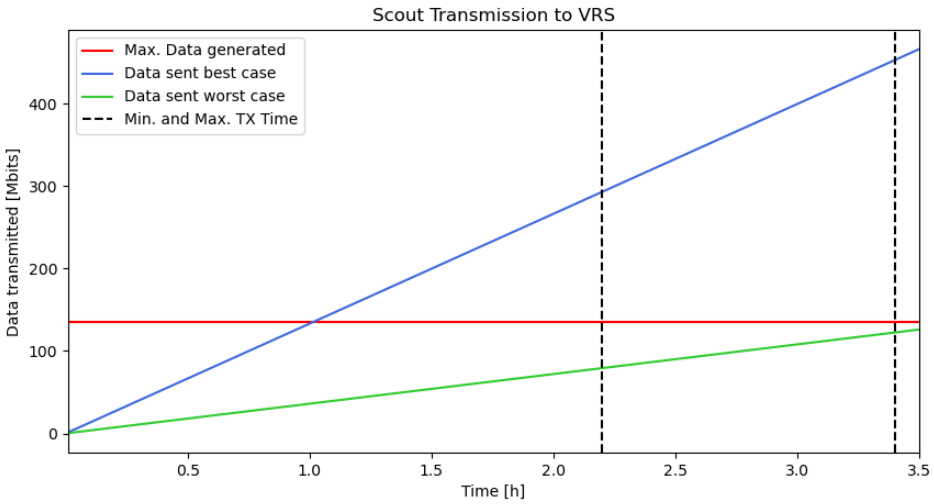

Figure 16.5: Communication with Scouts simulation. The worst and best case scenarios for transmission of the data are plotted against time of transmission. Maximum data generated is displayed.

Data Budget

Before the mission data budget can be analysed, the required runtime of the SAR has to be determined first. Figure 16.6 shows the minimum required runtime of the SAR to map a desired area. For these calculations, the rotation and the curvature of Venus were neglected. With a single look approach, a swath width of about 100 km and an average ground speed of 61.5 m/s,

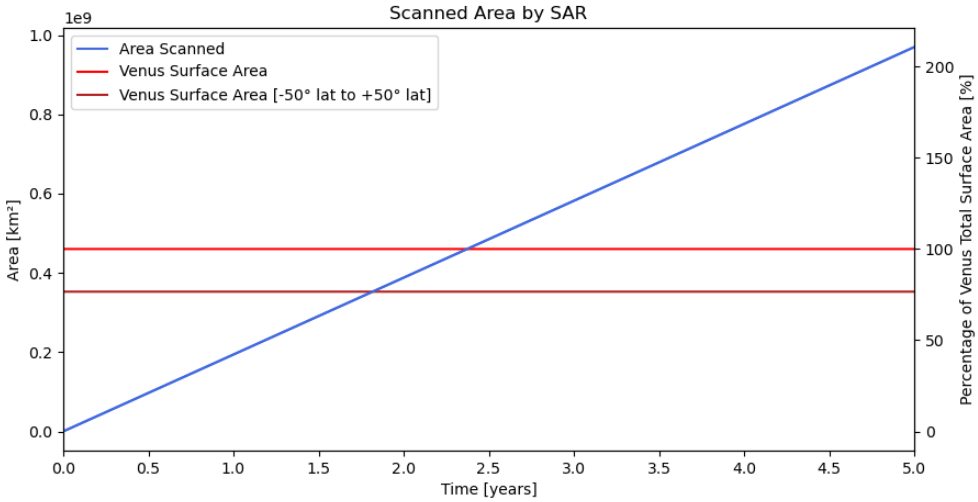

Figure 16.6: Simulation of necessary runtime of SAR. Area scanned plotted against time including the area of Venus total surface area and the area between $\Phi = -50°$ to $+50°$.

this results in an area coverage of the SAR of 6.15 km^2/s. To map Venus globally the SAR would need to operate for roughly 2.5 years. Since this concept is restricted to Φ from $-50°$ to $+50°$, it needs at least 1.85 years.

Based on the concept that the SAR operates one circumnavigation (Mode: SO1) and then the other instruments operate for a second circumnavigation (Mode: SO2), the number of Relay Satellites required to transmit all the data generated in these two circumnavigations is determined. Figure 16.7 shows the required data rate depending on the number of Relay Satellites in the same orbit.

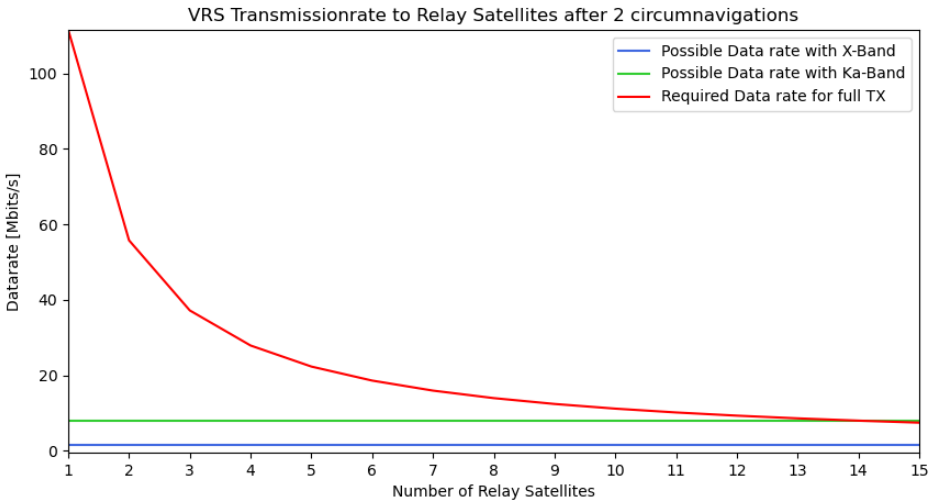

Figure 16.7: Necessary transmission rate depending on the number of Relay Satellites. Possible data rates using X- or Ka-Band are displayed.

The necessary data rate for transmission with 14 Relay Satellites to send all data that is generated in these two circumnavigations in the same time period is 7.44 Mbits/s, which is achieved with the actual transmission rate of 8.0 Mbits/s using the Ka-Band. Therefore the number of Relay Satellites is set to 14. Figure 16.8 displays the resulting data budget including storage over the two circumnavigations using 14 Relay Satellites. This results in a maximum memory utilization of approximately 3950 Gbits, which corresponds to 25 % of the possible memory capacity. If the SAR was running continuously for two years then the necessary storage would be approximately 231.92 Tbits, which is much higher than possible storage of 16 Tbits. Table 16.1 lists all the results of the simulation after the individual circumnavigations, as well as the overall results after both.

Circumnavigation	**1 (SO1)**	**2 (SO2)**	**Together**
Total Data Generated [Gbits]	31772.97	93.02	31865.99
Compr. Data Generated [Gbits]	7960.88	46.51	8007.39
Data stored [Gbits]	3943.19	0.0	0.0

Table 16.1: Results simulation data budget after two circumnavigations. First circumnavigation includes collecting the data of 2 Scouts (worst case). Transmitted data per circumnavigation: 4017.69 Gbits and total: 8035.38 Gbits.

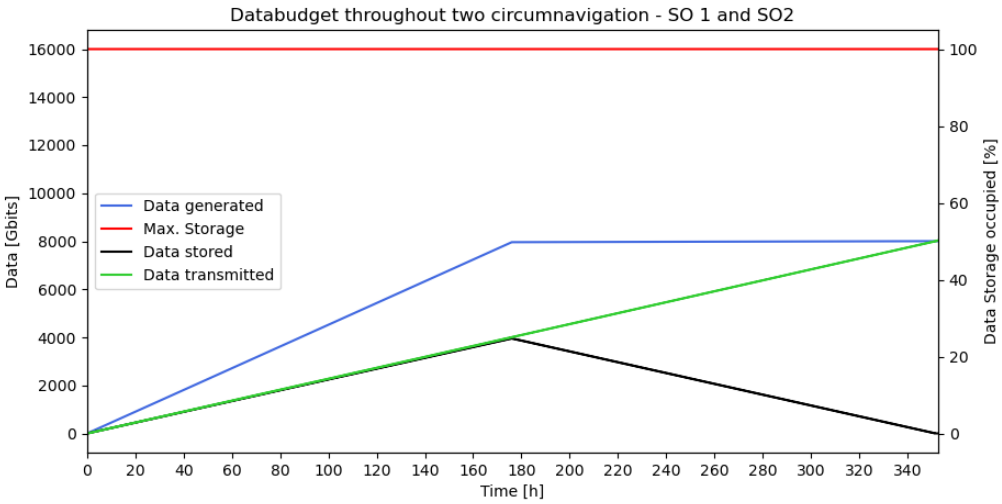

Figure 16.8: Data budget over two circumnavigations. First circumnavigation (176 h) SO1 Mode (SAR) and second circumnavigation SO2 Mode (all other instruments). Display of max. storage, data generated, data transmitted and data stored over the time period of 352 h.

Based on the number of Relay Satellites the max. possible SAR runtime $t_{SAR,max}$ is calculated as follows using the max. amount of data that can be transmitted $D_{TX,max}$, the amount of data generated without the SAR D_0, the SAR data rate R_{SAR}, the payload compression factor of 0.5 and the SAR filter factor of 0.5.

$$t_{SAR,max} = \frac{D_{TX,max} - D_0}{R_{SAR} \cdot 0.5^2} = \frac{(999857254.998\,\text{Mbits} - 7762710.570\,\text{Mbits})}{50\,\text{Mbits/s} \cdot 0.5^2} \approx 2.51\,\text{years} \tag{16.7}$$

This results in the SAR obtaining a runtime of two years to map Venus. Within two years the SAR maps an area of 387892800.0 km^2, which is roughly 85 % of Venus total surface area and 110 % of the area between $-50°$ to $+50°$ latitude.

According to the mission scenario, refer to Chapter 5, not only the SAR will run for two years during the entire five-year mission, but also the other instruments will run for two years in total. The only exception is the experiment for the search for life in Venus‘ atmosphere, which will run in the last year of the mission. Figure 16.9 displays the amount of compressed data that will be generated during the entire mission. The data from the Scouts is considered an offset, as they can be transferred to the VRS randomly during the entire mission. The necessary data rate for transmission over the whole mission without considering storage capacity is 6.41 Mbits/s.

The results of the simulation show that with this concept it is possible to transmit all data from the VRS to the Relay Satellites. The theoretical maximum amount of data that can be transmitted is significantly higher than the amount of data generated over the entire mission. Further simulations in Section 17.3 will vary parameters in order to gain further insights into the theoretically possible data budget over the entire mission and the effects on storage.

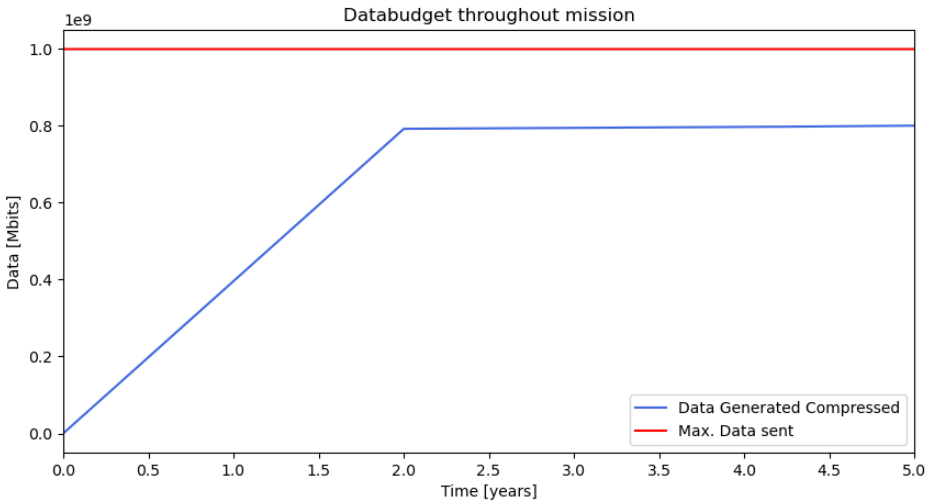

Figure 16.9: Simulation of mission data budget. Operation times: SAR for two years (0-2), all other instruments for two years (2-4) and the experiment for search for life in Venus‘ atmosphere for one year (4-5). Max. possible data amount that can be transmitted during the overall mission is displayed.

CHAPTER 17

Sensitivity Analysis

by Carolin Bösch and Matthais Finzel

In this Chapter a sensitivity analysis is carried out in which the simulation, presented in Chapter 16 yields further results. For this purpose, parameters with a very large influence are varied and the new results analysed.

17.1 Propulsion System

The results of the average thrust simulation showed that operation at an altitude of 45 km is not feasible. The required thrust exceeds that of the chosen propulsion system, with peak average required thrust being slightly above 2000 N. As a result, the VRS was not able to hold its latitude beyond 35° and consequently lost control. For this reason, operating the VRS at an altitude of 45 km was not considered to be unfeasible. With increasing altitude, the average thrust required for station keeping decreases as the atmospheric density decreases. At 50 km altitude, the average required thrust had a peak of 1468 N at 42° latitude. This is well within the range of the capabilities of the propulsion system and provides sufficient additional thrust for changing the latitude of the VRS. The lowest amount of thrust is required at an altitude of 55 km with a peak of 1010 N. The comparison between the required average amount of thrust depending on latitude for different altitudes can be found in Figure 17.1.

17.2 Power System

At 45 km altitude, the solar efficiency is at 6.94 %. The resulting power balance is not sufficient to allow continuous operation at all latitudes at this altitude. Beyond latitudes of ±21° latitude, the power balance is negative (see Figure 17.2), which also leads to rapid depletion of the batteries. Only inside that latitude range, the battery can be fully charged without reaching critical levels during nighttime (see Figure A.10). The efficiency of the solar generation rises rapidly from 9.79 % at 50 km altitude to 15.47 % at 55 km altitude, refer to Chapter 12. Both simulation modes showed that the batteries will be depleted at latitudes beyond ±26° if the VRS operates at 50 km altitude. This is avoided if the VRS flies at altitudes above 52 km. Thus, to avoid critical power levels, the VRS should operate at higher altitudes or should only operate at latitudes where sufficient power generation can be guaranteed. As a compromise, the VRS could rise to higher altitudes if it reaches regions where the power generation becomes critically low and descend to lower altitudes in safer regions. As a safety margin,the battery capacity was chosen to be 2 MWh, which resulted in a total battery mass of 6667 kg and a total vehicle mass of 14832 kg. Bigger capacities for the batteries could in theory overcome the problem of battery depletion during the nighttimes at high latitudes and low altitudes.

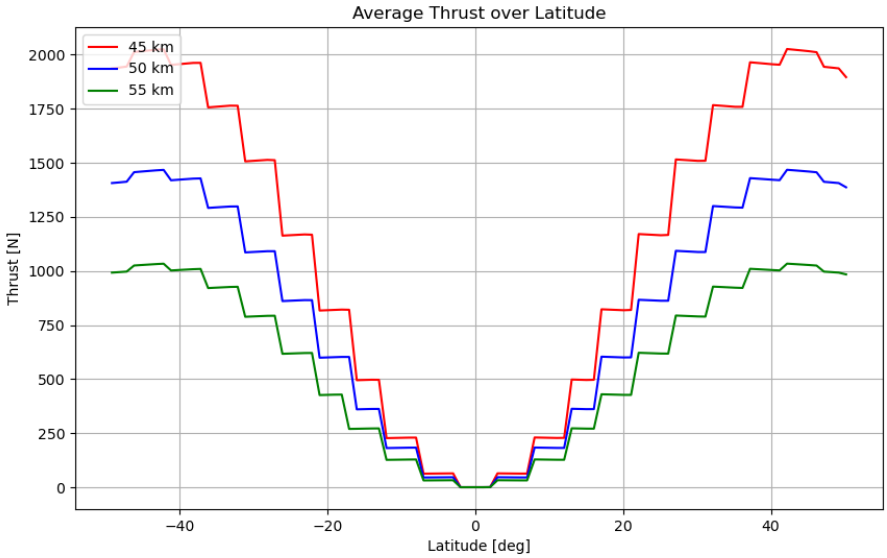

Figure 17.1: The plot shows the typical average thrust curve over the latitudes at different altitudes. The required thrust decreases at higher altitudes.

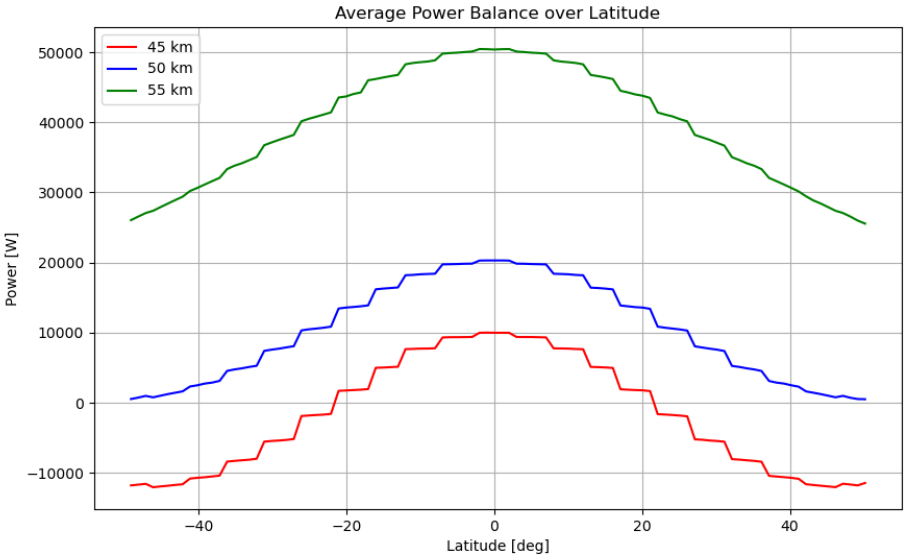

Figure 17.2: The average power balance over latitudes increases with the altitude. Towards the poles, the average power balance decreases.

In practice this leads to further problems as a bigger capacity leads to a higher mass of the VRS which in turn requires more powerful propulsion. The gain in capacity cannot be compensated through a more powerful propulsion system, as this has a negative impact on the power balance. Furthermore, by looking at Figure A.11, it becomes clear that the amount of time that the power balance is positive throughout a Venus day at higher latitudes is not sufficient to fully charge the batteries. By increasing the size of the balloon, more solar panels could be mounted on it and thus the power generation would be increased. But increasing the diameter of the balloon would greatly increase the drag force acting on the VRS during station keeping, which would quickly exceed the limits of the propulsion system. Thus, only the length was increased. Increasing the length also increases the drag force, acting on the VRS by the East-West-Wind. In the following simulation runs, no adequate length could be found without exceeding the calculation limits for the initial drag forces that were acting on the VRS during the commissioning phase. This means that a research station with such large measurements would likely break up early during the mission. Thus, it was concluded that the current size and power configurations of the VRS are already optimal for its purpose and consequently choosing higher altitudes for its operation should be favoured.

17.3 Data Budget

The biggest influencer for communication and data handling is the SAR. It generates the most data by far, as seen in Figure 16.3. This Section variates different aspects of the SAR and their influence on the communication and data handling, as well as the entire mission.

Mapping whole Venus

For a theoretically complete mapping of Venus, the SAR would have to run for a minimum of 2.5 years (SO1 mode). Based on the mission scenario, the other experiments of the Venus Research Station (VRS) (SO2 mode) operate for the same amount of time. This means that all instruments will run for 2.5 years except for the experiment to find life on Venus (SO3 mode), which will run for only one year. Since the mission is limited to 5 years of planning, SO1 and SO2 would run alternately for one circumnavigation for the entire mission, and the experiment to find life would additionally run continuously in the last year. Figure 17.3 shows the hypothetical mission data budget for this scenario. The VRS would produce 997.65 Tbits during the entire mission, whereas with the given communication system (14 Relay Satellites and Ka-Band with 8.0 Mbits/s transmission rate) would be able to send a total of 999.86 Tbits to the Relay Satellites. The necessary data rate for transmission over the whole mission without considering storage capacity is 7.98 Mbits/s, which is less than the transmission rate of the Ka-band. The scenario is therefore possible from a transmission point of view.

Regarding the storage it is possible to operate the SAR and other experiments alternating for one circumnavigation each, refer to Section 16.5 and transmit all the generated data in the same period of time. The only difference regarding storage takes place during the last year, in which additionally the experiment to search for life is taking place. Figure 17.4 displays the storage consideration during that last year. Table 17.1 tabulates the data budget for two circumnavigations.

If the experiment for search of life would run continuously for one year (50 circumnavigations, or rather 25 cycles of two alternating circumnavigations, it would require a total storage capacity of 1.00 Tbits (Data stored at end of cycle times number of cycles). With the integrated memory of 16 Tbits it possible to store the data. In order to transmit the stored data it is necessary to

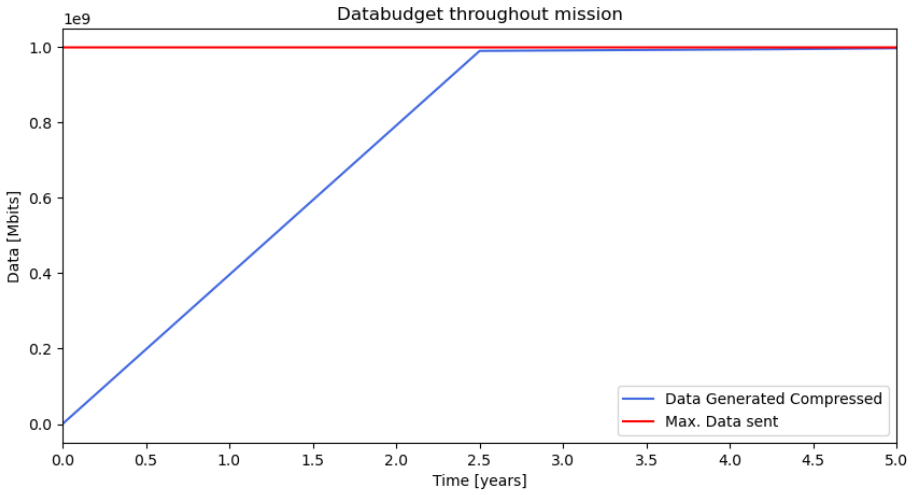

Figure 17.3: Simulation of mission data budget plotting whole Venus. Operation times: SAR for 2.5 years (0-2.5), all other instruments for 2.5 years (2-4.5) and the experiment for search for life in Venus‘ atmosphere for one year (4-5).

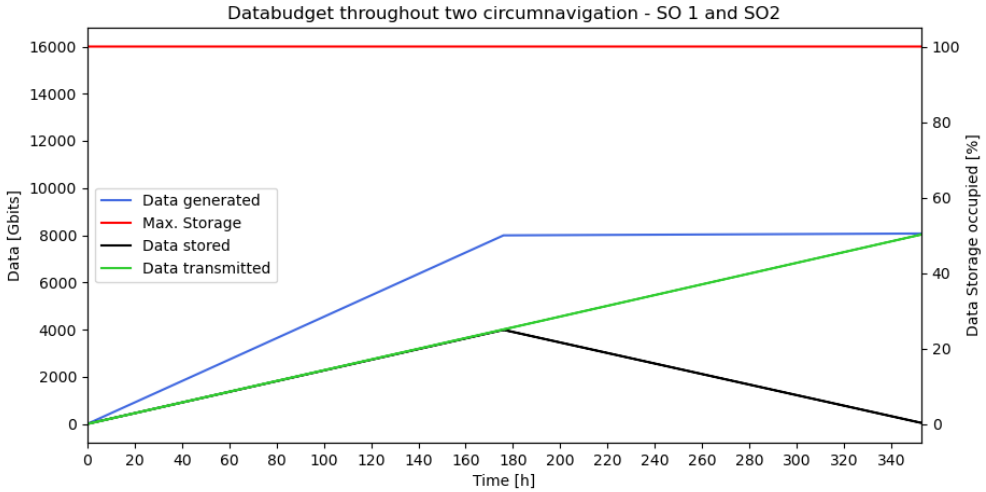

Figure 17.4: Data budget over two circumnavigations with life experiment. First circumnavigation (176 h) SO1 + SO3 Mode (SAR) and second circumnavigation SO2 + SO3 Mode (all other instruments). Display of max. storage, data generated, data transmitted and data stored over the time period of 352 h.

have a period of time in which the VRS produces fewer data than it transmits. Without the experiment of life, the VRS produces 28.00 Gbits less than it transfers in two circumnavigations. Therefore it would require 35 cycles with two circumnavigations each after the experiment to search for life to transmit all the stored data from the experiment to search for life. This equals approximately 1.5 years.

Circumnavigation (both: SO3)	1 (SO1)	2 (SO2)	Together
Total Data Generated [Gbits]	31836.33	156.38	31992.70
Compr. Data Generated [Gbits]	7992.56	78.19	8070.74
Data transmitted [Gbits]	4017.69	4017.69	8035.38
Data stored [Gbits]	3986.11	40.00	40.00

Table 17.1: Results simulation data budget after two circumnavigations for the scenario of complete mapping of Venus. First circumnavigation: collecting the data 2 Scouts (worst case).

In conclusion, it is with a change of mission scenario possible with the current concept to plot all of Venus from a communication and data handling point of view. A possible scenario is to operate the SAR and the other experiments alternating each circumnavigation for the entire mission. The experiment to search for life is running for the first year of the mission continuously. In this case, all data from that experiment would be sent after 2.5 years of the mission.

Less compression of Payload

The following section analyses different compression rates and their impact on the mission. Although a high compression rate reduces the amount of data considerably, it can also lead to the loss of data. If it is too high, the original data can no longer be decompiled without errors. The simplest approach to reducing the amount of data at a low compression rate is to operate the SAR for a shorter time. Table 17.2 lists the mission data budget for a SAR operation time of two years for different compression rates for payload (including Scouts) up to no compression. Since not all compression rates are realizable with the current communication concept and the SAR operating for two years, the subsequent max. running time of the SAR, that the current communication concept (14 Relay Satellites and Ka-Band with 8.0 Mbits/s transmission rate) allows, is calculated. The max. runtime of the SAR relates directly to the max. possible scanned area with the SAR, which is also tabulated. Figures A.12 to A.17 show the mission data budget plot for the different compression rates.

Compression factor	0.5	0.6	0.7	0.8	0.9	1.0
Compr. Data Gen. [Tbits]	800.69	958.80	1116.91	1275.01	1433.12	1591.23
TX Data Rate [Mbits/s]	6.41	7.67	8.94	10.20	11.47	12.73
Max. Time SAR [years]	2.52	2.10	1.80	1.57	1.40	1.26
Area scanned [$\times 10^6$ **km**^{2}]	488.74	407.29	349.10	304.50	271.52	244.37
Area of Venus [%]	106.19	88.50	75.85	66.16	59.00	53.10
Area between $\Phi = \pm 50°$ **[%]**	138.63	115.52	99.02	86.37	77.02	69.31

Table 17.2: Results simulation mission data budget for different compression rates.

The max. compression rate for payload (including Scouts) the communication concept allows for the SAR operating for two years is 0.625. In that case the VRS generates 998.32 Tbits of compressed data over the entire mission. This leads to a necessary transmission data rate of 7.99 Mbits/s, which is fulfilled by the actual transmission data rate of 8.00 Mbits/s. Figure A.18 displays the mission data budget for a compression rate of 0.625.

Higher SAR Data Rates

A big factor of a SAR is its data rate. SARs can also have much higher data rates than 50 Mbits/s. Table 17.3 lists the data budget for the VRS after one circumnavigation in SO1 Mode (only running the SAR as payload) for SAR data rates of 50 Mbits/s, 100 Mbits/s, 250 Mbits/s and 500 Mbits/s.

SAR Data Rates [Mbits/s]	**50**	**100**	**250**	**500**
Total Data Generated [Gbits]	31772.97	63452.97	158492.97	316892.97
Compr. Data Generated [Gbits]	7960.88	15880.88	39640.88	79240.88
Data Stored [Gbits]	3943.19	11863.19	35623.19	75223.19
Data Stored [%]	24.6	74.1	222.6	470.1

Table 17.3: Results simulation data budget after one circumnavigation in SO1 Mode for different SAR data rates.

It is possible to store the data of one circumnavigation in SO1 for a SAR with up to 100 Mbits/s while keeping a buffer of free memory. The effective transmission rates amount to 7.92681 Mbits/s in SO2 and to 7.93570 Mbits/s with no payload running. Based on these transmission rates it would take 415.72 h to transmit the 11.9 Tbits in SO2 Mode or 415.25 h if no payload was operating.

The maximum data rate possible with two years runtime and 0.5 payload compression and SAR filtering is 62.5 Mbits/s. In that case the VRS generates 997.79 Tbits and is able to transmit 999.86 Tbits of data. Figure A.19 displays the mission data budget for this scenario.

Figure 17.5 displays the necessary number of Relay Satellites that the mission would need to transmit all the data after two circumnavigations (first: SO1, second: SO2). Only for a SAR data rate of 50 Mbits/s are 14 Relay Satellites sufficient. All other rates would need either more than 15 Relay Satellites or higher transmission rates. Table 17.4 tabulates the necessary transmission rate [Mbits/s] from VRS to Relay Satellites for the different SAR data rates and for a different number of Relay Satellites.

SAR Data Rates [Mbits/s]	**50**	**100**	**250**	**500**
5 Relay Satellites	18.60	37.00	92.20	184.1
10 Relay Satellites	10.15	20.19	50.29	100.47
14 Relay Satellites	7.44	14.80	36.88	73.68

Table 17.4: Results simulation necessary transmission data rate [Mbits/s] to transmit all data after two circumnavigations for different SAR data rates.

To ensure the transmission for higher SAR data rates, or even lower compression and filtering factors, the VRS would need a higher transmission rate, more Relay Satellites would have to be employed or it would require a higher storage capacity and enough time to transmit all the stored data. Each of those solutions are with the current concept either not feasible or realizable. But these can be the solution for further research and other design approaches to enable higher amounts of data from the SAR.

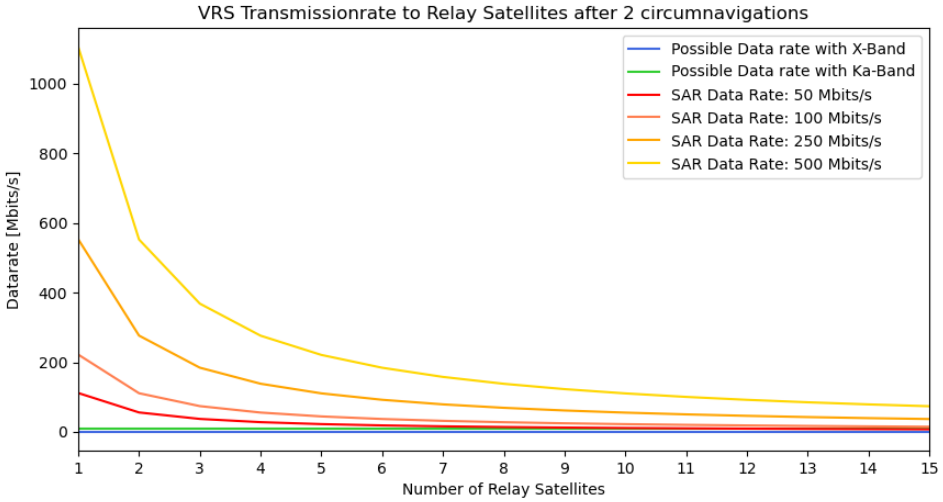

Figure 17.5: Necessary transmission rate depending on the number of Relay Satellites with alternating SAR data rates. Possible data rates using X- or Ka-Band are displayed.

CHAPTER 18

Conclusion

by Carolin Bösch[1]

In this work, a Venus Research Station that operates within Venus‘ atmosphere was developed on a conceptual basis. This includes the definition of the mission, i.e. the mission statement, mission objectives (scientific and technological) and requirements, starting with the user requirements up to the functional requirements and boundary conditions. For the definition of the mission the physical environment of Venus was analyzed in detail and scientific objectives were developed. The final concept, contains not only the atmospheric Venus Research Station (VRS), but also multiple deployable atmospheric Scouts for the exploration of Venus‘ atmosphere at different altitudes. A total of 15 single-use Scouts are evenly distributed on Venus and dropped from a Carrier Vehicle in orbit.

A mission scenario including operating modes for the operation of the Research Station was developed. The scenario allocates operating times to the individual systems ensuring that the objectives and requirements of the mission are met. The challenge in developing the mission scenario was to ensure sufficient power supply at all times and allocation of instrument operating times to A) meet the ambitious objectives and requirements of the mission and B) ensure the transmission of all data.

This mission concept also includes the system environment, which defines the external elements of the mission, such as Launch Systems, Ground Support, Relay Satellites, or Interplanetary Trajectories. Further it includes the more detailed concept of certain mission scenarios, e.g. Launch Scenario or End-of-Life Disposal and Decommissioning. One of the critical challenges faced during the design of the mission scenario from a system environment perspective is the limited payload capacity of the launch system. This issue leads to multiple launches thus increasing the complexity of the mission. The mission timeframe to start within the next 30 years allows Arianespace or other upcoming European launching companies to build higher capacity launchers in the coming years, thereby reducing mission complexity. The second critical challenge was the close dependence on the system-level design of multiple elements of the mission. Small changes in mass or volume, affected launch systems along with the entire mission scenario. Finally, the issue regarding planet sustainability needs a deeper analysis. This analysis could allow the mission to reduce the number of orbiting elements around the planet as well as on the planet‘s surface without hampering the ability to achieve all the mission requirements.

Based on the scientific objectives and requirements, the payload system of the VRS was designed. The selected instruments for the VRS and the deployable atmospheric Scouts can accomplish the scientific objectives within the predefined design constraints. There are technological challenges for this mission that require targeted development of certain instruments. These include some high-level payload instruments, such as the SlimSAR and the Venus Acoustic

[1] established by entire team, written by Carolin Bösch

Anemometer, that are not yet technologically ready for use onboard the VRS. However, with appropriate continued research and engineering, they could be ready for use within 30 years. The biggest challenge in payload development is the SlimSAR, which must be able to penetrate thick clouds and provide high-resolution images of the planet's surface while requiring a low mass, low power and low data generation.

The structure of the VRS is a non-rigid airship with a balloon and an aluminuim based payload carrier. The methodology used in this report for the design of the VRS is a useful tool for the conceptual design of a non-rigid airship. It is helpful to meet specific operational requirements and to determine the sensitivity of different parameters of the airship such as payload mass, changing pressure with altitude, or cruising speed. This can help identify the requirements that drive the design, and to investigate several 'what-if' scenarios. The final overall mass of the entire VRS exceeds the mass range given by the boundary conditions. Therefore multiple launches are required for the VRS. The individual components of the VRS are within the mass limits of the launch system and can be attached during docking phase. The biggest challenge during the design of the VRS was the determination of the total mass due to a cyclic dependency of mass, size of balloon and necessary thrust/power. One solution could be to implement multidisciplinary design optimization along with concurrent engineering techniques to avoid complete iterations by optimizing systems concurrently. The methodology can be continuously upgraded and fine-tuned as more accurate information becomes available. It can also be adopted for carrying out multi-disciplinary design optimization of an airship system.

After a comparison between different levitation options, for the VRS to float at 50 km altitude, a helium filled balloon was chosen. The relevant forces acting on both the VRS during its flight as well as on the Scouts during their descent were modelled and simulated. From this the overall mass estimations for the size of the balloon were made, leading to a diameter of 14 m and a length of 57 m. Due to the flight dynamics of the Scouts, they will only be able to preform their experiments starting at an altitude of 76 km. Thus, the requirement to explore the Venus atmosphere from an altitude of 130 km is not met with this concept. The balloon sizing depends on the final mass of the overall VRS and the balloon size itself has an effect on mass, via its own mass and the necessary propulsion due to its size, which directly transfers to the size and mass of the batteries. This leads to the already mentioned cyclic dependency when it comes to overall mass and balloon size. Solving this cycle posed the largest issue for flight dynamics. Due to the Hadley circulation of Venus, the polar regions (above approximately $\pm 50°$ latitude) can not be reached by a mainly levitating and wind-driven airship. Thus, the requirements aiming for global coverage of Venus are not met with this concept, e.g. including global mapping of Venus.

The propulsion system was developed to actively steer the VRS and to overcome gust winds, while floating mostly passively along with the atmospheric winds. The designed propulsion concept is based on a cyclocopter. Various challenges were faced throughout the development of the propulsion system. The main challenges included the limitations of power availability while meeting the necessary thrust requirements. Several iterations using various mathematical approaches and propeller mechanisms were used. In addition, fitting the actuator into the allotted space of the payload section was a difficult mechanical and transportational problem. This problem is bypassed by a folding mechanism that uses actuators to secure the propulsion system in its final location.

To control the movement of the VRS, a guidance, navigation and control (GNC) system was developed. The biggest challenge regarding GNC was the initial localization of the VRS, as well as the calibration of the attitude sensors. Both of these problems were solved with the help of the SAR payload instrument via Simultaneous Localization and Mapping (SLAM) algorithms and n-vector attitude determination methods. The drawback of this approach is that the SAR instrument must be operational at least intermittently throughout the mission

in order to ensure accurate localization and attitude estimation. This puts pressure on the On-Board Computer (OBC) and power subsystems. Attitude control could be achieved relatively easily via thrust vector control and aerodynamic control surfaces. However, position control is somewhat more difficult due to the power constraints (and subsequent thrust limitations) of the propulsion system. This means that position control cannot be ensured in certain regions within the Venusian atmosphere due to high wind speeds restricting this mission concept to latitudes within $\pm 50°$. Furthermore, altitude control is achieved primarily via high pressure ballast tanks, which could pose a threat to the entire station if one of the tanks fails. For this reason, large safety margins were considered when determining tank wall thickness. Certain aerodynamic considerations were omitted in this analysis. Thus, more detailed research is required to ensure the feasibility of autonomous navigation in the harsh environment of Venus atmosphere.

The Scouts are powered by a sufficient battery for their one-time use. To ensure the power supply of the VRS, a solar-based power concept was developed. The design of the power system was challenging because of the environment of Venus. The challenge of identifying the power source was solved fairly well by selecting the suitable altitude and latitude range for operating the VRS. This solution was analyzed by calculating the power demand of the station and the power generated by the source. The results were simulated for verification. The energy and power demand of the VRS is very high, mainly coming from the propulsion system. To meet this demand at night time the VRS requires a battery with high specific energy density. After a thorough research, a battery was selected but with very limited details, so the sizing of batteries could not be accomplished completely. Only the mass of batteries required to meet the demand was calculated. The high mass of the batteries led to an increase in mass and size of the station especially of the balloon, which increased the power demand of propulsion. This led to the before mentioned cyclic dependency of flight dynamics, structure, propulsion and power.

To ensure the functionality of the VRS and the Scouts, a certain internal temperature must be maintained. For the Scouts a layer of aerogel insulation and a heat shield, used during the entry phase, are employed. The VRS is also insulated by a 30 cm aerogel insulation layer, which already significantly reduces the heat flow. Moreover the VRS is equipped with two Stirling Cycle Cryocoolers to ensure the final temperature regulation. Both, the aerogel insulation and the Stirling Cycle Cryocoolers, need further research for this specific application to ensure the temperature regulation. In order to determine all heat loads for the calculation of the internal temperatures good models of radiation and albedo flux depending on height within the Venus atmosphere are needed. Finding these models posed a challenge during the development of the VRS‘s thermal system. Another challenge was modelling the VRS for thermal calculations. Due to the shape of the balloon it would be too complex to determine the exact value. This was solved by assuming a cylinder and approximation instead of calculation. If it were possible to design a smaller VRS the heat flows could be reduced drastically. In addition it would decrease the mass of the insulation layer assuming the same thickness.

The Command and Data Handling of the VRS and the data storage before transmission of the Scouts‘ data to the VRS is ensured. The utilization of OBC characteristics onboard the VRS is critical for real-time command, execution, and feedback, allowing for precise control of all operations. The impact of data management and handling was meticulously reviewed and simulated during the operation, taking into account numerous obstacles and trade-offs. The biggest challenge during the tradeoff was the data generation rate of SAR which is six times greater than the transmission rate creating the need for large data storage and leading to a high power consumption. The amount of data can be reduced by applying a greater compression ratio, but that reduces picture integrity, thereby affecting image quality received on Earth. By addressing these considerations, the mission‘s concept can be ensured to achieve optimal success and efficiency.

The communication aspect of this mission involves the exchange of data between the Scouts and the VRS, as well as between the VRS and the Relay Satellites. The major challenge in achieving effective communication lies in attaining high data transmission rates, which are limited due to atmospheric absorption and defocusing loss. However, this limitation can be overcome by utilizing 14 Relay Satellites. Having a direct communication with Earth and the Research Station is very challenging due to the high free space path loss, and it is unnecessary since redundant communication is ensured with 14 Relay Satellites in use. To achieve high data transmission rates, Free Space Optical Communication can be considered. This method offers a substantial bandwidth and high data rate. Additionally, it is more compact than radio frequency communication and requires lower power. Nonetheless, optical communication currently faces challenges due to atmospheric conditions on Venus, such as cloud covers, high wind speeds, sun intensity, and atmospheric turbulences, leading to significant loss and radiation background noise. As a result, using optical communication is not feasible at the moment. However, future technologies may emerge to overcome these challenges.

Performance of the sensitivity analysis for the propulsion aspect showed that station keeping of the VRS is feasible at an altitude of 50 km and above without exceeding the limits of the propulsion system. Increasing the maximum thrust would also enable the VRS to perform station keeping at lower altitudes but at the same time increase the power demand which cannot be met at such low altitudes as the sensitivity analysis of the power system concluded that the optimal operating altitude for the VRS is between 52 km and 53 km altitude. Furthermore, the ideal battery capacity is 20 MWh and the chosen size of the balloon of 14.3 m in diameter and 57 m in length provides the optimal surface area for the power generation of the solar panels. Further analysis in the communications and data handling area has shown that the VRS would even be capable of mapping Venus completely if it were not limited by the Hadley circulation over $\pm 50^\circ$ latitude. It was also shown that the maximum achievable SAR data rate and payload compression factor are close to the values of this concept.

In summary, the designed concept provides all the desired functionalities and fulfils almost all the requirements, except for the launch exploration height of the Scouts and the global coverage regarding the scientific objectives. The results were verified with the help of a simulation. In some cases, the simulation was even used to perform further analyses.

Appendices

APPENDIX A

Further Tables and Plots

A.1 Physical Environment

H Km	T K	P (bar)	r kg/m³	U m/s	m Pa*s	n s/m²	Cp J/kg*K	Cp/Cv	A m/s	K W/m*K
0	735.3	92.1	64.79	0.6	3.35E-05	5.17E-07	1181	1.193	410	0.0588
1	727.7	86.45	61.56	0.7	3.12E-05	5.07E-07	1177	1.194	408	0.0575
2	720.2	81.09	58.45	0.8	2.89E-05	4.95E-07	1172	1.195	406	0.0561
3	712.4	76.01	55.47	0.9	2.67E-05	4.81E-07	1168	1.196	404	0.0548
4	704.6	71.2	52.62	1.0	2.44E-05	4.63E-07	1163	1.197	402	0.0534
5	696.8	66.65	49.87	1.2	2.21E-05	4.43E-07	1159	1.198	400	0.0521
6	688.8	62.35	47.24	1.3	2.18E-05	4.62E-07	1155	1.199	398	0.0511
7	681.1	58.28	44.71	1.9	2.16E-05	4.83E-07	1151	1.200	396	0.0501
8	673.6	54.44	42.26	2.4	2.13E-05	5.04E-07	1146	1.200	393	0.0490
9	665.8	50.81	39.95	3.4	2.11E-05	5.27E-07	1142	1.201	391	0.0480
10	658.2	47.39	37.72	4.5	2.08E-05	5.51E-07	1138	1.202	389	0.0470
11	650.6	44.16	35.58	6.3	2.25E-05	6.33E-07	1134	1.203	387	0.0462
12	643.2	41.12	33.54	8.2	2.42E-05	7.23E-07	1129	1.204	385	0.0455
13	635.5	38.26	31.6	10.8	2.60E-05	8.22E-07	1125	1.205	383	0.0447
14	628.1	35.57	29.74	13.4	2.77E-05	9.31E-07	1120	1.206	381	0.0440
15	620.8	33.04	27.95	16.1	2.94E-05	1.05E-06	1116	1.207	379	0.0432
16	613.3	30.66	26.27	19.6	2.91E-05	1.11E-06	1111	1.208	377	0.0425
17	605.2	28.43	24.68	22.0	2.88E-05	1.17E-06	1106	1.209	374	0.0417
18	597.1	26.33	23.18	24.5	2.84E-05	1.23E-06	1101	1.211	372	0.0410
19	589.3	24.36	21.74	26.0	2.81E-05	1.29E-06	1096	1.212	369	0.0402
20	580.7	22.52	20.39	27.6	2.78E-05	1.36E-06	1091	1.213	367	0.0395
21	572.4	20.79	19.11	28.8	2.76E-05	1.44E-06	1085	1.214	365	0.0388
22	564.3	19.17	17.88	29.9	2.74E-05	1.53E-06	1079	1.216	362	0.0382
23	556.0	17.66	16.71	30.6	2.71E-05	1.62E-06	1074	1.217	360	0.0375
24	547.5	16.25	15.62	31.3	2.69E-05	1.72E-06	1068	1.219	357	0.0369
25	539.2	14.93	14.57	32.3	2.67E-05	1.83E-06	1062	1.220	355	0.0362
26	530.7	13.7	13.59	33.3	2.64E-05	1.94E-06	1056	1.222	352	0.0357
27	522.3	12.56	12.65	34.0	2.61E-05	2.06E-06	1049	1.223	350	0.0352
28	513.8	11.49	11.77	34.6	2.58E-05	2.19E-06	1043	1.225	347	0.0346
29	505.6	10.5	10.93	35.0	2.55E-05	2.33E-06	1036	1.226	345	0.0341
30	496.9	9.851	10.15	35.5	2.52E-05	2.48E-06	1030	1.228	342	0.0336
31	488.3	8.729	9.406	36.0	2.49E-05	2.65E-06	1023	1.230	339	0.0331
32	479.9	7.94	8.704	36.4	2.46E-05	2.83E-06	1016	1.232	337	0.0325
33	472.7	7.211	8.041	36.7	2.44E-05	3.03E-06	1010	1.234	334	0.0320
34	463.4	6.537	7.42	36.9	2.41E-05	3.25E-06	1003	1.236	332	0.0314
35	455.5	5.917	6.831	37.3	2.38E-05	3.48E-06	996	1.238	329	0.0309
36	448.0	5.346	6.274	37.6	2.35E-05	3.75E-06	990	1.240	326	0.0304
37	439.9	4.822	5.762	38.2	2.33E-05	4.04E-06	983	1.242	324	0.0300

H Km	T K	P (bar)	r kg/m³	U m/s	m Pa*s	n s/m²	Cp J/kg*K	Cp/Cv	A m/s	K W/m*K
38	432.5	4.342	5.276	38.7	2.30E-05	4.36E-06	977	1.244	321	0.0295
39	425.1	3.903	4.823	39.7	2.28E-05	4.72E-06	970	1.246	319	0.0291
40	417.6	3.501	4.404	40.7	2.25E-05	5.11E-06	964	1.248	316	0.0286
41	410.0	3.135	4.015	42.6	2.23E-05	5.55E-06	958	1.250	314	0.0282
42	403.5	2.802	3.646	44.5	2.21E-05	6.05E-06	953	1.252	311	0.0277
43	397.1	2.499	3.303	47.4	2.18E-05	6.61E-06	947	1.253	309	0.0273
44	391.2	2.226	2.985	50.3	2.16E-05	7.24E-06	942	1.255	306	0.0268
45	385.4	1.979	2.693	54.2	2.14E-05	7.95E-06	936	1.257	304	0.0264
46	379.7	1.756	2.426	57.4	2.11E-05	8.71E-06	930	1.259	302	0.0260
47	373.1	1.556	2.186	59.4	2.09E-05	9.55E-06	923	1.261	299	0.0256
48	366.4	1.375	1.967	61.0	2.06E-05	1.05E-05	917	1.264	297	0.0251
49	358.6	1.213	1.769	61.2	2.04E-05	1.15E-05	910	1.266	294	0.0247
50	350.5	1.066	1.594	60.9	2.01E-05	1.26E-05	904	1.268	292	0.0243
51	342.0	0.9347	1.432	60.2	1.97E-05	1.38E-05	895	1.272	288	0.0239
52	333.3	0.8167	1.284	59.4	1.94E-05	1.51E-05	886	1.276	284	0.0235
53	323.0	0.7109	1.153	59.3	1.90E-05	1.65E-05	877	1.279	281	0.0231
54	312.8	0.616	1.032	59.2	1.87E-05	1.81E-05	868	1.283	277	0.0227
55	302.3	0.5314	0.9207	59.9	1.83E-05	1.99E-05	859	1.287	273	0.0223
56	291.8	0.4559	0.8183	60.5	1.80E-05	2.20E-05	851	1.290	270	0.0219
57	282.5	0.3891	0.7212	62.7	1.77E-05	2.45E-05	844	1.294	266	0.0215
58	275.2	0.3306	0.6289	65.0	1.73E-05	2.76E-05	836	1.297	263	0.0212
59	268.7	0.2796	0.5448	71.1	1.70E-05	3.12E-05	829	1.301	259	0.0208
60	262.8	0.2357	0.4694	77.2	1.67E-05	3.56E-05	821	1.304	256	0.0204
61	258.7	0.2008	0.40525	85.4	1.66E-05	4.09E-05	818	1.306	255	0.0201
62	254.5	0.1659	0.3411	92.0	1.64E-05	4.82E-05	815	1.307	253	0.0197
63	250.0	0.14075	0.2927	94.0	1.63E-05	5.57E-05	811	1.309	252	0.0194
64	245.4	0.1156	0.2443	94.5	1.62E-05	6.62E-05	808	1.310	250	0.0190
65	243.2	0.09765	0.2086	95.0	1.61E-05	7.69E-05	805	1.312	249	0.0187
66	241.0	0.0797	0.1729	94.4	1.59E-05	9.21E-05	802	1.314	247	0.0184
67	238.2	0.06709	0.14695	93.8	1.58E-05	1.07E-04	799	1.315	246	0.0180
68	235.4	0.05447	0.121	93.2	1.57E-05	1.29E-04	795	1.317	244	0.0177
69	232.6	0.04569	0.102465	92.6	1.55E-05	1.52E-04	792	1.318	243	0.0173
70	229.8	0.0369	0.08393	92.0	1.54E-05	1.83E-04	789	1.320	241	0.0170
71	227.0	0.03083	0.07084	89.4	1.53E-05	2.15E-04	786	1.322	239	0.0167
72	224.1	0.02476	0.05775	86.8	1.51E-05	2.61E-04	783	1.324	238	0.0164
73	221.4	0.02061	0.04854	84.2	1.50E-05	3.08E-04	779	1.325	236	0.0161
74	218.6	0.01645	0.03933	81.6	1.48E-05	3.76E-04	776	1.327	235	0.0158
75	215.4	0.01363	0.03298	79.0	1.47E-05	4.44E-04	773	1.329	233	0.0155
76	212.1	0.01081	0.02663	74.6	1.45E-05	5.44E-04	770	1.331	231	0.0151
77	208.7	0.00891	0.022235	70.2	1.44E-05	6.45E-04	767	1.333	230	0.0148

H Km	T K	P (bar)	r kg/m³	U m/s	m Pa*s	n s/m²	Cp J/kg*K	Cp/Cv	A m/s	K W/m*K
78	205.3	0.00701	0.01784	65.8	1.42E-05	7.96E-04	763	1.334	228	0.0145
79	201.2	0.00589	0.01485	61.4	1.41E-05	9.46E-04	760	1.336	227	0.0142
80	197.1	0.00476	0.01186	57.0	1.39E-05	1.17E-03	757	1.338	225	0.0139
81	193.5	0.00378	0.009793	52.4	1.38E-05	1.41E-03	755	1.340	223	0.0138
82	189.9	0.00281	0.007725	47.8	1.36E-05	1.77E-03	752	1.341	222	0.0136
83	186.9	0.00227	0.006326	43.2	1.35E-05	2.14E-03	750	1.343	220	0.0135
84	183.8	0.00173	0.004926	38.6	1.34E-05	2.72E-03	747	1.344	219	0.0133
85	181.0	0.00139	0.004007	34.0	1.33E-05	3.31E-03	745	1.346	217	0.0132
86	178.2	0.00105	0.003088	30.4	1.31E-05	4.25E-03	743	1.347	215	0.0131
87	175.9	0.00084	0.002493	26.8	1.30E-05	5.21E-03	740	1.349	214	0.0129
88	173.6	0.00063	0.001898	23.2	1.29E-05	6.78E-03	738	1.350	212	0.0128
89	171.5	0.0005	0.001525	19.6	1.27E-05	8.35E-03	735	1.352	211	0.0126
90	169.4	0.00037	0.001151	16.0	1.26E-05	1.09E-02	733	1.353	209	0.0125
91	168.3	0.0003	0.000917	15.0	1.26E-05	1.38E-02	734	1.353	209	0.0125
92	167.2	0.00022	0.000684	14.0	1.27E-05	1.85E-02	734	1.353	210	0.0126
93	167.2	0.00017	0.000542	13.0	1.27E-05	2.34E-02	735	1.353	210	0.0126
94	167.2	0.00013	0.0004	12.0	1.27E-05	3.18E-02	735	1.353	211	0.0126
95	168.2	0.0001	0.000315	11.0	1.28E-05	4.04E-02	736	1.353	211	0.0127
96	169.2	7.5E-05	0.000231	10.8	1.28E-05	5.52E-02	736	1.352	211	0.0127
97	170.6	6E-05	0.000183	10.6	1.28E-05	7.00E-02	737	1.352	212	0.0127
98	172.0	4.5E-05	0.000135	10.4	1.28E-05	9.53E-02	737	1.352	212	0.0127
99	173.7	3.6E-05	0.000107	10.2	1.29E-05	1.21E-01	738	1.352	213	0.0128
100	175.4	2.7E-05	7.89E-05	10.0	1.29E-05	1.63E-01	738	1.352	213	0.0128

Figure A.1: An overview of different atmospheric conditions on Venus at different heights [23].

A.2 Flight Dynamics

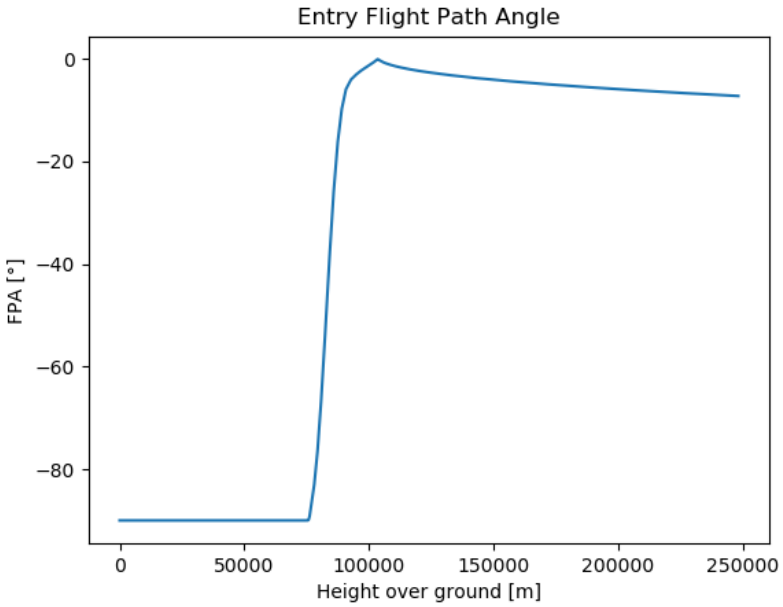

Figure A.2: The Flight Path Angle of the Scouts during atmospheric entry based on their height.

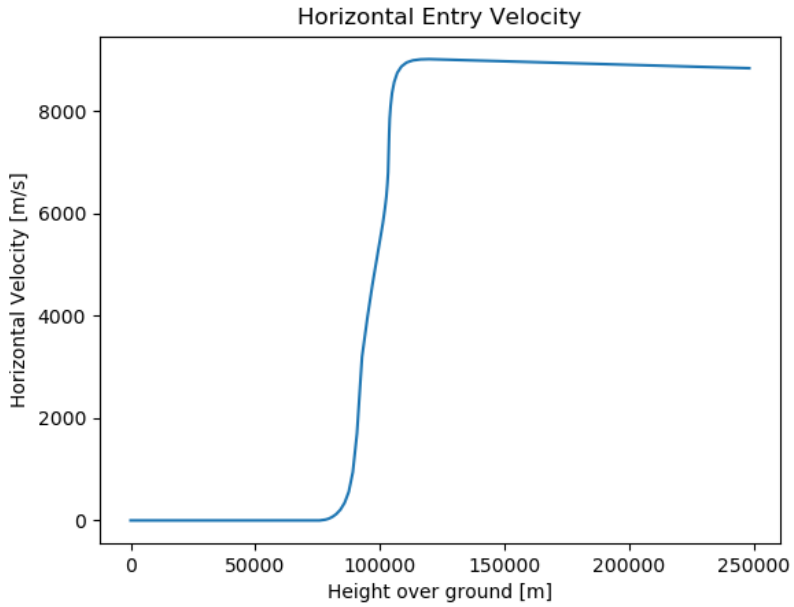

Figure A.3: The horizontal velocity of the Scouts during atmospheric entry based on their height.

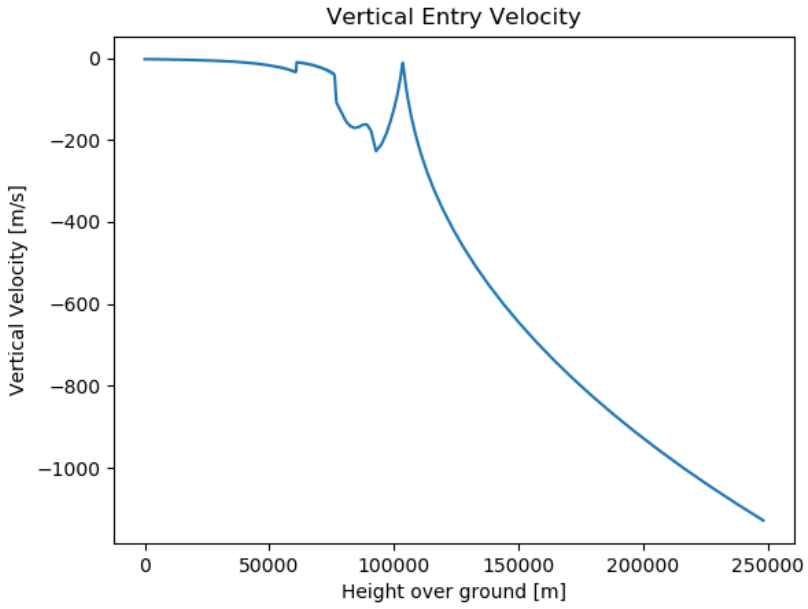

Figure A.4: The vertical velocity of the Scouts during atmospheric entry based on their height.

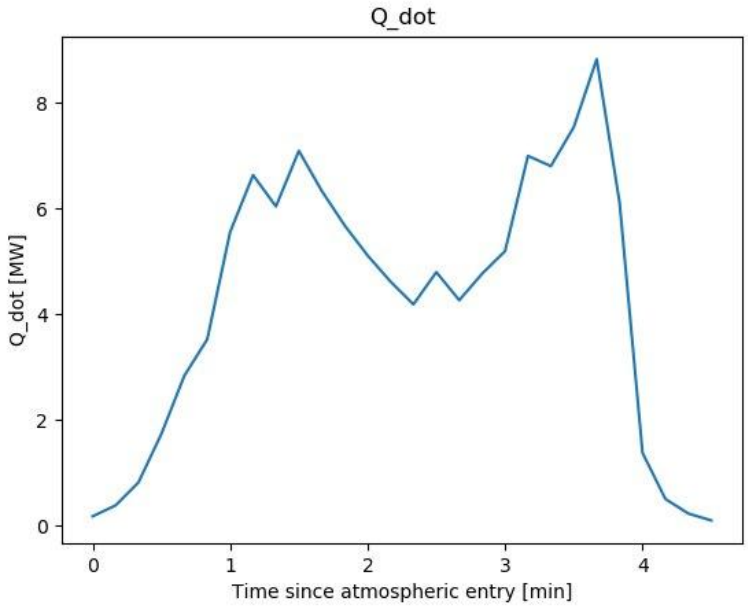

Figure A.5: The heat load on the Scouts during the phase of atmospheric entry with the strongest heat loads.

A.3 Simulation

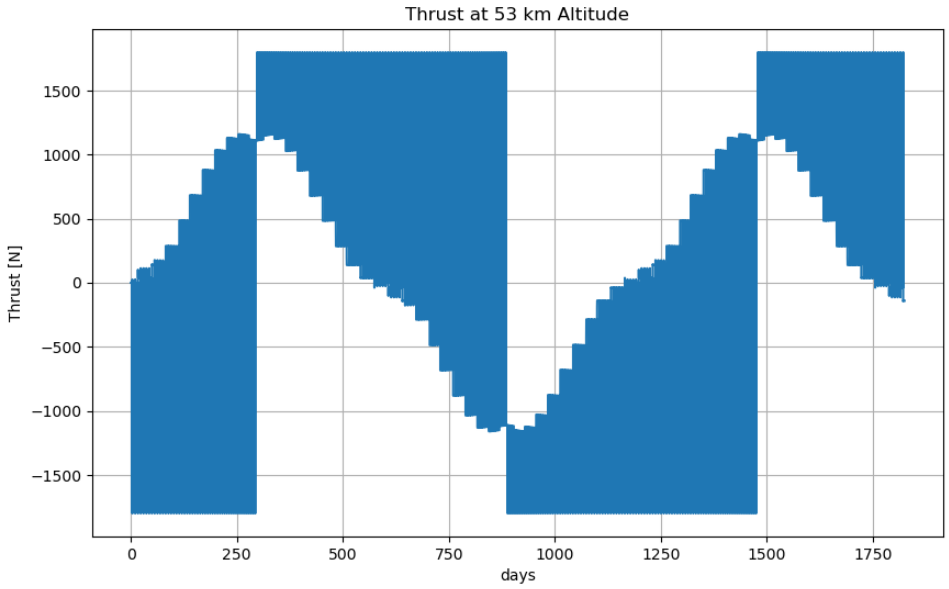

Figure A.6: The required thrust of the VRS changes depending on its position on Venus and direction of movement. For travelling to a new latitude, the thrust usually reaches the maximum thrust value as it needs to reach its target as fast as possible. For station keeping, it usually compensates the drag force of the wind. This plot represents the thrust curve simulated at 53 km altitude.

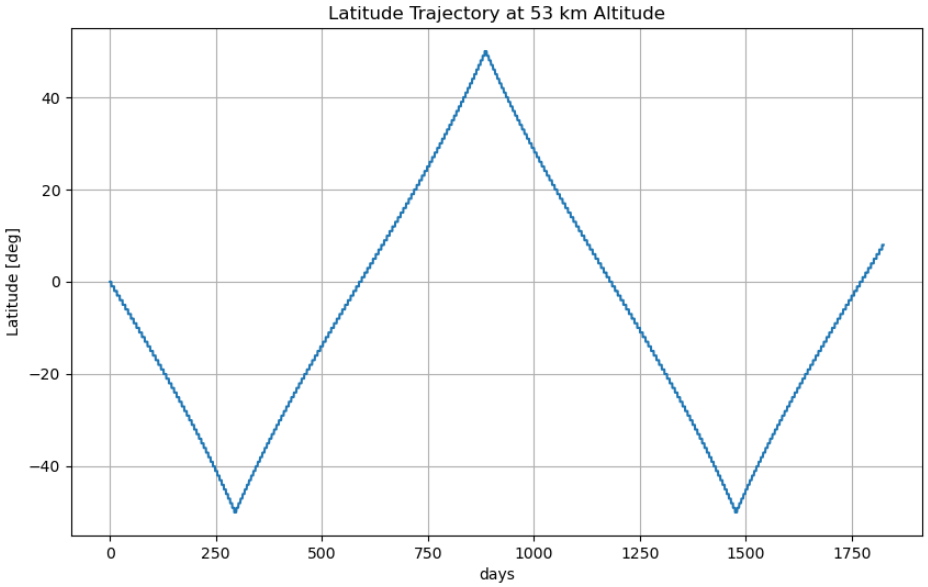

Figure A.7: This plot shows the latitude trajectory that the VRS followed during a full mission simulation at 53 km altitude.

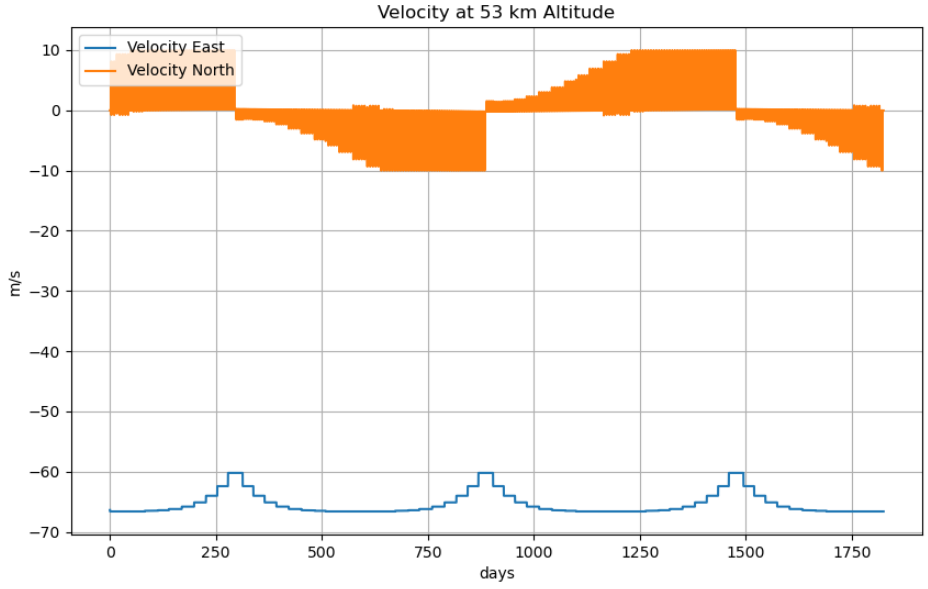

Figure A.8: The velocity of the VRS depends on its position. The westbound velocity decreases with increasing distance relative to the equator. The northbound velocity on the other hand depends on the station keeping and travelling across the latitudes. Positive velocities indicate that the VRS is moving south, negative velocities translate to northbound movement.

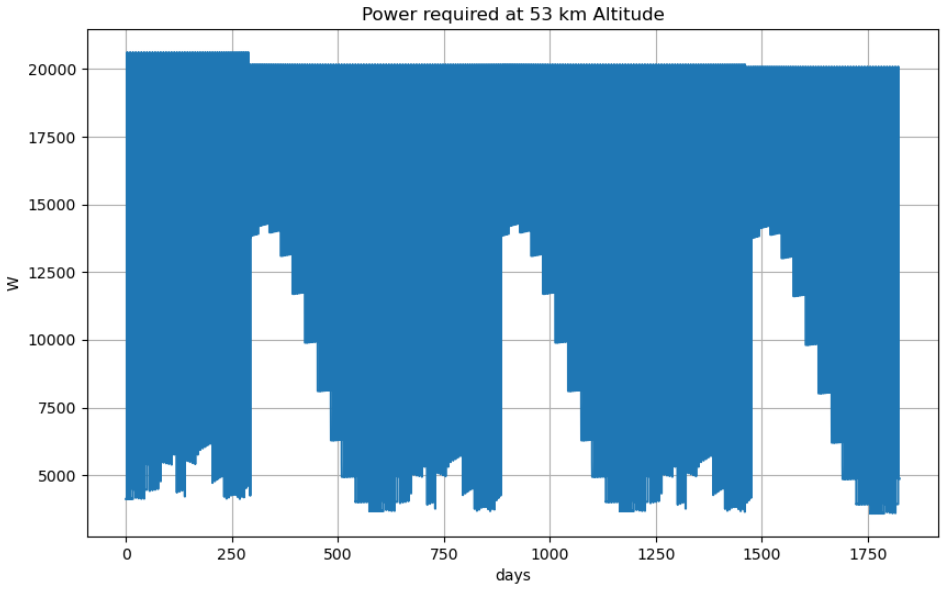

Figure A.9: The required power changes over time. Depending on the mission phase, the maximum required power decreases towards the end of the mission. The total range of the required power varies and is mostly dependent on the Propulsion system.

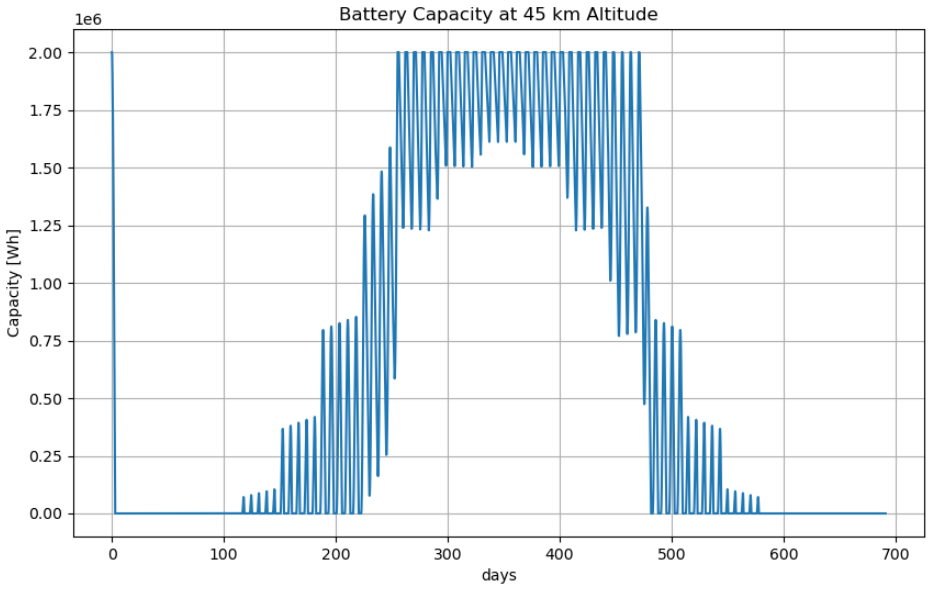

Figure A.10: At 45 km altitude, the power system does not generate enough power to maintain a sufficient power level on the VRS.

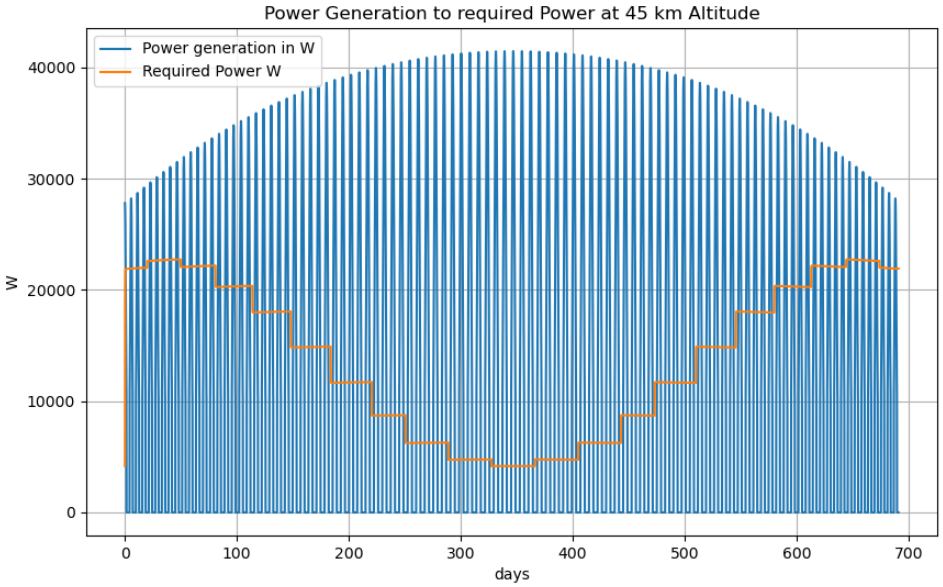

Figure A.11: Simulation of the generated power to the required power. The starting point is at 50° latitude, moving over the equator until it reaches −50° latitude.

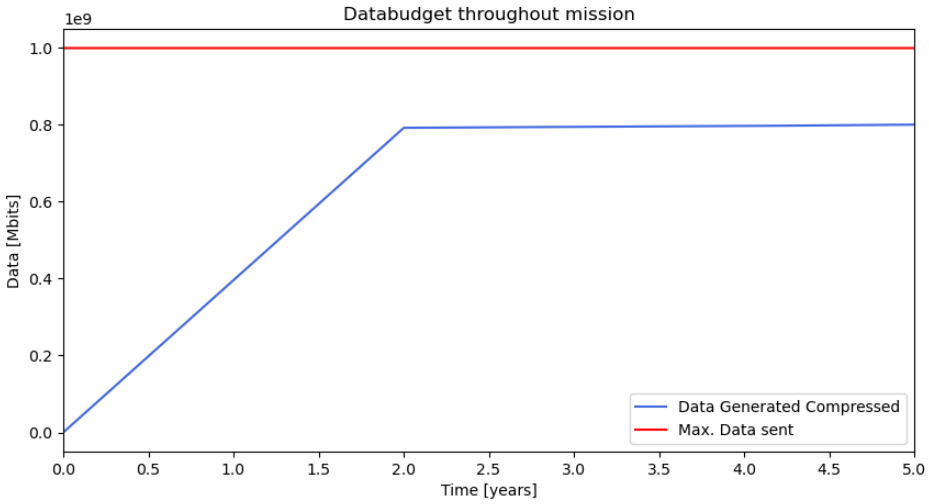

Figure A.12: Simulation of mission data budget with payload compression of 0.5. Operation times: SAR for two years (0-2), all other instruments for two years (2-4) and the experiment for search for life in Venus‘ atmosphere for one year (4-5). Max. possible data amount that can be transmitted during the overall mission is displayed.

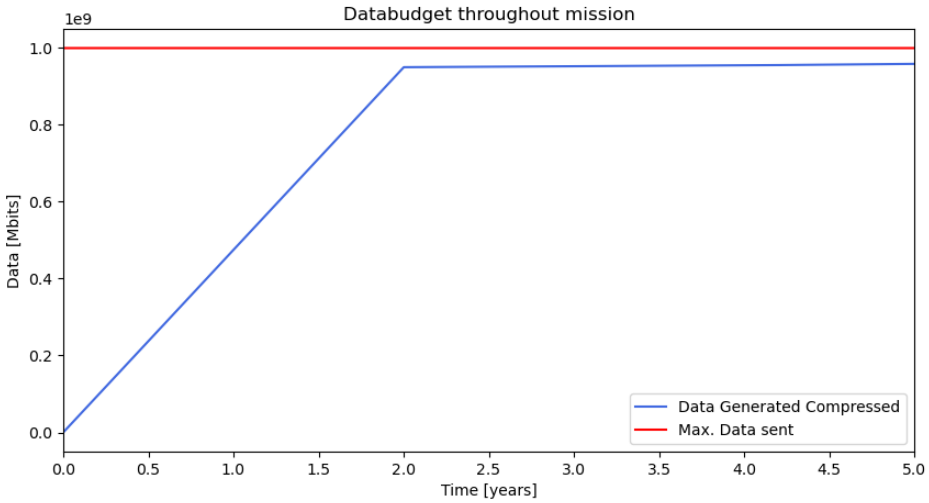

Figure A.13: Simulation of mission data budget with payload compression of 0.6. Operation times: SAR for two years (0-2), all other instruments for two years (2-4) and the experiment for search for life in Venus‘ atmosphere for one year (4-5). Max. possible data amount that can be transmitted during the overall mission is displayed.

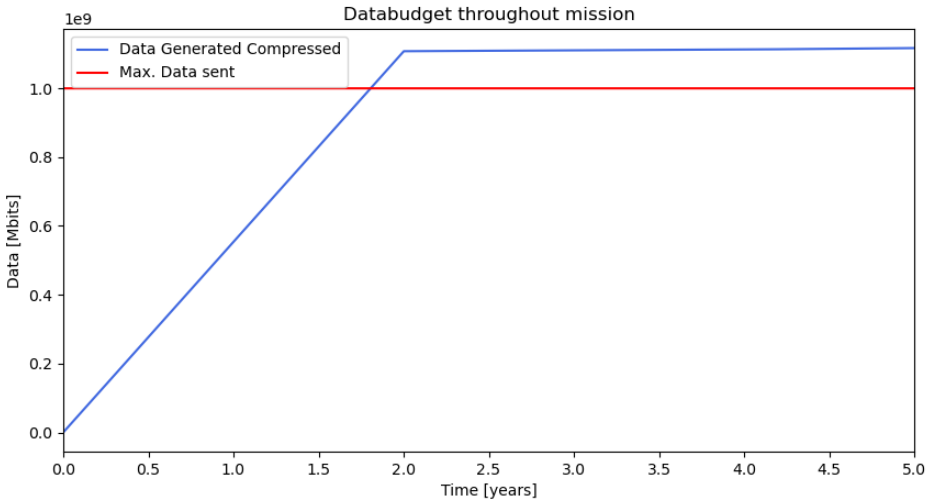

Figure A.14: Simulation of mission data budget with payload compression of 0.7. Operation times: SAR for two years (0-2), all other instruments for two years (2-4) and the experiment for search for life in Venus‘ atmosphere for one year (4-5). Max. possible data amount that can be transmitted during the overall mission is displayed.

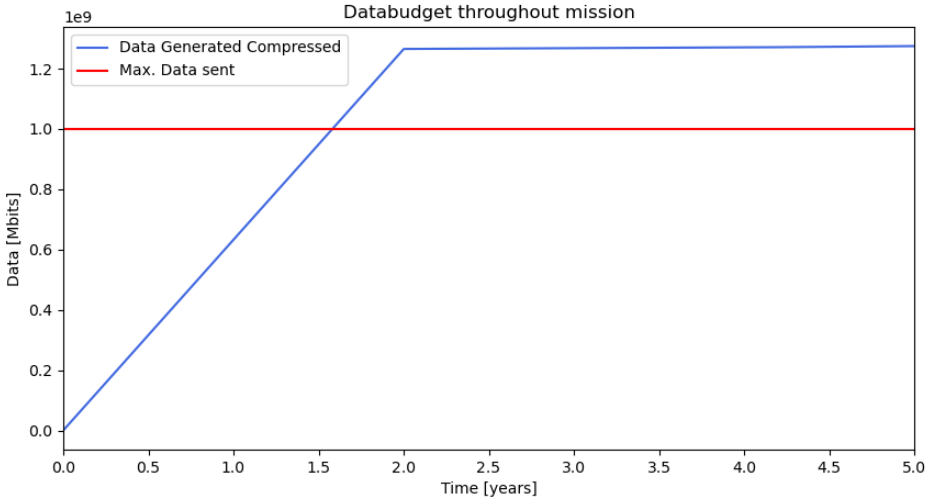

Figure A.15: Simulation of mission data budget with payload compression of 0.8. Operation times: SAR for two years (0-2), all other instruments for two years (2-4) and the experiment for search for life in Venus‘ atmosphere for one year (4-5). Max. possible data amount that can be transmitted during the overall mission is displayed.

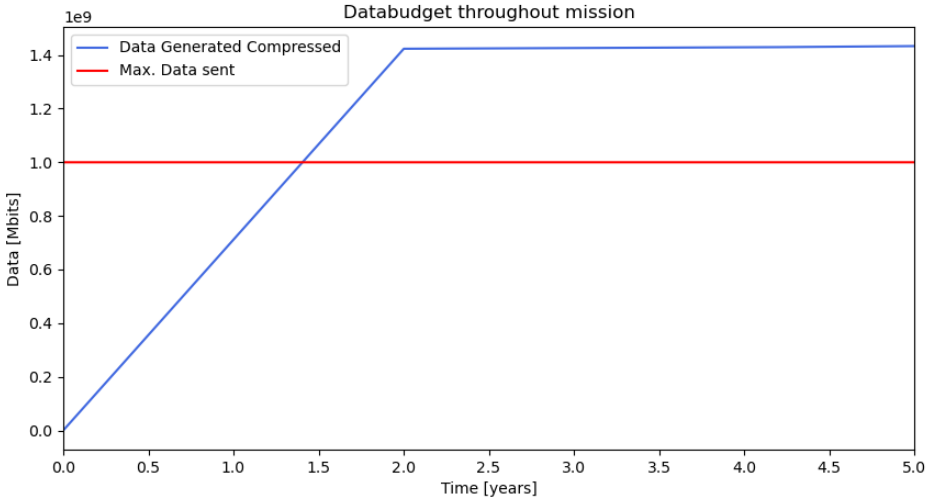

Figure A.16: Simulation of mission data budget with payload compression of 0.9. Operation times: SAR for two years (0-2), all other instruments for two years (2-4) and the experiment for search for life in Venus‘ atmosphere for one year (4-5). Max. possible data amount that can be transmitted during the overall mission is displayed.

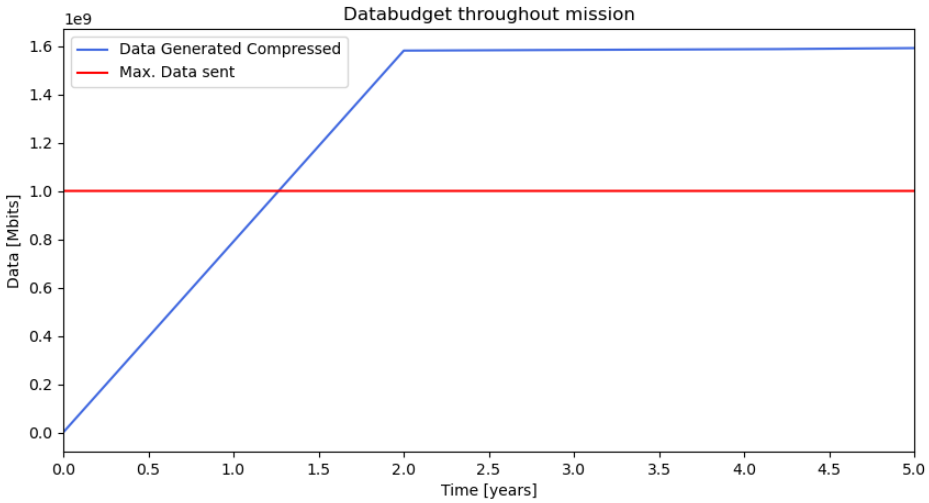

Figure A.17: Simulation of mission data budget with no payload compression. Operation times: SAR for two years (0-2), all other instruments for two years (2-4) and the experiment for search for life in Venus‘ atmosphere for one year (4-5). Max. possible data amount that can be transmitted during the overall mission is displayed.

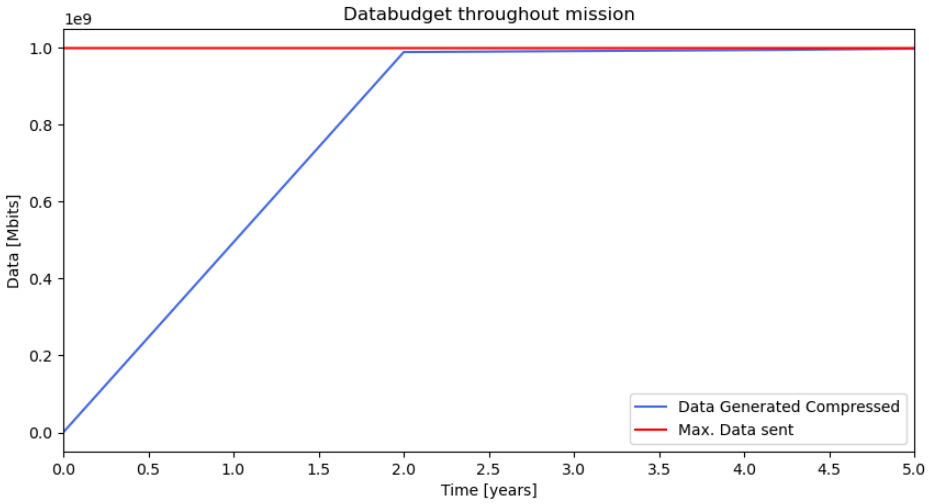

Figure A.18: Simulation of Mission Data Budget with Payload Compression of 0.625. Operation times: SAR for two years (0-2), all other instruments for two years (2-4) and the experiment for search for life in Venus‘ atmosphere for one year (4-5). Max. possible data amount that can be transmitted during the overall mission is displayed.

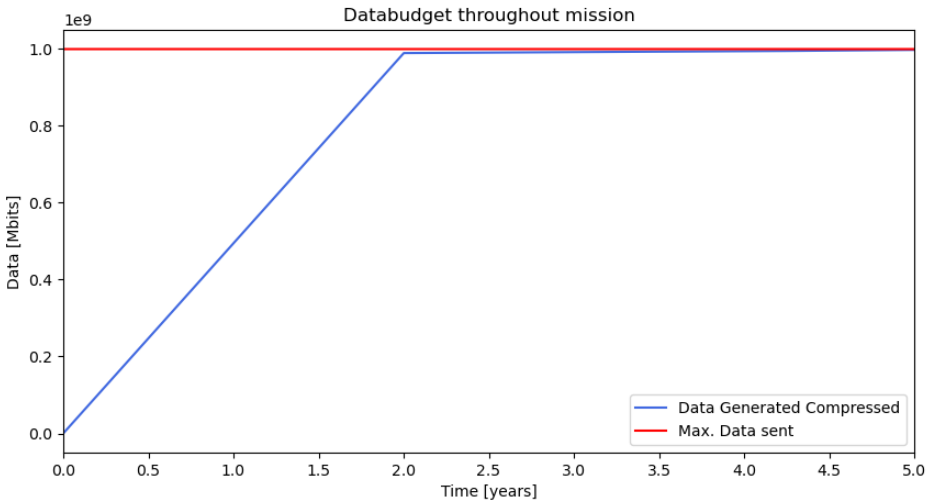

Figure A.19: Simulation of Mission Data Budget with SAR Data Rate of 62500 Mbits/s. Operation times:SAR for two years (0-2), all other instruments for two years (2-4) and the experiment for search for life in Venus‘ atmosphere for one year (4-5). Max. possible data amount that can be transmitted during the overall mission is displayed.

Bibliography

1. Justh, H., Cianciolo, A. D. & Hoffman, J. *Venus Global Reference Atmospheric Model (Venus-GRAM): User Guide* Accessed: 21.07.2023. 2021. https://ntrs.nasa.gov/citations/20210022168.
2. NASA. *Venus Global Reference Atmospheric Model (Venus-GRAM) 2005, Version 1.0 (MFS-32314-1)* Accessed: 21.07.2023. https://software.nasa.gov/software/MFS-32314-1.
3. Morbidelli, A., Lunine, J. I., O'Brien, D. P., Raymond, S. N. & Walsh, K. J. Building terrestrial planets. *Annual Review of Earth and Planetary Sciences* vol. 40, 251–275 (2012).
4. Smrekar, S. E. *et al.* Recent hotspot volcanism on Venus from VIRTIS emissivity data. *Science* vol. 328, 605–608 (2010).
5. Gülcher, A. J., Gerya, T. V., Montési, L. G. & Munch, J. Corona structures driven by plume–lithosphere interactions and evidence for ongoing plume activity on Venus. *Nature Geoscience* vol. 13, 547–554 (2020).
6. De Bergh, C. *et al.* Deuterium on Venus: observations from Earth. *Science* vol. 251, 547–549 (1991).
7. Donahue, T., Grinspoon, D., Hartle, R. & Hodges Jr, R. Ion/neutral escape of hydrogen and deuterium: Evolution of water. *Venus II: Geology, geophysics, atmosphere, and solar wind environment* vol. 385 (1997).
8. Taylor, F. W., Svedhem, H. & Head, J. W. Venus: the atmosphere, climate, surface, interior and near-space environment of an Earth-like planet. *Space Science Reviews* vol. 214, 1–36 (2018).
9. Way, M. J. *et al.* Was Venus the first habitable world of our solar system? *Geophysical research letters* vol. 43, 8376–8383 (2016).
10. Way, M. J. & Del Genio, A. D. Venusian habitable climate scenarios: Modeling Venus through time and applications to slowly rotating Venus-like exoplanets. *Journal of Geophysical Research: Planets* vol. 125, e2019JE006276 (2020).
11. Amato, P. *et al.* Active microorganisms thrive among extremely diverse communities in cloud water. *PloS one* vol. 12, e0182869 (2017).
12. Morowitz, H. & Sagan, C. Life in the Clouds of Venus? *Nature* vol. 215, 1259–1260 (1967).
13. Limaye, S. S. *et al.* Venus' Spectral Signatures and the Potential for Life in the Clouds. *Astrobiology* vol. 18. PMID: 29600875, 1181–1198 (2018).

14. Seager, S. *et al.* The Venusian lower atmosphere haze as a depot for desiccated microbial life: A proposed life cycle for persistence of the Venusian aerial biosphere. *Astrobiology* vol. 21, 1206–1223 (2021).

15. Hamano, K., Abe, Y. & Genda, H. Emergence of two types of terrestrial planet on solidification of magma ocean. *Nature* vol. 497, 607–610 (2013).

16. Hashimoto, G. L. & Sugita, S. On observing the compositional variability of the surface of Venus using nightside near-infrared thermal radiation. *Journal of Geophysical Research: Planets* vol. 108 (2003).

17. Ivanov, M. A. & Head, J. W. Global geological map of Venus. *Planetary and Space Science* vol. 59, 1559–1600 (2011).

18. ECSS. *ECSS-M-ST-10C* Accessed: 02.08.2023. https://ecss.nl/standards/active-standards/management/.

19. Taylor, F. W. *The scientific exploration of Venus* (Cambridge University Press, 2014).

20. Schuler, T. K., Bowman, D. C., Izraelevitz, J. S., Sofge, D. & Thangavelautham, J. Long duration flights in Venus' atmosphere using passive solar hot air balloons. *Acta Astronautica* vol. 191, 160–168. https://www.sciencedirect.com/science/article/pii/S0094576521005725 (2022).

21. Pätzold, M. *et al.* The structure of Venus' middle atmosphere and ionosphere. *Nature* vol. 450, 657–660 (2007).

22. Royal Belgian Institute for Space Aeronomy. *Temperature and greenhouse effect* http://venus.aeronomie.be/en/venus/temperaturegreenhouseeffect.htm. Accessed: 03.08.2023. 2023.

23. Colozza, A. & Landis, G. *Solar powered flight on Venus* tech. rep. (2004).

24. Titov, D. V., Ignatiev, N. I., McGouldrick, K., Wilquet, V. & Wilson, C. F. Clouds and hazes of Venus. *Space Science Reviews* vol. 214, 1–61 (2018).

25. Ekonomov, A. *et al.* Scattered UV solar radiation within the clouds of Venus. *Nature* vol. 307, 345–347 (1984).

26. Schofield, J. & Taylor, F. Net global thermal emission from the Venusian atmosphere. *Icarus* vol. 52, 245–262 (1982).

27. Zasova, L., Moroz, V., Esposito, L. & Na, C. SO2 in the middle atmosphere of Venus: IR measurements from Venera-15 and comparison to UV data. *Icarus* vol. 105, 92–109 (1993).

28. Lee, Y. J. *et al.* Vertical structure of the Venus cloud top from the VeRa and VIRTIS observations onboard Venus Express. *Icarus* vol. 217, 599–609 (2012).

29. Sánchez-Lavega, A., Lebonnois, S., Imamura, T., Read, P. & Luz, D. The atmospheric dynamics of Venus. *Space Science Reviews* vol. 212, 1541–1616 (2017).

30. Taylor, F. & Grinspoon, D. Climate evolution of Venus. *Journal of Geophysical Research: Planets* vol. 114 (2009).

31. Smith, R. & West, G. *Space and planetary environment criteria guidelines for use in space vehicle development. Volume 1: 1982 revision* tech. rep. (1983).

32. ECSS. *ECSS-E-ST-10C* Accessed: 02.08.2023. https://ecss.nl/standards/active-standards/engineering/.

33. ESA. *The electromagnetic spectrum* Accessed: 02.08.2023. https://www.esa.int/Science_Exploration/Space_Science/Integral/The_electromagnetic_spectrum.
34. AG, G. R. S. Interferometric SAR Processor j ISP. *Documentation j User, s Guide. Vers* vol. 1 (2010).
35. Peralta, J. *et al.* A long-lived sharp disruption on the lower clouds of Venus. *Geophysical Research Letters* vol. 47, e2020GL087221 (2020).
36. Gilmore, M., Beauchamp, P., Lynch, R., Amato, M. *et al.* Venus flagship mission decadal study final report. *A Planetary Mission Concept Study Report Presented to the Planetary and Astrobiology Decadal Survey* vol. 8 (2020).
37. Kane, S. R. *et al.* Venus as a laboratory for exoplanetary science. *Journal of Geophysical Research: Planets* vol. 124, 2015–2028 (2019).
38. Greeley, R. *et al.* Aeolian features on Venus: preliminary Magellan results. *Journal of Geophysical Research: Planets* vol. 97, 13319–13345 (1992).
39. Schubert, G. & Walterscheid, R. L. Propagation of small-scale acoustic-gravity waves in the Venus atmosphere. *Journal of Atmospheric Sciences* vol. 41, 1202–1213 (1984).
40. Byrne, P. K. *et al.* Venus tesserae feature layered, folded, and eroded rocks. *Geology* vol. 49, 81–85 (2021).
41. Kumar, H., Syed, T. & Rajak, D. R. *Damage Assessment Post Severe Cyclonic Storm" YAAS" Using Synthetic Aperture Radar* in *2021 IEEE International India Geoscience and Remote Sensing Symposium (InGARSS)* (2021), 173–176.
42. Haas, J. Laboratoriet för Digital Arkeologi DARK Lab The joint faculties of humanities and theology.
43. Elfadaly, A., Abate, N., Masini, N. & Lasaponara, R. SAR sentinel 1 imaging and detection of palaeo-landscape features in the mediterranean area. *Remote Sensing* vol. 12, 2611 (2020).
44. Saepuloh, A., Koike, K. & Omura, M. Applying Bayesian decision classification to Pi-SAR polarimetric data for detailed extraction of the geomorphologic and structural features of an active volcano. *IEEE Geoscience and Remote Sensing Letters* vol. 9, 554–558 (2012).
45. Sabrian, P. G., Saepuloh, A., Hede, A. N. H. *et al. Identification of Altered Minerals Based on Synthetic Aperture Radar (SAR) For Mineral Exploration in a Tropical Area* in *IOP Conference Series: Earth and Environmental Science* **71** (2017), 012021.
46. Bishop, C., Rivard, B., de Souza Filho, C. & Van Der Meer, F. *Geological remote sensing* 2018.
47. Gilmore, M. S., Mueller, N. & Helbert, J. VIRTIS emissivity of Alpha Regio, Venus, with implications for tessera composition. *Icarus* vol. 254, 350–361 (2015).
48. Romdhane, M. B. *et al.* Optimization of polysaccharides extraction from watermelon rinds: Structure, functional and biological activities. *Food Chemistry* vol. 216, 355–364 (2017).
49. Nimmo, F. & McKenzie, D. Volcanism and tectonics on Venus. *Annual Review of Earth and Planetary Sciences* vol. 26, 23–51 (1998).
50. Mulder, V., De Bruin, S., Schaepman, M. E. & Mayr, T. The use of remote sensing in soil and terrain mapping—A review. *Geoderma* vol. 162, 1–19 (2011).

51. Haest, M., Cudahy, T., Laukamp, C. & Gregory, S. Quantitative mineralogy from infrared spectroscopic data. I. Validation of mineral abundance and composition scripts at the rocklea channel iron deposit in Western Australia. *Economic Geology* vol. 107, 209–228 (2012).
52. Robling, A. G. *et al.* Mechanical stimulation of bone in vivo reduces osteocyte expression of Sost/sclerostin. *Journal of Biological Chemistry* vol. 283, 5866–5875 (2008).
53. Özdemir, G. & Clark, D. B. An overview of conceptual change theories. *Eurasia Journal of Mathematics, Science and Technology Education* vol. 3, 351–361 (2007).
54. Kokaly, R. F. *PRISM: Processing routines in IDL for spectroscopic measurements (installation manual and user's guide, version 1.0)* tech. rep. (US Geological Survey, 2011).
55. Breunig, F. M., Galvão, L. S. & Formaggio, A. R. Detection of sandy soil surfaces using ASTER-derived reflectance, emissivity and elevation data: potential for the identification of land degradation. *International Journal of Remote Sensing* vol. 29, 1833–1840 (2008).
56. Dabney, S. M. *et al.* Using cover crops and cropping systems for nitrogen management. *Advances in nitrogen management for water quality* vol. 66, 231–82 (2010).
57. DeMore, W. & Yung, Y. L. Catalytic processes in the atmospheres of Earth and Venus. *Science* vol. 217, 1209–1213 (1982).
58. Luhmann, J., Elphic, R., Russell, C., Mihalov, J. & Wolfe, J. Observations of large scale steady magnetic fields in the dayside Venus ionosphere. *Geophysical Research Letters* vol. 7, 917–920 (1980).
59. O'Rourke, J., Buz, J., Fu, R. & Lillis, R. Detectability of remanent magnetism in the crust of Venus. *Geophysical Research Letters* vol. 46, 5768–5777 (2019).
60. Cloutier, P. *et al.* Venus-like interaction of the solar wind with Mars. *Geophysical research letters* vol. 26, 2685–2688 (1999).
61. Doglioni, C., Pignatti, J. & Coleman, M. Why did life develop on the surface of the Earth in the Cambrian? *Geoscience Frontiers* vol. 7, 865–873 (2016).
62. Loper, D. E. & Roberts, P. H. Compositional convection and the gravitationally powered dynamo. *Stellar and planetary magnetism,* 297–327 (1983).
63. O'Rourke, J. G. & Stevenson, D. J. Powering Earth's dynamo with magnesium precipitation from the core. *Nature* vol. 529, 387–389 (2016).
64. Lagier, R. *ARIANE 6 USER'S MANUAL* Senior Vice President, Chief Technical Officer. Issue 2 Revision 0. Arianespace (Feb. 2021).
65. Rebecca M. Hahn, P. K. B. *KERNEL DENSITY ANALYSIS OF VOLCANOES ON VENUS AT VARYING SPATIAL SCALES.* in (Lunar and Planetary Science Conference, 2022), 2437.
66. Löw, S., Herman, J., Schulze, D. & Raschke, C. *Modes and More Finding the Right Attitude for TET-1* Accessed: 02.08.2023. June 2012. https://elib.dlr.de/76299/1/id1274662-Paper-002.pdf.
67. Izzo, D. *Pygmo and pykep: Open source tools for massively parallel optimization in astrodynamics (the case of interplanetary trajectory optimization)* in *Proceedings of the Fifth International Conference on Astrodynamics Tools and Techniques, ICATT* (2012).
68. *Kourou Antenna* Accessed: July 30, 2023. European Space Agency (ESA). http://estracknow.esa.int/#/2023-08;station=KRU.

69. *New Norcia 2 Antenna* https://www.esa.int/Enabling_Support/Operations/New_Norcia. Accessed: July 30, 2023. European Space Agency (ESA).

70. *ESA tracking stations* European Space Agency (ESA). http://estracknow.esa.int/ (2023).

71. European Space Agency (ESA). *Cool tech to almost double deep space data* https://www.esa.int/Enabling_Support/Operations/ESA_Ground_Stations/Cool_tech_to_almost_double_deep_space_data (2023).

72. *UCS Satellite Database* Union of Concerned Scientists (UCS). https://www.ucsusa.org/resources/satellite-database (2023).

73. *Ansys Systems Tool Kit (STK)* https://www.ansys.com/products/missions/ansys-stk. Version 12.1.

74. Deutsch, L. J., Townes, S. A., Liebrecht, P. E., Vrotsos, P. A. & Cornwell, D. M. *Deep space network: The next 50 years* in *14th International Conference on Space Operations* (2016), 2373.

75. Giorgini, J. & Group, J. S. S. D. *JPL Solar System Dynamics Group, NASA/JPL Horizons On-Line Ephemeris System* https://ssd.jpl.nasa.gov/horizons/. Data retrieved 2023-06-21.

76. European Space Agency (ESA). *CleanSat disposal essential for swelling satellite population* https://www.esa.int/Space_Safety/Clean_Space/CleanSat_disposal_essential_for_swelling_satellite_population (2023).

77. Rummel, J., Stabekis, P., Devincenzi, D. & Barengoltz, J. COSPAR's planetary protection policy: A consolidated draft. *Advances in Space Research* vol. 30, 1567–1571 (2002).

78. Kminek, G. *ESA planetary protection requirements, Technical Report ESSB-ST-U-001* 2012.

79. European Space Agency (ESA). *No bugs please, this is a clean planet!* https://www.esa.int/Science_Exploration/Space_Science/Cassini-Huygens/No_bugs_please_this_is_a_clean_planet (2023).

80. Zaugg, E., Edwards, M. & Margulis, A. *The slimsar: a small, multi-frequency, synthetic aperture radar for uas operation* in *2010 IEEE Radar Conference* (2010), 277–282.

81. Koenig, E. W. *High resolution infrared radiation sounder (HIRS) for the Nimbus F spacecraft* tech. rep. (1975).

82. Fimmel, R. O. *OMAG for magnetic field* (Scientific, Technical Information Branch, National Aeronautics and Space ..., 1983).

83. Ksanfomaliti, L. *et al.* Venus Acoustic Anemometers for wind measurement. *Soviet Astronomy Letters, vol. 8, July-Aug. 1982, p. 227-229. Translation Pisma v Astronomicheskii Zhurnal, vol. 8, July 1982, p. 419-423* vol. 8, 227–229 (1982).

84. Hiesinger, H. *et al.* MERTIS for thermal infrared radiation. *Space Science Reviews* vol. 216, 1–37 (2020).

85. Van der Heide, P. *Ion mass spectrometer for solar wind interaction* (John Wiley & Sons, 2014).

86. Park, I. *et al.* UFFO for the observation of early photons from gamma-ray bursts. *New Journal of Physics* vol. 15, 023031 (2013).

87. Wrbanek, J. D. *et al. Development of a Venus Surface Wind Sensor Based on a Miniature Drag-Force Anemometer* tech. rep. (2020).

88. Muhiyudin, M. *et al.* Miniaturised Infrared Spectrophotometer for Low Power Consumption Multi-Gas Sensing. *Sensors* vol. 20, 3843 (2020).

89. Arnold, G. *et al.* MERTIS-Mercury Radiometer and Thermal Infrared Spectrometer-a novel thermal imaging spectrometer for the exploration of Mercury (2007).

90. Taylor, H., Brinton, H., Wagner, T., Blackwell, B. & Cordier, G. Bennett ion mass spectrometers on the Pioneer Venus Bus and Orbiter. *IEEE Transactions on Geoscience and Remote Sensing,* 44–49 (1980).

91. Bae, H. *et al.* Miniature diamond-based fiber optic pressure sensor with dual polymer-ceramic adhesives. *Sensors* vol. 19, 2202 (2019).

92. Loftin Jr, L. K. *Subsonic aircraft: Evolution and the matching of size to performance* tech. rep. (1980).

93. Khoury, G. A. *Airship technology* (Cambridge university press, 2012).

94. Young, A. D. *The calculation of the total and skin friction drags of bodies of revolution at zero incidence* tech. rep. (HM Stationery Office, 1939).

95. Kuraray. vectran HT. *xyz* (2017).

96. Gawale, A. & Pant, R. S. *Design, fabrication and flight testing of remotely controlled airship* in *Proceedings of National Conference on LTA Technologies, Aerial Delivery R&D Establishment, Agra, India* (2002).

97. Liao, L. & Pasternak, I. A review of airship structural research and development. *Progress in Aerospace Sciences* vol. 45, 83–96 (May 2009).

98. The Editors of Encyclopaedia. *Airship* https://www.britannica.com/technology/airship. Accessed: 31.07.2023. 2023.

99. Jeff Scott. *Drag of Cylinders & Cones* https://aerospaceweb.org/question/aerodynamics/q0231.shtml. Accessed: 02.08.2023. 2005.

100. Pepermans, L. *et al. Comparison of Various Parachute Deployment Systems for Full Rocket Recovery of Sounding Rockets* in (July 2019), 7.

101. Seager, S. *et al.* Venus Life Finder Missions Motivation and Summary. *Aerospace* vol. 9. https://www.mdpi.com/2226-4310/9/7/385 (2022).

102. Kim, S., Yun, C., Kim, D., Yoon, Y. & Park, I. *Design and performance tests of cycloidal propulsion systems* in *44th AIAA/ASME/ASCE/AHS/ASC Structures, Structural Dynamics, and Materials Conference* (Norkfolk, virginia, 2003), 1786.

103. Boirum, C. & Post, S. *Review of historic and modern cyclogyro design* in *45th AIAA/ASME/SAE/ASEE Joint Propulsion Conference & Exhibit* (Danver, colorado, 2009), 5023.

104. Benedict, M. & Chopra, I. *Design and development of an unconventional VTOL micro air vehicle: The Cyclocopter* in *Micro-and Nanotechnology Sensors, Systems, and Applications IV* **8373** (Baltimore, Maryland, United States, 2012), 330–350.

105. Sachse, H. Kirsten-Boeing Propeller. Technical Memorandums–National Advisory Committee For Aeronautics. *Zeitschrift für Flugtechnik und Motorluftschifffahrt. S,* 1–4 (1926).

106. Kirsten, F. K. Cycloidal propulsion applied to aircraft. *Transactions of the American society of Mechanical Engineers* vol. 50, 25–47 (1928).

107. Strandgren, C. *The theory of the strandgren cyclogiro* tech. rep. (1933).

108. Nozaki, H. *et al. Research and development on cycloidal propellers for airships* in *18th AIAA Lighter-Than-Air Systems Technology Conference* (Seattle, Washington, 2009), 2850.

109. Moble, B. *Fundamental understanding of the cycloidal-rotor concept for micro air vehicle applications* (University of Maryland, College Park, Maryland, 2010).

110. Lee, C. H., Yong Min, S., Lee, J. W. & Kim, S. J. Design, analysis, and experimental investigation of a cyclocopter with two rotors. *Journal of Aircraft* vol. 53, 1527–1537 (2016).

111. Choudhury, N. *(THEORETICAL ASPECTS AND PRACTICAL US AGE OF HOERNER WING TIP)* Accessed: 02.08.2023. 2013. https://www.myplane.nl/cherrydocs/THEORETICAL_ASPECTS_AND_PRACTICAL_US_AGE.pdf.

112. Smith, R., Self, M. & Cheeseman, P. in *Autonomous robot vehicles* 167–193 (Springer, 1990).

113. *SDI500/SDI505 Quartz MEMS Tactical Inertial Measurement Unit* https://emcore.com/products/sdi500-tactical-grade-imu-inertial-measurement-unit/. Accessed: 07.06.2023.

114. *HDI Series amplified pressure sensors* https://www.first-sensor.com/cms/upload/datasheets/DS_Standard-HDI_E_11650.pdf. Accessed: 07.06.2023.

115. Markley, L. *Attitude determination using two vector measurements* in *NASA Conference Publication* (1999), 39–52.

116. Gomes, S. B. V. & Ramos, J. G. *Airship dynamic modeling for autonomous operation* in *Proceedings. 1998 IEEE International Conference on Robotics and Automation (Cat. No. 98CH36146)* **4** (1998), 3462–3467.

117. Pant, R. *A methodology for determination of baseline specifications of a non-rigid airship* in *AIAA's 3rd Annual Aviation Technology, Integration, and Operations (ATIO) Forum* (2003), 6830.

118. J, S., Wilcox, B. & Cutts, J. *An Airborne Turbine for Power Generation on Venus* in *15th Meeting of the Venus Exploration and Analysis Group (VEXAG)* **15** (2017), 8037.

119. Bechtel & Ryan. Multi-mission radioisotope thermoelectric generator (MMRTG). *NASA Facts* (2013).

120. Hall, J. L., Bullock, M., Senske, D. A., Cutts, J. A. & Grammier, R. *Venus Flagship Mission Study:Report of the Venus Science and Technology Definition Team* Accessed: 02.08.2023. 2009. https://www.lpi.usra.edu/science/kiefer/Publications/venusSTDT2009_finalreport.pdf.

121. Group, S. S. B. *3.6 V Primary lithium-thionyl chloride (Li-SOCl 2) High power, high temperature, super robust D-size spiral cell* Accessed: 02.08.2023. https://www.saftlithium.nl/datasheets/BIN_2013LSH_20_HTS.pdf.

122. Anthony, C. & Landis, G. *Solar powered flight on Venus* tech. rep. (2004).

123. Landis, G. A. & Harrison, R. Batteries for Venus surface operation. *Journal of propulsion and power* vol. 26, 649–654 (2010).

124. Energy, Z. *Litjium-Sulphur Batteries* Accessed: 02.08.2023. https://zetaenergy.com/.

125. Palissat, G. *Lithium-sulphur batteries: opportunities and challenges for space applications* in *Proceedings of the 8th European Conference for Aeronautics and Space Sciences. Madrid, Spain, 1-4 july 2019* (2019).

126. Khoury & Alexander, G. in *Airship technology* chap. 20 (Cambridge university press, 2012).

127. Landis, A, G., Haag & Emily. *Analysis of solar cell efficiency for Venus atmosphere and surface missions* in *11th International Energy Conversion Engineering Conference* (2013), 4028.

128. GmbH, A. S. S. P. *30% Triple Junction GaAs Solar Cell Type: TJ Solar Cell 3G30C - Advanced Large Area: 120mm x 60mm* Accessed: 02.08.2023. https://www.azurspace.com/images/products/0003422-02-02_DB_3G30C.pdf.

129. Technologies, E. *3High energy and high power lithium-ion cell for demanding applications* Accessed: 02.08.2023. https://www.eaglepicher.com/sites/default/files/SLC-203%200523.pdf.

130. Krause *et al.* High specific energy lithium primary batteries as power sources for deep space exploration. *Journal of The Electrochemical Society* vol. 165, A2312 (2018).

131. Subramanian, R. S. Conduction in the Cylindrical Geometry. *Department of Chemical and Biomolecular Engineering, Clarkson University.* https://web2.clarkson.edu/projects/subramanian/ch330/notes/Conduction%20in%20the%20Cylindrical%20Geometry.pdf.

132. Promat. MICROTHERM® PANEL technical datasheet. https://etex.azureedge.net/pi508569/original/1604591721/microtherm-panel_tds_de.pdf.

133. NASA. Aerogel Factsheet. https://solarsystem.nasa.gov/stardust/aerogel_factsheet.pdf.

134. Landis, G. *et al. Venus Rover Design Study* in (Sept. 2011).

135. Alutronic. *PR 264 Heatsink* https://alutronic.de/en/products/standardprofile/pr-264/.

136. Landis, G. & Mellott, K. Venus surface power and cooling systems. *Acta Astronautica* vol. 61, 995–1001 (Dec. 2007).

137. Vladimirova, T., Fayyaz, M., Sweeting, M. N. & Vitanov, V. I. A novel autonomous low-cost on-board data handling architecture for a pin-point planetary lander. *Acta Astronautica* vol. 68, 811–829 (2011).

138. Kraft, S. *et al.* On the concepts of a highly integrated payload suite for use in future planetary missions: The example of the BepiColombo Mercury planetary orbiter. *Acta astronautica* vol. 59, 823–833 (2006).

139. ESA. *Architectures of Onboard Data Systems* Accessed: 25.06.2023. https://www.esa.int/Enabling_Support/Space_Engineering_Technology/Onboard_Computers_and_Data_Handling/Architectures_of_Onboard_Data_Systems.

140. ESA. *Architectures of Onboard Data Systems* Accessed: 25.05.2023. https://www.esa.int/Enabling_Support/Space_Engineering_Technology/Onboard_Computers_and_Data_Handling/Architectures_of_Onboard_Data_Systems.

141. ESA. *Onboard Computers and Data Handling* Accessed: 25.05.2023. https://www.esa.int/Enabling_Support/Space_Engineering_Technology/Onboard_Computers_and_Data_Handling/Onboard_Computers_and_Data_Handling.

142. Airbus. *Onboard computers* Accessed: 15.06.2023. https://www.airbus.com/en/products-services/space/equipment/avionics/platform-electronics.

143. Beyond gravity. *Next Generation On Board Computer* Accessed: 25.06.2023. https://products.beyondgravity.com/d/SVq1aavsDmtE/library/show/eyJpZCI6MTM5NywidGltZXN0YW1wIjoiMTY4NzMwNDQzMSJ9:beyond-gravity:_ZD4GnvlxBSMhMefvfOXPhes3kwbYVG7Rkz8-ku9MnE.

144. Aerospace, M. *COMMAND AND DATA HANDLING (C&DH)* Accessed: 25.06.2023. https://magellan.aero/product/space/avionics/.

145. Airbus. *CMCU Clock Monitoring and Control Unit* Accessed: 25.06.2023. https://www.airbus.com/sites/g/files/jlcbta136/files/2021-11/Publication-sce-PP-NAV-CMCU-old.pdf.

146. Airbus. *NEMO-2 2041 High-End Non-Volatile Mass Memory* Accessed: 27.06.2023. https://www.airbus.com/sites/g/files/jlcbta136/files/2023-02/Nemo2-2041.pdf.

147. STAR-Dundee. *SpaceWire Router Mk2S* Accessed: 27.06.2023. https://www.star-dundee.com/wp-content/star_uploads/product_resources/datasheets/SpaceWire-Router-Mk2S.pdf.

148. BST. *PAYLOAD SUPPORT UNIT* Accessed: 27.06.2023. https://www.berlin-space-tech.com/portfolio/payload-support-unit/.

149. Beyond gravity. *Remote Terminal Unit (RTU)* Accessed: 27.06.2023. https://products.beyondgravity.com/d/SVq1aavsDmtE/library/show/eyJpZCI6MTQ1MiwidGltZXN0YW1wIjoiMTY4NzMwNDA3beyond-gravity:3MGYt74aVMuZFxHAODfOl5TYUW97XBoJNNeRiGJ7wD4.

150. Labs, K. *Leopard - Data Processing Unit for AI applications* Accessed: 25.05.2023. https://satsearch.co/products/kplabs-leopard-data-processing-unit.

151. Satsearch. *Spotlight: on-board data processing for next-generation satellites – with Unibap* Accessed: 25.05.2023. https://blog.satsearch.co/2022-03-23-on-board-data-processing-with-unibap.

152. ESA. *Remote Terminal Units* Accessed: 25.05.2023. https://www.esa.int/Enabling_Support/Space_Engineering_Technology/Onboard_Computers_and_Data_Handling/Remote_Terminal_Units.

153. Satsearch. *A guide to advanced data processing and AI for satellite missions* Accessed: 25.05.2023. https://blog.satsearch.co/2021-11-16-a-guide-to-advanced-data-processing-and-ai-for-satellite-missions#products.

154. NASA-CR-1146040. *A Study of an Orbital Radar Mapping Mission to Venus* Accessed: 25.05.2023. https://ntrs.nasa.gov/api/citations/19730023003/downloads/19730023003.pdf.

155. ESA. *Telemetry & Telecommand* Accessed: 25.05.2023. https://www.esa.int/Enabling_Support/Space_Engineering_Technology/Onboard_Computers_and_Data_Handling/Telemetry_Telecommand.

156. Steiger, C., Furnell, R. & Morales, J. *On-board control procedures for ESA's Deep space missions rosetta and venus express* in *DASIA 2005-Data Systems in Aerospace* **602** (2005).

157. ETSI. *Final draft ETSI EN 301 927 V1.1.1* Accessed: 25.05.2023. https://www.etsi.org/deliver/etsi_en/301900_301999/301927/01.01.01_40/en_301927v010101o.pdf.

158. SPACE, A. C. *Command and Data handling - kryten-M3* Accessed: 27.06.2023. https://www.aac-clyde.space/wp-content/uploads/2021/11/AAC_DataSheet_Kryten.pdf.

159. Du Toit, C. F., Everett, D. & Lorenz, R. D. Modeling of Venus Atmospheric RF Attenuation for Communication Link Purposes, 1–20 (2019).

160. A. J. Kliore V. I. Moroz, G. M. K. *The Venus International Reference Atmosphere.* 1–304 (Pergamon Press, Oxford, 1985).

161. NASA. *The Drag Equation.* Accessed: 02.08.2023. https://www.grc.nasa.gov/www/k-12/rocket/drageq.html.

162. Type, M. *Destination point given distance and bearing from start point.* Accessed: 04.08.2023. https://www.movable-type.co.uk/scripts/latlong.html.

163. Sena, S. *Solar Elevation Angle* Accessed: 04.08.2023. https://solarsena.com/solar-elevation-angle-altitude/.

164. Society, T. P. *Planetary Facts - Web archive* Accessed: 04.08.2023. https://web.archive.org/web/20120511011542/http://www.planetary.org/explore/space-topics/compare/planetary-facts.html.

Raumfahrttechnik und Extraterrestrik

Advances in Space Technology and Exploration

In der Schriftenreihe „Raumfahrttechnik und Extraterrestrik“ erscheinen Beiträge zu neuen Entwicklungen aus dem Bereich der Raumfahrttechnik sowie der Erforschung und Nutzung des Weltraums. Diese können sehr gute studentische Arbeiten, Dissertationen, Aufsätze zu relevanten Themen oder Ergebnisse von Projektarbeiten beinhalten.

Herausgeber:
Prof. Dr.-Ing. Hakan Kayal

Julius-Maximilians-Universität Würzburg
Prof. Dr.-Ing. Hakan Kayal
Professur für Raumfahrttechnik
Informatik VIII
Universität Würzburg
Emil-Fischer-Str. 32
D-97074 Würzburg
Tel.: +49-931-31-86649
Fax: +49-931-31-81368
hakan.kayal@uni-wuerzburg.de

ISSN: 2747-9374

Zitiervorschlag:

Bösch, Carolin; et al.: Venus Research Station, Raumfahrttechnik und Extraterrestrik, Nr. 4 (2023). DOI: 10.25972/OPUS-32869